STRENGTH AND DURABILITY OF BLENDED GEOPOLYMER COMPOSITE

THESIS SUBMITTED FOR THE FULFILMENT OF
DOCTOR OF PHILOSOPHY DEGREE IN ENGINEERING

by

DEBABRATA DUTTA

Department of Civil Engineering
Faculty of Engineering & Technology
Jadavpur University
Kolkata, India
2018

DEPARTMENT OF CIVIL ENGINEERING
FACULTY OF ENGINEERING AND TECHNOLOGY
JADAVPUR UNIVERSITY
KOLKATA
INDIA

CERTIFICATE FROM THE SUPERVISOR

This is to certify that the thesis entitled **"STRENGTH AND DURABILITY OF BLENDED GEOPOLYMER COMPOSITE",** submitted by Shri **Debabrata Dutta,** who got his name registered on **25.01.2012** for the award of **Ph.D. (Engineering)** degree of Jadavpur University, is absolutely based upon his own work under the supervision of Dr. Somnath Ghosh and that neither his thesis nor any part of the thesis has been submitted for any degree/diploma or any other academic award anywhere before.

Date

(Signature of the Supervisor)
Dr. Somnath Ghosh
Professor

(Office Seal)

JADAVPUR UNIVERSITY

KOLKATA- 700 032, INDIA

INDEX. NO. - 264/12/E

Title of Thesis:

STRENGTH AND DURABILITY OF BLENDED GEOPOLYMER COMPOSITE

Name, Designation & Institution of the Supervisor

Dr. Somnath Ghosh
Professor
Department of Civil Engineering,
Jadavpur University, Kolkata- 700032

List of publications:
International Journal Publications

SL.	TITLE	UGC APPROVED JOURNAL	Volume/ Issue/ Year/ Pg. No.	ISSN /ISBN	UGC JOURNAL NO.	SOURCE
1	Comparative study on the performance of blended and non-blended fly ash geopolymer composite as durable construction materials	Advances In Civil Engineering	Volume 2018, Article ID 2940169 19 February 2018, Pg.1-12	ISSN-1687-8086	11739	SCOPUS SCI Indexed
2	The role of delayed water curing in improving the mechanical and microstructural properties of alkali activated fly ash based geopolymer paste blended with slag	World Journal of Engineering	Accepted June,2018	ISSN 1708-5284	33153	SCOPUS SCI Indexed
3	Enhancing the mechanical and micro-structural properties of silica fume blended fly ash based geopolymer using murram as a tertiary supplement	Rasayan Journal	Vol. 11, No. 3, July-September, 2018, Pg. 1018 - 1033	ISSN 0974-1496	10001	SCOPUS
4	Effect of silica fume additions on porosity of Fly ash geopolymers	ARPN Journal of Engineering and Applied Sciences	Vol. 5, No. 10, October 2010, Pg.74-79	ISSN 1819-6608	8551	SCOPUS
5	Sustainable construction material under cyclic freezing-thawing in high saline exposure	International Journal of Civil and Structural Engineering	Volume 7, No 1, 2016, Pg.11-20	ISSN 0976 – 4399	2709	ICI
6	Evaluation of geopolymer properties with temperature imposed on activator prior mixing with fly ash	International Journal of Civil and Structural Engineering	Volume 3, No 1, 2012, Pg.205-213	ISSN 0976 – 4399	2709	ICI

SL.	TITLE	UGC APPROVED JOURNAL	Volume/ Issue/ Year/ Pg. No.	ISSN /ISBN	UGC JOURNAL NO.	SOURCE
7	Investigation on slag as supplement in fly ash geopolymer at various curing regime	International Journal Of Pure And Applied Research In Engineering And Technology	Volume 3, Issue 6, 2015, Pg.64-74	ISSN: 2319-507X	43791	UNIV
8	Effect of curing profile on fly ash geopolymer with slag as supplementary	International Journal of Engineering Sciences & Research Technology	Volume 3, Issue 12, December 2014, Pg.142-148	ISSN: 2277-9655	48486	UNIV
9	Optimization of temperature imposed on activator before mixing	International Journal of Engineering Science Invention	Volume 3, Issue 11, November 2014, Pg.56-62	ISSN (Online) : 2319 – 6734	43302	UNIV
10	Effect of lime stone dust on geopolymerisation and geopolymeric structure	International Journal of Emerging Technology And Advanced Engineering	Volume 2, Issue 11, November 2012, Pg.757-763	ISSN 2250-2459	44256	UNIV

SL.	TITLE	OTHER JOURNAL	Volume/ Issue/ Year/ Pg. No.	ISSN /ISBN	NAME OF PUBLISHERS
11	Microstructure of fly ash geopolymer paste with Blast furnace slag	Current Advances In Civil Engineering (CACE)	Volume 2, Issue 3, Jul. 2014, Pg.95-101	p-ISSN: 2332-9963 e-ISSN: 2332-998X	American V-King Scientific Publishing.
12	Durability study of geopolymer paste blended with blast furnace slag	IOSR Journal Of Mechanical And Civil Engineering (IOSR-JMCE)	Volume 11, Issue 2 Ver. I (Mar- Apr. 2014), Pg.73-79	p-ISSN: 2320-334X, e-ISSN: 2278-1684,	International Organization of Scientific Research (IOSR)
13	Effect of activator solution on compressive strength of fly ash geopolymer blended with slag	Int. Journal of Engineering Research and Applications	Volume 4, Issue 12 (Part 2), December 2014, Pg.72-76	ISSN : 2248-9622	IJERA Publication
14	Study on fly ash based geopolymer blended with calcium at different curing profile	SSRG International Journal of Civil Engineering (SSRG-IJCE)	Volume 1, Issue-6, Nov 2014, Pg.1-6	ISSN: 2348 -8352	SSRG International Journal
15	Prediction of optimal curing temperature for fly ash based Geopolymer blended with blast furnace slag	International Journal of Emerging Technology & Research	Volume 1, Issue 7, Nov - Dec, 2014, Pg.104-110	e-ISSN: 2347-5900 p-ISSN: 2347-6079	Innovation And Emerging Technology Group Publisher
16	The effect of Na_2O concentration in activator for fly ash based geopolymer blended with slag	Int. Journal of Applied Sciences And Engineering Research	Vol. 3, Issue 6, 2014, Pg.1096-1101	ISSN: 2277 -9442	IJASER Publishers

SL.	TITLE	OTHER JOURNAL	Volume/ Issue/ Year/ Pg. No.	ISSN /ISBN	NAME OF PUBLISHERS
17	Parametric study of geopolymer paste with the different combination of activators	International Journal of Engineering Innovation & Research	Volume 3, Issue 6, 2014, Pg.787-793	ISSN: 2277 -5668	Timeline Publication Pvt. Ltd.
18	Strength and durability of fly ash geopolymer blended with lime stone dust	International Journal of Engineering Research & Technology (IJERT)	Vol. 2 Issue 7, July – 2013, Pg.60-67	ISSN: 2278-0181	International Research Publication House
19	Comparative study of geopolymer paste prepared from different activators	Recent Trends in Civil Engineering & Technology	Volume 2, Issue 3, December-2012, Pg.1-10	ISSN: 2249 -8753	STM Journals

List of International and National Conferences

SL.	TITLE	CONFERENCE	Volume/ Issue/ Year/ Pg. No.	Venue & Time	NAME OF ORGANISER
01	Durability study of geopolymer paste blended with blast furnace slag	International Conference on "Global Trends In Engineering and Management"	Volume 1, March,2013, Pg.531-536	Nagpur, India / March 21-22,2013	J D College of Engineering

THESIS IS DEDICATED TO MY BELOVED

SIR & MADAM

ACKNOWLEDGEMENTS

First and foremost, enormous gratitude to Prof. (Dr.) Somnath Ghosh who has been there as my supervisor for the whole research period and has been unstinting in his support and constructive idea. He provided critical advice in my calculation and suggested many important additions and improvement. It has been a great enriching experience to me to work under his authoritative guidance. In fact, it was only because of his keen interest and continuous encouragement that gave my work this extent form.

I'd like to use this opportunity to express my very sincere gratitude to my parents and my wife who have offered me invaluable guidance, counseling, and helpful hints, which have greatly inspired myself to the work.

I would like to express the deepest appreciation to all my respected committee members and Head of Civil Engineering Department.

Particular thanks must also be recorded to Dr. Suresh Thokchom, Dr. Nadeem Qureshi, Mr. Samrat Sengupta, Late Supratim Dey, my friends and my Departmental Professors.

Debabrata Dutta

TABLE OF CONTENTS

CERTIFICATE

LIST OF PUBLICATIONS

ACKNOWLEDGEMENT

TABLE OF CONTENTS i

LIST OF FIGURES xii

LIST OF TABLES xix

LIST OF ABBREVIATIONS xxi

SYNOPSIS xxii

1. INTRODUCTION 1

1.1 Preamble 1

1.2 Geopolymerization 1

1.2.1 Base Material and Activator 1

1.2.2 Curing Profile 2

1.3 Geopolymer and Zeolite 3

1.4 Supplements with Base Materials 5

1.5 Use of Activators in Geopolymer 6

1.6 Drawbacks in Alkali activated Fly ash based Geopolymer 7

1.7 Scope of work 8

1.8 Organization of the Thesis 10

2. REVIEW OF EXISTING LITERATURE 12

2.1 Preamble 12

2.2 Instability of Geopolymer with Aging 13

2.3 Reactivity of precursors with variation of Base material and Alkali 13

2.4 Parametric study on the performance of Non-Blended Geopolymer 18

2.5 Parametric study on the performance of Blended Geopolymer 22

2.5.1 Geopolymer Blended with Supplementary Calcium compound 22

2.5.2 Cast-in-situ Geopolymer 26

2.5.3 Geopolymer Blended with Supplementary Silica compound 26

2.6 Objectives of the Present research 27

2.6.1 Study on Optimal parameters of Activator and its impact on Non-Blended Fly Ash Geopolymer 27

2.6.2 Study on Fly Ash based Geopolymer Blended with Supplementary Calcium based Compound 27

2.6.3 Study on Fly Ash based Geopolymer Blended with Supplementary Silica based Compound 28

3. EXPERIMENTAL INVESTIGATION 29

3.1 Preamble 29

3.2 Raw Materials 32

3.2.1 Base Material 32

3.2.1.1 Fly Ash 32

3.2.2 Supplementary Materials 33

3.2.2.1 Silica Fume 33

3.2.2.2 Lime Stone Dust 34

3.2.2.3 Ground Granulated Blast Furnace Slag (GGBS) 34

3.2.2.4 Murram 35

3.2.2.5 Commercial Borax 36

3.2.3 Alkali Activator 37

3.3 Manufacturing process of Geopolymer composites 39

3.3.1 Preparation 39

3.3.2 Curing 41

3.3.2.1 Hot Curing 41

3.3.2.2 Water Curing 41

3.4 Test setup 41

3.4.1 Test setup for the study on Physico -Mechanical performance 41

3.4.1.1 Workability Test 41

3.4.1.2 Strength Test 42

3.4.1.3 Water Absorption Test 44

3.4.1.4 Density and Apparent Porosity Test 44

3.4.1.5 Sorptivity Test 44

3.4.2 Test Setup for Durability Study 46
3.4.2.1 Sulfate Exposure 46
3.4.2.2 Weight change and Residual Strength Test 46
3.4.2.3 Physical Changes and Optical Microscopy 46
3.4.2.4 Thermal Fluctuation (Freezing –Thawing) Set up 47
3.4.3 Test Setup for the Microstructural Study 48
3.4.3.1 Field Emission Scanning Electron Microscopy (FESEM) 48
3.4.3.2 Scanning Electron Microscopy (SEM) and Energy Dispersive X-ray (EDX) Analysis 49
3.4.3.3 X-Ray Diffraction Analysis 50
3.4.3.4 MIP Analysis 51
3.4.3.5 Thermo Gravimetric Analysis (TGA) 52
3.5 Typical outline of the different phases of the entire experimental investigation 53
3.5.1 Preamble 53
3.5.2 Study on Activator and its Impact on Non-blended Fly ash Geopolymer 54
3.5.2.1 Temperature Imposed (By Pre-Heating) On Activator Prior Mixing to Manufacture Geopolymer 54
3.5.2.2 Blended Alkali activator with dual Alkali oxide 54
3.5.3 Study on Fly ash Geopolymer with Supplementary Calcium compound 54
3.5.3.1 Fly ash Geopolymer blended with Lime stone dust and its mechanical properties 54
3.5.3.2 Microstructure with Mechanical performance of Lime stone dust 55
3.5.3.3 Durability Study on Fly ash Geopolymer blended with Lime Stone Dust 55
3.5.3.4 Development of Fly ash Geopolymer blended with Slag and its properties 55
3.5.3.5 Microstructure with Mechanical performance of Fly Ash Geopolymer blended with Slag 56
3.5.3.6 Durability study on Fly ash Geopolymer blended with Slag 56
3.5.3.7 Fly ash Geopolymer blended with Slag (Water cured) 56
3.5.4 Study on Fly ash Geopolymer blended with Supplementary Silica compound 57

3.5.4.1 Development of Fly ash Geopolymer blended with Silica fume in presence of Borax and its performance 57

3.5.4.2 Physical and Microstructural study on Fly ash Geopolymer blended with Silica Fume and Murram 57

3.6 Geopolymer Mix proportion and other parameters 58

3.6.1 Study on Activator parameters of Non-blended Fly ash based Geopolymer 59

3.6.1.1 Details of specimens for studying Activator parameters of Non-blended Fly ash based Geopolymer 61

3.6.2 Study on Fly ash Geopolymer blended with supplementary Calcium compound 62

3.6.2.1 Details of specimens for study on Fly ash Geopolymer blended with supplementary Calcium compound 70

3.6.3 Study on Fly ash Geopolymer blended with supplementary Silica compound 71

3.6.3.1 Details of specimens for study on Fly ash Geopolymer blended with supplementary Silica compound 74

4. RESULT AND DISCUSSION 75

4.1 Preamble 75

4.2 Parameters of Activator and its impact on Non-Blended Fly ash Geopolymer 76

4.2.1 Physical Property 76

4.2.1.1 Workability 76

4.2.1.1.1 Effect of Temperature level of Activator on Workability of Fly ash based Geopolymer 76

4.2.1.1.2 Effect of dual oxides in Activator (K_2O+Na_2O) on Workability of Fly ash based Geopolymer 78

4.2.1.2 Compressive strength 79

4.2.1.2.1 Effect of Temperature level of Activator on Compressive strength of Fly ash based Geopolymer 79

4.2.1.2.2 Effect of dual oxides in Activator (K_2O+Na_2O) on Compressive strength of Fly ash based Geopolymer 80

4.2.2 Microstructural property 81

4.2.2.1 Scanning Electron Microscopy and EDX analysis 81

4.2.2.1.1 Effect of Temperature level of Activator on microstructural properties of Fly ash based Geopolymer 81

4.2.2.1.2 Effect of dual oxides in Activator (K_2O+Na_2O) on microstructural properties of Fly ash based Geopolymer 84

4.3 Fly ash based Geopolymer blended with supplementary Calcium compound 86

4.3.1 Physical property 86

4.3.1.1 Workability 86

4.3.1.1.1 Effect of Lime stone dust blending on Workability of Fly ash based Geopolymer 86

4.3.1.1.2 Effect of Slag blending on Workability of Fly ash based Geopolymer 87

4.3.1.2 Compressive strength 89

4.3.1.2.1 Compressive strength of Heat cured specimens 89

4.3.1.2.1.1 Effect of Aging on the Compressive strength of Fly ash based Geopolymer blended with Blast furnace slag 89

4.3.1.2.1.2 Effect of Curing profile (curing temperature and duration) on Compressive strength of Fly ash based Geopolymer blended with Lime stone dust 91

4.3.1.2.1.3 Effect of Curing profile on Compressive strength of Fly ash based Geopolymer blended with Slag 93

4.3.1.2.1.4 Effect of Alkali concentration on Compressive strength of Fly ash based Geopolymer blended with Slag 95

4.3.1.2.2 Compressive Strength of Water cured samples 101

4.3.1.2.2.1 Effect of Rest period on Compressive strength of Alkali activated Fly ash blended with Slag, cured in water 101

4.3.1.3 Water Absorption and Apparent Porosity 104

4.3.1.3.1 Water absorption and Apparent porosity of Heat cured specimens 104
4.3.1.3.1.1 Effect of Lime stone dust blending on Apparent porosity and Water absorption of Fly ash based Geopolymer 104
4.3.1.3.1.2 Effect of Slag blending on Water absorption and Apparent porosity of Fly ash based Geopolymer 105
4.3.1.4 Sorptivity 106
4.3.1.4.1 Sorptivity of Heat cured specimens 106
4.3.1.4.1.1 Effect of Lime stone blending on Sorptivity of Fly ash Geopolymer 106
4.3.1.4.1.2 Effect of Slag blending on Sorptivity of Fly ash based Geopolymer 108
4.3.2 Microstructural Property 110
4.3.2.1 Microstructural Property of Heat cured specimens 110
4.3.2.1.1 Microstructural properties analysis by SEM & EDX 110
4.3.2.1.1.1 Effect of Lime stone dust blending on Microstructural property of Fly ash based Geopolymer 110
4.3.2.1.1.2 Effect of blast furnace slag blending on Microstructural property of Fly ash based Geopolymer 113
4.3.2.1.2 Mercury Intrusion Porosimetry (MIP) 117
4.3.2.1.2.1 Effect of Lime stone dust blending on Pore distribution of Fly ash Geopolymer 117
4.3.2.1.2.2 Effect of Slag Blending on Pore Distribution of Fly Ash based Geopolymer 119
4.3.2.2 Microstructural Property of Water cured specimens 121
4.3.2.2.1 Property analyzed by FESEM 121

4.3.2.2.1.1 Effect of Rest period on the microstructure of Alkali activated Fly ash blended with Slag and cured in water 121

4.3.2.2.2 XRD Analysis to study Mineralogical changes 123

4.3.2.2.2.1 Effect of Rest period after casting on mineralogical change of Alkali activated Fly ash blended with Slag and cured in water 123

4.3.2.2.3 Thermo-Gravimetric Analysis (TGA) 126

4.3.2.2.3.1 Effect of Rest period on Thermal stability of Alkali activated Fly ash blended with Slag and Cured in water 126

4.3.3 Durability performance 129

4.3.3.1 Durability performance analysis of Heat cured specimens 129

4.3.3.1.1 Change in weight under aggressive exposure 129

4.3.3.1.1.1 Effect of Lime stone dust blending on the Weight change of Fly ash based Geopolymer exposed to 10% Magnesium sulfate solution 129

4.3.3.1.1.2 Effect of Slag blending on the Weight change of Fly ash based Geopolymer exposed to 10% Magnesium sulfate solution 130

4.3.3.1.1.3 Effect of Slag blending on the Weight change of Fly ash based Geopolymer under cyclic Freezing thawing exposed to 20% Magnesium sulfate solution 131

4.3.3.1.2 Residual strength under aggressive exposure 133

4.3.3.1.2.1 Effect of Lime stone dust blending on the Residual strength of Fly ash based Geopolymer exposed to 10% Magnesium sulfate solution 133

4.3.3.1.2.2 Effect of Slag blending on the Residual strength of Fly ash based Geopolymer exposed to 10% Magnesium sulfate solution 133

4.3.3.1.2.3 Effect of Slag blending on the Residual strength of Fly ash based Geopolymer under cyclic Freezing thawing exposed to 20% Magnesium sulfate solution 134

4.3.3.1.3 Physical change in appearance 136

4.3.3.1.3.1 Effect of Lime Stone dust blending on the Physical appearance of Fly ash based Geopolymer under 10% Magnesium sulfate solution exposure 136

4.3.3.1.3.2 Effect of Slag blending on the Physical appearance of Fly ash based Geopolymer under 10% Magnesium sulfate solution exposure 138

4.3.3.1.3.3 Effect of Slag blending on the Physical appearance of Fly ash based Geopolymer under cyclic Freezing thawing and exposed to 20% Magnesium sulfate solution 139

4.3.3.2 Durability performance analysis of Water cured specimens 140

4.3.3.2.1 Change in weight for specimens exposed to Aggressive exposure 140

4.3.3.2.1.1 Effect of Rest period on Weight change of Alkali activated Fly ash blended with Slag and Water cured, under cyclic Freezing-thawing exposed to 20% Magnesium sulfate exposure 140

4.3.3.2.2 Residual strength for specimens exposed to Aggressive exposure 141

4.3.3.2.2.1 Effect of Rest period on Residual strength of Alkali activated Fly ash blended with Slag and Water cured, subjected to cyclic Freezing-thawing exposed to 20% Magnesium sulfate solution 141

4.3.3.2.3 Physical change in appearance 142

4.3.3.2.3.1 Effect of Rest period on Efflorescence of Alkali activated Fly ash blended with Slag and Water cured under ambient environment 142

4.4 Fly ash based Geopolymer blended with Supplementary Silica compound 143

4.4.1 Physical property 143

4.4.1.1 Workability 143

4.4.1.1.1 Effect of Silica fume blending in Fly ash based Geopolymer in presence of Murram 143

4.4.1.2 Compressive strength 145

4.4.1.2.1 Effect of Silica fume blending in Fly ash based Geopolymer in presence of Borax on Compressive strength 145

4.4.1.2.2 Effect of Silica fume blending in Fly ash based Geopolymer in presence of Murram on Compressive strength 147

4.4.2 Microstructural Property 149

4.4.2.1 Scanning Electron Microscopy (SEM) & Energy Dispersive X-ray (EDX) 149

4.4.2.1.1 SEM and EDX report on the effect of Silica fume blending 149

4.4.2.1.1.1 Report on the effect of Silica fume blending in the presence of Borax in Fly ash based Geopolymer 149

4.4.2.1.1.2 Report on the effect of Silica fume blending in presence of Murram in Fly ash based Geopolymer 151

4.4.2.2 Mercury Intrusion Porosimetry (MIP) 156

4.4.2.2.1 Effect of Silica fume blending on the pore characteristics of Fly ash based Geopolymer in the presence of Murram 156

4.4.2.2.2 Effect of Silica fume blending on the pore characteristics of Fly ash based Geopolymer in the presence of Borax 158

4.4.3 Durability performance in Aggressive and Room exposure 161

4.4.3.1 Effect of Silica fume and Borax in Fly ash Geopolymer on Efflorescence in room exposure 161

4.4.3.2 Effect of Silica fume and Borax blending on the durability performance Fly ash Geopolymer under Sulfate exposure (10% concentration) 162

4.4.3.2.1 Change in Physical appearance (Micro and Macro Level) 162

4.4.3.2.2 Changes in Weight and Strength exposed to 10% concentrated sulfate exposure 165

5. CONCLUSION 168

5.1 Preamble 168

5.1.1 Study on Activator parameter and its Impact on Non-Blended Fly Ash Geopolymer 169

5.1.1.1 Level of temperature induced on Activator (pre heating) prior to use to manufacture Geopolymer 169

5.1.1.2 Combination of oxides in activator 169

5.1.2 Study on Fly ash Geopolymer blended with Supplementary Calcium compound 170

5.1.2.1 Study on Workability 170

5.1.2.2 Study on Heat cured specimens 170

5.1.2.2.1 Study on Compressive strength 170

5.1.2.2.1.1 Effect of Aging on Compressive strength 170

5.1.2.2.1.2 Effect of Curing temperature on Compressive strength 170

5.1.2.2.1.3 Effect of Curing duration on Compressive strength 171

5.1.2.2.1.4 Effect of Alkali concentration on Compressive strength 171

5.1.2.2.1.5 Study on Microstructure 172

5.1.2.2.1.6 Study on Durability performance 172

5.1.2.3 Study on Water cured specimens 173

5.1.2.3.1 Study on Compressive strength 173

5.1.2.3.2 Study on Mineralogical and Microstructural properties 173

5.1.2.3.3 Study on Durability performance 173

5.1.3 Study on Fly ash Geopolymer blended with supplementary Silica compound 173

5.1.3.1 General observation 173

5.1.3.2 Study on Workability 174

5.1.3.3 Study on Compressive Strength 174

5.1.3.4 Study on Micro-structure 174

5.1.3.5 Study on Durability 174

5.2 Scope of future study 175

6. REFERENCE 176

APPENDIX-I Calculation for constituent proportion of activator and geopolymer paste

APPENDIX-II Reprints of some published papers

LIST OF FIGURES

Figure No.	Description	Page No.
Figure 1.1	Schematic diagram of drawbacks in fly ash geopolymer	07
Figure 3.1	Flow chart of Present Investigation	31
Figure 3.2	Microscopic Image of Fly Ash	32
Figure 3.3	Microscopic Image of Silica Fume	33
Figure 3.4	Microscopic Image of Lime Stone Dust	34
Figure 3.5	Microscopic Image of Blast Furnace Slag	35
Figure 3.6	Microscopic Image of Murram	36
Figure 3.7	Microscopic Image of Borax	37
Figure 3.8	Activator Preparation	38
Figure 3.9	Preparation of test specimens	40
Figure 3.10	Workability Test Setup	42
Figure 3.11	Split Tensile Strength Testing Setup	43
Figure 3.12	Digital Compression Test Machine	43
Figure 3.13 (a)	Setup for Sorptivity	45
Figure 3.13 (b)	Samples for Sorptivity Test	46
Figure 3.14	Crack Detection Microscope	47
Figure 3.15	Setup for Freezing-Thawing Test in Magnesium Sulfate Solution	48
Figure 3.16	Specimen after Freezing in Freezing-Thawing Exposure in Sulfate Solution	48
Figure 3.17	Field Emission Scanning Electron Microscopy Unit	49
Figure 3.18	QUANTA 2000 for Scanning Electron Microscope	50
Figure 3.19	X-Ray Diffractometer Unit for X-Ray Diffraction Analysis and its Mechanism	51
Figure 3.20	Micromeritics Autopore for MIP	52
Figure 3.21	Thermo Gravimetry/Differential Thermal Analyser	52
Figure 4.1	The experimental setup	77
Figure 4.2	The expansion of past sample PS35	77
Figure 4.3	Zero flow for sample PS15 (Area factor =1)	77
Figure 4.4	Sample PS35 after flow (Area factor =13.44)	77

Figure 4.5	3-day Compressive strength of Fly ash based Geopolymer paste specimens	79
Figure 4.6	Compressive strength of Fly ash based Geopolymer specimens with age	80
Figure 4.7(a)	SEM @ 600x zoom and EDX of specimen PS15	81
Figure 4.7(b)	SEM @ 640x zoom and EDX of specimen PS20	82
Figure 4.7(c)	SEM @ 300x zoom and EDX of specimen PS35	82
Figure 4.7(d)	SEM @ 1550x zoom and EDX of specimen PS65	82
Figure 4.7(e)	SEM @700x zoom and EDX of specimen PS75	83
Figure 4.7(f)	SEM @ 4000x zoom and EDX of specimen PS80	83
Figure 4.7(g)	SEM @ 1520x zoom and EDX of specimen PS90	83
Figure 4.7(h)	SEM @ 4000x zoom and EDX of specimen PS95	84
Figure 4.8(a)	SEM @ 1200x zoom and EDX of specimen GP1-L	85
Figure 4.8(b)	SEM @ 600x zoom and EDX of specimen GP1	85
Figure 4.8(c)	SEM @ 600x zoom and EDX of specimen GP1	86
Figure 4.8(d)	SEM @ 300x zoom and EDX of specimen GPX1	86
Figure 4.9	Workability Test Setup	87
Figure 4.10	Expansion of sample GL2	87
Figure 4.11	Flow of sample GB2	88
Figure 4.12	Sample GB2 after flow	88
Figure 4.13	3-Day Compressive strength of Fly ash based Geopolymer blended with Blast furnace slag	90
Figure 4.14	Effect of Aging on Compressive strength of Fly ash based Geopolymer blended with Blast furnace slag	91
Figure 4.15	Compressive strength at different curing profile for Lime stone dust Blended Fly ash based Geopolymer specimens	93
Figure 4.16	Compressive strength at different curing profile for Slag Blended Fly ash based Geopolymer specimens	95
Figure 4.17	Effect of percentage Na2O on Compressive strength of Slag Blended Fly ash based Geopolymer specimens	98
Figure 4.18	Effect of Silicate modulus on Compressive strength of Slag Blended Fly ash based Geopolymer specimens	99
Figure 4.19	Combined effect of Curing temperature and Activator concentration on Compressive strength of Fly ash Geopolymer blended with Slag	100
Figure 4.20 (a)	1 and 20 day Compressive strength after curing of specimens (for varying rest periods)	102

Figure 4.20 (b)	1 and 20 day Compressive strengths (expressed as percentages of 20 day strength) after Water curing of specimens (for different rest periods)	102
Figure 4.20 (c)	Strength gain of Water cured specimens (for varying rest periods)	103
Figure 4.21	Apparent porosity of Fly ash based Geopolymer blended with Slag	104
Figure 4.22	Water absorption of Fly ash based Geopolymer blended with Lime stone dust	105
Figure 4.23	Apparent porosity of Fly ash based Geopolymer blended with Slag	106
Figure 4.24	Water absorption of Fly ash based Geopolymer blended with Slag	106
Figure 4.25(a)	Trend of cumulative absorption of water for Fly ash based Geopolymer blended with Lime stone dust	107
Figure 4.25(b)	Initial trend of cumulative absorption of Fly ash based Geopolymer blended with Lime stone dust	107
Figure 4.26	Sorptivity of Fly ash based Geopolymer blended with Lime stone dust	108
Figure 4.27(a)	Cumulative absorption of Fly ash based Geopolymer blended with Slag	109
Figure 4.27(b)	Initial trend of cumulative absorption of Fly ash based Geopolymer blended with Slag	109
Figure 4.28	Water Sorptivity of Fly ash based Geopolymer blended with Slag	110
Figure 4.29(a)	SEM @ 620x zoom and EDX of specimen GP1	111
Figure 4.29(b)	SEM @ 300x zoom and EDX of specimen GL1	111
Figure 4.29(c)	SEM @ 300x zoom and EDX of specimen GL2	112
Figure 4.30	SEM @ 9000x zoom; presence water crystal in specimen GP1-HL	112
Figure 4.31(a)	SEM @ 600x zoom and EDX of specimen GP1	114
Figure 4.31(b)	SEM @ 1200x zoom and EDX of specimen GB1	114
Figure 4.31(c)	SEM@ 1600x zoom and EDX of specimen GB2	114
Figure 4.31(d)	SEM @ 800x zoom of specimen GP1	115
Figure 4.31(e)	SEM @1918x zoom of specimen GP1	115
Figure 4.31(f)	SEM @ 8000x zoom of specimen GP1	115
Figure 4.31(g)	SEM @ 18041x zoom of specimen GP1	115
Figure 4.31(h)	SEM @ 13000x zoom of specimen GP1	115
Figure 4.31(i)	SEM @ 50000x zoom of specimen GP1	115
Figure 4.31 (j)	SEM @ 6000X zoom and EDX of crystalline compound within the pore of specimen	116

Figure 4.32	SEM of GP1 on typical interior point under progressive zoom	116
Figure 4.33	Typical plot of MIP analysis of specimen GP1	118
Figure 4.34	Typical plot of MIP analysis of specimen GL2	118
Figure 4.35	Typical plot of MIP analysis for specimen GP1	120
Figure 4.36	Typical plot of MIP analysis for specimen GB1	120
Figure 4.37(a)	Scanning Electron Microscopy @ 800x zoom of Specimen GB_R(2)_WC after 20 days water curing	122
Figure 4.37(b)	Scanning Electron Microscopy @ 1524x zoom of Specimen GB_R(2)_WC after 20 days water curing	122
Figure 4.37(c)	Scanning Electron Microscopy @ 3231x zoom of Specimen GB_R(8)_WC after 20 days water curing	122
Figure 4.37(d)	Scanning Electron Microscopy @ 6866x zoom of Specimen GB_R(8)_WC after 20 days water curing	122
Figure 4.37(e)	Scanning Electron Microscopy @ 9609x zoom of Specimen GB_R(14)_WC after 20 days water curing	122
Figure 4.37(f)	Scanning Electron Microscopy @ 16479x zoom of Specimen GB_R(14)_WC after 20 days water curing	122
Figure 4.37(g)	SEM @ 6866x zoom of Specimen GB_R(24)_WC after 20 days water curing	122
Figure 4.37(h)	SEM @ 20974x zoom of Specimen GB_R(24)_WC after 20 days water curing	122
Figure 4.38(a)	XRD pattern of specimen GB_R (2) _WC	125
Figure 4.38(b)	XRD pattern of specimen GB_R (12) _WC	125
Figure 4.38(c)	XRD pattern of specimen GB_R (24)_WC	125
Figure 4.39	TG/DTA Thermo-gram for specimen GB_R (2) _WC	127
Figure 4.40	TG/DTA Thermo-gram for specimen GB_R (24) _WC	127
Figure 4.41	Thermo-grams for specimens GB_R (2) _WC and GB_R (24) _WC (indicating remaining weight with the change in temperature)	128
Figure 4.42	Thermo-grams for specimens GB_R (2) _WC and GB_R (24) _WC (indicating heat flow out of each specimen during TGA analysis)	128
Figure 4.43	Weight changes for Lime stone dust blended Geopolymer paste specimens	129
Figure 4.44	Weight changes for Slag blended Geopolymer paste specimens	130
Figure 4.45	Change in weight after different immersion time of GP1 & GB2 specimens	132
Figure 4.46	Residual strength of Lime stone dust blended Geopolymer paste	133

Figure 4.47	Residual strength of Slag blended Geopolymer paste	134
Figure 4.48	Residual strength after different immersion times for GP1 & GB2 Specimens	135
Figure 4.49 (a)	Geopolymer paste specimen GP1, after 6 weeks in 10% Magnesium sulfate solution	136
Figure 4.49(b)	Geopolymer paste specimen GL1, after 6 weeks in 10% Magnesium sulfate solution	137
Figure 4.49 (c)	Geopolymer paste specimens GL2, after 6 weeks in 10% Magnesium sulfate solution	137
Figure 4.49(d)	SEM @ 3000x zoom and EDX of white deposit on the surface of specimen after exposure	137
Figure 4.50 (a)	Geopolymer paste specimens GP1, after 6 weeks in 10% Magnesium sulfate solution	138
Figure 4.50(b)	Geopolymer paste specimens, GB1 after 6 weeks in 10% Magnesium sulfate solution	138
Figure 4.50(c)	Geopolymer paste specimens, GB after 6 weeks in 10% Magnesium sulfate solution	139
Figure 4.50(d)	SEM @ 400x zoom and EDX of white deposit on the surface of specimen after exposure	139
Figure 4.51 (a)	Cylinder specimen of the GP1 specimen	140
Figure 4.51(b)	Crack in the GP1 specimen	140
Figure 4.52 (a)	Change in Weight after different immersion times for specimens GB_R(24) _WC and GB_R (2) _WC Specimens	141
Figure 4.52(b)	Residual strength after different immersion times of specimens GB_R (24)_WC and GB_R_(2)_WC Specimens	142
Figure 4.53 (a)	Efflorescence in specimen GB_R (2) _WC after 3 months from casting	143
Figure 4.53(b)	Efflorescence in specimen GB_R (16) _WC after 3 months from casting	143
Figure 4.53 (c)	Efflorescence in specimen GB_R (24) _WC after 3 months from casting	143
Figure 4.54 (a)	Workability set up	145
Figure 4.54(b)	Raising of cylinder	145
Figure 4.54 (c)	Specimen GPC-1	145
Figure 4.54(d)	Specimen GSC1R-N	145
Figure 4.54 (e)	Specimen GPC	145
Figure 4.54 (f)	Specimen GPC1-N	145
Figure 4.54(g)	Specimen GPC-N	145
Figure 4.54(h)	Specimen GPC-M (failed to form normal specimen)	146
Figure 4.55 (a)	Specimen GSC at different phase of Manufacturing	147

Figure 4.55(b)	Specimen GSCB1 at different phase of Manufacturing	147
Figure 4.55 (c)	Specimen GSCB2 at different phase of Manufacturing	147
Figure 4.56 (a)	SEM @ 300x zoom on surface of specimen GPC after 3 days of manufacturing	149
Figure 4.56(b)	SEM @ 1200x zoom on surfaces of specimen GPC after 30 days of manufacturing	150
Figure 4.56(c)	SEM @ 800x zoom on surfaces of specimen GPC after 60 days of manufacturing	150
Figure 4.57(a)	SEM @ 300x zoom on surface of specimen GSCB2 after 3 days of manufacturing	150
Figure 4.57(b)	SEM @ 1500x zoom on surfaces of specimen GSCB2 after 30 days of manufacturing	151
Figure 4.57(c)	SEM @ 1200x zoom outer surfaces for specimen GSCB2 after 60 days of Manufacturing	151
Figure 4.58(a)	4.58(a) SEM @ 3647x zoom of specimen GPC-1	152
Figure 4.58(b)	SEM @ 3336x zoom of specimen GPC-1	152
Figure 4.58(c)	SEM @ 3526x zoom of specimen GSC1R	153
Figure 4.59(a)	SEM @ 600x zoom of specimen GSCR	153
Figure 4.59(b)	SEM @ 800x zoom of specimen GSCR-N	153
Figure 4.59(c)	SEM @ 600x zoom of specimen GSC1-N	154
Figure 4.59(d)	SEM @ 600x zoom of specimen GSC1R-N	154
Figure 4.60(a)	EDX of specimen GPC-1	155
Figure 4.60(b)	EDX of specimen GSC1	155
Figure 4.60(c)	EDX of specimen GSC1R	156
Figure 4.61(a)	MIP curve for specimen GPC-1	157
Figure 4.61(b)	MIP curve for specimen GSC1R	158
Figure 4.62	Intruded volume of Mercury for Geopolymer specimen GPC	159
Figure 4.63	Intruded volume of Mercury for Geopolymer specimen GSC	160
Figure 4.64	Intruded volume of Mercury for Geopolymer specimen GSCB1	160
Figure 4.65	Intruded volume of Mercury for Geopolymer specimen GSCB2	161
Figure 4.66 (a)	Specimen GPC after 30 days of manufacturing	162
Figure 4.66(b)	Specimen GSCB2 after 30 days manufacturing	162
Figure 4.67(a)	Specimen GPC showing needle like structure after 1 month exposure to 10% Magnesium sulfate solution	163

Figure 4.67(b)	Specimen GPC showing white precipitant after 6 months exposure to 10% Magnesium sulfate solution	163
Figure 4.68(a)	SEM @ 16708x zoom of the white deposit on specimen GPC	164
Figure 4.68(b)	EDX of white precipitant on specimen GPC	164
Figure 4.69(a)	Specimen GSCB2 showing fresh surface after 1 month exposure to Magnesium sulfate solution	164
Figure 4.69(b)	Specimen GSCB2 showing very little precipitants on surface after 6 months exposure to Magnesium sulfate solution	165
Figure 4.70 (a)	SEM @ 4000x zoom of specimen GPC shows crystal structure	166
Figure 4.70(b)	SEM @ 8000x zoom of specimen GPC, showed micro crack	166
Figure 4.71 (a)	Percentage gain or loss in weight with time of exposure to magnesium sulfate solution	167
Figure 4.71(b)	Percentage gain or loss in strength with time of exposure to magnesium sulfate solution	167

LIST OF TABLES

Table No.	Description	Page No.
Table 3.1	XRF Elemental Analysis Report of Fly ash	32
Table 3.2	XRF Elemental Analysis Report of Silica Fume	33
Table 3.3	XRF Elemental analysis report of Lime stone dust	34
Table 3.4	XRF Elemental analysis report of Ground granulated blast furnace slag	35
Table 3.5	XRF Elemental analysis report of Murram	35
Table 3.6	XRF Elemental analysis report of Borax	36
Table 3.7	Mix composition of Alkali activator for studying effect of Temperature imposed on it before mixing	59
Table 3.8	Mix compositions for studying the effect of Dual oxide in activator on Non-blended Fly ash Geopolymer composites	60
Table 3.9	Mix compositions for Studying on Fly ash based Geopolymer blended with Lime stone dust at different Curing profile	62
Table 3.10	Mix compositions for studying on Microstructure and Mechanical performance of Fly ash based Geopolymer blended with Lime stone dust	63
Table 3.11	Mix compositions for Durability study on Fly ash based Geopolymer blended with Lime stone dust	64
Table 3.12	Mix compositions for studying on Fly ash based Geopolymer blended with slag at different Curing profile	64
Table 3.13	Mix compositions for studying on Fly ash based Geopolymer blended with Slag under different Curing profile and Alkali concentration	66
Table 3.14	Mix composition for studying on Microstructure of Slag blended Fly ash Geopolymer	67
Table 3.15	Mix composition for Durability study on Fly ash Geopolymer blended with Blast furnace slag	68
Table 3.16	Mix composition for studying Activated Fly ash blended with Slag under water curing	68
Table 3.17	Mix composition for studying the development of Fly ash Geopolymer blended with Silica fume in presence of Borax and its performance	71
Table 3.18	Mix composition for studying the development of Fly ash Geopolymer blended with Silica fume in presence of Murram and its performance	72
Table 4.1	Results of Workability test of the Geopolymer paste	78
Table 4.2	Results of Workability test of the Geopolymer paste	79

Table 4.3	EDX report of Geopolymer specimens	85
Table 4.4	Workability test result for Geopolymer blended with Lime stone dust	87
Table 4.5	Result of Workability test on Geopolymer paste with different Slag content	88
Table 4.5.1	Test result on Workability vs. Time of Fly ash based Geopolymer blended with Slag with time (mix id: GB - 6% Na_2O in activator and 15 % slag as supplementary material (ref. to Table 3.16))	89
Table 4.6	Compressive strength of Lime stone dust Blended Fly ash based Geopolymer with different curing profile (Curing temperature and duration)	92
Table 4.7	Compressive strength of Slag Blended Fly ash based Geopolymer specimens with different curing profile (Curing temperature and duration)	94
Table 4.8	Compressive strength of Fly ash Geopolymer blended with Slag for varying Alkali concentration and Curing profile	95
Table 4.9	Compressive strengths 1 and 20 days after Water curing of Alkali activated Fly ash specimens (for varying rest periods - 2 to 24 hrs.)	103
Table 4.10	XRD peak list for Water cured blended Alkali activated fly ash	124
Table 4.11	Change in Weight after different immersion time of specimens GP1 and GB2	132
Table 4.12	Residual strength after different immersion times for GP1 and GB2 Specimens	135
Table 4.13	Results of Workability test of the Geopolymer paste	144
Table 4.14	day Compressive strength of non-blended and blended specimen	146
Table 4.15	Compressive strength of Geopolymer paste specimen (Fly ash +Silica fume +Murram)	148

LIST OF ABBREVIATIONS

AAFA	Alkali Activated Fly Ash
AAS	Alkali Activated Slag
ASR	Alkali Silica Reaction
ASTM	American Society for Testing and Materials
BET	Brunauer-Emmett-Teller Surface Area
CFA	Coal Fly Ash
CGCRI	Central Glass and Ceramic Research Institute
CSH	Calcium Silicate Hydrate
DTA	Differential Thermal Analysis
EDS	Energy Dispersive Spectroscopy
EDAX/EDX	Energy Dispersive X-ray
FESEM	Field Emission Scanning Electron Microscope
GGBS	Ground Granulated blast Furnace Slag
IUPAC	International Union of Pure and Applied Chemistry
IS	Indian Standard
BIS	Bureau of Indian Standards
MAS NMR	Magic Angle Spinning
MIP	Mercury Intrusion Porosimetry
MPa	Mega Pascal
MK	Metakaoline
NIST	National Institute of Standards and Technology
***p*H**	Power of Hydrogen (Negative logarithm of Hydrogen ion)
SEI	Secondary electron imaging
SEM	Scanning Electron Microscope
SSD	Saturated Surface Dry
TG	Thermogravimetry
XRD	X-ray Diffraction
XRF	X-ray Fluorescence

SYNOPSIS

Interest on geopolymer as a new construction material has been growing fast. Industrial waste utilization is the prime reason behind this development. Understanding the presence of huge amount of wastes, priority has been given in Govt. policies of different countries including India, to utilize of these waste. It is also true that proper attention has not been received to explore the potential of waste and utilize it to produce high performance comparatively cheaper construction material. Again, the research on new alternative of conventional cement binder, with considerably lower CO_2 emission, is the need of the day for different reasons. Geopolymer from waste is one of such new materials. Basically, the geopolymers are produced from waste like fly ash, metakaolin etc. which are rich in alumina and silica. Manufacturing process involves activation of these base material in alkaline environment followed by heat curing. Different types of silicates are added to increase the performance of the product. Researchers took interest about fly ash based geopolymer and its properties like early strength, better durability etc. Several types of waste materials have been also tried by some researchers. Geopolymer produced at completely amorphous stage as an alternative construction material in place of conventional cement based composites. Several influencing parameters like composition of base material, concentration of alkali activator, level of curing temperature, curing duration etc. are need to be studied in a systematic way to develop guidelines for manufacturer. Based on research different parameters have been optimized to produce high performance geopolymer. Several elemental terminologies like silica-alumina ratio, percentage of alkali oxide, silicate modulus, water/solid ratio etc., have been brought in this kind of material development for proper scientific interpretations and developing recommendations. In most of the studies, fly ash was selected as base material. The chemical composition of base material plays a major role on performance of the final product. Most of studies concentrated on a particular base material and alkali. Study on the incorporation of supplementary materials with base material and proper understanding of the effect of synthesizing parameters in regard to the performance of the final product, are very limited. Again, research on supplements in activator has not received much attention in the past. Most of the studies made based on heat cured products and compared with conventional cement concrete. Geopolymer is a different product compared to conventional cement based products because of the property of gel formed. Therefore, it is better to compare performance of a particular geopolymer with another one to identify pathway to have ultra-high performance geopolymer.

Research indicated some noticeable drawbacks of fly ash based geopolymer like hardening characteristics, cracking with age, efflorescence, low reactivity level etc. Studies on the water cured fly ash based geopolymers, has not received proper attention in the past. Some more drawbacks may be noted here. It is observed that dissolution of sodium hydroxide in lower ambient temperature (in winter) is very low. The optimization of temperature level of activator prior mixing is essential to overcome this problem and have a considerably better geopolymer. Again, the rate of poly-

condensation is dependent on the choice of alkali combination for different base and supplementary material/additives. Slow synthesis may provide an amorphous structure but partly crystalline. The sequential development of crystallized compound within the pores affects the product performance. An investigation program may be designed to investigate the pre-mixing and post-mixing performance of different combination of activators. It may be noted here that the silicate solution consists of more than 65% of water which is mainly responsible for porous character and semi crystalline phases in geopolymer. But this reactive silica is also essential to initiate the primary poly-condensation. The scope of supplementary reactive silica (like silica fume) as an alternative of sodium silicate may be investigated. Most of the research is confined with the effect of supplements added to the base material, concerning strength and durability properties. The parametric study on blended fly ash based geopolymer considering the influence of silicate modulus, combination of oxides in activator solution, curing regime on synthesis etc. needs systematic study. Fly ash may be blended with Calcium / Silicon intensive supplementary materials like lime stone dust, blast furnace slag, silica fumes etc.

Workability and strength are the most important aspects. Breed of geopolymer is completely different from conventional cement based products and therefore new measurement procedure need to be used. It is again a big challenge to have non heat cured fly ash based geopolymer, as the polymeric reaction mostly takes place at a temperature of 60-90^{0}C. In alkali activated mixture, the accretion of alkali activator and base material brings a dissolved aqueous state which is thermodynamically effective for the geopolymeric reaction. But when ions dissolve in water, releases heat energy due to the stabilizing interaction. This energy is an accumulation of lattice energy and heat of hydration due to the dissolution of ionic solid. The water curing of activated calcium blended fly ash may incorporate secondary heat input to enhance the partial polymer formation. The concept, dealing with the typical alkali activated and water cured new blended product may be investigated. Though earlier study reveals better performance of geopolymer exposed to sulfate solution compared to conventional cement based products. However, it is observed that weight and strength decreases with more time, might be due to the ionic transaction between the geopolymer structure and exposure environment. A systematic study is required to evaluate performance of blended geopolymer with less permeable pores in severe exposure to assess long term performance.

Present study was inclined towards the long term performance of geopolymer, optimization of strength, suitable parameter for measuring workability, choice of supplementary materials, choice of combination of oxides in activator solution and combinations, choice of curing profile etc. Present research deals with the incorporation of supplementary materials to improve the performance of fly ash based geopolymer. Base material used is fly ash / fly ash blended with lime stone dust, blast furnace slag, silica fumes. The entire research work may be divided into three different aspects. Firstly, use of activator/combination of two activators, to study the performance of fly ash based non blended/ blended geopolymer. Secondly, the impact of supplementary materials on the performance

of fly ash based non blended/ blended geopolymer at fresh and hardened state. Lastly, on water cured fly ash based blended geopolymer. Performance of combination of oxides in activator solution was examined with non-blended (only fly ash) and blended base material. Optimum temperature of alkali activator prior mixing and its effect on the performance of geopolymer, was studied. Preheating of alkali activator was made to arrive at a particular temperature. Choice of alkali with respect to base material, has been evaluated. Silica fume as an alternative of silicate solution and its impact on strength and durability of the improved geopolymer, were evaluated. Incorporation of Borax and murrum as tertiary input to compensate the lack in source alumina was studied and briefed. The incorporation of supplementary materials (calcium based compound) and its positive effect on workability, strength, curing type, curing regime and durability, were investigated. New parameter like 'Area factor' for measuring workability, has been introduced. Long term strength optimization, long term exposure in cyclic freezing-thawing in sulfate exposure etc., have been introduced and new findings were presented.

The following combinations of non-blended and blended geopolymer have been studied

1. Fly ash + KOH + Na_2SiO_3
2. Fly ash + NaOH + Na_2SiO_3
3. Fly ash + NaOH + Na_2SiO_3 + supplementary material (Lime stone dust)
4. Fly ash + NaOH + Na_2SiO_3 + supplementary material (Blast furnace slag)
5. Fly ash + KOH + Na_2SiO_3 + supplementary material (Silica fume and Borax)
6. Fly ash + KOH + Na_2SiO_3 + supplementary material (Silica fume and Murram)

For all the studies, the mechanical performance of geopolymer was carried out and typical microstructural studies like SEM, XRD, MIP, FESEM, EDAX, TG/DTA etc., were made for proper scientific interpretations. This research provides new information based on systematic microstructural and mechanical studies of fly ash based non blended/ blended geopolymer. New areas of research have been explored to assess workability. Newly introduced workability parameter added new dimension in understanding the performance of fresh geopolymer. This research has provided pathway to produce high performance fly ash based non blended and blended geopolymers in different forms overcoming present drawbacks as discussed earlier.

1. INTRODUCTION

1.1 Preamble

Due to growing industrial production, the generation of wastes has been increased many folds with time and disposition is a challenging problem. On the other hand, carbon dioxide emission has increased to a great extent causing global warming. There is scarcity of ore also. Under this circumstances fruitful application of the waste materials is the need for the day. Limited use of waste materials (like slag, fly ash etc.) are made in cement manufacturing but major portion is used in road construction or for any filling purpose. This may create ground water contamination problem due to leaching of toxic and heavy metals, ultimately reaching to underground water reservoir. Joseph Davidovits introduced geopolymer as a synthetic material primarily. Later on it is observed that geopolymer may be developed from the waste materials containing silica and alumina, in an alkaline environment. Waste materials such as fly ash, metakaolin, slag, silica fumes etc. are considered as the prime base material to make waste based polymer. Geopolymer is imported from the geo-synthesis of polymeric aluminosilicate and alkali silicates which results a tetrahedral structure of SiO_4 and AlO_4 [72]. Geopolymer is stated to retain better strength and durability [73] and geopolymer may be substitute of cement [6].

1.2 Geopolymerization

1.2.1 Base Material and Activator

Geopolymerization is a geo-synthesis which includes naturally arising silico-aluminates [56]. Any type of pozzolanic compound has the possibility to act as geopolymer precursor species in alkali solution and contributes in geopolymerization [137]. In geopolymerization process the geopolymer is usually amalgamated through the triggering of an aluminosilicate waste sources like fly ash, slag etc.in presence of activator (generally, an alkali hydroxide or a combination of alkali hydroxide and silicate). These source materials are distinguished as the base material. Usually, highly soluble silicate concentrations are often used as an activating solution to produce geopolymers in a way to achieve better setting and mechanical properties [132]. The rate of geopolymerization and the leaching of alkali may be influenced by the cation anion pair theory. It may be identified by this fact that despite having the same electric charges, the Na^+ and K^+ affect differently only because of dissimilar size. In this connection, the smaller sized cations emphasize the ion-pair reactivity in presence of small sized silicate oligomers like monomers, dimers and trimmers [55, 91 and 121]. Earlier research shows that the smaller silicate oligomer like monomer, dimer which subsist during the dissolution of Al-Si

minerals are better stabilized by Na^+ (Sodium ion) having smaller size, resulting in higher extent of dissolution. On the contrary, larger silicate oligomers increase considerably with the addition of more silicate solution which is better coordinated by K^+ cation (larger size) and extended to a higher level of geopolymerization [137]. Literally geopolymer file contains an amorphous aluminosilicate complex, where the alkali-cations balance the charges of tetrahedral aluminium [20]. Contrivance of geopolymers comprises the poly-condensation of geopolymeric precursors, which produces Si–O–Al link ultimately [28, 54, 99, and 128]. In fact the basic formula of a polymer is expressed as $Py[-(Si-O_2)x-Al-O]y. wH_2O$ where P, x and y represent the alkaline element, numeric value (1,2,3 etc.) and the degree of poly-condensation respectively [54].

The process of geopolymerization is based on several factors, comprising the contents of the raw materials, curing regime, water quantity, alkali percentage etc. [68]. Outcome of geopolymerization i.e. Geopolymer is an alkali aluminosilicate material with superior chemical, mechanical characteristics paralleled to conventional cement based products and does not contribute significant CO_2 [34].

1.2.2 Curing Profile

The exact chemistry and formation methodology of geopolymer are not yet fully known. Previous study recommended that the mechanism of geopolymer is comprised of the dissolution, orientation and poly-condensation [70]. Curing at high temperature may emphasize polymer development in higher alkali concentration. In fact, the higher curing temperature increases the rate of polymerization indeed. The influence of heat curing to the evolution of geopolymeric-structure was investigated and established to some extent [109]. Beside the composition of mixture, the curing temperature has an important impact on different aspects of heat cured geopolymer prepared from fly ash [131]. Again duration of heat curing also has significant contribution on the amalgamation of the mix and subsequent drying shrinkage [33] [21]. Different types of curing mode have been reported in literatures for different combination of base materials and activators. Since, stimulation energy is greater for fly ash in compare to slag, the high temperature curing is much essential for the first event [41], [42], [105]. Study on alkali-activated slag (GGBS) confirmed that curing at high temperature tends to lower strength for alkali hydroxide plus water glass as an activator medium [41]. However, the result is reversed in absence of water glass. Other authors [12] noticed that prolonged exposure of alkali-activated slag in higher curing temperature gradually lowers the strength with time though initially it tends to the strength-gaining. Again it has been observed

that the solubility of slag is increased with curing temperature [46]. But, other authors consider that the drop in strength is resulted from the development of new hydrated product which creates barrier around the slag grains and makes obstacle towards further hydration [117]. According to some studies [118], the generation of unreacted material is emphasized with raised curing temperature. Some researchers [84] observed the successive drop in compressive strength with prolonged heat curing. Sanjayan et. al. [23, 24] investigated on slag activated with water glass (powder) under heat curing. Some authors [102] also spotted to the requirement of the separation of the toughened samples in a manner to resist evaporation of water. Higher strength in compare to non-isolated water and air curing was observed for the same with isolation. Criado [25] studied on the activation of fly ash under alkali and proposed the separation of the samples to prevent carbonation process which leads to lower pH and mechanical strength. Few studies [77] defined specific curing temperature for optimum strength gaining for the mixture of metakaolin and fly ash with activation. Though, prolonged exposure in heat curing deteriorates the structure due to excessive shrinkage. Brough et. al. [15] studied on the activated GGBS (slag) and found curing profile of 80^0C for 12 hours, as best fitted for achieving maximum strength. Significant rise (7 MPa to 72 MPa) in strength was detected along with the increment of curing temperature after 20^0C onward. Wang et al. [135] similarly studied on slag with activation and correlated the types of activator profiles with that of curing profiles. Bakha [11] highlighted on thermal activated barrier for AAFA which need to be overcome to initiate the reaction. This statement was further established by other research [83], which depicts a remarkable increment in strength along the raised curing heat. Change in curing temperature from the range of (45^0C-65^0C) to (65^0C-85^0C) enhances the rate of strength gaining to a remarkable extent [4].

However, there have been very few studies [145] found in the literature regarding water curing and ambient curing of fly ash based geopolymer. In fact, best choice of curing style and profile highly subjected to the combination of base material, alkali activator and their inherent chemistry of reactiveness.

1.3 Geopolymer and Zeolite

The term Geopolymer and Zeolite are referred to an X-ray amorphous structure and fine crystalline structure respectively [103]. The activation process of the material comprising of silica and alumina, follows four consecutive steps: firstly, the surface disbanding of Al, Si within alkaline medium; secondly, the dispersion of the disbanded species through the solution; thirdly, the poly-condensation of the Al and Si with the added silicate solution and

formation of gel; fourthly, the strengthening of gel phases towards final polymeric outcome [35]. Now, zeolites are generally synthesized from a gel comprising of an insoluble solid phase and confined liquid phase which in fact maintains a balanced distribution of silicate and aluminosilicate anions, the supply of which is controlled by the dissolution of the solid phase [55]. The degree of crystallization is greatly influenced by the condition of synthesis of geopolymer [76]. In most of the existing literature the presence of nano-crystalline particles (zeolite structure) within the body of geo-polymeric structure was found [5], [76] and [107]. The chances of formation of amorphous and crystalline structure depend on several factors like curing profile, curing type, rest period (time lag between mixing and curing), alkaline activator concentration, composition of base material (fly ash, slag, silica fume etc.), water to base material ratio, environmental coverage and others [3, 5, 27, 75, 76, 89, 96, 133]. In AAFA (alkali activated fly ash) system, hydroxide activator emphasizes the production of more crystals in compare to silicate activators (like sodium silicate). Again, the zeolite phase formation is enhanced by the presence of sodium ion rather than potassium ion [75, 76 and 96]. Synthesis of zeolite-phase is also influenced by the existence of high volume of water within the mixture [27]. Earlier study suggested that the mild curing temperature is appropriate for the formation of zeolite-phase [3]. Sometimes the vitreous component of fly ash is rapidly dissolved in alkali activator without forming well-crystallized structure because of the limited time and space [33], [80], [126]. Again zeolite phase may be crystallized from the dilute aqueous solution if the precursor species have sufficient time and space to achieve proper coordination which forms crystal structure [33]. Na–Al–Si part(s) (Purely amorphous) which is an initial product of polymerization, progressively biased to semi-crystalline part(s) through lengthy curing exposure [103]. Some studies [35] were carried out over alkali activated multiphasic product. Presence of higher calcium content in slag allows the existence of C-S-H precipitation parallel to aluminosilicate network which starts decomposing under alkaline medium. In fact, in this process Ca^{2+} moves within the solution and precipitates as calcium hydroxide which forms calcium silicate hydrated phases with time being [35]. Even in the presence of calcium compound under the high alkali concentration metakaolin yields to amorphous aluminosilicate [110, 111]. This discussion concludes that the possibility of the development of C-S-H inside the polymeric structure is increased at mild pH medium [18]. Already, the concept of geopolymer with the accumulation of nano-crystalline zeolitic phases and aluminosilicate gel has broadly studied at a chemical thermodynamic and mechanistic viewpoint [76].

1.4 Supplements with Base Materials

Some studies have been done on fly ash based geopolymer. Fly ash contains large amount of silica and alumina. It is understood that geopolymerization process mainly includes alkaline activation of base material by alkali activator (alkali hydroxide/silicate solution) followed by heat curing [131]. The geopolymer chemistry explains the development of 3D polymeric chain by Si-O-Al-O bond with alkali activation of the base material rich in silica-alumina [32]. Though the geopolymer material shows notable performance [13] in compare to conventional cement concrete but the performance of geopolymer changes with the combination of base materials and alkalis [90]. It is really important to search new type of geopolymer to achieve better properties associated with it. An idea of blended geopolymer may be tried to improve the microstructural and mechanical properties. Previous study [67] explored that incorporation of calcium supplements may improve hardened characteristics of fly ash based geopolymer under ambient heat curing. Calcium compound in geopolymer improves microstructural morphology and strengthens the geopolymer by enhancing amorphous framework through polymerization [48, 129, 130 and 134]. Some literatures [16] suggested that GGBS generates calcium containing composites like silicates, aluminate hydrates and silico-aluminates associated with calcium which affects consistency at green level indeed [129]. Gaining of higher early strength was observed for geopolymer prepared from calcined material while non-calcined materials provides notable strength with time [48]. Jaarsveld et al. [130] described a typical context where better strength was found for the geopolymer comprising kaolin. Though the literature in this connection is limited but quite enough to realize the influence of calcium on strength and durability of fly ash based geopolymer. Presence of water in higher extent is the prime drawback of developing better geopolymer composite. In fact, the sodium silicate solution is the prime source of water which itself contains a huge amount of water. Sequentially additional water makes the structure more porous and sometime permeable to some extent. To eliminate this problem and initiate faster reaction, a suitable compensator of sodium silicate like micro silica or silica fume may be introduced as the primary source of reactive silica. Use of new supplements comprising reactive silica, alumina or calcium in fly ash based geopolymer, is required. New research should be executed on blended geopolymer. Blending of two or more base materials may be tried. An idea of blending of base materials to produce better fresh/hardened geopolymer in micro and macro level. Again, parametric studies of blended geopolymer should be revisited.

1.5 Use of Activators in Geopolymer

Selection of activator is highly dependent on several parameters like types/chemical composition of base material, supplementary materials, silicate content etc. Major drawbacks of geopolymer is correlated with the wrong choice of activator. The rheological characteristics of geopolymer is interfered mainly by the viscosity of alkali activator [100]. Choice of activator is again important in this context. Like fly ash in activation with highly concentrated sodium hydroxide plus silicate solvent, generates cracks with aging in some cases [30]. This is mainly because of the development of pore pressure within the hardened composite by the late precipitated alkali compound [30]. Though at the infancy level of development, it exhibits sequential rising in strength [30]. Use of alternative hydroxide to bring the stable structure is a subject of interest in this connection. The size of cations has great impact on the ion-pair reaction which in fact determine the differential performance of alkali in activation of a particular base material under defined ambience [55], [91], [121]. Again, the concentration of silicate solution has major impact on the choice of alkali hydroxide for better dissolution and stabilization of geopolymer [137]. As already discussed that the higher presence of monomer and dimer which exist during dissolution of Al-Si, supports sodium hydroxide for better stabilization [137]. Whereas, potassium hydroxide is favored as alkali activator for larger silicate oligomers in the sense of better co-ordination of geopolymer framework [137]. So, the choice of alkali hydroxide is subjected to the concentration of reactive silica (available from silicate solution, base material and supplementary materials) in the mixture. Again, the role of alkali cation is to balance the charges of aluminium indeed. Hence, the presence of supplementary cation like calcium (available from calcium supplement) minimize the requirement of alkali cation in activator or claims lower concentration of alkali hydroxide. Therefore, choice of alkali for different mixture, is extremely important to have best performance of the activated product.

1.6 Drawbacks in Alkali activated Fly ash based Geopolymer

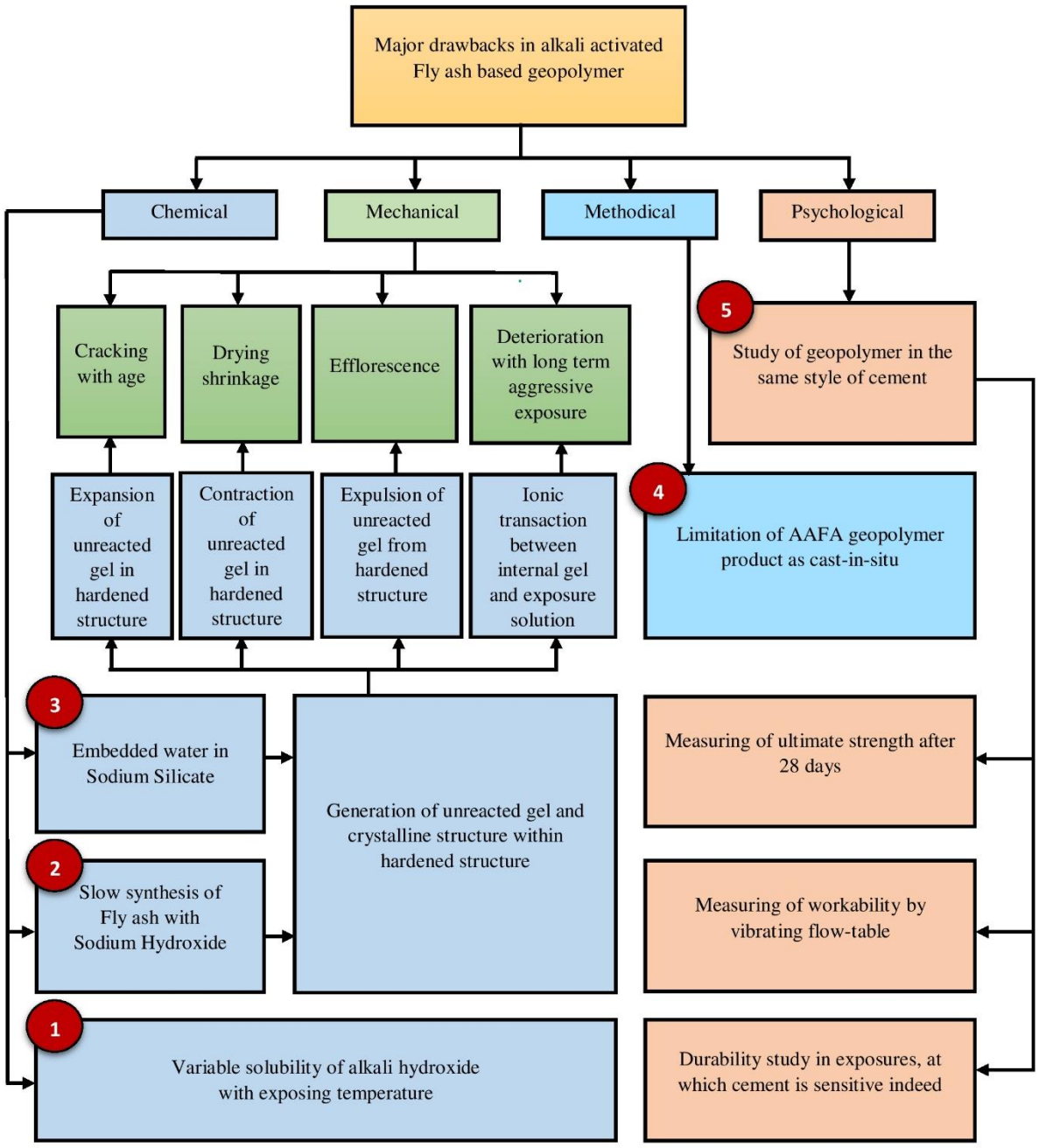

Figure 1.1 Schematic Diagram of Drawbacks in Fly ash Geopolymer

The major drawbacks associated with alkali activated fly ash based geopolymer is depicted schematically in Figure 1.1. The major drawbacks have been categorized by four types like chemical, mechanical, methodical and psychological drawbacks. All above mentioned drawbacks were taken care while framing scope of work as discussed below.

1.7 Scope of work

Research indicated some noticeable drawbacks of fly ash based geopolymer like hardening characteristics, cracking with age, efflorescence, low reactivity level etc. Studies on the water cured fly ash based geopolymers, has not received proper attention in the past. Some more drawbacks may be noted here. It is observed that dissolution of sodium hydroxide in lower ambient temperature (in winter) is very low. The optimization of temperature level of activator prior mixing is essential to overcome this problem and have a considerably better geopolymer. Again, the rate of poly-condensation is dependent on the choice of oxide/combination of oxides in activator solution for different base and supplementary material/additives. Slow synthesis may provide an amorphous structure but partly crystalline. The sequential development of crystallized compound within the pores affects the product performance. An investigation program may be designed to investigate the pre-mixing and post-mixing performance of different combination of activators. It may be noted here that the silicate solution consists of more than 65% of water which is mainly responsible for porous character and semi crystalline phases in geopolymer. But this reactive silica is also essential to initiate the primary poly-condensation. The scope of supplementary reactive silica (like silica fume) as an alternative of sodium silicate may be investigated. Most of the research is confined with the effect of supplements added to the base material, concerning strength and durability properties. The parametric study on blended fly ash based geopolymer considering the influence of silicate modulus, oxide/combination of oxides in activator solution, curing regime on synthesis etc. needs systematic study. Fly ash may be blended with Calcium / Silicon intensive supplementary materials like lime stone dust, blast furnace slag, silica fumes etc.

Workability and strength are the most important aspects. Breed of geopolymer is completely different from conventional cement based products and therefore new measurement procedure need to be used. It is again a big challenge to have non heat cured fly ash based geopolymer, as the polymeric reaction mostly takes place at a temperature of 60-90^{0}C. In alkali activated mixture, the accretion of alkali activator and base material brings a dissolved aqueous state which is thermodynamically effective for the geopolymeric reaction. But when ions dissolve in water, releases heat energy due to the stabilizing interaction. This energy is an accumulation of lattice energy and heat of hydration due to the dissolution of ionic solid. The water curing of activated calcium blended fly ash may incorporate secondary heat input to enhance the partial polymer formation. The concept, dealing with the typical alkali activated and water cured new blended product may be investigated. Though earlier study

reveals better performance of geopolymer exposed to sulfate solution compared to conventional cement based products. However, it is observed that weight and strength decreases with more time, might be due to the ionic transaction between the geopolymer structure and exposure environment. A systematic study is required to evaluate performance of blended geopolymer with less permeable pores in severe exposure to assess long term performance.

Present study was inclined towards the long term performance of geopolymer, optimization of strength, suitable parameter for measuring workability, choice of supplementary materials, choice of oxide/combination of oxides in activator solution, choice of curing profile etc. Present research deals with the incorporation of supplementary materials to improve the performance of fly ash based geopolymer Base material used is fly ash / fly ash blended with lime stone dust, blast furnace slag, silica fumes. The entire research work may be divided into three different aspects. Firstly, use of oxide/combination of oxides in activator solution, to study the performance of fly ash based non blended/ blended geopolymer. Secondly, the impact of supplementary materials on the performance of fly ash based non blended/ blended geopolymer at fresh and hardened state. Lastly, on water cured fly ash based blended geopolymer. Performance of potassium hydroxide, sodium hydroxide or combination of oxides in activator solution, was examined with non-blended (only fly ash) and blended base material. Optimum temperature of alkali activator prior mixing and its effect on the performance of geopolymer, was studied. Preheating of alkali activator was made to arrive at a particular temperature. Choice of alkali with respect to base material, has been evaluated. Silica fume as an alternative of silicate solution and its impact on strength and durability of the improved geopolymer, were evaluated. Incorporation of Borax and Murram as tertiary input to compensate the lack in source alumina was studied and briefed. The incorporation of supplementary materials (calcium based compound) and its positive effect on workability, strength, curing type, curing regime and durability, were investigated. New parameter like 'Area factor' for measuring workability, has been introduced. Long term strength optimization, long term exposure in cyclic freezing-thawing in sulfate exposure etc., have been introduced and new findings were presented.

The following combinations of non-blended and blended geopolymer have been studied

1. Fly ash + KOH + Na_2SiO_3
2. Fly ash + NaOH + Na_2SiO_3
3. Fly ash + NaOH + Na_2SiO_3 + supplementary material (Lime stone dust)
4. Fly ash + NaOH + Na_2SiO_3 + supplementary material (Blast furnace slag)
5. Fly ash + KOH + Na_2SiO_3 + supplementary material (Silica fume and Borax)
6. Fly ash + KOH + Na_2SiO_3 + supplementary material (Silica fume and Murram)

For all the studies, the mechanical performance of geopolymer was carried out and typical microstructural studies like SEM, XRD, MIP, FESEM, EDAX, TG/DTA etc., were made for proper scientific interpretations. This research provides new information based on systematic microstructural and mechanical studies of fly ash based non blended/ blended geopolymer. New areas of research have been explored to assess workability. Newly introduced workability parameter added new dimension in understanding the performance of fresh geopolymer. This research has provided pathway to produce high performance fly ash based non blended and blended geopolymers in different forms overcoming present drawbacks as discussed earlier.

1.8 Organization of the Thesis

Synopsis

Brief introduction of the research area and its importance. Described scope of present research work.

Chapter 1: Introduction

Introduction of the research area and its importance in an elaborate way. Described scope of the present research work in detail.

Chapter 2: Review of existing literature

Critical review of the existing literature close to the aims and objective of the present research work and described scope of the present research work in detail.

Chapter 3: Experimental investigations

Detail of extensive experimental investigations made on Fly ash based geopolymer.

The typical series of specimens, manufacturing methodology, mixing proportion, phases of investigation and testing procedure (including new methods proposed), have been included properly in this chapter.

Chapter 4: Results and discussion

Presented systematically the test results of experimental investigations on non-blended and blended geopolymer including physical, mechanical, microstructural, mineralogical and durability studies. Studies on synthesizing parameters like alkali concentration and combination of oxides in activator solution, curing temperature and duration, rest period etc., were also made.

Chapter 5: Conclusions and suggestions for future research.

Specific conclusions are made and indicated future research areas.

Appendix

Presented typical calculation for obtaining ingredients to produce fly ash based non blended and blended geopolymer and reprints of some published papers.

2. REVIEW OF EXISTING LITERATURE

2.1 Preamble

Past literature were reviewed with the aim to collect specific information on the research area to identify the drawbacks of fly ash based geopolymer as indicated in the earlier chapters and also to develop a pathway to resolve drawbacks to have a high performance fly ash based geopolymer. Testing methods are also reviewed to understand their shortcomings and to develop a better one to appreciate the performance of the product in a more scientific way. Literature in this regard is very limited. Literature on the experience of using supplementary materials were collected. Most of the available literatures on geopolymer with supplements dealt with mostly strength. But literature on the synthesizing parameters like optimization of curing temperature, curing duration, alkali concentration, possibility of water curing etc. is limited. Comparative analysis in view of pore morphology, microstructure and durability study on blended geopolymer is very limited. Review aimed at to stretch the research from single phase composites to multiphase primarily, by blending supplementary materials with fly ash to develop new geopolymer and its parametric trend. Lot of works have been done on geopolymer from MK-Fly ash-based geopolymers and MK-rock-forming minerals [4], [5], [53], [129], [137]. It is well known that strength and durability of geopolymeric binders is better compared to conventional cement binders in general [71], [125]. The polymeric reaction product and their proportion should be monitored to satisfy some important properties e.g. durability, porosity, strength and stability which are expected from a high performance binder. A concept of blended geopolymer for the betterment in connection with improved structural performance may be drawn in a manner to compensate the major drawbacks of fly ash based geopolymer. In this chapter a review on previous studies mainly related to blended geopolymer and their properties have been done. Again, considering the structural stability as the prime concern, the review has been also focused towards the study related to the basic chemistry of activators, reactivity of precursors with the variation of base materials, methodology concerning curing types and profile, phase generation or transformation or deterioration of activated product with time in ambient and aggressive exposure. The entire review is divided into four sections (i) Instability of Geopolymer with Aging (ii) Reactivity of precursors with variation of Base material and Alkali (iii) Parametric study on the performance of Non-Blended Geopolymer (iv) Parametric study on the performance of Blended Geopolymer.

2.2 Instability of Geopolymer with Aging

Carsten Kuenzel. et.al. (2012) [146] focused on the instability of geopolymer over time. Drying shrinkage is observed at normal environment with low moisture for geopolymer pastes prepared from metakaolin. This research tried to correlate the impact of mixing composition like water content, silica alumina ratio, sodium to aluminium ratio, sodium ions and potassium ions on drying shrinkage at normal temperature. The study suggested the reduction of gel contraction and successive drying shrinkage with the possible reduction in structural water content. The study reveals the consequence of the whole quantity of cations, density of ionic charge, the relative measures and permanencies of cation, presence of aluminate combines in the mixing on shrinkage with aging. It is quite enough to understand that the existence of excessive water in the polymeric product which ascends by means of improper control on mixing parameters, choice of alkali and lack of chemical understanding, may bring the instability of geopolymer with time.

2.3 Reactivity of precursors with variation of Base material and Alkali

Van Jaarsveld. et.al. (2002) [131] examined that the fundamental research on geopolymerization process is under demand, due to extreme exposure of the marketable application. In fact, differential reactiveness of base material affects the final characteristics of the material indeed. Apropos the same it matters a lot on the typical level of synthesis. These pragmatic deviations in measureable characteristics take place owing to the inadequate suspension of those waste solids. Several parameter including water to solid ratio, percentage ash of kaolinite, category of silicate involved, keep considerable influence on the ultimate characteristics of the product. The specific work exhibits that two important elements basically control the performance of the developed geopolymer. One is the thermal account of the base material and the second one is the curing profile. Again the investigation suggests to consider these major elements before scheming this product for particular tender. Also an inter-relationship exists amid the numerous parameters which influence developed structure and characteristics of geopolymers. The clay content lies a great impact on the hardened characteristics. The clay gets abided into the formation but some portion of the clay may not react in the same manner which creates inconvenience like water retaining nature. Heat curing at higher magnitude and intensity may bring in humid environment exhibits cracking. Whereas, the same under moderate intensity of heat curing appears with better compound. Present research has revealed that cautious attention on the mixing procedure, heat curing

profile, environmental moisture content is required for manufacturing geopolymer composite to meet categorical needs.

J G S Jaarsveld. et.al. (2003) [78] proposed in this research work that not every waste material is dissolved in alkali solution. Because of that the author mentioned that original structure of some waste particles remain intact and contribute to either quicken or toughen those developed frameworks. In this research, distinctive parameters like dissolution behavior, reactivity, mechanical performances of fly ash based geopolymer has been analyzed through XRD and FTIR techniques. Author recognized the degree of crystalinity of the geopolymer is the prime influencing parameter for strength perspective. Again, the presence of calcium in fly ash and its role towards strength development has been found out. The extent of particle, calcium contamination, metals in alkaline medium and base material category directly influence initial synthesis and the final product.

M N Qureshi. et.al. (2013) [94] first time introduced blast furnace slag as a base material activated by potassium hydroxide and sodium silicate. The author used the term flow diameter in a manner to evaluate workability and setting times were maintained. The typical parameters like liquid to solid ratio, alkaline medium, amount of silicate solvent, base material to activating solution, and silicate solvent to metal hydroxide. Again, the typical characteristic like consistency, setting behaviour were broadly investigated. Research outcome shows, consistency and setting behaviour of activated GGBS depend mainly on the feature of the activating solvent indeed. In this research, the verification of the potentiality of blast furnace slag as source material was exercised.

H Djwantoro. et.al. (2006) [49] reported several vital research not only on the progress, behaviour, production, but also on the uses of Low-C Fly Ash Geopolymer. Above all, the cement is deliberated to be the most significant part in the conventional concrete. Understanding the issue of greenhouse gases and its negative impacts like its high energy and natural resources consumption, a new alternative infrastructure development constituent was targeted. Author again concentrated on the generation of vast quantity of fly ash which may be beneficially used in this purpose throughout the world; very few fly ashes are efficiently recycled indeed. Basically this fly ash can be assumed as the prime constituent of the new vista.

Xiaolu Guo. et.al. (2010) [136] organized geopolymers from fly ash (CFA) comprising calcium more than 25% in presence sodium hydroxide and sodium silicate solution as activator. Maximum compressive strength was obtained for molar ratio of 1.5 and Na_2O 10 wt. % of CFA. The compressive strength reached up to 63.4 MPa. Those samples were cured at 75^0C for 8 hours followed a regime of 23^0C for 28 days. At 1036 and 1400 cm^{-1} the main peak was attributed associated with asymmetric stretching of Al–O/Si–O bonds in FTIR spectroscopy. Again Si–O–Si/Si–O–Al bending band was observed at 747 cm^{-1}. The polymeric structure was associated with (C–S–H) gel mutually (predicted from SEM and EDAX) due to the existence of higher calcium.

Xu H. et.al. (2000) [137] anticipated that the chemical composition of geopolymer is almost same like zeolites. But these particles possess a complete amorphous characteristic. As per author mutual polymerization of the species of alumina and silicate was formed by this process. This product was actually originated by dissolving source material comprising of silicon and aluminium high value of pH. It only occurred with the presence of alkali silicate solvent. The research includes the investigation on geopolymerization from fifteen natural Al-Si minerals in a way to govern the consequence of mineral characteristics on the strength of developed geopolymer. Again the research output defines maximum dissolution of alkali solution for framework silicates in compare to chain, sheet and ring structures. The author suggests KOH instead of NaOH in maximum cases out of the fifteen minerals. The research appropriately correlates the ion pair mechanism with the mineral dissolution as well as the geopolymerization. The research on the other hand, exhibited the several source of materials which can be potentially used in the purpose of geo-synthesis.

Catherine A. Rees. et.al. (2008) [20] mainly focused on the growth of the seeding of geopolymer mixture with higher superficial extent of alumina particles. Conspicuous variation in kinetics of reaction along with the developed structure was observed. At the early stages, the development of face isolated gels due to the seed surface nucleation was happen. These phenomena exclude the initiation time before the establishment of polymeric gel, generally spotted through the activation of hydroxide. Despite the development of few sections with very higher silica gel inside the arrangement, the characteristics of leading polymeric gel part remain almost unaltered. Lengthy heat exposure exhibits the development of zeolite part generated from both of the seeded and unseeded medium.

Hua Xu. et.al. (2003) [51] studied on the consequence of metallic cations organized in alkali-feldspars on the development of water phase in geopolymers through typical experiments like Si MAS NMR EDAX, SEM practices. Again the author introduces tests like ICP, PAS-FT-IR etc.in the same connection. The suspension of alkali-feldspars was originated to be repressed in a concentrated alkaline solution. As per DSC results it was investigated that the presence of potassium in the water phase, may be resulted from potassium hydroxide solvent or sometime from dissolved K-feldspar. The Si-MAS-NMR analysis was done to find out polymerizing movement among silicate and aluminosilicate species driven in the occurrence of potassium certainly. Author investigated through microstructure study like SEM and EDAX. The study confirmed highest synthesizing and strengthening of polymer from the alkali-feldsper-kaolinit (AFK) grounds with sodium to potassium choices for the value of 3.5 up to 85.6. The research correspondingly expressed that greater dissolving affinity with the engrossment of potassium may give rise to the strength of the product amalgamated as of activation of the AFK matrices.

B A Latella. et.al. (2008) [10] responsible the total porosity as a limiting parameter to control the structure in connection with physical and microstructural properties. In this research four typical types of geopolymer having equal composition (like ratio of sodium and aluminium, ratio of silicon and aluminium as 1 and 2 respectively) were monitored in respect to mechanical performance considering typical combination of precursor. The combinations were like sodium aluminate, colloidal solvent of SiO_2, Ludox; sodium hydroxide, fumed silica, MK; Ludox, sodium hydroxide, metakaolin; commercial sodium silicate, metakaolin. The same trend was followed for fracture toughness and modulus of elasticity. The author differentiated the change in mechanical properties like toughness and modulus of elasticity for paste and mortar sample.

J L Provis. et.al. (2005) [76] found a major constituent of the geopolymer binder phase is consisted of nanometer-sized crystalline structures. This structure was closed to the nuclei around which zeolites crystallize. The remaining aluminosilicate material accumulated these nano-crystallites abide with the amorphous. Existence of the unreacted particles were observed within the developed matrix by chemical or physical means. By the degree of crystalline ordering, the physicochemical properties of the developed geopolymer was significantly influenced. These was subjected to the primary mix formulation and reaction conditions in this work. The research found that using of more alkali silicate emphasize the crystalline structure more in the polymer product in compare to that, activated with alkali

hydroxide only. In fact, the rapid nucleation of species in presence of soluble silicates was the basic cause behind. In the evaluation of geopolymerization, calorimetric data were possibly of great significance. But some contradictory outcomes were also found there in this work. Again the conflict was suitable resolved by collaborating data in connection with mechanical analysis, phase identification of the matrix. Author pointed out the proper identification was possibly the best way to correlate the chemical composition of the source material and the reacted product. To conclude that higher knowledge of chemistry might be applied again for the better understanding of geopolymer, to elevate the performance of the product.

N Murayama. et.al. (2002) [96] focused on the synthesis of zeolite from coal fly ash. In this study, the author investigated on the hydrothermal reaction in presence of various alkali. In this typical process, an autoclave of volume (800 cc) with 393.0 K and 100 gm. /400cc of solid–liquid ratio were maintained for zeolite synthesis. During the hydrothermal reaction, the alterations of physical, chemical and other properties, like crystal structure, surface structure, cation interchange capacity and dissolved amount of Si_4^+ and Al_3^+ in alkali solution were examined. The author considered the process of mechanism of zeolite crystallization and the role of alkali solution on the synthesis reaction in this research. From coal fly ash, Zeolite P and chabazite were mainly taken as the category of crystal in zeolite for the fulfillment of the purpose of synthesis. Three steps were there in alkali hydrothermal reaction of zeolite synthesis: firstly, the dissolution step of Si_4^+ and Al_3^+ from source, secondly, the condensation in alkali solution to made aluminosilicate gel, and finally, the crystallization of aluminosilicate gel to form zeolite crystal. In the dissolution step of Si_4^+ and $Al_3^+$of coal fly ash, the OH^- in alkali solution had a remarkable involvement. On the other hand, it was also pointed out that Na^+ in alkali solution influenced the crystallization step of zeolite P which had a tenacity of capturing potassium ion specifically.

C Chotetanorm. et.al. (2013) [17] made a clear investigation on the resistance to sulfate attack, sorptivity, compressive strength, and pore size of high-calcium bottom ash geopolymer mortars and so on. In this analysis, author used ground lignite bottom ashes (BAs) having average particle sizes of 16, 25, and 32 μm. NaOH and sodium silicate was used as activator. Temperature curing was executed for the process of geopolymerization. Research outcome revealed higher strength value (40.0–54.5 MPa) for the geopolymer mortars prepared from high-calcium bottom ash. The strength and durability were modified by the use of fine BA to prepare geopolymer which attributes better performances. The

workability of mixes was improved by the incorporation of water but its affect the porosity a lot.

J Temuujin. et.al. (2009) [68] introduced the power driven or mechanical activation of ash and its impact on the features of the geopolymers developed at ambient heat exposure. Essentially this process influenced by grain size and morphological stand point. The author indicates towards the fact that the harden property of polymeric compound were reduced along with the introduction of free water in the reaction mix. For raw and routinely activated samples, strength under room temperature curing was found 16 (2) MPa and 45 (8) MPa, respectively. This procedure was performed in a typical methodology where milling agent to powder ratio was controlled as 10:1. This activation was proved efficient to improve the size and shape of the grains in connection with better reactive potentiality without allowing major alteration in mineral arrangement. Around 80% increment was observed for the fly ash activated by this technology rather than ordinary one. The key role to increase the strength of polymeric product was endorsed through this methodology by minimizing the grain size and modifying the morphological extent. There by this methodology directly emphasize the higher rate of suspension or reactivity by tuning the size of grains or particles through mechanical process of activation.

2.4 Parametric study on the performance of Non-Blended Geopolymer

Khale D. et.al. (2007) [33] addressed geopolymerization as a broad scope of research for utilizing solid waste products. Khale D. et.al briefly elaborated various factors which influence the mechanism of geopolymerization and development of geopolymer. The impact of various parameters like starting materials, alkali activators, super-plasticizers, curing temperature, curing time, Silicate-Hydroxide ratio, alkali concentration, Silicate-Aluminium ratio, liquid-solid ratio have been briefly described. Again the author has focused on few important terms in connection with geopolymerization like calcination, relative humidity. Immobilization of toxic metal by geopolymer along with micro-structural characterization are worked out in this research. The author depicted geopolymerization as embryonic tool for the operation of several waste disposal.

Pre De Silva. et.al. (2008) [104] explored on the progress of typical phases and its growth at micro level in set of geopolymers. He also enquired into several parameters such as silicon oxide, aluminate, sodium oxide and water at alkali response of metakaolin. Here, the author investigated on the possessions and impacts of cure duration on strength and others physical properties. The distinguishing molar ratios of the typical mix of geopolymers were governed

as silicon-aluminium ratio and aluminium-sodium ratio separately. The makings were tested from time to time by XRD, SEM practices. With the prolonged curing exposure (40^0C for 28 weeks), amorphous Na–Al–Si parts (generated at initial age), was converted to semi-crystalline parts. The primary silicon oxide, aluminate, sodium oxide substances in mixes were seemed as the important criteria of prevailing the phase transformation. It was also noticed in few mixtures that well-amplified zeolite parts include chabazite, faujasite, zeolite A & P. Compressive strength development undertook several deviations resulting of corresponding phase changes with elongated curing. Essentially, after prolonged curing, crystalline phases which were developed by mixture development provide low strengths.

P Rovnaník (2010) [109] observed the metakaolin-based geopolymer properties which are not directly resulted by the use of primary source material metakaolin and its constituent. It is also subjected to specific surface area, configuration and comparative extent of activator. It is also hinged upon the primary level of circumstances. The author also explained the upshot of the curing intensity and duration (varied from 10 to 80^0C) on the typical physical performance and its correlation in micro level. It is resulted though the handling mix at raised heat curing which speeds up the strengths improvement. It was examined that mechanical performance were declined after 28 days of heat exposure. Whereas, mixes which was preserved at moderate or room temperature performed well enough. Impact of raising in curing temperature on geopolymer was tested in micro structurally including MIP. An inclination towards higher value of pore size and volume was observed parallel to the increment of curing intensity, which was again confirmed through mechanical enactment.

N V Chanh (2008) [21] observed that geopolymer is an aluminosilicate amorphous solid which may be amalgamated from the poly-condensation response of geopolymeric predecessor and polysilicates induced from silicate solution. The resources, mix complex, micro level induction and factors influencing characteristics of geopolymer were represented. Investigation on the applicability of fly ash as the primary home of silicon and aluminium was considered. Best result was obtained at a curing temperature range of 60^0C to 90^0C .The strength value at this level was found appreciable. Also, higher strength of the product was emphasized through the longer curing duration one to four days. Nonetheless, the rise in strength after 2 days was not noteworthy indeed. Through the rise of additional water in the combination, slump value of the fresh geopolymer was observed to be increased. The strength value of heat-cured geopolymer is not highly dependent on age (study on strength

was confined for a short period). Even composite exhibits good resistance in acidic and saline exposure.

R N Thakur. et.al. (2009) [106] experimented on the growth of macro and microstructure of geopolymer with or without introducing sand. It was organized by thermal activation of fly ash in alkaline medium. Author again studied on the chief amalgamation factors like (Na_2O/Al_2O_3), (SiO_2/Al_2O_3), water to ash ratio, percentage of sand, heat curing profile and its impact on the change of the typical characteristics at micro and macro level. The compressive strength was optimized at a curing regime of 85^0 C for 2 days. Establishment of a novel amorphous aluminosilicate part, which affects the improvement of the strength was found out through typical micro level analysis like (SEM), (XRD). The study results that alkali metal, silicon and water level of mixture has a noteworthy impact on the hardened properties. Author found that water in mixture plays a significant role throughout several stages like suspension, poly-condensation and toughening of geopolymerisation. Again, research depicts the strength under compression is improved along the reduction of the presence of external water in the mix. The research was inclined towards the optimization of strength considering heat curing profile including the temperature regime and time extent. As per the researcher, hotness crosses stimulation blockade and enriches the rate of dissolving of the source material. Raising strength was visualized with the application of heat influx in the system. Here amorphous phase with partly water phases was observed under high resolution microscopy. The existence like aluminosilicate part (s) like hydroxysodalite, herschelite etc. was confirmed through mineralogical studying equipment, such as X-ray diffractometer. The investigation ensures 1:1 ash to sand ratio is best for having good strength indeed. In certain industrial applications, the geopolymer binders are considered as future eco-friendly alternative to Portland cement.

T Bakharev. et.al. (2005) [123] examined on the durability of geopolymer materials when exposed to 5% solutions of sulfuric and acetic acids. In this investigation, a class F fly ash (FA) and alkaline activators were used. The change in weight, compressive strength and microstructural changes were considered as the key parameters in this study. When exposed to acid solutions, the durability of geopolymer components was higher to OPC (Ordinary Portland cement) paste. In selected geopolymer materials prepared by mixing sodium silicate with a mixture of sodium and potassium hydroxide (activators), conspicuous dilapidation of strength was detected. This study revealed that the degradation was associated with

depolymerisation of the aluminosilicate polymers in acidic exposure and formation of zeolites. In few cases, these led to a major drop of strength. The geopolymer material prepared with sodium hydroxide followed by elevated temperature curing displayed finest presentation. It exhibited sustainable cross-linked aluminosilicate polymer structure formed.

X J Song. et.al. (2005) [119] anticipated that the earlier issue was unresolved unless a long-standing study under sulfuric acid corrosion is observed. On the durability of fly ash based geopolymer concretes, the investigational data was based on specimens exposed to 10% sulfuric acid solutions up to eight weeks. The author stated that fly ash (class F) based geopolymer concrete was cured for 24 hours under alternate temperature (23^0C and 70^0C) at the initial stage.28 days' compressive strength of 50-mm cubes lied from 53MPa to 62MPa that was also being pointed out in this study. Samples were examined at 7, 28, and 56 days with the exposure in a 10% sulfuric acid carrying considering a relation between acid volume to specimen surface area of 8 ml/cm^2. Confirming ASTM C267 tests, the weight loss, residual compressive strength, and the residual alkalinity were controlled here. The test confirms minimum weight loss (less than 3wt. %), for geopolymer concrete under sulfuric acid. Geopolymer cubes were intact enough to take considerable load further. In compare to PC concretes, AAFG binders exhibited much lower mass change. Moreover, in such low pH environments, steel reinforcement cannot be used properly. Therefore, either alternate reinforcement needs to be used or the permeability of geopolymer materials has to be considerably amended. To conclude, author recommended essentially the high purity siliceous aggregates in this investigation.

S Thokchom. et.al. (2009) [115] correlated durability with apparent porosity and sorptivity for fly ash based geopolymer mortar specimens. By activating a Class F fly ash with a mixture of NaOH and Na_2SiO_3, geopolymer mortar specimens were manufactured. This mixture of NaOH and Na_2SiO_3 was consisted of Na_2O in the range of 5% to 8%. For the immersion of geopolymer mortar specimens, Nitric acid solution was used and the evaluation was performed to predict durability. This was executed on the basis of changes in weight and residual compressive strength at the end of 24 weeks. Higher apparent porosity and water sorptivity were found for specimens containing lesser Na_2O. In Nitric acid solution, even after 24 weeks, substantial compressive strength was retained by geopolymer mortar specimens. For specimen with higher porosity and sorptivity exhibited excessive loss of weight and reduction in compressive strength. At the end, research the research indicates that

the performance of geopolymer mortars in Nitric acid is influenced by porosity and sorptivity of geopolymer mortar specimens.

2.5 Parametric study on the performance of Blended Geopolymer

2.5.1 Geopolymer Blended with Supplementary Calcium compound

J Temuujin. et.al. (2009) [67] minutely observed the impact of calcium supplements on the characteristics of geopolymer prepared from ash. In this present research, Calcium supplements was replaced to ash from 1 to 3 wt. (%). Again, the research was focused to the development of polymer structure at heat & ambient curing (20^0C to 70^0C). This research briefly indicates that calcium supplements is highly beneficial towards the enhancement of typical characteristics at green and harden condition. For Calcium Oxide and Calcium Hydroxide as supplements in weight 3% within the mix of fly ash geopolymer inaugurate better strength characteristics. The author indicates calcium hydroxide as a beneficial additive than calcium oxide. In this experimental program it was resulted that addition of Calcium compound developed secondary input as generation of CSH and others hydrates associated with Alumina, Silicon and Calcium. In the same way, increment of suspension of ashes comprising silica in activator along with higher poly-condensation reactivity was observed. Again the author suggested that the sudden drop or degradation of the characteristics of polymer exposed in raising temperature might be due to the inadequate formation of 3D network. The efflorescence made on the geopolymer synthesized from collie ash was confirmed as hydrate comprising Na and P, as decided from mineral analysis.

C K Yip. et.al. (2005) [18] introduced Scanning Electron Microscopy to evaluate the consequence of GGBFS on the characteristic of polymer composites prepared from metakaolin at micro and macro standard. The author also found the coexistence of the geopolymeric and CSH gel within the body of the binder. The author confirmed that this phenomenon is dependent on the feature of alkali and base to supplements ratio by weight. Again, the research conveys that the appearance of hydrate and polymeric gel mutually is mainly possible under lower alkaline medium. Mutual existence of dual phases was absent unless considerable calcium supplements is available at the primary level. The author suggests, CSH may fill the internal hollow spaces of the porous polymeric file. The particular process may help to interconnect the deviation amongst the hydrated parts and unreacted elements which in fact results in improved strength phenomena. It was also found that moderate amount of calcium dissolvable calcium from GGBFS participates in the development of CSH at low alkalinity. The author again mentioned that the precipitation of

Calcium Hydroxide is enhanced in presence of excessive metal hydroxide in the mixing system. The author concludes that the mutual development of CSH and polymeric binder brings the structural homogeneity with compact bonding and a strengthen feature.

H M Khater. et.al. (2012) [50] examined the impact of calcium hydroxide on the mechanical and microstructural characteristics of geopolymer. In this program a product of alkaline activation of aluminosilicate wastes collected from demolition process. This wastes were considered as coarse aggregates. It included waste concrete and demolished walls comprising cement binder. The aggregates were passed through sieve size of 90 micron. The aggregate was prepared by mixing demolished walls and concrete waste as 6:4 (weight percent). Lime content was incorporated 0wt. % –25wt. %. Two distinct curing procedure like ambient temperature curing at (23^0C) in tap water and under a mild temperature were accomplished. On each specimen mix, drying treatment at 80^0C for 24 hours was performed. This act was executed to refine the mechanical properties of dried and wet samples. The mechanical and microstructural properties of the specimens were rectified by the addition of the calcium compound through rise of hydrated lime up to 10wt. % which were subjected to water curing. In contrary, the properties slightly decreased for those specimens cured in 100% RH at 40^0C. In the presence of calcium hydroxide, aluminosilicate wastes produce more aluminosilicate geopolymer using sodium hydroxide and sodium silicate as 3:3wt. %. This geopolymer accelerated both mechanical and microstructural properties, respectively. Finally, the author concluded that alkaline activation of aluminosilicate wastes served as an aid to generate valuable constituents. In the building industry, these materials may be applied for further investigation.

K Wang. et.al. (2004) [82] made and investigation on fly ash binder from cement kiln dust and several parameters controlling its characteristics. The research exhibited good performance of fly ash binder with cement kiln dust as supplements by 50 wt. %. The concentration of alkali hydroxide was maintained as 2 wt. % to 5 wt. %. The curing temperature was controlled as 24, 38 and 50^{o}C. The gravimetric analysis and x-ray diffraction test were carried out to examine the hydration product of the binder in this research. The XRD defined ettringite as a long term (observed for 100 days) stable system which was the prime product of CKD-FA binders with hydration. Curing temperature has favouarble effect on strength development rather than hydroxide.

A Palomo. et.al. (2004) [4] characterized the reaction products developed during alkaline activation by means of MASNMR. The research is mainly focused to find out the role of curing profile actually. The initial development of tecto-silicates as an amorphous product diverted into two consecutive phases. The study deals with the Si/Al ratio of zeolite precursor attained at 85^0C reaches at 1.86 from 0.95 with curing duration of 5 hrs. to 7 days. The mechanical, chemical, micro-structural properties of prepared products were discussed. In this research, an aluminum-rich phase was first made that left as the reaction proceeded, to lastly produce a silicon-rich zeolite precursor as detailed by MASNMR. The research refers the mechanical properties as function of intensity and duration of temperature. Prolonged curing time with high temperature emphasize the formation of continuous alumino-silicate matrix that heightens mechanical behavior of the molded product.

S Alonso. et.al. (2001) [111] projected metakaolin as another reactive source of silica which is able to form cementitious product which better physical characteristics. The interesting findings is that the developed product in presence of calcium hydroxide is similar to that in absence of calcium hydroxide with high alkali medium. The product was identified as sodium alumino silicate. CSH gel as a secondary product was also distinguished in this study. The research work again stated that salient parameters such as curing temperature, concentration of alkali, content of initial solids etc. controlled the rate of polymer formation. Although the temperature accelerates its formation, with the rise of the activator concentration, delayed polymer formation was found to be increased in activator concentration. Again the study shows that the ratio of metakaolin to $Ca(OH)_2$) made no impact on the rate of aluminosilicate formation.

C K Yip. et.al. (2003) [16] proved the existence of geopolymeric and CSH gel within a single product. Morphology and elemental composition of the two phases were checked by scanning electron microscopy. The SEM results showed the consistency of elemental composition within the different phases. Still, CSH gel formulated in this system possessed a considerably lower Ca/Si ratio rather than that usually formed with the hydration of OPC. Few calcium precipitates were there along the interface of CSH and geopolymeric gels, respectively. Such recommendation was there that the properties such as size, elemental composition etc. of the geopolymeric and CSH gels formed concurrently along the interfacial region, the reactivity of calcium precipitates held on to the key which reformulate a new trend of concrete to improve durability. A brief view on the consequence of slag on the typical properties of alkali activated metakaolin was elaborated.

Z Li. et.al. (2007) [139] made a considerable inspection on the progression of the strength of FA-based geopolymer subjected to low level temperature of heat curing. Slag as supplement was incorporated up to 4 wt. % into fly ash-based geopolymer. Combination of 10 wt. % metakaolin and 90 wt. % fly ash showed improved compressive strength. Compressive strength of 53.1 MPa and 70.4 MPa were achieved when cured at 30 and 70^0C respectively for 14 days. The author pointed out the improvement in structural strength by introducing XRD, FTIR, XPS, and MIP. At curing temperature of 70^o C, the rise in strength was about 15 MPa. The geopolymers showed diffuse hump under XRD at about 20–35^0 2θ max, Cu K. Variation of temperature (30^0C and 70^0C) did not have significant effect on compressive strength for geopolymer with 4wt. % of slag as supplements. The study revealed that incorporation of slag as supplements help to make the system more amorphous. Thus, a chances of the presence of new amorphous phase CSH is highlighted in this study. The test results showed that slag addition increases the compressive strength significantly. The change in MIP pattern suggests that higher curing temperature (70^0C) emphasizes the development of finer pores. The abridged pores have significant contribution to the strength characteristics.

Zuhua Z. et.al. (2009) [140] executed a program on the role of water as a key parameter in synthesis of calcined kaolin based geopolymer. It was observed in X-ray diffraction (XRD) and thermo-gravimetry (TG) that the activity growth of calcined kaolin was decreased by the residual water prior to the formation of stable crystalline phases. Reaction heat evolution capacity showed that high liquid/solid ratio may increase the rate of dissolution of raw materials and the hydrolysis of Si_4^+ and Al_3^+ compounds. The author suggests that the effect of non-evaporable water is a key parameter in connection with the strength variation of geopolymers. In this study the results point out that non-evaporable water is indispensable to maintain the strength stable and the optimum content was about 7.4%. In kaolin calcination, remaining water ebbed the activity growth of calcined product before the formation of the stabled crystalline phases. The higher liquid/solid ratio could increase the percentage of dissolution and hydrolysis, if OH^- concentration was high enough, but it might hinder poly-condensation process. Geopolymers exhibited large shrinkage property while cured in air unlike in a little expanded hydrothermal condition. Finally, to conclude that for the upcoming application of this new material, the environmental condition, especially humidity and temperature should be taken into consideration.

2.5.2 Cast-in-situ Geopolymer

Hu Mingyu. et.al. (2009) [57] investigated on the synthesis of geopolymer at ambient temperature. For this purpose, author introduced fly ash and bentonite as base material and supplementary material. A combination of NaOH and CaO was used. Reactivity of metakaolin was found better in compare to fly ash. This low reactivity is basically responsible for the poor rate of reaction at ambient temperature at the time of geopolymerization. In this research methodology the supplementary material was introduced in a way to have better rate of geopolymerization which enhance the properties of fly ash based geopolymer as well. This research explored the differential nature between fly ash and geopolymer made by the same. The comparison was carried out through X-ray spectra. The spectra were almost similar for every case except the pics of $CaCO_3$. From the result the author indicated that geopolymerization reaction did not allow the formation of new crystalline phases indeed. Secondary electron image proves the existence of zeolite in the matrix. Again, some unreacted fly ash particles were visualised even after sixty days of curing in ambient temperature. Some networked outcome was also observed microscopically at the top surface of fly ash particles which was arbitrarily dispersed. Due to the presence of these products over fly ash the structure exhibited lesser porosity. The author found bentonite as the prime cause behind this phenomenon. The durability exposure tests observed the better performance for the geopolymer comprising zeolites. Lower weight loss was observed after sixty days of emersion in magnesium sulfate. At the end of the research the author suggested that geopolymer comprising zeolite was much imtact under aggressive environment and exhibited no fracture as confirmed by short term (two months) sulfate exposure.

2.5.3 Geopolymer Blended with Supplementary Silica compound

Prud'homme. et.al. (2010) [36] stated that the synthesis of geopolymers on the basis of alkaline polysialate was achieved at low temperature (~25–80^{0}C), by the alkaline activation of raw minerals and silica fume. Dehydroxylated kaolinite and alkaline hydroxide pellets solution (dissolved in potassium silicate) were used to prepare the materials. After that, the constituents were transmitted to a polyethylene mold sealed with a top. Then the materials were employed to oven at 70^{0}C for 24 hours. FTIR-ATR spectroscopy studied that a polycondensation reaction was used in the formation of the amorphous solid for all geopolymer materials following dissolution of the raw materials. It was occurred since the thermal measurement having a 0.22 W m^{-1} K^{-1} value.

Again, TGA-MS experiments confirmed that there was a synthesization of in situ inorganic foam based on silica fume from the in situ gaseous production of dihydrogen owing to the oxidation of free silicon (content in the silica fume) by water in alkaline medium. For the applications in building materials, this substance had potentiality as an insulating material.

2.6 Objectives of the Present research

The objective of the present research is to develop blended geopolymer by eliminating the major drawbacks discussed in earlier chapters. There are three major aspects. Firstly, the investigation on the optimal parameters of activator prior mixing and its impact on non-blended fly ash. Secondly, the effect of supplementary material on the properties of geopolymer at green and hardened state. Thirdly, to develop water cured blended geopolymer as a cast-in-situ product. Finally, the resolved aspects will be useful to align in a way to compensate the major drawbacks of Alkali activated fly ash based geopolymer. The study is aimed to develop a new stable blended geopolymer in connection with physical, mechanical, microstructural performance in ambient and aggressive environment.

The scope of studies comprised of (i) optimization of temperature level of activator solution prior mixing. (ii) incorporation of combination of oxides in activator solution (iii) supplementation of external calcium based material (lime stone dust, silica fumes and blast furnace slag) in fly ash geopolymer. (iv) parallel study on alkali activated fly ash blended with calcium subjected to water curing (v) Silica fume blending with flyash to compensate the role of sodium silicate. (vi) new approach to assess workability and durability. For all the studies physical, mechanical, microstructural and mineralogical studies were made separately to appreciate the non-blended and blended geopolymer characteristics clearly. Considering the major aspects, the entire research can divided into three parts.

2.6.1 Study on Optimal parameters of Activator and its impact on Non-Blended Fly Ash Geopolymer

- Temperature imposed on activator before mixing
- Activator with dual oxides

2.6.2 Study on Fly Ash based Geopolymer Blended with Supplementary Calcium based Compound

- Development of fly ash based geopolymer blended with calcium based compound (lime stone dust / slag) and its parametric studies related to mechanical properties.
- Appreciation of microstructure with mechanical properties of fly ash based geopolymer blended with calcium based compound (lime stone dust / slag).

- Durability study on fly ash based geopolymer blended with calcium based compound (lime stone dust / slag)
- Water cured fly ash based geopolymer blended with slag

2.6.3 Study on Fly Ash based Geopolymer Blended with Supplementary Silica based Compound

- Development of fly ash based geopolymer blended with silica fumes in presence of aluminium compensator (Borax / Murram) and its parametric studies related to mechanical properties.
- Appreciation of microstructure with mechanical properties of fly ash based geopolymer blended with silica fumes.
- Durability study on fly ash based geopolymer blended with silica fumes.

At all stages of investigation comparative studies were made between blended and non-blended fly ash based geopolymer.

The following combinations of non-blended and blended geopolymer have been studied

1. Fly ash + KOH + Na_2SiO_3
2. Fly ash + NaOH + Na_2SiO_3
3. Fly ash + NaOH + Na_2SiO_3 + supplementary material (Lime stone dust)
4. Fly ash + NaOH + Na_2SiO_3 + supplementary material (Blast furnace slag)
5. Fly ash + KOH + Na_2SiO_3 + supplementary material (Silica fume and Borax)
6. Fly ash + KOH + Na_2SiO_3 + supplementary material (Silica fume and Murram)

For all the studies, the mechanical performance of geopolymer was carried out and typical microstructural studies like SEM, XRD, MIP, FESEM, EDAX, TG/DTA etc., were made for proper scientific interpretations. This research provides new information based on systematic microstructural and mechanical studies of fly ash based non blended/ blended geopolymer. New areas of research have been explored to assess workability. Newly introduced workability parameter added new dimension in understanding the performance of fresh geopolymer. This research has provided pathway to produce high performance fly ash based non blended and blended geopolymers in different forms overcoming present drawbacks as discussed earlier.

3. EXPERIMENTAL INVESTIGATION

3.1 Preamble

This particular chapter deals with the detail of experimental investigation carried out on fly ash based blended and non-blended geopolymer. Experimental procedures has been discussed in detail. Detail of test specimens have been furnished.

The experimental investigation was carried out with the following objective

1. Development and analysis of geopolymer from Class F fly ash. Fly ash blended with other supplementary materials.
2. Comparative study on the performance of geopolymer prepared with different activators of dual oxide combinations.
3. Comparative study on workability of fresh and mechanical properties of hardened blended geopolymer.
4. Microstructural study on blended geopolymer.
5. Parametric study of blended geopolymer, Alkali content, Curing regime etc.
6. Comparative performance study and analysis of blended geopolymer with different mix combination exposed to severe exposure such as freeze-thaw cycle and exposition to magnesium sulfate solution.

The following combinations of non-blended and blended geopolymer have been studied

1. Fly ash + KOH + Na_2SiO_3
2. Fly ash + NaOH + Na_2SiO_3
3. Fly ash + NaOH + Na_2SiO_3 + supplementary material (Lime stone dust)
4. Fly ash + NaOH + Na_2SiO_3 + supplementary material (Blast furnace slag)
5. Fly ash + KOH + Na_2SiO_3 + supplementary material (Silica fume and Borax)
6. Fly ash + KOH + Na_2SiO_3 + supplementary material (Silica fume and Murram)

For all the studies, the mechanical performance of geopolymer was carried out and typical microstructural studies like SEM, XRD, MIP, FESEM, EDAX, TG/DTA etc., were made for proper scientific interpretations. This research provides new information based on systematic microstructural and mechanical studies of fly ash based non blended/ blended geopolymer. New areas of research have been explored to assess workability. Newly introduced workability parameter added new dimension in understanding the performance of fresh geopolymer. This research has provided pathway to produce high performance fly ash based

non blended and blended geopolymers in different forms overcoming present drawbacks as discussed earlier.

Most of the experimental investigations have been carried out at the Concrete Laboratory of Civil Engineering Department, Jadavpur University, Kolkata, India. Tests like SEM, FESEM, EDX, TG/DTA and XRD were conducted at Department of Condensed Matter Physics and Material Sciences, S. N. Bose National Center for Basic Sciences, Kolkata, India for microstructural characterization and micro-analysis. Few samples for XRD have been carried out at Department of Physics, Jadavpur University, Kolkata. MIP (Mercury Intrusion Porosimetry) test for the geopolymer composites have been carried out at Central Glass and Ceramic Research Institute (CGCRI), Kolkata, India.

Brief description of the raw materials used for the manufacturing of fly ash based geopolymer and the test procedures for the characterization of geopolymer are included in this chapter. The investigation steps were divided into two parts; firstly, the manufacturing of blended geopolymer specimens and secondly the characterization of the same. New method to assess workability has been introduced. XRD, SEM, EDX, TG/DTA and MIP have been used to explain the mineralogical and microstructural changes for the characterization of blended and non-blended geopolymer composites. Properties like Sorptivity, Water absorption, Dry density, Apparent porosity etc. were carried out. Polar chart has been introduced in the new proposed method to assess workability. Investigation on durability involves immersion of non-blended and blended geopolymer samples in concentrated saline solutions (10% and 20%) for 6 months/one year. have been considered. Assessment of its resistivity was made in terms optical appearance (surface texture), change in weight and residual strength at different interval of exposure time. An investigation to assess freezing-thawing effect on blended and non-blended geopolymer sample exposed to saline water for a period of one year. Details of materials, manufacturing methodology, testing tools and procedures, typical series of samples, mix composition related to every phases of study, have been briefly furnished in this chapter. The detail outline of the different phases of investigation has been discussed in Section 3.5. A complete flow chart of the present investigation is furnished in Figure. 3.1.

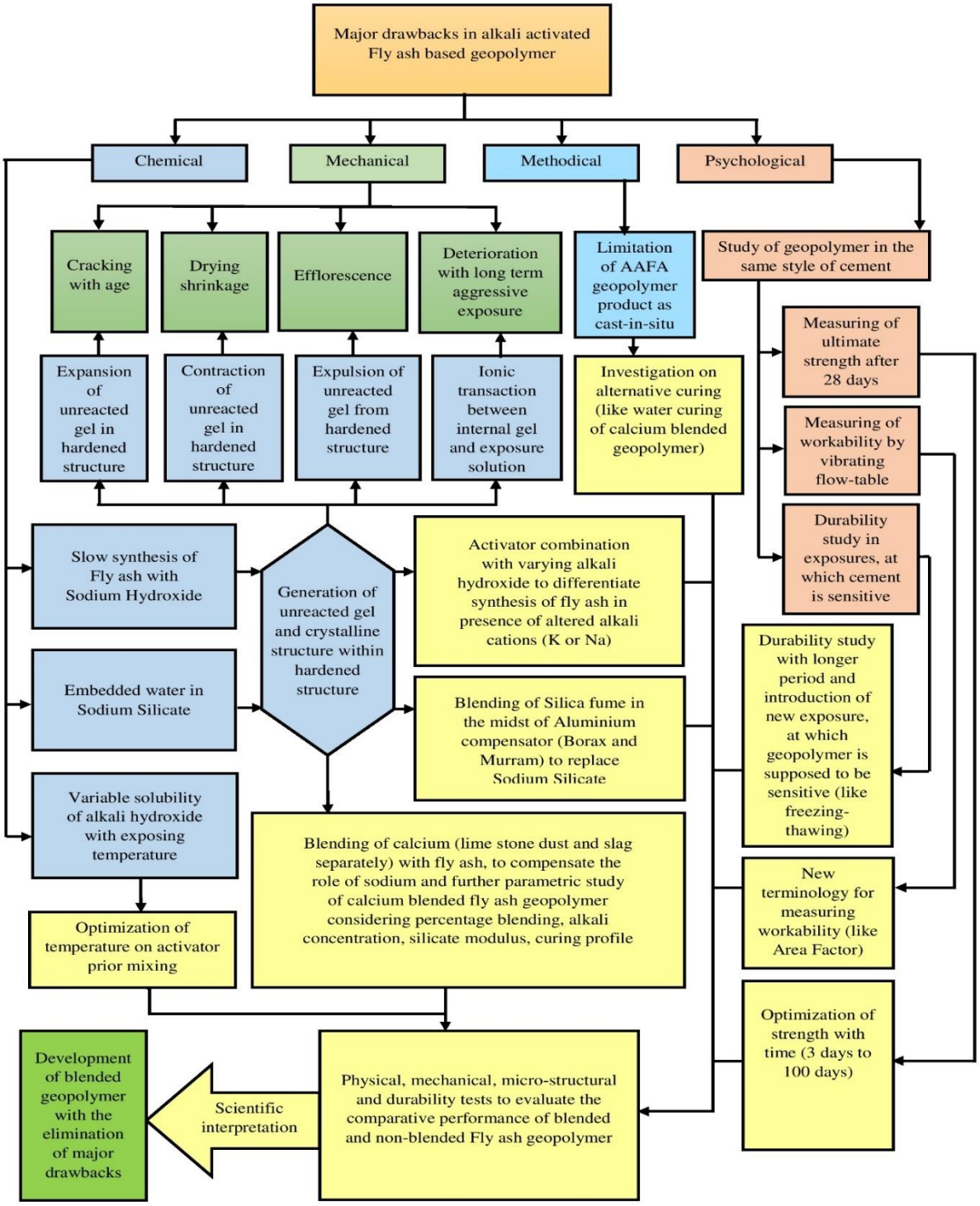

Figure 3.1 Flow Chart of Present Investigation

3.2 Raw Materials

3.2.1 Base Material

3.2.1.1 Fly Ash

For manufacturing of geopolymer from low calcium Fly ash (Class F; also conforming to ASTMC618 and IS 3812-1987 specifications), was collected from Kolaghat Thermal Power Station, Kolaghat, East Midnapore, India. It was utilized as the solid aluminosilicate base material. The collected fly ash was oven dried and sieved. Before the commencement of research work, all the dried and sieved fly ash was mixed thoroughly to ensure homogeneity. More than 75% portion of fly ash was passed through 45μ and Blaine fineness measurement was 380m^2 per kg. The XRF elemental analysis report and SEM micrograph of the fly ash are specified in Table 3.1 and Figure 3.2 respectively. It is shown in the Table 3.1 that the summation of silicon and aluminium content of fly ash is about 80% of the total mass.

Table 3.1 XRF Elemental analysis report of Fly ash

Elemental composition	SiO_2	Al_2O_3	Fe_2O_3	TiO_2	CaO	K_2O	Na_2O	P_2O_5	MgO	LOI
Percentage	56.01	29.80	3.58	1.75	2.36	0.73	0.61	0.44	0.30	0.40

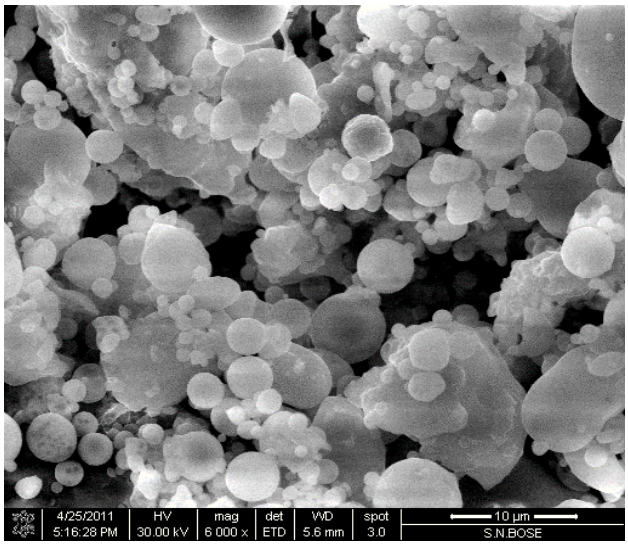

Figure 3.2 Microscopic image of Fly ash

3.2.2 Supplementary Materials

3.2.2.1 Silica Fume

Silica fume was supplied by Oriental Trexim Pvt. Ltd. Interestingly, pozzalonic material consisted of amorphous silica is produced through electric arc incinerators. It is basically a byproduct in the process of preparing ferrosilicon alloy. In silica fume, about 92% of silicon oxide was present. Silica fume had specific surface area of 18900 m^2/kg, moisture content of 0.60%, pH value of 7.6, specific gravity of 2.36 and bulk density of 450.6 gm/cc. In Table 3.2 and Figure 3.3, the chemical composition and SEM micrograph of the silica fume are shown respectively.

Table 3.2 XRF Elemental analysis report of Silica fume

Elemental Composition	SiO_2	Fe_2O_3	K_2O	Al_2O_3	K_2O	Na_2O	CaO	MgO	SO_3	TiO_2	P_2O_5	LOI
Percentage	92.00	1.60	0.61	0.46	0.61	0.51	0.29	0.28	0.19	0.0	0.0	1.00

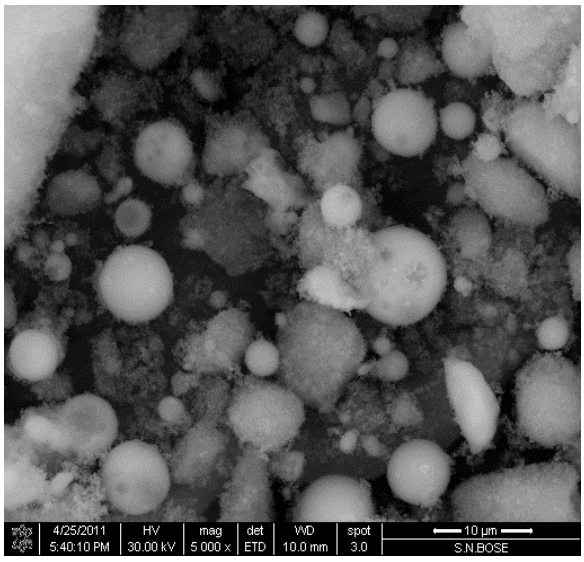

Figure 3.3 Microscopic image of Silica fume

3.2.2.2 Lime Stone Dust

Limestone dust, a solid material, was collected from BCC Limited, Dhanbad, India. Ground limestone had bulk density and specific gravity of 1425 kg/m^3 and 2.7 respectively. It had finer particles in the range between 10 to 70 microns. The typical mean size of grains was around 25 µ. The chemical analysis report and scanning electron micrographs of Lime stone dust are provided in Table 3.3 and Figure 3.4 respectively.

Table 3.3 XRF Elemental analysis report of Lime stone dust

Elemental Composition	CaO	MgO	Fe_2O_3	Al_2O_3	SiO_2	K_2O	TiO_2	Na_2O	LOI
Percentage	51.01	0.28	0.36	2.74	3.92	0.04	0.09	0.0	41.56

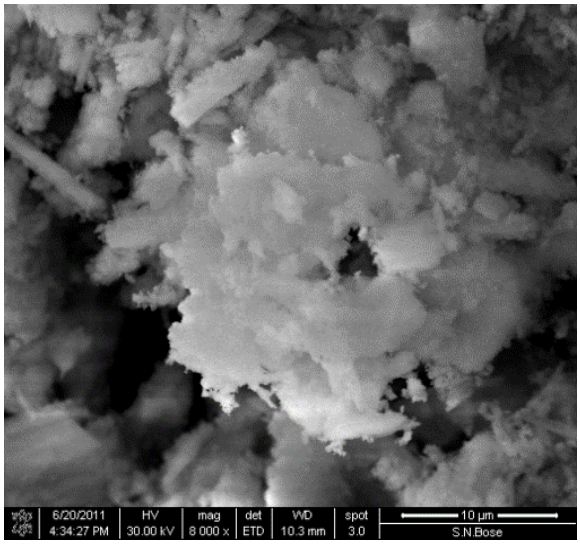

Figure 3.4 Microscopic image of Lime stone dust

3.2.2.3 Ground Granulated Blast Furnace Slag (GGBS)

GGBS complying BA 669 (1992), collected from TATA Metaliks, Kharagpur, West Bengal, was used in this work. The blast furnace slag had 39.07% CaO content. It had bulk density and specific gravity of 1236 kg/m^3 and 2.8. It was in granular form and converted to powder form by grinding. It had fine particles having mean size close to 35 microns. To increase the reactivity level of slag special stone grinding was done by DRD Educational & Consultancy Pvt. Ltd. The specific surface area was brought to 960 m^2/Kg. In fact, it was done to bring the reactivity level as like lime stone dust. The XRF elemental composition and SEM micrograph of slag particles are given in Table 3.4 and Figure 3.5 respectively.

Table 3.4 XRF Elemental analysis report of Ground granulated blast furnace slag

Elemental Composition	CaO	SiO_2	MgO	Fe_2O_3	MnO	Al_2O_3	LOI
Percentage	39.07	30.26	8.95	1.87	0.44	15.18	0.04

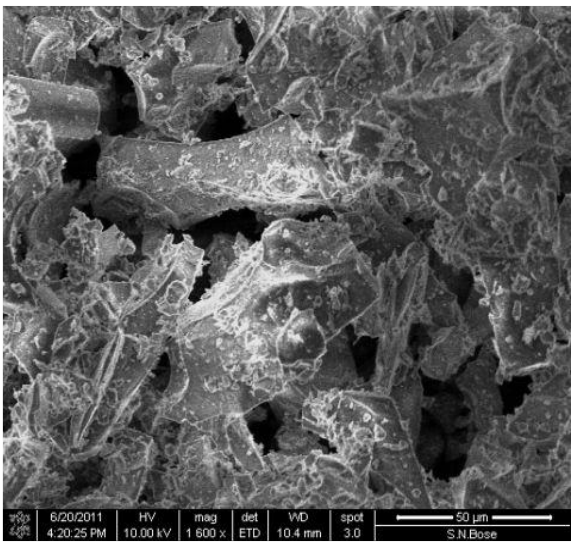

Figure 3.5 Microscopic image of Blast furnace slag

3.2.2.4 Murram

Murram, a mixture of solid and metallic oxides, was collected from Ujjal Chemical Works, Ranaghat, Kolkata, India. Murram as an industrial waste was available from aluminium production industry. About 26% of aluminium oxide was present in Murram used. Typical values of other constituents in Murram were also obtained. The mean particle size below 75 µm. The specific surface area (BET) of Murram was 171 m^2/Kg. The chemical composition and SEM micrograph of Murram are furnished in Table 3.5 and Figure 3.6 respectively.

Table 3.5 XRF Elemental analysis report of Murram

Elemental Composition	SiO_2	Al_2O_3	CaO	Fe_2O_3	Na_2O	TiO_2	MgO	K_2O	LOI
Extent in Percentage	21.06	26.01	17.12	13.02	5.3	4.21	2.22	2.04	9.02

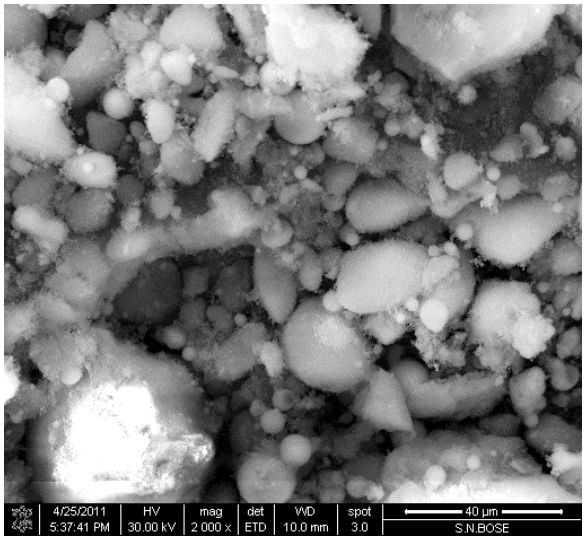

Figure 3.6 Microscopic image of Murram

3.2.2.5 Commercial Borax

Commercial borax ($Na_2B_4O_7 \cdot 10H_2O$), was collected from DRD Educational & Consultancy Pvt. Ltd, North 24 Parganas, India. The IUPAC name of the natural mineral is sodium tetraborate decahydrate. Commercial borax having specific gravity equal to 1.7 and BET surface area 557m^2/Kg, were used in powder form. In market, Borax is available as sodium borate, sodium tetraborate or disodium tetraborate. It arises in nature as evaporated dump which is formed by the continual evaporation of seasonal lakes. The chemical composition and SEM micrograph of commercial borax are provided in Table 3.6 and Figure 3.7 respectively.

Table 3.6 XRF Elemental analysis report of Borax

Elemental Composition	**B_2O_3**	**Na_2O**	**SO_3**	**Fe_2O_3**	**SiO_2**	**Al_2O_3**	**P_2O_5**	**LOI**
Extent in Percentage	39.00%	17.0%	1.0%	1.0%	0.0	0.0	0.0	28.32%

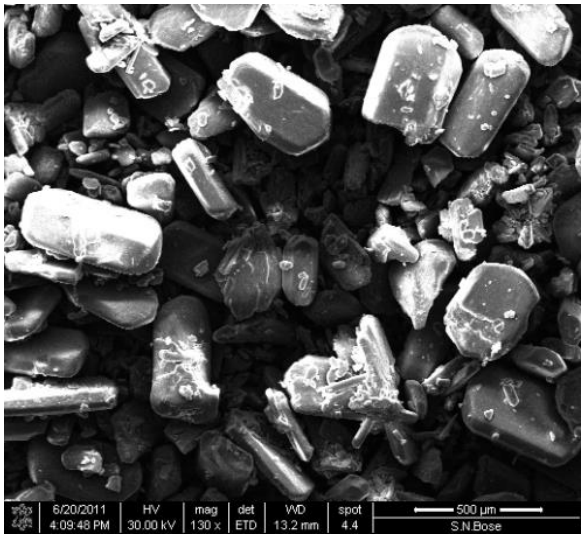

Figure 3.7 Microscopic image of Borax

3.2.3 Alkali Activator

Alkali activator is a combination of alkali silicate and alkali hydroxide. Laboratory standard potassium hydroxide pellets (84 percent pureness and specific gravity 2.04) and sodium hydroxide pellets (98 percent pureness and specific gravity 2.11) were used. Sodium silicate solution contains Na_2O= 8%, SiO_2=26.5% and 65.5% having a bulk density and silicate modulus 1410 kg/m^3 and 3.3 respectively. Merck Ltd, India is the manufacturer of hydroxide and Loba Chemie Ltd, India is the manufacturer of silicate solution. In initial stage, required quantities of hydroxide pellets and water were mixed depending on the desired X_2O content (Here X refers to alkali cation; X_2O indicates Na_2O, K_2O or sometime combination of Na_2O and K_2O in this research) of the activator solution. Dissolution of hydroxide pellets in water is an exothermic reaction. So, generation of hotness from this solution indicates the reactivity level. The activator solution was kept undisturbed for a duration of 24 hours before use in every cases. Thereafter, required amount of sodium silicate and hydroxide were mixed thoroughly 3 hours prior use, to manufacture geopolymer composite. It was mixed in a way to have desired quantity of SiO_2, Na_2O etc. in activator. It was observed that the reaction of hydroxide solution with silicate solution is an exothermic reaction and takes few hours to reach in room temperature. Sometime, it takes more time and a white precipitation within the solution, occurs. Hence, 3 hours rest was decided and maintained in this research.

Figure 3.8 Activator Preparation

3.3 Manufacturing process of Geopolymer composites

Different types of base materials and activators have been used to manufacture alkali activated product. Most of the previous studies involve heat curing. Study on the blended geopolymer and its comparison with the non-blended geopolymer is the prime objective of this experimental procedure. Very limited technical literatures are available on water cured activated products. The detail experimental study has been carried out by varying oxides in activator, base material, supplementary material, curing condition to investigate the performance of new blended geopolymer composites.

3.3.1 Preparation

1. Firstly, the fly ash with or without supplements were properly mixed in completely dry condition in Hobart pan mixer. The Hobart mixture [Figure 3.9(c)] of model P660 of capacity 600cc and speed of 60 cps was used for mixing the raw materials.
2. Required quantity of hydroxide pellets and water were mixed depending on the desired X_2O (Here X refers to alkali cation; X_2O indicates Na_2O, K_2O or sometime combination of Na_2O and K_2O in this research) content in the activator solution. The hydroxide solution was kept undisturbed for 24 hours. Required amount of sodium silicate was added 3 hours prior use of activator.
3. Activator solution was added to the blended materials (base material + supplements) and the Hobart mixture was used to mix for five minutes to have geopolymer paste ready for casting test specimens.
4. Then, the geopolymer paste was transferred to 50 x 50 x 50 mm^3 cubical wooden mould [as shown in Figure 3.9] and 50 mm dia × 100 mm height cylindrical wooden mould [as shown in Figure 3.9], followed by vibration in a vibrating table [as shown in Figure 3.9] for 5 minutes to remove entrapped air bubbles.
4. Geopolymer test specimens were kept in hot air oven at a prefixed temperature for heat curing.
5. However, some geopolymer test specimens were immersed in water after a rest period of zero to 24 hours.

Figure 3.9 Preparation of test specimens

3.3.2 Curing

3.3.2.1 Hot Curing

For heat curing the samples were placed in the oven along with the mould for a period of 24 to 48 hours at 55°C to 85°C. After the heat curing the samples were allowed to be within the oven, keeping the door of the oven open.

3.3.2.2 Water Curing

Immediately after placing the geopolymer paste in the mould, it was covered with plastic paper to protect from external contact. The samples were kept at room temperature for zero to 24 hours and then the specimens were immersed in a water basin. Specimens were cured for 20 days water curing after prefixed rest period as indicated above.

3.4 Test setup

The performance of non-blended/blended geopolymer specimens with respect to strength and durability were examined. Tests like sorptivity, water absorption, dry density, apparent porosity etc. were conducted. Relevant Indian standard codes of practice have been followed to conduct the experiments. Moreover, some experiments were also conducted based on the ASTM standard. Scanning electron microscopy (FSEM/SEM), Energy dispersive X-ray (EDX), Mercury intrusion porosimetry (MIP) and Thermo-gravimetry /Differential thermal analysis (TG/DTA) experiments have been used for microstructural characterization. In some cases, XRD (X-ray diffraction) analysis have been used to study the mineralogical status of material. Typical test set up for measuring the durability of geopolymer product through visual and optical observation, change of weight and change of strength at different interval of time, have been briefed in this section. Special test set up for measuring the performance of geopolymer specimen in aggressive saline water under cyclic freezing and thawing has been also explained.

3.4.1 Test setup for the study on Physico -Mechanical performance

3.4.1.1 Workability Test

Workability of geopolymer paste at green state was assessed. A new concept of testing has been introduced. A polar graph was used which had 50 circular concentric loops and 40 radial lines. The total domain was subdivided into fragments to find the areal variation of the extent of flow. The n^{th} circle has n cm diameter. A brass cylindrical container (6 cm diameter, 8cm height) and a circular glass slab were used. The thickness and diameter of the glass slab were 7mm and 50cm respectively (as shown in the Figure 3.10). The polar chart was kept under a thick glass piece. The cylindrical brass container was positioned accurately at the midpoint of

the circular plate, confirming that the midpoint of the container matches with the midpoint of the polar chart (as shown in the Figure 3.10). The brass mould was then filled up by geopolymer paste immediately after mixing or a prefixed time. Initially the brass cylinder was used to hold the paste. After one minute of detention period the cylinder was allowed to be raised up vertically. In this way mixture composite in green state was allowed to move radially. After reaching more or less static condition, measurements were taken. Change in the rate of poly condensation has direct impact on the workability. Consistency or workability of geopolymer was expressed by the term "Area factor". "Area factor" denotes the ratio of the area of unconfined paste (when reaching more or less static condition) to that of confined paste (initially when within container). This set up was also used to have an idea of setting ti.

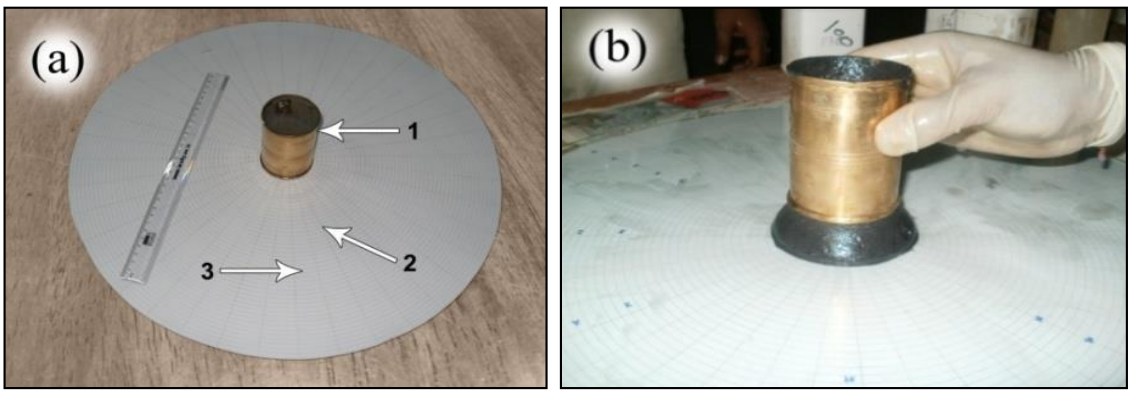

Figure 3.10 Workability Test Setup

1. Brass cylindrical 2. Polar chart 3.Rounded glass piece

3.4.1.2 Strength Test

Compressive strength and split tensile test of test specimens were conducted by a 2000 KN capacity digital compression testing machine (model no. EM500 supplied by ENKAY Enterprise). The least count was 0.001 KN. (3 to 100) day direct compressive strength of hardened geopolymer specimens were determined. Compressive strength of cube specimens was done as per ASTM C109. The split tensile strength of cylindrical specimens (as shown in Figure 3.11) was measured and the formula $\sigma_t = \frac{2P}{\pi dl}$, was used, where P, l and d are the load at failure, length of the cylinder and diameter of the cylinder respectively, as per ASTM C496. The compressive and split tensile strength tests have been also conducted at different intervals of exposure in aggressive solution. In each case, at least six specimens were tested as per ASTM C-109-02 [7] and average values were considered. In fact breakage pattern of specimens were frequently random. Even some parts were chipped of before the final fracture.

The crushing was not considered perfect unless the specimens crush distinctly with a breakage [86]. A typical test setup for split tensile strength is presented in Fig. 3.11.

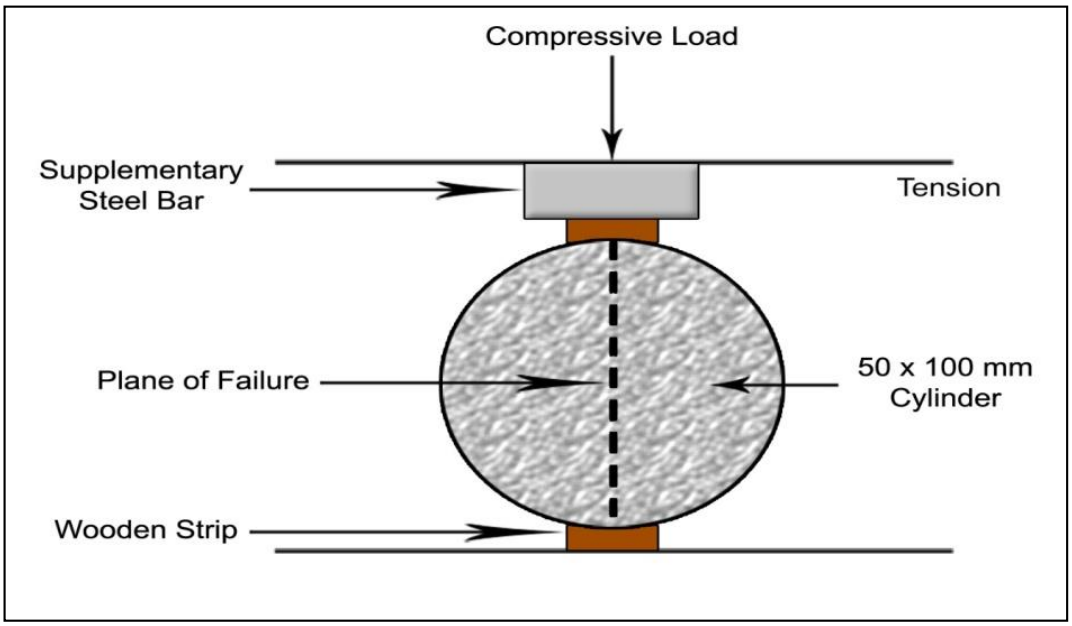

Figure 3.11 - Split Tensile Strength Testing Setup

Figure 3.12 Digital Compression Test Machine

3.4.1.3 Water Absorption Test

Water absorption was obtained after immersion in water and the amount of water absorbed is obtained and expressed in terms of percentage rise. Drying process continues till the specimen to reach a constant weight and then it was immersed in water for 24 hours. Six specimens from each series of studies were considered. The drying temperature was kept below the curing temperature.

3.4.1.4 Density and Apparent Porosity Test

This test method followed by S. Thokchom et.al. [112] was considered. The bulk density and apparent porosity were determined for different series of samples at same prefixed age.

The following steps were followed in the test:

1. The specimens were oven dried for one day at a temperature less than the curing temperature.
2. Weight of the dried samples was measured and considered as $\mathbf{W_d}$.
3. Specimens were then soaked in water for 24 hours.
4. Sample was freely suspended in water and its weight was recorded as $\mathbf{W_i}$.
5. The specimens were brought to surface saturated dry condition and its weight was measured as $\mathbf{W_s}$.

Dry density and Apparent porosity were determined using the following relationships:

$$\text{Dry density (kg/m}^3) = \mathrm{W_d}/(\mathrm{W_s} - \mathrm{W_i}) \times 1000$$

$$\text{Apparent porosity (\%)} = [\frac{W_s - W_d}{\mathrm{W_s} - \mathrm{W_i}}] \times 100$$

3.4.1.5 Sorptivity Test

This test method followed by S. Thokchom et.al [112] was considered. Sorptivity test was conducted at room temperature as per the ASTM C 1585 -04 with a change of specimens size used 50 mm x 50 mm x 50 mm Rate of absorption (sorptivity) through capillary action of water, was measured. Increase in mass due to absorption, when only one surface of the specimen is exposed to water and water absorption takes place due to capillary suction with time. The surfaces unexposed to water, were painted to avoid any moisture absorption from the environment. The arrangement as shown in Figure 3.13(a). Test specimens were rested on wire mesh. Specimens were immerged 2 to 5 mm from bottom surface as dipped in water. Along the testing period the weight rise of the test specimen was recorded. Figure 3.13(b) shows typical coated specimen for water sorptivity test. Absorbed water per elemental area with the square root of period in minute, was plotted. The slope of the trend line indicates as 'Sorptivity'. The uplift of fluid through solid was designated by this standard plotting indeed

[52]. It can be utilized as an indicator of durability as it is linked with pores connectivity [22], [47], [93]. This test brings a relation between water absorption into porous and permeable materials with the square root of the elapsed time (t) after submersion. But the relation stands only considering a continuous source of fluid through the entry face [92]. Firstly, these specimens were coated with water proof enamel paint on all sides except the bottom and top surfaces in a way to permit the unidirectional capillary flow of water from bottom surface only. Ingress of water per elemental area from bottom face I (gm /mm^2) was plotted against root of period (t) in minute, which is expressed with the relation

$$I = S\sqrt{t}$$

Here, S = Sorptivity in $mm/min^{0.5}$

I = Rise in mass per elemental area (gm/mm^2) (Considering unit density of water)

t = Time (generally limited to 3-4 hours), measured in minutes corresponding to reading.

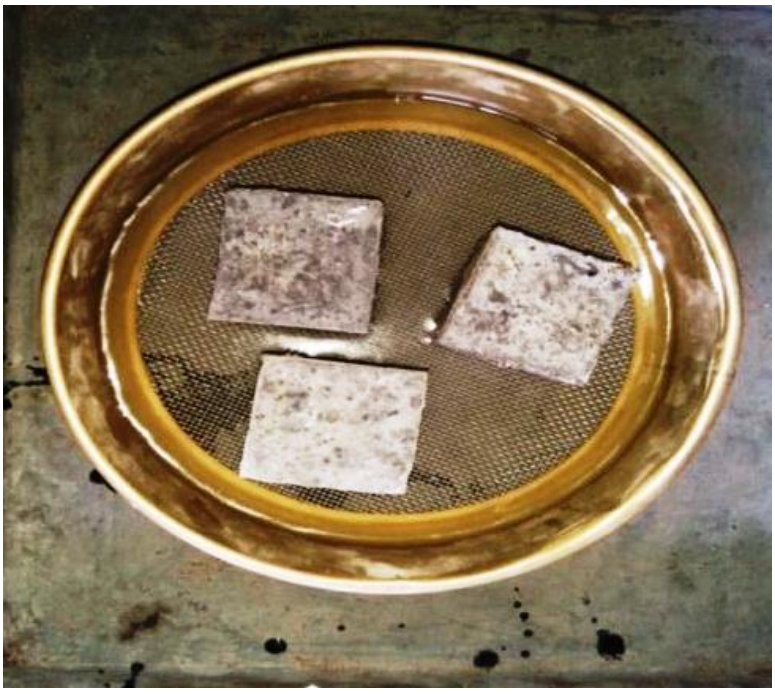

Figure 3.13(a) Setup for Sorptivity

Figure 3.13(b) Samples for Sorptivity Test

3.4.2 Test Setup for Durability Study

3.4.2.1 Sulfate Exposure

Before immersion in saline water, every specimen was kept submerged in potable water for 1 hour. At the very outset vertical immersion of samples (cylindrical and cubical) in magnesium sulfate solvent of 10% - 20% concentration was made. To prepare the solution, Magnesium Sulfate powder (99% pureness) was liquefied in water to achieve required concentration (%). Solution level was maintained 4cm - 5cm over test specimens for allowing free open air evaporation. Both the cube and cylinder specimens were used this sulfate resistance test. Residual strength and change in weight were conducted at different interval of time.

3.4.2.2 Weight change and Residual Strength Test

Specimens were weighed before immersion and after every prefixed time of immersion. Weight was taken after cleaning surfaces of the specimen at saturated dry condition using mild air blower as required. Change in weight in percentage (increase or decrease) for specimens at different time, recorded. Similar procedure followed in case of strength measurement.

3.4.2.3 Physical Changes and Optical Microscopy

Variations in physical appearance were recorded by an optical microscope at every stages of observation. this crack detection microscope WF 10X, manufactured by C&D (Micro services) Ltd., U.K, shown in Figure 3.14 was introduced. It provides surface texture in normal condition and after exposing to sulfate solutions.

Figure 3.14: Crack Detection Microscope

3.4.2.4 Thermal Fluctuation (Freezing –Thawing) Set up

Chest freezer of Model No. VT3-NUCAB 400L Glass top, manufactured by Hindustan Unilever, India, has been used in this study. The temperature fluctuating domain was ranged from +8^{o}C to - 20^{o}C. Each specimen was subjected to consecutive cycles for the entire period of program, sometime one year. The temperature change rate was controlled on the basis of the exposure time. The test specimens (cylinder/cube) were immersed vertically in the horizontal chest freezer. After immersion water level was maintained 4cm to 5cm above top surface of the specimens. Initial temperature of water was adjusted 8^{o}C during immersion. The salinity of the water was adjusted by making it 20% concentrated with Magnesium Sulfate as shown in Figure 3.15 and Figure 3.16. Actually, the assembly was monitored in a way so that it could create consecutive phase of cool (8^{o}C) to chill (-20^{o}C). Long term residual strength and change in weight test were carried out for different geopolymer specimens submerged in 20% concentrated Magnesium sulfate solution along with cyclic freezing and thawing.

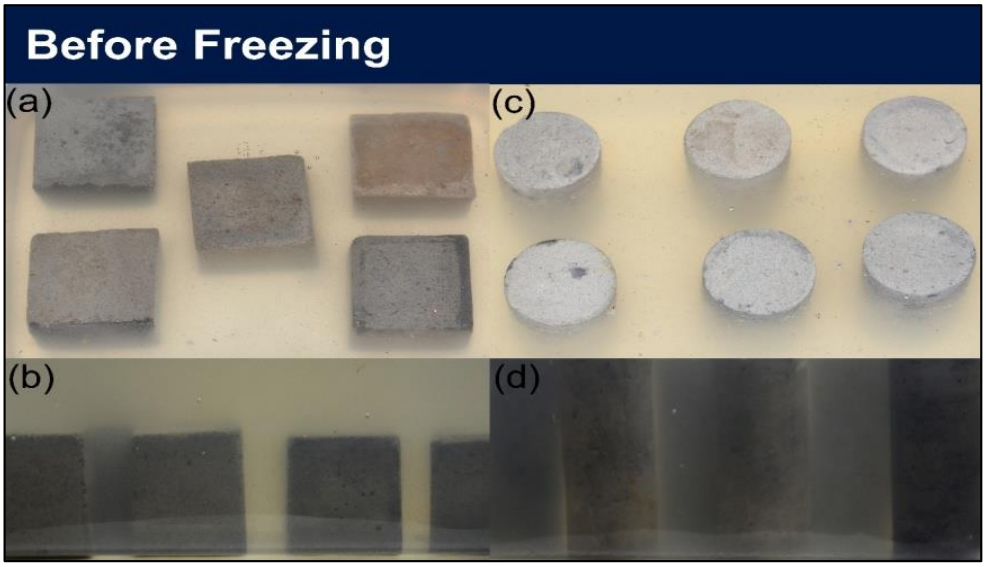

Figure 3.15: Setup for Freezing-Thawing Test in Magnesium Sulfate Solution

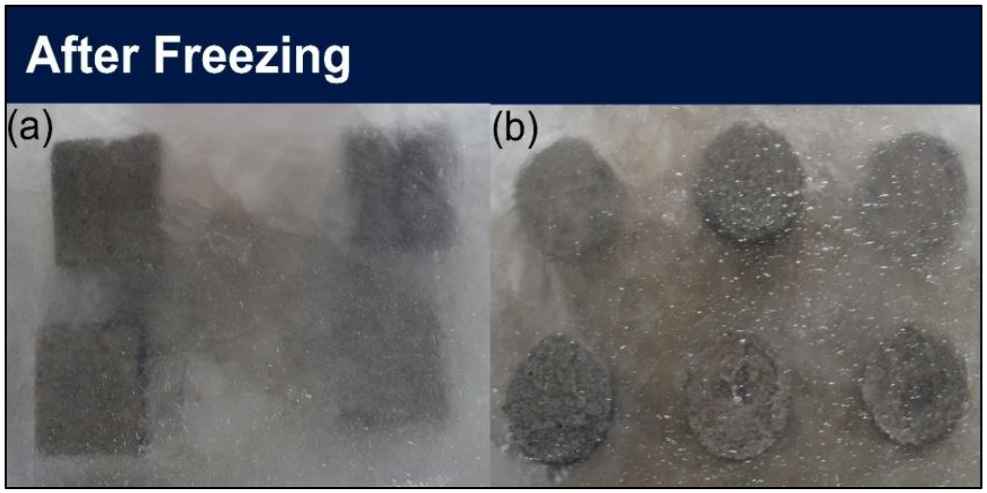

Figure 3.16: Specimen after Freezing in Freezing-Thawing Exposure in Sulfate Solution

3.4.3 Test Setup for the Microstructural Study

3.4.3.1 Field Emission Scanning Electron Microscopy (FESEM)

FESEM was executed to comprehend pore-morphological details and observe the reactivity extent of the outcome indeed. This test was conducted through QUANTA FEG 250 unit. Samples with irregular shape were collected at the time of crushing. The geopolymer samples were selected as a small scrap (very small cheap) form to perform this study. To have best outcome in this research, scraps were collected from inner part of the specimen. Sometimes grinding or polishing were done for FESEM analysis for better image indeed.

Figure 3.17: Field Emission Scanning Electron Microscopy Unit

3.4.3.2 Scanning Electron Microscopy (SEM) and Energy Dispersive X-ray (EDX) Analysis

SEM was conducted by QUANTA 2000 with a capacity of 2.4 nm at 30 kv at high vacuum condition to study the reaction status and morphological characteristics of the reacted products. Microstructure of specimens from fractured test specimens, were observed. With the aid of ED spectrometer, few selected spots were considered for further analysis to have elemental configuration. It is a fact that SEM is not sufficient to gather proper statistics regarding the distribution and measurement of pores clearly. Previous investigation suggests that minimum 25 mm^2 of sampling area is needed to obtain a reliable result [69]. For this test, samples were collected in the form of chips from fractured test specimens. But the size of the samples was kept about 5-8 mm. Age for each sample was kept more or less same so as to eliminate the effects due to time.

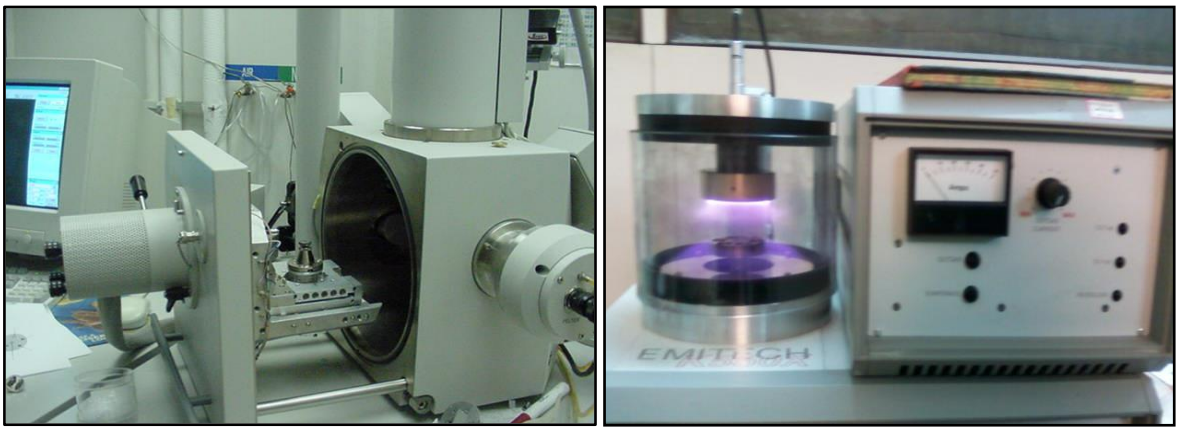

Figure 3.18: QUANTA 2000 for Scanning Electron Microscope

3.4.3.3 X-Ray Diffraction Analysis

X-Ray Diffractometer unit of model PAN analytical X-PERT PRO was used to determine the electron spreading outline of the solid sample in powder form. Cu Kα anticathode, 1.54A^{o} (wavelength) was used to record X-ray diffractograms from 5^{o} to 140^{o}, 2-theta range in a manner to get the mineralogical information. In some cases X-ray diffraction analysis was also made using Rigaku Mini Flex machine with Cu-Kα radiation with 40 kV, 22.5 mA. The methodology of X-ray diffractometer is established on the principal of Bragg [69]. This principle demonstrates the correlation of electron emission to the mineralogical formation. The formation allows the availability of information regarding the geometrical orientation of typical atoms. It is expressed by the equation $\lambda = 2\ d \sin\theta$, here λ and θ indicate the wavelength of emitting energy and angle of occurrence. In powder method, λ is conserved persistent while the emission angle is changeable. As per Bragg's principal the angle is marked corresponding to the emission with peak value. The peak value and d spacing (lift of electron) is plotted then. Each compound formation of the structure is characterized by a set diagram. In the XRD diagram the prime matter of finding in connection with developed compounds correspond to the recorded peaks. For information, hump shaped XRD features is observed for amorphous structural configuration. At this case the arrangement of atoms is supposed to be poorly organized [26]. When the component is partially crystalline, the shape is appeared through halo formation with a group of peaks. For example, slags (typically glassy) presents both halo diagram and halo- peaks spectrum [95]. X-ray diffraction technique was convenient method for mineralogical analysis of new trend of geopolymer with varying parameters in this study.

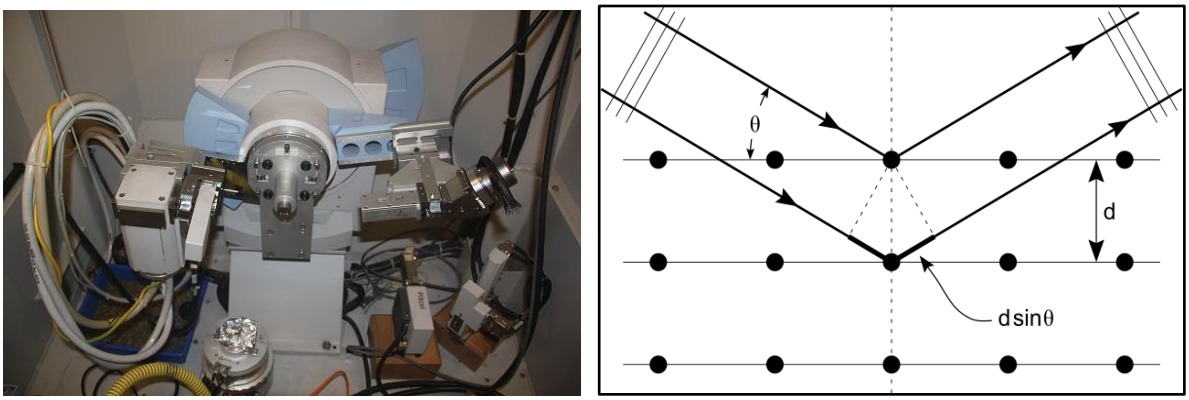

Figure 3.19: X-Ray Diffractometer Unit for X-Ray Diffraction Analysis and its Mechanism

3.4.3.4 MIP Analysis

MIP (Mercury Intrusion Porosimetry) provides PSD distribution curve for penetrable pores in the form of pore volume versus apparent pore entry radius. In these study section was prepared by cutting a cylinder with a dimension of ¼ inch diameter to ½ inch height by concrete cutter. The sample had a bulk volume of 1 cc. Micromeritics Autopore II set up was used at CGCRI, Kolkata. The test was conducted at a pressure of 0 to 60,000 psi. The mercury surface tension was maintained as 480.000 erg/sq.cm. with the angle of contact (I) equal to 140.000, (E) 140.000. MIP test reposts on the typical statistics regarding mean-median size of pores, distribution of pores, total porosity, bulk density and apparent density. Mercury was intruded under pressure in an evacuated sample and volume of intruded mercury was checked against pressure. Mercury intrusion procedure (being a non-wetting liquid) within the solids (especially for cement based materials and ceramics), follows Washburn's equation. The equation actually relates the pressure to equivalent pore entry radius. In this way, radius versus intruded volume curves could be obtained. The function of distribution was represented through F = - dV / d log D, where V is the combined volume of pores. This was indicative of towards the portion as a function within the range of typical diameter of pores which is yielded volume of pores within that array.

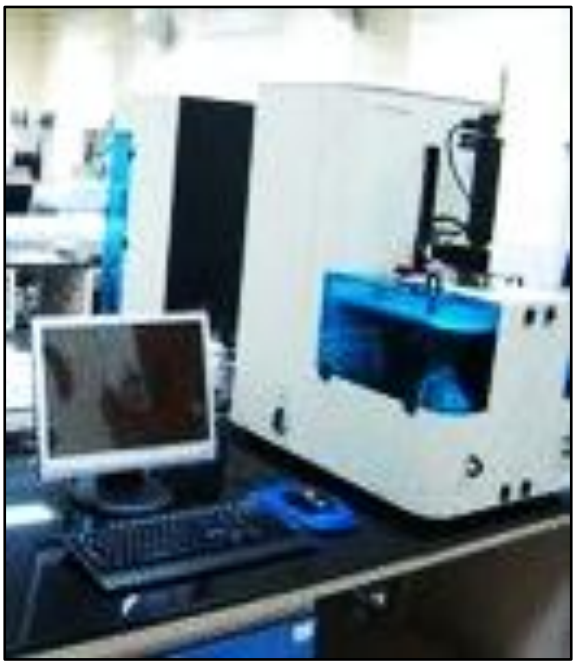

Figure 3.20: Micromeritics Autopore for MIP

3.4.3.5 Thermo Gravimetric Analysis (TGA)

Thermo Gravimetric Analysis was done using Thermo Gravimetry or Differential Thermal Analyzer (TG/DTA), a system made by Perkin Elmer. The testing was aimed to regulate structural aquatic content by the variation of weight and heat energy. Throughout the phase transition, the temperature value was controlled within the range of 30ºC to 1000ºC.

Figure 3.21: Thermo Gravimetry/Differential Thermal Analyser

3.5 Typical outline of the different phases of the entire experimental investigation

3.5.1 Preamble

The whole experimental program has been suitably designed to appreciate the changes of non-blended and blended fresh and hardened geopolymer along with microstructural and mineralogical changes to understand and overcome present problems as indicated in earlier chapters to trace the correct pathway to have high performance geopolymer.

Phase 1: Activator and its impact on non-blended Fly ash Geopolymer

At the very early stage, this research includes the review on fundamental chemistry of non-blended fly ash based geopolymer and its control parameters, like processing of raw materials, mix proportion, activator combination, mixing and curing regime etc. But before finding the effect of the blending of supplements with base material (fly ash), it is essential to fix up the general controlling parameters of the activator. Controlling parameters of activators imply the parameters of the activator itself which impact directly on the potentiality of the activator and the performance of the activated product. This phase of investigation was focused to find out the optimal value of the parameter like imposing temperature (by pre-heating) on activator prior use to manufacturing geopolymer. Furthermore, the existence of dual oxide in activator and its impact on the performance of the activated product was also examined.

Phase 2: Fly ash Geopolymer blended with supplementary Calcium compound

In the second stage of investigation, the research includes the concept of calcium blending to overcome drawbacks of fly ash geopolymer as indicated in earlier chapters. Blending of various supplementary materials like lime stone dust, blast furnace slag and the performance of alkali activated products, both in green and hardened state, have been experimentally studied. Parameters like alkali concentration, alkali oxide combination, curing types, curing factors in connection with physical, mechanical and microstructural and mineralogical features. Again, this research was focused towards the durability performance of blended geopolymer subjected to saline exposure, freezing thawing for short and long period. Study was made for both the heat cured and water cured blended geopolymer.

Phase 3: Fly ash Geopolymer blended with supplementary Silica compound

In the third stage, a study was made based on mechanical, durability and microstructural features of fly ash geopolymer blended with Silica fume. Again, various parameters like concentration of alkaline solution, water content in the mixture, base material, supplementary material, heat curing temperature and duration were discussed. Properties at fresh and hardened state were studied.

Comparative study on the performance of blended and non-blended fly ash based geopolymer related to strength and durability along with XRD, TGA, MIP and EDAX, have been made.

3.5.2 Study on Activator and its Impact on Non-blended Fly ash Geopolymer

3.5.2.1 Temperature Imposed (By Pre-Heating) On Activator Prior Mixing to Manufacture Geopolymer

This part of the experimental investigation was focused towards the assessment of the consequence of imposing temperature on alkaline solution prior mixing to manufacture geopolymer and to appreciate the characteristics of the developed product. NaOH solution (Na_2O - 8%) was exposed to varying temperatures from 15^oC to 95^oC, for a period of 24 hours. Then sodium silicate was added prior to mixing to manufacture geopolymer. Workability and strength parameters are compared. Scanning Electron Microscopy (SEM) and Energy-dispersive X-ray spectroscopy (EDX) have been done to appreciate the variations micro-structure along with the mineralogical status.

3.5.2.2 Blended Alkali activator with dual Alkali oxide

This part dealt with parametric study of geopolymer paste resulting from various combination of alkali activation (dual oxide). In this section, four series of geopolymer paste were prepared by activating fly ash (class F). Prior mixing activator to manufacture geopolymer mixing, the activators were kept under a controlled temperature (35^oC) for 24 hours. The geopolymer specimens were subjected to heat curing at 85^oC temperature for 48 hours. The parameters like compressive strength (3days and 28 days), workability and micro-structural (SEM) and mineralogical change (EDAX) were compared.

3.5.3 Study on Fly ash Geopolymer with Supplementary Calcium compound

3.5.3.1 Fly ash Geopolymer blended with Lime stone dust and its mechanical properties

This part dealt with fly ash based geopolymer blended with lime stone dust as calcium supplements was investigated. Lime stone dust(as supplementary material) up to 15 wt. % and remaining portion fly ash were mixed together. Sodium silicate solution (Na_2SiO_3) and Sodium hydroxide (NaOH) was treated as alkali. The silicate modulus (SiO_2/Na_2O) was maintained as 1.00. The Na_2O percentage in the activator was kept at 8% of the total mass of fly ash plus lime stone dust. Three typical series of mix were subjected to varying curing regime like the curing exposure at 35^oC to 85^oC for 24 and 48 Hrs. The workability and compressive strength were assessed. A link between the mechanical properties, curing regime (curing temperature and period) and mixing parameters was scientifically interpreted.

3.5.3.2 Microstructure with Mechanical performance of Lime stone dust

The objective of the investigation was to find the effect of lime stone dust as a supplement on the physico-mechanical and microstructural properties of fly ash geopolymer. 0 wt. %, 10wt. % and 15wt. % of lime stone dust of total was incorporated in fly ash to prepare geopolymer. Sodium silicate solution (Na_2SiO_3) and sodium hydroxide (NaOH) pellets were mixed keeping the silicate modulus SiO_2/ Na_2O =1. The percentage of Na_2O was kept at 8% of the total mass of Fly ash plus lime stone dust. Three series of mix were subjected to controlled-temperature (65°C) curing temperature for a period of 48 Hrs. Firstly, the compressive strength (considering aging also), apparent porosity, sorptivity and water absorption tests were conducted to have basic mechanical performance of geopolymer pastes. Microstructure categorisation of the developed products were executed by the scanning electron microscopy (SEM), (EDX) and Mercury intrusion porosimetry (MIP).

3.5.3.3 Durability Study on Fly ash Geopolymer blended with Lime Stone Dust

This part consists of studies to find the influence of the incorporation of lime stone dust on durability performance of the blended fly ash geopolymer product. Lime stone dust from 10wt. % to 15 wt. % of the total (fly ash plus supplements) was incorporated. In the activator, Na_2O and SiO_2 content were maintained as 8 wt. % of fly ash and SiO_2/Na_2O = 1. Water to total material (base plus supplements) was taken as 0.33. In this program blended geopolymer samples were submerged in a 10% magnesium sulfate solution up to an exposure duration of 15 weeks. The resistivity was examined by monitoring visual appearance, change in weight and compressive strength with time.

3.5.3.4 Development of Fly ash Geopolymer blended with Slag and its properties

In this section, fly ash geopolymer were developed by incorporating blast furnace slag as supplement in the mix (slag content 0 wt. %, 10 wt. % and 15 wt. % of the total of fly ash plus slag). Percentage of Na_2O content in the activator solution was 6% and 8% of the total weight of fly ash plus supplements. Effect of SiO_2 content in the activator was studied by changing the silicate modulus of the activator by 0, 1 and 1.5. Again different curing regimes (temperature of 35ºC, 55ºC, 85ºC for 1 day and 2 days duration) were considered to observe the performance of fly ash geopolymer with slag as supplementary material. The workability and compressive strength were recorded. The main objective was to regulate the mixed design parameter like percentage of alkali, silicate modulus in a way to obtain the best possible performance of the blended geopolymer.

3.5.3.5 Microstructure with Mechanical performance of Fly Ash Geopolymer blended with Slag

This part of investigation aims to study the performance of blended fly ash geopolymer (in presence of slag as supplementary material) at curing temperature of 85^{o}C for 48 hours. Slag content varies i.e. 0 wt. %, 10 wt. % and 15 wt. % of (fly ash plus slag). Activator composition was kept constant (8% Na_2O and silicate modulus =1). In fact, the developed semi-crystallized compound within the amorphous structure, creates internal pore pressure for non-blended fly ash geopolymer with age. This increased pressure enhances the compressive strength of fly ash geopolymer paste initially but causes micro-cracks later on, under extreme pore pressure. Strength was monitored and optimized through long time observation. Investigation including MIP, SEM, EDX was conducted to appreciate the changes in physical, mechanical and microstructural characteristics of fly ash geopolymer due to incorporation of slag.

3.5.3.6 Durability study on Fly ash Geopolymer blended with Slag

This part of investigation aims at to study the impact of slag as supplements on durability of blended fly ash geopolymer specimens. Water to total material (base material plus supplement) ratio was of 0.33. Na_2O content of activator is equal to 8 wt. % of (fly ash plus slag). SiO_2/Na_2O ratio was kept equal to 1. Geopolymer specimens were subjected to 10% concentrated magnesium sulfate solution up to 15 weeks. Periodical observation of its resistivity in aggressive medium was checked in terms of visual appearance, change in weight and residual strength. Long term durability test was conducted imposing alternative freezing-thawing cycle on different specimens submerged in sulfate solution for one year. The experiment was conducted in a Freeze- Thaw set up, where the individual specimen was exposed (immerged) to 20% concentrated Magnesium sulfate solution. This section is focused to the long time durability test for fly ash geopolymer with the incorporation of blast furnace slag as supplement. Performance of blended fly ash geopolymer specimens (15% slag as supplementary material) were compared to non-blended geopolymer specimens.

3.5.3.7 Fly ash Geopolymer blended with Slag (Water cured)

In this part of the investigation slag was taken 15% as supplementary material. The percentage Na_2O in activator solution (Sodium hydroxide plus Sodium silicate) was 6% of total material (fly ash + slag). Low alkalinity was preferred to investigate the effect of delayed water curing after 2 hours to 24 hours rest period in the formation of zel as along with calcium silicate hydrate (CSH) zel. The aqueous condition (mixture of fly ash and activator) is thermodynamically suitable for the geopolymeric reaction itself. Only heat is required to

initiate the primary poly-condensation. The presence of external calcium compound in the presence of delayed water curing may include secondary heat input to enhance the formation of partial polymer with CSH precipitation. To analyze the mechanical, microstructural, mineralogical and durability properties of the product, compressive strength, FESEM, XRD, TGA, DTA and freezing-thawing under sulfate exposure tests, were carried out.

3.5.4 Study on Fly ash Geopolymer blended with Supplementary Silica compound

3.5.4.1 Development of Fly ash Geopolymer blended with Silica fume in presence of Borax and its performance

This investigation was carried out to study mechanical, microstructural and durability characteristics of fly ash geopolymer blended with Silica Fume and Borax as primary and secondary supplements respectively. In fact fly ash itself contains silica and alumina, which is essential for geopolymerization but adequate amount of highly reactive silica may be effective for quick geopolymerization. Potassium hydroxide pellets and sodium silicate solution, were considered for making the activator solution. Alkaline activator was prepared from potassium hydroxide and sodium silicate solution, keeping 6% K_2O concentration in activator. In mixture, silicate solution was reduced to a great extent (i.e. SiO_2 from 6% to 0.6%) to find the role of reactive silica fume as a better alternative of silicate solution. Silica fume and Borax were used as supplementary material with fly ash up to 10% and 5% by weight respectively. The samples were heat cured at 85°C for 48 hours. Parameters like workability and strength along with microstructural studies were conducted to examine the influence of primary supplementary material (silica fume). The categorization of the different specimens were done through tests like SEM, EDX and MIP. Again, specimens were exposed to a 10% magnesium sulfate solution for 12 months. At prefixed interval of time, the physical and mechanical performance of geopolymer specimens, were examined.

3.5.4.2 Physical and Microstructural study on Fly ash Geopolymer blended with Silica Fume and Murram

In this part of the investigation, Murram was used as a compensator of additional alumina rather than borax. Silica fume was substituted for fly ash at the rate of 10% by weight. The K_2O concentration in the alkaline activator solution was taken as 6wt. % and 8wt. %, whereas the silicate modulus was considered as 1.0 and 0.0. The silicate modulus value zero indicates that the activator prepared without taking silicate solution. The macro and microstructural study of fly ash based geopolymer blended with silica fume and Murram were studied. Workability was assessed with the help of polar graph. Compressive strength was recorded. Mercury Intrusion Porosimetry, Scanning Electron Microscopy, Energy Dispersive X-Ray

Analysis (EDX) etc., were carried out to observe the change in microstructure of the composites with different combination of ingredients and activator parameters. This study was made to appreciate the correct path in achieving best possible geopolymer composite.

3.6 Geopolymer Mix proportion and other parameters

Mix proportion for geopolymer composites are furnished in the following tables. Sample proportion has also been presented along with the tables. Some calculations have been briefly provided in Appendix I.

3.6.1 Study on Activator parameters of Non-blended Fly ash based Geopolymer

Table 3.7: Mix composition of Alkali activator for studying effect of Temperature imposed on it before mixing

Activator ID	Temperature imposed on Hydroxide solution prior mixing	Na_2O content in activator (%) of total material	Silicate modulus (SiO_2/ Na_2O)	SiO_2 content in activator (%) of total material	Water / total material ratio	Curing Temp.	Curing Duration
PS15	15°C	8	1	8	0.33	85°C	48Hrs.
PS20	20°C	8	1	8	0.33	85°C	48 Hrs.
PS25	25°C	8	1	8	0.33	85°C	48 Hrs.
PS30	30°C	8	1	8	0.33	85°C	48 Hrs.
PS35	35°C	8	1	8	0.33	85°C	48 Hrs.
PS40	40°C	8	1	8	0.33	85°C	48 Hrs.
PS50	50°C	8	1	8	0.33	85°C	48 Hrs.
PS60	60°C	8	1	8	0.33	85°C	48 Hrs.
PS65	65°C	8	1	8	0.33	85°C	48 Hrs.
PS75	75°C	8	1	8	0.33	85°C	48 Hrs.
PS80	80°C	8	1	8	0.33	85°C	48 Hrs.
PS90	90°C	8	1	8	0.33	85°C	48 Hrs.
PS95	95°C	8	1	8	0.33	85°C	48 Hrs.

Sample Mix

Activator ID	Fly Ash (gm.)	Sodium silicate (gm.)	NaOH pellets (with 98% purity) (gm.)	Water added (gm.)
PS15	1000	302	74	116
PS20	1000	302	74	116
PS30	1000	302	74	116
PS35	1000	302	74	116
PS45	1000	302	74	116
PS50	1000	302	74	116
PS60	1000	302	74	116
PS65	1000	302	74	116
PS75	1000	302	74	116
PS80	1000	302	74	116
PS90	1000	302	74	116
PS95	1000	302	74	116

Table 3.8: Mix compositions for studying the effect of Dual oxide in activator on Non-blended Fly ash Geopolymer composites

Mix ID	X_2O* content in activator (%) of total material	Equivalent Silicate modulus (SiO_2/X_2O)	SiO_2 content in activator (%) of total material	K_2O Content in activator (%) of total material	Na_2O content in activator (%) of total material	Type of specimen	Water / total material ratio	Curing temp. and duration
GP1-L	8	0.5	4	0	8	Paste	0.33	85°C and 48 Hrs.
GP1	8	1.0	8	0	8	Paste	0.33	85°C and 48 Hrs.
GPX1-L	8	0.5	4	6.79	1.21	Paste	0.33	85°C and 48 Hrs.
GPX1	8	1.0	8	5.58	2.42	Paste	0.33	85°C and 48 Hrs.

Sample Mix

Mix ID	Fly Ash (gm.)	Sodium silicate (gm.)	NaOH pellets (with 98% purity) (gm.)	KOH pellets (with 84% purity) (gm.)	Water added (gm.)
GP1-L	1000	151	89	0	211
GP1	1000	302	74	0	116
GPX1-L	1000	151	0	96	216
GPX1	1000	302	0	79	120

X_2O refers the combination K_2O and Na_2O in activator. X refers the alkali cations in activator.

3.6.1.1 Details of specimens for studying Activator parameters of Non-blended Fly ash based Geopolymer

Properties to be evaluated	**Studying Parameters**	**State of Product**	**Test conducted**	**Form of test Sample**	**No of Distinctive Series**	**No of Cubical (5cm×5cm×5cm) Specimens required**
Physical & mechanical	Temperature Prior mixing 15^0 to 95^0	Green State	Workability	Fluid Gel	10	N/A*
		Hardened state	Compressive strength	Cubical solid	16	128 no. (Considering 8 no. per series)
Microstructural	X_2O** content 8% Silicate Modulus (0.5,1.0)		SEM & EDX	Scrap (small but greater than 25 mm^2)	16	N/A***
	***Test is conducted before molding **X_2O indicates combination of Na_2O & K_2O *** Test sample is collected from crushed specimens subjected to strength test.**					

3.6.2 Study on Fly ash Geopolymer blended with supplementary Calcium compound

Table 3.9 Mix compositions for Studying on Fly ash based Geopolymer blended with Lime stone dust at different Curing profile

Mix ID	Sample ID	Na_2O content in activator (%) of total material in wt.	SiO_2 content in activator (%) of total material in wt.	Lime stone dust (%) of total material by wt.	Type of specimen	Water / total material ratio	Curing temp.	Curing duration
GP1	GP1-LS	8	8	0	Paste	0.33	35ºC	24 Hrs.
	GP1-LL	8	8	0	Paste	0.33	35ºC	48 Hrs.
	GP1-MS	8	8	0	Paste	0.33	55ºC	24 Hrs.
	GP1-ML	8	8	0	Paste	0.33	55ºC	48 Hrs.
	GP1-HS	8	8	0	Paste	0.33	85ºC	24 Hrs.
	GP1-HL	8	8	0	Paste	0.33	85ºC	48 Hrs.
GL1	GL1-LS	8	8	10	Paste	0.33	35ºC	24 Hrs.
	GL1-LL	8	8	10	Paste	0.33	35ºC	48 Hrs.
	GL1-MS	8	8	10	Paste	0.33	55ºC	24 Hrs.
	GL1-ML	8	8	10	Paste	0.33	55ºC	48 Hrs.
	GL1-HS	8	8	10	Paste	0.33	85ºC	24 Hrs.
	GL1-HL	8	8	10	Paste	0.33	85ºC	48 Hrs.
GL2	GL2-LS	8	8	15	Paste	0.33	35ºC	24 Hrs.
	GL2-LL	8	8	15	Paste	0.33	35ºC	48 Hrs.
	GL2-MS	8	8	15	Paste	0.33	55ºC	24 Hrs.
	GL2-ML	8	8	15	Paste	0.33	55ºC	48 Hrs.
	GL2-HS	8	8	15	Paste	0.33	85ºC	24 Hrs.
	GL2-HL	8	8	15	Paste	0.33	85ºC	48 Hrs.

Sample Mix

Mix ID	Sample ID	Fly Ash (gm.)	Lime stone (gm.)	Sodium silicate (gm.)	NaOH pellets (with 98% purity) (gm.)	Water added (gm.)
GP1	GP1-LS	1000	0	302	74	116
	GP1-LL	1000	0	302	74	116
	GP1-MS	1000	0	302	74	116

	GP1-ML	1000	0	302	74	116
	GP1-HS	1000	0	302	74	116
	GP1-HL	1000	0	302	74	116
GL1	GL1-LS	900	100	302	74	116
	GL1-LL	900	100	302	74	116
	GL1-MS	900	100	302	74	116
	GL1-ML	900	100	302	74	116
	GL1-HS	900	100	302	74	116
	GL1-HL	900	100	302	74	116
GL2	GL2-LS	850	150	302	74	116
	GL2-LL	850	150	302	74	116
	GL2-MS	850	150	302	74	116
	GL2-ML	850	150	302	74	116
	GL2-HS	850	150	302	74	116
	GL2-HL	850	150	302	74	116

Table 3.10 Mix compositions for studying on Microstructure and Mechanical performance of Fly ash based Geopolymer blended with Lime stone dust

Mix ID	**Na_2O Content in activator (%)**	**SiO_2 content in activator (%)**	**Lime stone dust (% by Wt. of total material)**	**Type of specimen**	**Water / total material ratio**	**Curing temp. and duration**
GP1	8	8	0	Paste	0.33	**65°C and 48 Hrs.**
GL1	8	8	10	Paste	0.33	**65°C and 48 Hrs.**
GL2	8	8	15	Paste	0.33	**65°C and 48 Hrs.**
Sample Mix						
Mix ID	**Fly Ash (gm.)**	**Lime stone dust (gm.)**	**Sodium silicate (gm.)**	**NaOH pellets (with 98% purity) (gm.)**		**Water added (gm.)**
GP1	1000	0	302	74		116
GL1	900	100	302	74		**116**
GL2	850	150	302	74		116

Table 3.11 Mix compositions for Durability study on Fly ash based Geopolymer blended with Lime stone dust

Mix ID	Na_2O Content in activator (%)	SiO_2 content in activator (%)	Lime stone dust (% by Wt. of total material)	Type of specimen	Water / total material ratio	Curing temp. and duration
GP1	8	8	0	Paste	0.33	65ºC and 48 Hrs.
GL1	8	8	10	Paste	0.33	65ºC and 48 Hrs.
GL2	8	8	15	Paste	0.33	65ºC and 48 Hrs.
Sample Mix						
Mix ID	**Fly Ash (gm.)**	**Lime stone dust (gm.)**	**Sodium silicate (gm.)**	**NaOH pellets (with 98% purity) (gm.)**	**Water added (gm.)**	
GP1	1000	0	302	74	116	
GL1	900	100	302	74	116	
GL2	850	150	302	74	116	

Table 3.12 Mix compositions for studying on Fly ash based Geopolymer blended with slag at different Curing profile

Mix ID	Sample ID	Na_2O content in activator (%) of total material by wt.	SiO_2 content in activator (%) of total material by wt.	Blast furnace slag (%) of total material in wt.	Type of specimen	Water / total material ratio	Curing temp.	Curing duration
GP1	GP1-LS	8	8	0	Paste	0.33	35ºC	24 Hrs.
	GP1-LL	8	8	0	Paste	0.33	35ºC	48 Hrs.
	GP1-MS	8	8	0	Paste	0.33	55ºC	24 Hrs.
	GP1-ML	8	8	0	Paste	0.33	55ºC	48 Hrs.
	GP1-HS	8	8	0	Paste	0.33	85ºC	24 Hrs.
	GP1-HL	8	8	0	Paste	0.33	85ºC	48 Hrs.
GB1	GB1-LS	8	8	10	Paste	0.33	35ºC	24 Hrs.
	GB1-LL	8	8	10	Paste	0.33	35ºC	48 Hrs.
	GB1-MS	8	8	10	Paste	0.33	55ºC	24 Hrs.
	GB1-ML	8	8	10	Paste	0.33	55ºC	48 Hrs.

	GB1-HS	8	8	10	Paste	0.33	85ºC	24 Hrs.
	GB1-HL	8	8	10	Paste	0.33	85ºC	48 Hrs.
GB2	GB2-LS	8	8	15	Paste	0.33	35ºC	24 Hrs.
	GB2-LL	8	8	15	Paste	0.33	35ºC	48 Hrs.
	GB2-MS	8	8	15	Paste	0.33	55ºC	24 Hrs.
	GB2-ML	8	8	15	Paste	0.33	55ºC	48 Hrs.
	GB2-HS	8	8	15	Paste	0.33	85ºC	24 Hrs.
	GB2-HL	8	8	15	Paste	0.33	85ºC	48 Hrs.

Sample Mix

Mix ID	Sample ID	Fly Ash (gm.)	Slag (gm.)	Sodium silicate (gm.)	NaOH pellets (with 98% purity) (gm.)	Water added (gm.)
GP1	GP1-LS	1000	0	302	74	116
	GP1-LL	1000	0	302	74	116
	GP1-MS	1000	0	302	74	116
	GP1-ML	1000	0	302	74	116
	GP1-HS	1000	0	302	74	116
	GP1-HL	1000	0	302	74	116
GB1	GB1-LS	900	100	302	74	116
	GB1-LL	900	100	302	74	116
	GB1-MS	900	100	302	74	116
	GB1-ML	900	100	302	74	116
	GB1-HS	900	100	302	74	116
	GB1-HL	900	100	302	74	116
GB2	GB2-LS	850	150	302	74	116
	GB2-LL	850	150	302	74	116
	GB2-MS	850	150	302	74	116
	GB2-ML	850	150	302	74	116
	GB2-HS	850	150	302	74	116
	GB2-HL	850	150	302	74	116

Table 3.13 Mix compositions for studying on Fly ash based Geopolymer blended with Slag under different Curing profile and Alkali concentration

Mix ID	Activator		Blast furnace slag (%) of total material in wt.	Type of specimen	Water / total material ratio
	%Na_2O	Silicate Modulus			
GP-L	6%	0.5	0	Paste	0.33
GP	6%	1	0	Paste	0.33
GP-H	6%	1.5	0	Paste	0.33
GP1-L	8%	0.5	0	Paste	0.33
GP1	8%	1	0	Paste	0.33
GP1-H	8%	1.5	0	Paste	0.33
GB-L	6%	0.5	15	Paste	0.33
GB	6%	1	15	Paste	0.33
GB-H	6%	1.5	15	Paste	0.33
GB2-L	8%	0.5	15	Paste	0.33
GB2	8%	1	15	Paste	0.33
GB2-H	8%	1.5	15	Paste	0.33

Hot Curing Exposure regimes								
Curing Duration→	24 Hours				48 Hours			
Curing Temperature→	55°C	65°C	75°C	85°C	55°C	65°C	75°C	85°C

Sample Mix

Mix ID	Fly Ash (gm.)	Slag (gm.)	Sodium silicate (gm.)	NaOH pellets (with 98% purity) (gm.)	Water added (gm.)
GP-L	1000	0	113	67	241
GP	1000	0	226	55	169
GP-H	1000	0	340	43	98
GP1-L	1000	0	151	89	211
GP1	1000	0	302	74	116
GP1-H	1000	0	453	58	20
GB-L	850	150	113	67	241
GB	850	150	226	55	169

GB-H	850	150	340	43	98
GB2-L	850	150	151	89	211
GB2	850	150	302	74	116
GB2-H	850	150	453	58	20

Table 3.14 Mix composition for studying on Microstructure of Slag blended Fly ash Geopolymer

Mix ID	**Na_2O content in activator (%) of total material in wt.**	**SiO_2 content in activator (%) of total material in wt.**	**Blast furnace slag (%) of total materialin wt.**	**Type of specimen**	**Water / total material ratio**	**Curing temp. and duration**
GP1	8	8	0	Paste	0.33	85ºC and 48 Hrs.
GB1	8	8	10	Paste	0.33	85ºC and 48 Hrs.
GB2	8	8	15	Paste	0.33	85ºC and 48 Hrs.
Sample Mix						
Mix ID	**Fly Ash (gm.)**	**Slag (gm.)**	**Sodium silicate (gm.)**	**NaOH pellets (with 98% purity) (gm.)**		**Water added (gm.)**
GP1	1000	0	302	74		116
GB1	900	100	302	74		116
GB2	850	150	302	74		116

Table 3.15 Mix composition for Durability study on Fly ash Geopolymer blended with Blast furnace slag

Mix ID	Na_2O content in activator (%)	SiO2 content in activator (%)	Blast Furnace Slag (% by wt. of total material)	Type of specimen	Water / total material ratio	Curing temp. and duration
GP1	8	8	0	Paste	0.33	85°C and 48 Hrs.
GB1	8	8	10	Paste	0.33	85°C and 48 Hrs.
GB2	8	8	15	Paste	0.33	85°C and 48 Hrs.
Sample Mix						
Mix ID	**Fly Ash (gm.)**	**Slag (gm.)**	**Sodium silicate (gm.)**	**NaOH pellets (with 98% purity) (gm.)**		**Water added (gm.)**
GP1	1000	0	302	74		116
GB1	900	100	302	74		116
GB2	850	150	302	74		116

Table 3.16 Mix composition for studying Activated Fly ash blended with Slag under water curing

Mix ID	Sample ID	Na_2O content in activator (%)	SiO_2 content in activator (%)	Blast Furnace Slag (% by wt. of total material)	Type of specimen	Water / total material ratio	Rest period after mixing (Hrs.)	Curing type
GB	GB_R(2)_WC	6	6	15	Paste	0.33	2	Water curing
	GB_R(4)_WC	6	6	15	Paste	0.33	4	Water curing
	GB_R(6)_WC	6	6	15	Paste	0.33	6	Water curing
	GB_R(8)_WC	6	6	15	Paste	0.33	8	Water curing
	GB_R(10)_WC	6	6	15	Paste	0.33	10	Water curing
	GB_R(12)_WC	6	6	15	Paste	0.33	12	Water curing

	GB_R(14)_WC	6	6	15	Paste	0.33	14	Water curing
	GB_R(16)_WC	6	6	15	Paste	0.33	16	Water curing
	GB_R(18)_WC	6	6	15	Paste	0.33	18	Water curing
	GB_R(20)_WC	6	6	15	Paste	0.33	20	Water curing
	GB_R(22)_WC	6	6	15	Paste	0.33	22	Water curing
	GB_R(24)_WC	6	6	15	Paste	0.33	24	Water curing

Sample Mix

Mix ID	Sample ID	Fly Ash (gm)	Slag (gm)	Sodium silicate (gm)	NaOH pellets (with 98% purity) (gm)	Water added (gm)
GB	GB_R(2)_WC	850	150	226	55	169
	GB_R(4)_WC	850	150	226	55	169
	GB_R(6)_WC	850	150	226	55	169
	GB_R(8)_WC	850	150	226	55	169
	GB_R(10)_WC	850	150	226	55	169
	GB_R(12)_WC	850	150	226	55	169
	GB_R(14)_WC	850	150	226	55	169
	GB_R(16)_WC	850	150	226	55	169
	GB_R(18)_WC	850	150	226	55	169
	GB_R(20)_WC	850	150	226	55	169
	GB_R(22)_WC	850	150	226	55	169
	GB_R(24)_WC	850	150	226	55	169

3.6.2.1 Details of specimens for study on Fly ash Geopolymer blended with supplementary Calcium compound

Properties to be evaluated	Studying Parameters	State of Product	Test conducted	Form of test Sample	No of Distinctive Series	No of Cubical (5cm×5cm×5cm) Specimens required
Physical & Mechanical	Fly ash geopolymer Blended with lime stone dust (10% & 15%) Fly ash geopolymer Blended with blast furnace slag (10% & 15%) Variation of curing regime 35^0 to 85^0@ 24 to 48 Hrs. on calcium blended geopolymer Na_2O content 6% & 8% with silicate modulus 0.5, 1.0 & 1.5 for calcium blended geopolymer Saline exposure*** and freezing thawing effect on calcium blended geopolymer Rest period and water curing after mixing (2 to 24 hr) on calcium blended geopolymer	Green State	Workability	Fluid Gel	05	N/A*
		Hardened state	Compressive strength	Cubical solid	131	1242 no. (Considering 6 no. per series)
			Water Absorption		06	36 no. (Considering 3 no. per series)
			Apparent Porosity		06	
			Sorptivity		06	
Microstructural			SEM & EDX	Scrap (small but greater than 25 mm^2)	06	N/A**
			FESEM		02	
			MIP	Cubical Solid $1cm^3$ Volume	04	
			XRD	Dust	03	
Durability			Weight Change	Cubical solid	06	42 no. (Considering saline & freezing thawing exposure)
				Cylindrical solid	02	24 no. (freezing thawing exposure)
			Residual Strength	Cubical solid	06	42 no. (Considering saline & freezing thawing exposure)
				Cylindrical solid	02	24 no. (freezing thawing exposure)
			Physical change	Cubical solid	06	14 no. (Considering saline & freezing thawing exposure)
				Cylindrical solid	02	8 no. (freezing thawing exposure)
	*Test is conducted before molding ** Test sample is collected from crushed specimens subjected to strength test. ***Exposure in 20% Concentration Magnesium Sulfate					

3.6.3 Study on Fly ash Geopolymer blended with supplementary Silica compound

Table 3.17 Mix composition for studying the development of Fly ash Geopolymer blended with Silica fume in presence of Borax and its performance

Sample Id.	Fly Ash* (%)	Silica Fume * (%)	Borax* (%)	K_2O Content in activator (%)	Apparent silicate modulus (SiO_2/K_2O in activator)	SiO_2 content in activator (%)	Water* (%)	Curing temp. and duration
GPC	100	0.0	0.0	6	1.0	6	33	85°C and 48 Hrs.
GPC-M	100	0.0	0.0	6	0.1	0.6	33	85°C and 48 Hrs.
GSC	90	10	0.0	6	1.0	6	33	85°C and 48 Hrs.
GSCB1	90	7.5	2.5	6	1.0	6	33	85°C and 48 Hrs.
GSCB2	90	5.0	5.0	6	1.0	6	33	85°C and 48 Hrs.
GSCB2-M	90	5.0	5.0	6	0.1	0.6	33	85°C and 48 Hrs.

Sample Id.	Fly Ash (gm)	Silica Fume (gm)	Borax (gm)	Sodium Silicate (gm)	KOH pellets (with 84% purity) (gm)	Water added (gm)
GPC	1000	0.0	0.0	226	85	168
GPC-M	1000	0.0	0.0	22.64	85	301
GSC	900	100	0.0	226	85	168
GSCB1	900	75	25	226	85	168
GSCB2	900	50	50	226	85	168
GSCB2-M	900	50	50	22.64	85	301

**of (fly ash + silica fume + borax) in weight*

Table 3.18 Mix composition for studying the development of Fly ash Geopolymer blended with Silica fume in presence of Murram and its performance

Sample Id	Silica Fume* (%)	Murram* (%)	K_2O content in activator (%)	Apparent silicate modulus SiO_2/K_2O in activator	SiO_2 content in activator* (%)	Water* (%)
GPC-1	0.0	0.0	8	1.0	8	33
GPC1-N	0.0	0.0	8	0.0	0	33
GPC	0.0	0.0	6	1.0	6	33
GPC-N	0.0	0.0	6	0.0	0	33
GSC1	10	0.0	8	1.0	8	33
GSC1-N	10	0.0	8	0.0	0	33
GSC	10	0.0	6	1.0	6	33
GSC-N	10	0.0	6	0.0	0	33
GSC1R	10	2.5	8	1.0	8	33
GSC1R-N	10	2.5	8	0.0	0	33
GSCR	10	2.5	6	1.0	6	33
GSCR-N	10	2.5	6	0.0	0	33
GSC1R1	10	2.5	8	1.0	8	25
GSCR1	10	2.5	6	1.0	6	25

Sample Id.	Fly Ash (gm)	Silica Fume (gm)	Murram (gm)	Sodium silicate (gm)	KOH pellets (with 84% purity) (gm)	Water added (gm)
GPC-1	1000	0.0	0.0	302	113	114
GPC1-N	1000	0.0	0.0	0	113	312
GPC	1000	0.0	0.0	226	85	168
GPC-N	1000	0.0	0.0	0	85	316
GSC1	900	100	0.0	302	113	114
GSC1-N	900	100	0.0	0	113	312
GSC	900	100	0.0	226	85	168
GSC-N	900	100	0.0	0	85	316

GSC1R	875	100	25	302	113	114
GSC1R-N	875	100	25	0	113	312
GSCR	875	100	25	226	85	168
GSCR-N	875	100	25	0	85	316
GSC1R1	875	100	25	302	113	34
GSCR1	875	100	25	226	85	88

% of (fly ash + silica fume+ murram) in weight

3.6.3.1 Details of specimens for study on Fly ash Geopolymer blended with supplementary Silica compound

Properties to be evaluated	Studying Parameters	State of Product	Test conducted	Form of test Sample	No of Distinctive Series	No of Cubical (5cm×5cm×5cm) Specimens required
Physical & Mechanical	Fly ash geopolymer Blended with silica fume & borax with silicate modulus 0 & 1.0 at 6% of K_2O in activator Fly ash geopolymer Blended with silica fume & Murram with silicate modulus 0 to 1.0 in activator of K_2O by 6% to 8% Exposure in saline*** and ambient climate	Green State	Workability	Fluid Gel	14	N/A*
		Hardened state	Compressive strength	Cubical solid	59	354 no. (Considering 6 no. per series)
Microstructural			SEM & EDX	Scrap (small but greater than 25 mm^2)	09	N/A**
			MIP	Cubical Solid 1cm^3 Volume	6	
Durability			Weight Change & Residual Strength	Cubical solid	08	48 no. (Considering 6 no. per series)
			Physical change		4	24 no. (Considering 6 no. per series)
	*Test is conducted before molding **Test sample is collected from crushed specimens subjected to strength test. *** Exposure in 20% Concentration Magnesium Sulfate					

4. RESULT AND DISCUSSION

4.1 Preamble

Experimental investigation was conducted to understand the comparative performance of non-blended and blended fly ash based geopolymer. At the very outset parameters like premixing temperature of activator was investigated. This result was crucial in a way to fix up the manufacturing process of fly ash based geopolymer in different seasons. Different alkali combinations were tried and the selection of alkali combination was made judiciously. Then the investigation was made to study the impact of blending which compensate some remarkable properties in fly ash geopolymer i.e. instability of strength, lack of control on workability, lack of control on strength, heat curing etc. The performance and character of blended geopolymer in fresh and hardened state along with its microstructural changes was simultaneously analyzed. Parameter like workability, strength, sorptivity, apparent porosity, water absorption for blended fly ash based geopolymer were studied. Again, mineralogical and micro-structural changes and its comparison with non-blended fly ash based geopolymer was also studied. Result of the water cured blended geopolymer with varying rest period was observed. Durability study on blended geopolymer exposed to magnesium sulfate solution also under freezing-thawing cycle was studied. Different combinations of source materials were studied and compared with non-blended fly ash based geopolymer composites. The parameters like alkali concentration, curing profile, curing type etc. were considered. All the results was presented in graphical / tabular form. Discussions were based on scientific interpretations and broadly divided into three phases:

Phase I: Activator and its impact on Non-blended Fly ash based Geopolymer

At the very early stage, this research includes the review on fundamental chemistry of non-blended fly ash based geopolymer and its control parameters, like processing of raw materials, mix proportion, activator combination, mixing and curing regime etc. But before finding the effect of the blending of supplements with base material (fly ash), it is essential to fix up the general controlling parameters of the activator. Controlling parameters of activators imply the parameters of the activator itself which impact directly on the potentiality of the activator and the performance of the activated product. This phase of investigation was focused to find out the optimal value of the parameter like imposing temperature (by pre-heating) on activator prior use to manufacturing geopolymer. Furthermore, the existence of dual oxide in activator and its impact on the performance of the activated product was also examined.

Phase 2: Fly ash based Geopolymer blended with supplementary Calcium compound

In the second stage of investigation, the research includes the concept of calcium blending to overcome drawbacks of fly ash geopolymer as indicated in earlier chapters. Blending of various supplementary materials like lime stone dust, blast furnace slag and the performance of alkali activated products, both in green and hardened state, have been experimentally studied. Parameters like alkali concentration, alkali oxide combination, curing types, curing factors in connection with physical, mechanical and microstructural and mineralogical features. Again, this research was focused towards the durability performance of blended geopolymer subjected to saline exposure, freezing thawing for short and long period. Study was made for both the heat cured and water cured blended geopolymer.

Phase 3: Fly ash Geopolymer blended with supplementary Silica compound

In the third stage, a study was made based on mechanical, durability and microstructural features of fly ash geopolymer blended with Silica fume. Again, various parameters like concentration of alkaline solution, water content in the mixture, base material, supplementary material, heat curing temperature and duration were discussed. Properties at fresh and hardened state were studied.

Comparative study on the performance of blended and non-blended fly ash based geopolymer related to strength and durability along with SEM, FESEM, EDX, XRD, TGA/DTA and MIP, have been made .

4.2 Parameters of Activator and its impact on Non-Blended Fly ash Geopolymer

4.2.1 Physical Property

4.2.1.1 Workability

4.2.1.1.1 Effect of Temperature level of Activator on Workability of Fly ash based Geopolymer

The dissolution of alkali hydroxide in water is an exothermic reaction, which follows the equation like; XOH (aq) = X^+ (aq) + OH^- (aq) + (heat). The Le' Chatelier's principle depicts that, any chemical arrangement moves to counter if experienced any type of changes in its concentration, volume, imposing temperature, pressure etc., in a way to rebuild new equilibrium indeed [87]. Hence, with the increase in imposing temperature the backward reaction is accelerated which results to the slower rate of dissolution of alkali hydroxide. Now, the dissolution of alkali hydroxide directly affects the availability of Na^+ and OH^- in the mixture. It is established that the proper suspension of fly ash is facilitated by the presence of OH^- [140]. Again the development of Si–O–Al–O network is progressed along with the balancing of charge loading on Al atoms by Na^+ ions [39]. Therefore, optimal polymerization

is difficult unless sufficient amount of Na^+ and OH^- exists in the medium. So, existence of Na^+ and OH^- in the mixture, dissolution of fly ash and rate of polymerization are directly and indirectly subjected to the imposing temperature on the activator. Workability was expressed in terms of area factor, i.e. the ratio of the area of the unconfined paste to that of confined paste (described in Chapter-3). Better results were observed for an imposing temperature within the range of 35ºC to 60ºC. Unit area factor was observed for samples PS15 and PS90 (described in Chapter- 3; Table 3.7) when activators were imposed to 15ºC and 90ºC prior to mixing. Unit area factor indicated very low level of consistency. At an imposing temperature nearly 35^0C to 40^0C, the reactivity level of activator was supposed to be maximum in regard to activation process.

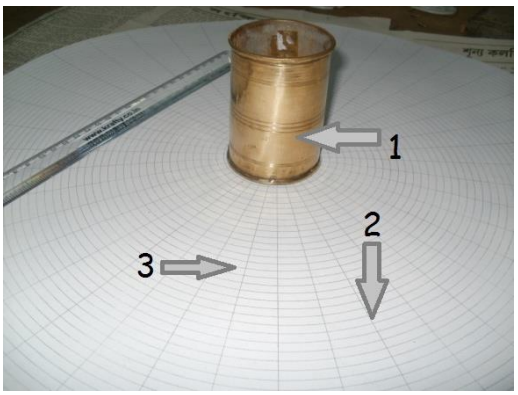

Figure 4.1 The experimental setup
1. Brass container 2.Polar graph 3.Glass slab.

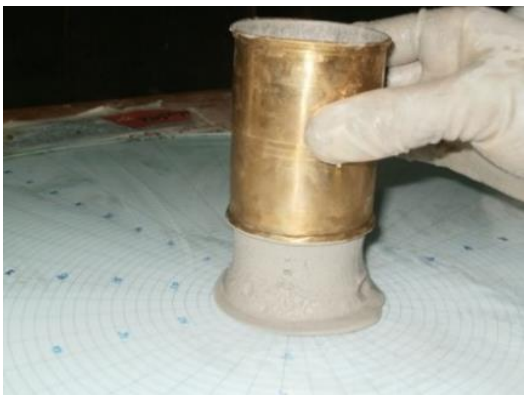

Figure 4.2 Flow of sample PS35

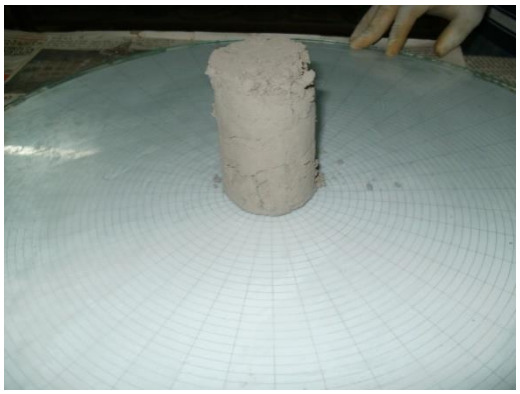

Figure 4.3 Zero flow for sample PS15 (Area factor =1)

Figure 4.4 Sample PS35 after flow (Area factor =13.44)

Table 4.1 Results of Workability test of the Geopolymer paste

Sample Id	Initial Diameter(D1) (cm)	Final equivalent Diameter (D2) (cm)	Initial Area (A1) (cm^2)	Final Area after flow (A2) (cm^2)	Area Factor=A2/A1
PS15	6	6	28.26	28.26	1.0
PS30	6	19	28.26	314	11.11
PS35	6	22	28.26	379.94	13.44
PS40	6	23	28.26	415.48	14.70
PS50	6	20	28.26	314.16	11.12
PS60	6	18	28.26	254.34	9.0
PS75	6	9	28.26	63.585	2.25
PS90	6	6	28.26	28.26	1.0

4.2.1.1.2 Effect of dual oxides in Activator (K_2O+Na_2O) on Workability of Fly ash based Geopolymer

The GP1-L, GPX1 (described in Chapter-3; Table 3.8) indicated better consistency and adhesiveness in compare to GPX1-L and GP1 respectively. The polymerization is initiated with sodium silicate at the infancy stage. It means at the very earlier stage polymerization is started with the SiO_2 presence in sodium silicate rather than the same in fly ash. But after that the formation of monomer, diamer, triamer, smaller oligomer, oligomer and polymer occurred successively. The SiO_2 presence in fly ash participates at this stage. So, at the initial level presence of smaller oligomers or larger oligomers extensively depend on the quantity of sodium silicate at the mixture [31]. It is already explained that Na^+ and K^+ affect differently mainly because of dissimilar size though having the same charges. The cation of smaller size makes the ion-pair reaction better with the smaller silicate oligomers, like silicate monomers, dimers and trimers [55], [91], [121]. Again, larger silicate oligomers increase significantly which can be better coordinated by K^+ cation having larger size, which evidently leads to a higher extent of geopolymerization [137].Here also higher presence of silicate (due to the addition of more silicate solution) enhances the activity of potassium regarding synthesis.Table:4.2 indicates better synthesis with potassium hydroxide at higher silicate modulus and better synthesis with sodium hydroxide at lower silicate modulus.

Table 4.2 Results of Workability test of the Geopolymer paste

Sample Id	Initial Diameter (D1) (cm)	Final equivalent Diameter (D2) (cm)	Initial Area (A1) (cm^2)	Final Area after flow (A2) (cm^2)	Area Factor=A2/A1
GP1-L	6	19	28.26	283.45	10.03
GP1	6	22	28.26	379.94	13.44
GPX1-L	6	17	28.26	226.86	8.03
GPX1	6	25	28.26	490.62	17.36

4.2.1.2 Compressive strength

4.2.1.2.1 Effect of Temperature level of Activator on Compressive strength of Fly ash based Geopolymer

3-day compressive strength of the geopolymer paste is presented in Figure 4.5. Specimen PS35 showed maximum compressive strength. Temperature level of activator ranging between 30ºC to 60ºC, indicated higher strength. However, in other range of temperature level, showed lower strength. Minimum compressive strength value of 14 MPa was obtained for specimen PS15 and for specimen PS95, the strength was around 18 MPa. The result indicates the impact of induced temperature level on the performance of activator as well as the performance of activated product.

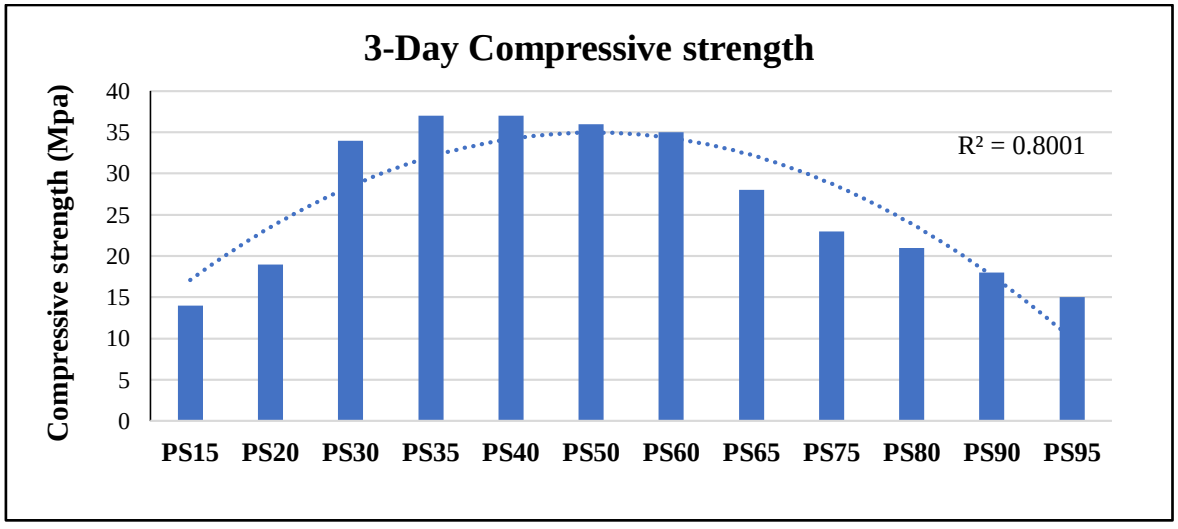

Figure 4.5 3-day Compressive strength of Fly ash based Geopolymer paste specimens

4.2.1.2.2 Effect of dual oxides in Activator (K_2O+Na_2O) on Compressive strength of Fly ash based Geopolymer

The compressive strength of geopolymer specimens were obtained after 3 days, 28 days and 60 days after manufacturing. The details of compressive strength observed for the fly ash based geopolymer specimens are shown in Figure 4.6. Two important factors may be noted here. First, combination of potassium hydroxide and sodium silicate (comprising dual oxide K_2O+Na_2O) exhibit better 3-day strength in presence of higher content of silicate. But the strength of the geopolymer sample in presence of sodium hydroxide and sodium silicate as activators indicated higher strength for silicate modulus equal to 0.5. The 3-day compressive strength of GPX1 sample is found maximum. The result supports that higher concentration of sodium silicate is better stabilized by potassium hydroxide while lower concentration of sodium silicate is compatible with sodium hydroxide in activation of fly ash. Secondly, although the 3-day strength of GPX1 is maximum but an increasing trend was observed in presence of sodium hydroxide (like sample GP1, GP1-L). The long term physical study shows that this increment of strength is continued for a long period but resulted in ultimate cracking of geopolymer specimens activated in presence of Na_2O. However, a stable behavior in connection with compressive strength was observed for geopolymers activated with activator comprising of dual oxide (Na_2O + K_2O).

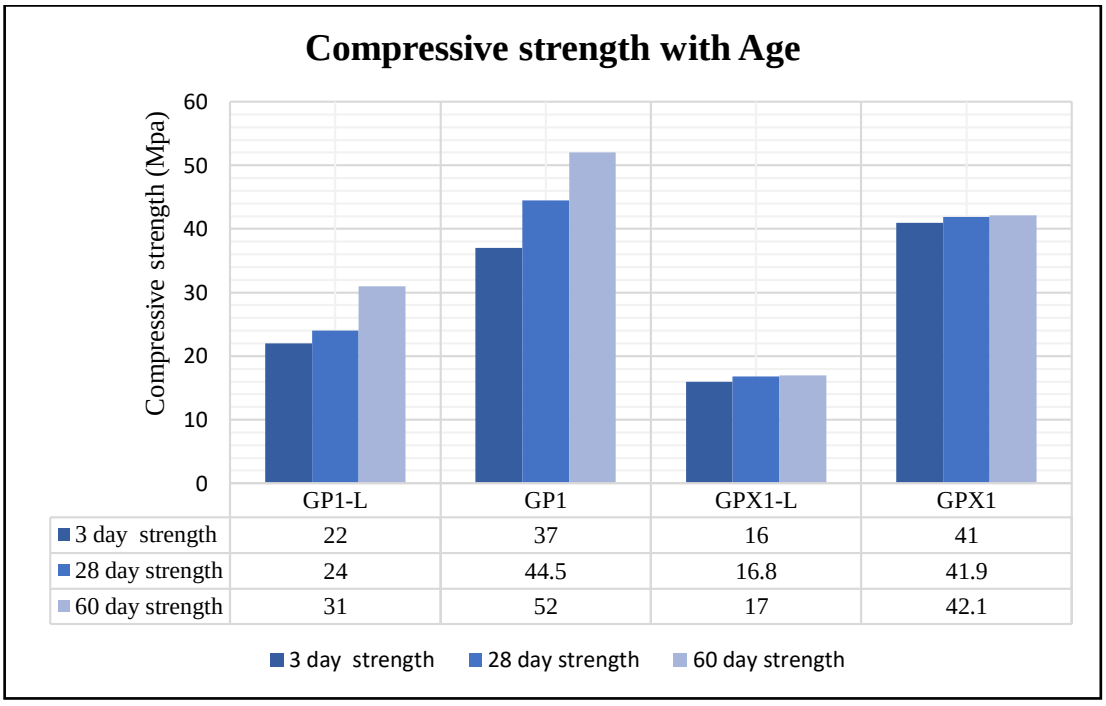

Figure 4.6 Compressive strength of Fly ash based Geopolymer specimens with age

4.2.2 Microstructural property

4.2.2.1 Scanning Electron Microscopy and EDX analysis

4.2.2.1.1 Effect of Temperature level of Activator on microstructural properties of Fly ash based Geopolymer

SEM micrographs for geopolymer specimens PS15, PS20, PS35, PS65, PS75, PS80, PS90 and PS95 including EDX traces are represented in Figure 4.7(a) to 4.7(j). For specimens PS15, PS20, PS90 and PS95, unreacted embedded particles were observed within gel body. Some of the samples showed micro crack. The micrographs revealed mostly a compact and well-connected part for specimen PS35.In samples PS15, PS20, P90 and PS95, unreacted crystalline elements were observed which may be considered as unreacted alkali. EDX spectra showed main elements like oxygen (O), aluminum (Al), silicone (Si) and sodium (Na) for typical selected spot on specific specimen. Few major elements (wt. %) conferring to EDX quantification of PS15 and PS95 were expressed in a pattern like O (40.18%), Na (11.39%) and O (27.62%), Na (20.5%) respectively. However, for sample PS65, the percentage of weight for above mentioned elements were changed in a pattern like O (35.7%), Si (17.27%), Al (9.02%) and Na (16.33%). Again, sample PS35 showed an elemental distribution like O (40.46%), Si (16.22%), Al (13.12%), Na (7.98%) and Ca (0.31%). These elemental changes were observed due to imposition of temperature to activator prior mixing.

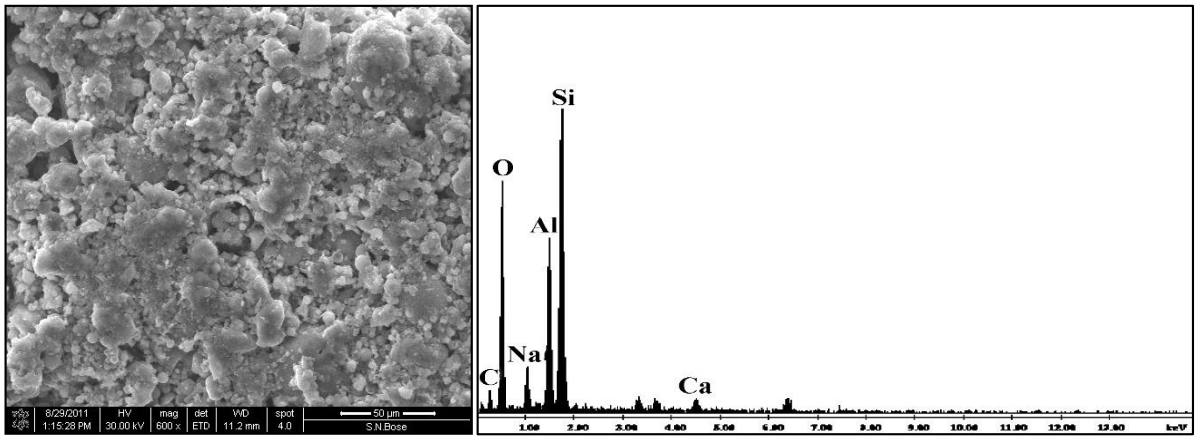

Figure 4.7(a) SEM @ 600x zoom and EDX of specimen PS15

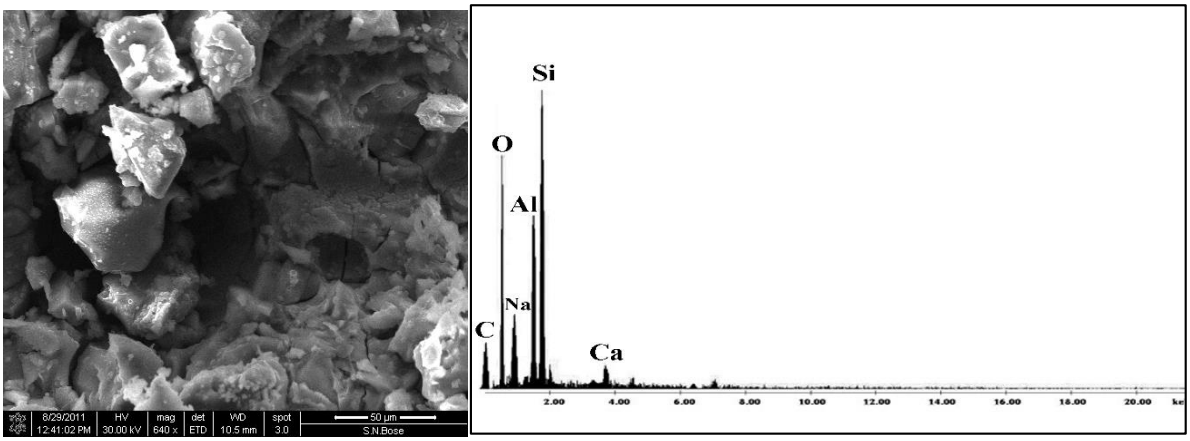

Figure 4.7(b) SEM @ 640x zoom and EDX of specimen PS20

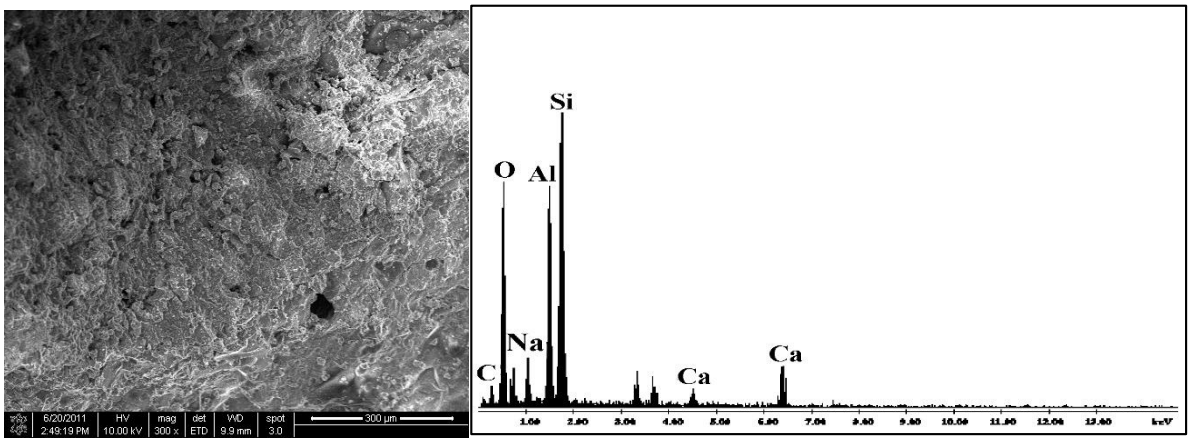

Figure 4.7(c) SEM @ 300x zoom and EDX of specimen PS35

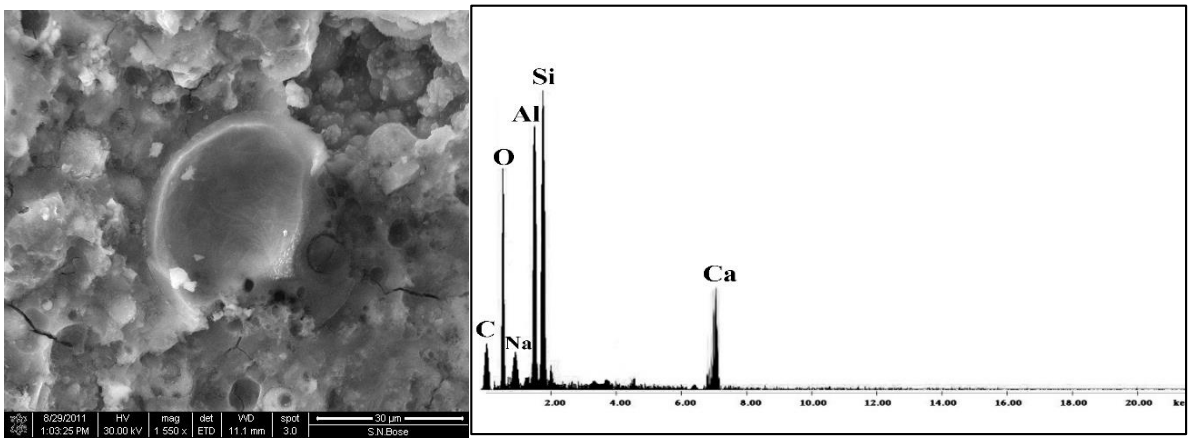

Figure 4.7(d) SEM @ 1550x zoom and EDX of specimen PS65

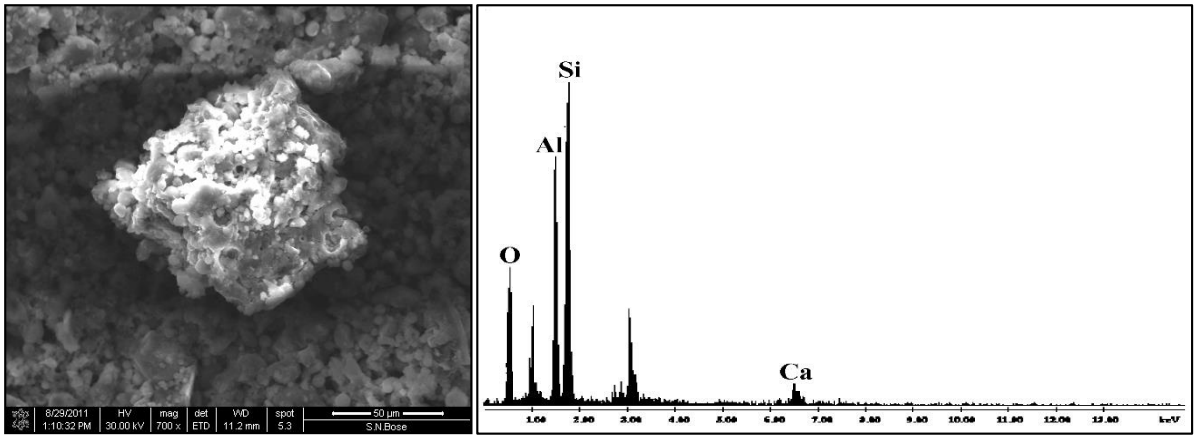

Figure 4.7(e) SEM @700x zoom and EDX of specimen PS75

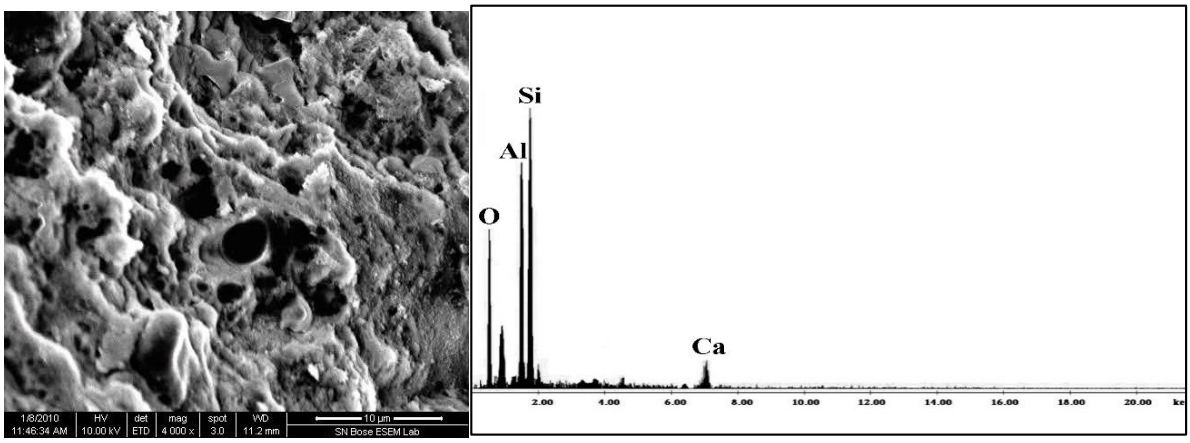

Figure 4.7(f) SEM @ 4000x zoom and EDX of specimen PS80

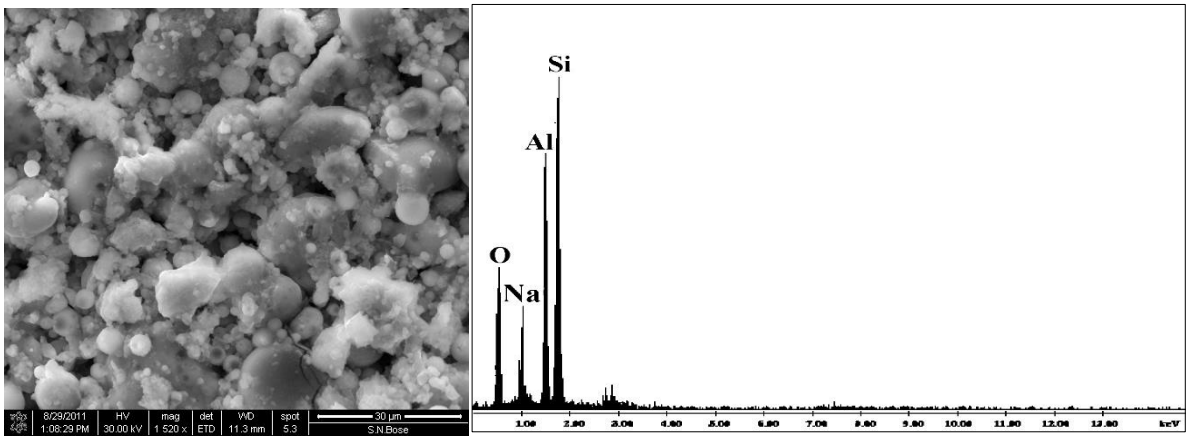

Figure 4.7(g) SEM @ 1520x zoom and EDX of specimen PS90

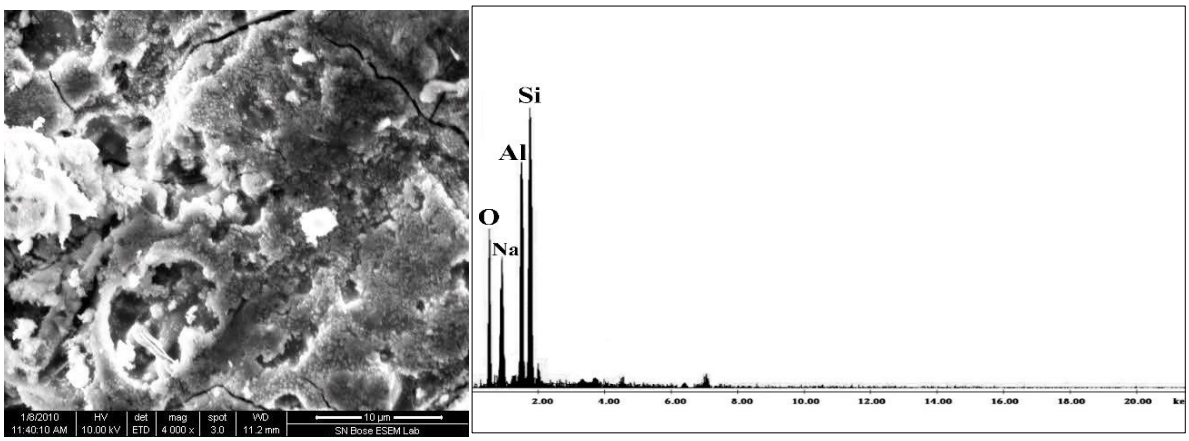

Figure 4.7(h) SEM @ 4000x zoom and EDX of specimen PS95

Figure 4.7 SEM micrographs and EDX spectra of Geopolymer paste specimens

4.2.2.1.2 Effect of dual oxides in Activator (K_2O+Na_2O) on microstructural properties of Fly ash based Geopolymer

The Figure 4.8 presents the SEM micrographs of geopolymer paste specimens GP1-L, GP1, GPX1-L and GPX1 along with their EDX traces. It showed a structure with huge amount of partially reacted or unreacted particles embedded within the gel in case of GP1 and GPX1-L. Almost an amorphous phase with fewer pores of different sizes was observed for GPX1 and GP1-L. Like the previous study here also the EDX spectra of specimens showed major elements such as silicone (Si), oxygen (O), aluminium (Al), potassium (K), sodium (Na) and Calcium (Ca). The percentages of few important elements by weight as per EDX quantification are tabulated. Though geopolymer is heterogeneous compound in nature, EDX at any tentative point is not enough to draw a conclusion. Perhaps EDX partially demonstrates the variation in the typical constitute elements of the geopolymer product. Data of few essential elements (wt. %) according to EDX quantification of GP1-L were counted as like O (21.89%), Si (13.39%), Al (7.79%), Na (15.39%), K (0%), Ca (0%) etc. The weight percentages of important elements for GP1 were reported as O (31.34%), Si (18.15%), Al (9.14%), Na (14.38%) and K (0%), Ca (0.08%) whereas, for GPX1-L sample, EDX analysis was showed the following ranges like, O (22.09%), Si (12.78%), Al (11.12%), K (8.91%), Na (3.36%) and Ca (0.11%). Again, for GPX1 specimen, EDX analysis was showed as O (33.39%), Si (20.13%), Al (10.09%), K (9.07%), Na (4.78%) and Ca (0.12%). EDX analysis confirmed the existence of both the Na and K in specimen GPX1 and GPX1-L.The SEM images for geopolymer specimens GP1-L, GP1, GPX1-L and GPX1 are given in Figure 4.8 along with their EDX spectrum. Figure 4.8(a) & Figure 4.8(d) exhibit better microstructure in compare to Figure 4.8(b) & Figure 4.8(c). This section demonstrates

that higher concentration of sodium silicate may be encouraged with KOH as an alkali hydroxide to prepare the activator. Sodium hydroxide plays better role in presence sodium silicate of lower concentration.

Table 4.3 EDX report of Geopolymer specimens

Sample ID	Oxygen (wt. %)	Silicon (wt. %)	Aluminium (wt. %)	Potassium (wt. %)	Sodium (wt. %)	Calcium (wt. %)
GP1-L	21.89	13.39	7.79	0	15.39	0
GP1	31.34	18.15	9.14	0	14.38	0.08
GPX1-L	22.09	12.78	11.12	8.91	3.36	0.11
GPX1	33.39	20.13	10.09	9.07	4.78	0.12

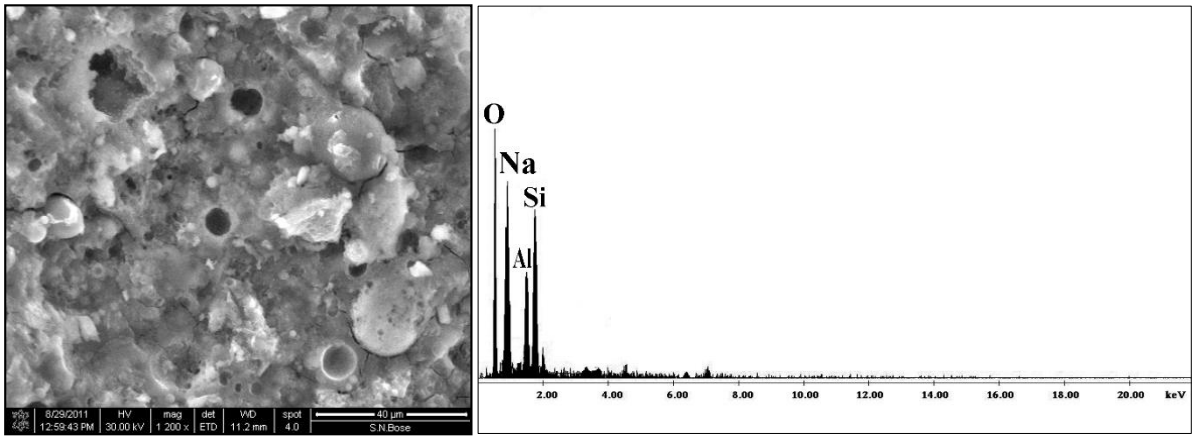

Figure 4.8(a) SEM @ 1200x zoom and EDX of specimen GP1-L

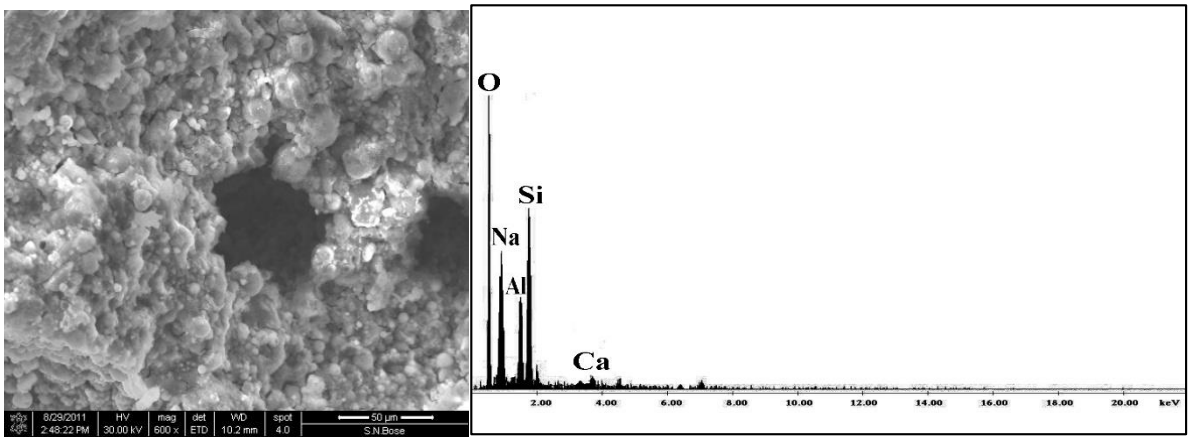

Figure 4.8(b) SEM @ 600x zoom and EDX of specimen GP1

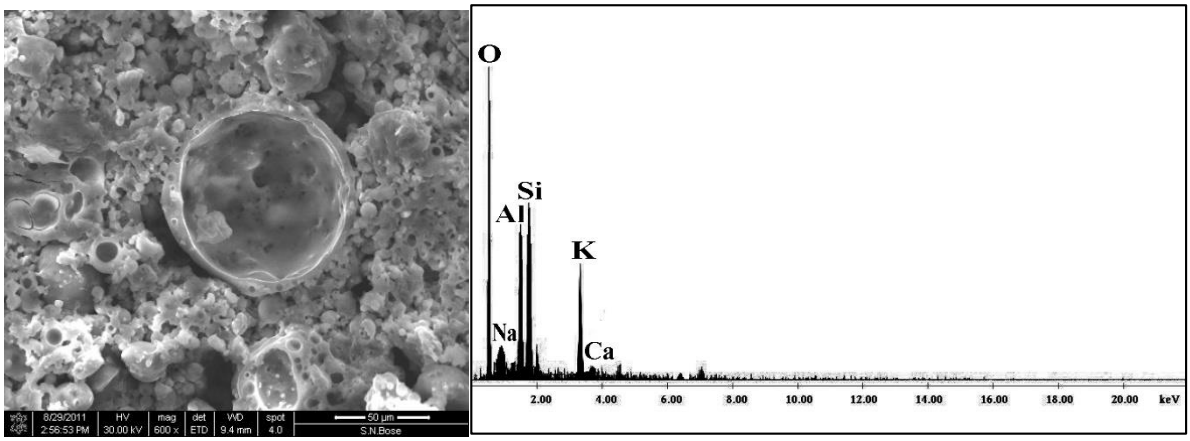

Figure 4.8(c) SEM @ 600x zoom and EDX of specimen GPX1-L

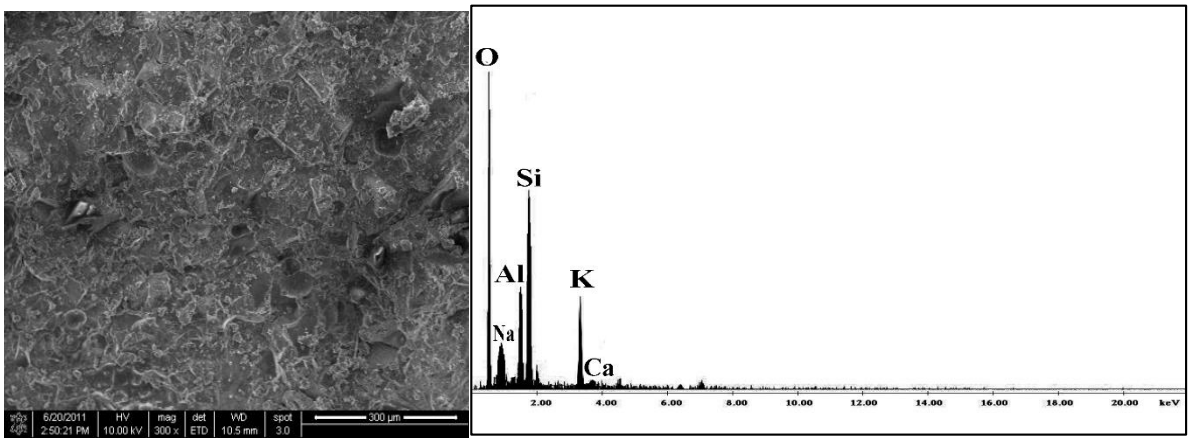

Figure 4.8(d) SEM @ 300x zoom and EDX of specimen GPX1

Figure 4.8: SEM micrographs and EDX spectra for Geopolymer paste specimens

4.3 Fly ash based Geopolymer blended with supplementary Calcium compound

4.3.1 Physical property

4.3.1.1 Workability

4.3.1.1.1 Effect of Lime stone dust blending on Workability of Fly ash based Geopolymer

Calcium based supplementary material (lime stone dust) when blended with fly ash, enhances the development of Ca-Al-Si amorphous structure rapidly at the primary phase of alkali activation [48], [78], [82]. Beside this the formation of calcium intense composites like calcium silicates, calcium aluminate hydrates were also perceived with synthesis in presence of calcium [16].It was found that high calcium compound may improve the microstructure as well as several hardened properties due to formation of Ca–Al–Si gel during geopolymerization [129], [130], [134]. Quick setting behaviour was observed for fly ash based geopolymer in presence of lime stone dust. In this section, the variation in workability was observed in terms area

factor. In fact, drop in the value of area factor was observed with the incorporation of lime stone dust. Maximum drop was observed for sample GL2 where area factor was found 7.11 and the mix was suitable for placing and casting.

Table 4.4 Workability test result for Geopolymer blended with Lime stone dust

Mix ID	Initial Diameter (D1) (cm)	Final equivalent Diameter (D2) (cm)	Initial Area (A1) (cm^2)	Final Area after flow (A2)(cm^2)	Area Factor =A2/A1
GP1	6.0	22.0	28.26	379.94	13.44
GL1	6.0	20.0	28.26	314.00	11.11
GL2	6.0	16.0	28.26	200.96	7.11

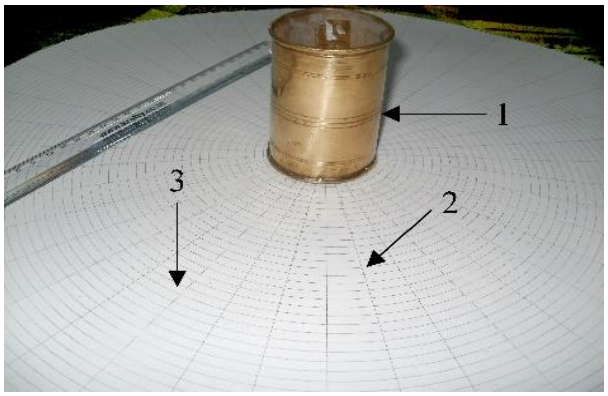

Figure 4.9 Workability Test Setup

Figure 4.10 Flow of sample GL2

4.3.1.1.2 Effect of Slag blending on Workability of Fly ash based Geopolymer

The study of fly ash based geopolymer blended with calcium based supplementary material has been made. Two types of calcium based supplementary material were used. Initially, laboratory grade lime stone dust was used which is a source of pure calcium. Later on after getting successful results, the experiment was focused to the blending of some calcium based waste supplements like Blast furnace slag. Similar kind of performance were observed in case of fly ash based geopolymer blended with blast furnace slag as observed in case of lime stone dust. Sample GB2 showed an area factor equal to 9.00 which is much less than that of GP1. But no casting problem was observed.

Table 4.5: Result of Workability test on Geopolymer paste with different Slag content

Mix ID	Initial Diameter (D1) (cm)	Final equivalent Diameter (D2) (cm)	Initial Area (A1) (cm^2)	Final Area after flow (A2) (cm^2)	Area Factor =A2/A1
GP1	6.0	22.0	28.26	379.94	13.44
GB1	6.0	21.0	28.26	346.19	12.25
GB2	6.0	18.0	28.26	254.34	9.00

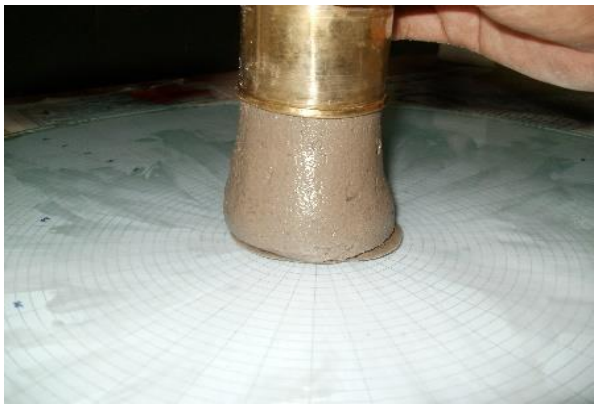

Figure 4.11 Flow of sample GB2

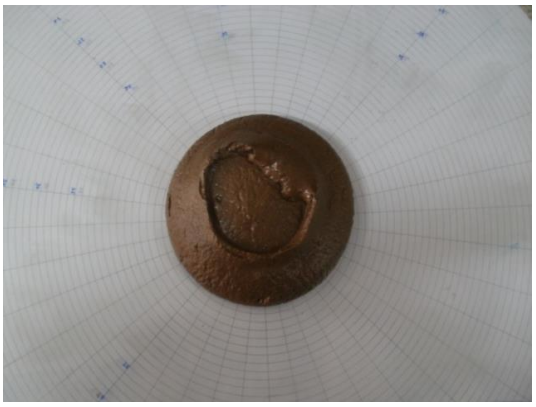

Figure 4.12 Sample GB2 after flow

It was reported earlier that there is a possibility of formation of calcium based composites such as silicates, aluminate hydrates etc. at the time of synthesis of fly ash based geopolymer in presence of calcium[16]. Rashad[141] also suggested that the workability of fresh alkali activated fly ash composites decreases with the increase in the supplementary slag content. Paste samples were collected at 9 different times, 5 to 45 minutes after mixing, at an interval of 5 minutes. It has indicated phase changes with time. The area factor dropped rapidly with time after mixing. Table 4.5.1 furnished the workability results, which demonstrate the rapid setting of the blended geopolymer. The area factor reached to unity between 35-40 minutes. A unit area factor may be considered as the end of the plastic state. This time was reduced to 2-3 minutes and 3-4 minutes in presence of lime stone dust and slag (around 18-20% of total source material). The present investigation was done in detail up to 15% replacement as supplementary material. Few latest research [148] has been done with higher percentage of slag. It may be noted here that this is entirely depends on physical and chemical properties of the slag. The reactivity level of the slag was enhanced in case of slag having higher specific surface area which was achieved through special stone grinding.

Table 4.5.1: Test result on Workability vs. Time of Fly ash based Geopolymer blended with Slag with time (mix id: GB - 6% Na_2O in activator and 15 % slag as supplementary material (ref. to Table 3.16))

Time Elapse After Mixing (Mints)	Initial Diameter (D1) (cm)	Final Equivalent Diameter (D2) (cm)	Initial Area (A1) (cm^2)	Final Area after flow (A2) (cm^2)	Area Factor =A2/A1
5	6.0	20.0	28.26	314.29	11.12
10	6.0	19.0	28.26	283.64	10.04
15	6.0	16.0	28.26	201.14	7.12
20	6.0	15.0	28.26	176.79	6.26
25	6.0	15.0	28.26	176.79	6.26
30	6.0	12.0	28.26	113.14	4.00
35	6.0	10.0	28.26	78.57	2.78
40	6.0	6.0	28.26	28.26	1.00
45	6.0	6.0	28.26	28.26	1.00

4.3.1.2 Compressive strength

4.3.1.2.1 Compressive strength of Heat cured specimens

4.3.1.2.1.1 Effect of Aging on the Compressive strength of Fly ash based Geopolymer blended with Blast furnace slag

Three distinct series of samples GP1, GB1 and GB2 (as shown in Chapter-3; Table 3.14**)** were selected to find the effect of aging on the compressive strength of fly ash based geopolymer blended with blast furnace slag. The compressive strength values of the test specimens were obtained after 3 days, 28 days, 60 days and 90 days after manufacturing to note the change in compressive strength with aging. Earlier study [30] found noticeable increment in compressive strength of fly ash based geopolymer with aging at ambient or room temperature [30]. The change in compressive strength with aging may be due to slow level of synthesis in presence sodium hydroxide [51]. Late precipitation (alkali hydroxide or silicate) within the internal pores may be the cause behind this increasing trend of strength of fly ash based geopolymer with aging [51]. This internal pore pressure may be responsible for the micro-cracking of the fly ash based geopolymer test specimens with aging. It was found from this study that around 50% of fly ash based geopolymer test specimens (non-blended) showed micro cracks with aging. The blending of blast furnace slag increase the presence of calcium ions in the fly ash based geopolymer. Earlier study [88] depicts that calcium ions may act as a charge balancer of aluminium at the time of synthesis and contributes to the faster formation of geopolymeric structure. This blended fly ash based geopolymer may be able to indicate less change of strength value with age. 3-day compressive strength for three typical

series of specimens are presented in Figure 4.13. 3 day-compressive strength values for specimen GP1, GB1 and GB2 were found as 37 MPa, 39 MPa and 41 MPa respectively. Blending of blast furnace slag in fly ash based geopolymer by 10% and 15%, increased the compressive strength by 5.4% and 10% respectively. The change in compressive strength with age is presented in Figure 4.14. For GP1 sample (non-blended) the 28-day, 60-day and 90-day compressive strength values were around 27.03 %, 40.54% and 100% greater than 3-day strength value. The 90-day compressive strength for blended fly ash based geopolymer like GB1 (10% blending of slag) was 12.02% higher than the 3-day compressive strength. For blended sample GB2 (15% blending of slag), this variation was accounted as only 1.2% only (Figure 4.13). The blended fly ash based geopolymer showed an increment in compressive strength (slag content 10% and 15% of base material i.e. fly ash + blast furnace slag). Again, it was observed less change of strength value with age, for fly ash based geopolymer blended with blast furnace slag.

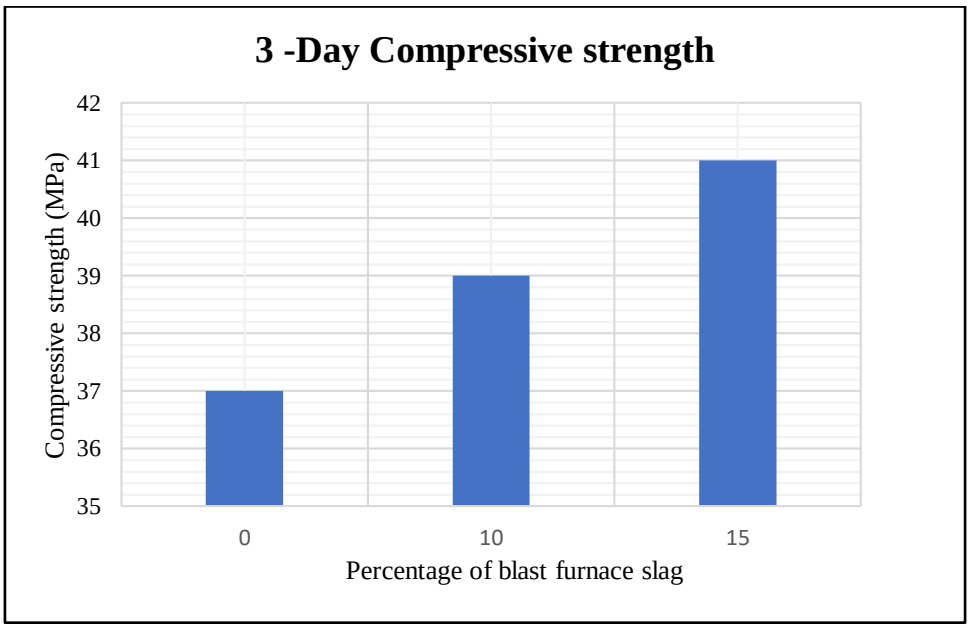

Figure 4.13: 3-Day Compressive strength of Fly ash based Geopolymer blended with Blast furnace slag

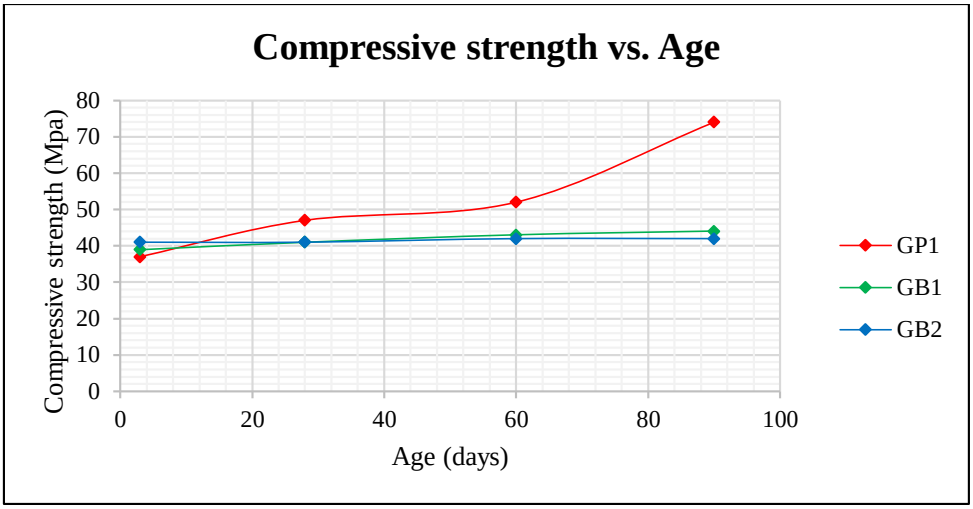

Figure 4.14 Effect of Aging on Compressive strength of Fly ash based Geopolymer blended with Blast furnace slag

4.3.1.2.1.2 Effect of Curing profile (curing temperature and duration) on Compressive strength of Fly ash based Geopolymer blended with Lime stone dust

3-day and 28-day compressive strength were studied for non-blended and blended geopolymer cured at different temperature and duration. Eighteen different series of specimens were studied based on curing temperature and curing duration (ref. to Table 4.6). In Table 4.6, the mix GP1, GL1 and GL2 contain lime stone dust 0%, 10% and 15% respectively (detail mixing composition is discussed in Chapter-3; Table 3.9). Beside the composition of mix, the curing temperature has an important impact on compressive strength of heat cured geopolymer manufactured from fly ash [131]. Again, duration of heat curing also has significant contribution on geopolymerization process, compressive strength and drying shrinkage [33] [21]. The curing temperature and duration was optimized for fly ash based geopolymer in earlier study [106]. But calcium based supplementary material like lime stone dust when blended with fly ash increase the amount of calcium in the geopolymer mix. For blended geopolymer, the poly-condensation process may be accelerated in presence of supplementary calcium compound. The calcium ions act as charge balancer of aluminium and take the role of alkali cation (sodium) which may emphasis faster dissolution of the silica and aluminium (reactive species) [88]. Earlier investigation [122] reports that the dissolution of reactive species are accelerated by the curing temperature for fly ash based geopolymer [122]. For fly ash based geopolymer blended with lime stone dust, the rate of dissolution is accelerated due to the presence of external calcium ions. Beside this, secondary amorphous structure (Ca–Al–Si gel) may be developed during geopolymerization in presence supplementary calcium content [48], [78], [79], [82]. Fly ash based geopolymer specimen GP1-LS (cured at a temperature of 35°C for 24hrs.), could not take any load (Table 4.6 and Figure

4.15), whereas, 3-day compressive strength of blended geopolymer GL2-LS (cured at 35ºC temperature for 24 hrs.) was found as 25.11 MPa. 3-day compressive strength of specimen GP1-MS (cured at 55ºC for 24hrs.) and GP1-HL (cured at 85ºC for 48hrs.) was recorded as 9.5MPa and 37MPa respectively i.e. increased four times. 3-day compressive strength of sample GL2-MS (cured at 55ºC for 24hrs.) and GL2-HL (cured at 85ºC for 48hrs.) was 33.09 MPa and 36 MPa respectively. Compressive strength of fly ash based geopolymer (non-blended) has been increased remarkably with the change of curing temperature from 55ºC to 85ºC.Similarly, the increase in curing duration (24hrs. to 48hrs.) had noteworthy impact on the increment of compressive strength. Blended fly ash based geopolymer did not show remarkable changes in compressive strength like the non-blended sample. Again, the variation of the 3-day and 28-day compressive strength for blended fly ash based geopolymer was found very less in compare to non-blended geopolymer (Table 4.6 and Figure 4.15).

Table 4.6 Compressive strength of Lime stone dust Blended Fly ash based Geopolymer with different curing profile (Curing temperature and duration)

Mix ID	Sample ID	Curing Temperature	Curing Duration	Compressive Strength (MPa)	
				After 3 days	After 28 days
GP1	GP1-LS	35ºC	24 Hrs.	0.0	0.0
	GP1-LL	35ºC	48 Hrs.	3.51	4.89
	GP1-MS	55ºC	24 Hrs.	9.50	10.90
	GP1-ML	55ºC	48 Hrs.	13.03	18.30
	GP1-HS	85ºC	24 Hrs.	28.31	35.00
	GP1-HL	85ºC	48 Hrs.	37.00	44.49
GL1	GL1-LS	35ºC	24 Hrs.	16.16	17.09
	GL1-LL	35ºC	48 Hrs.	19.70	20.00
	GL1-MS	55ºC	24 Hrs.	26.00	27.90
	GL1-ML	55ºC	48 Hrs.	28.57	29.34
	GL1-HS	85ºC	24 Hrs.	31.89	32.00
	GL1-HL	85ºC	48 Hrs.	33.21	33.50
GL2	GL2-LS	35ºC	24 Hrs.	22.17	23.50
	GL2-LL	35ºC	48 Hrs.	25.11	26.30
	GL2-MS	55ºC	24 Hrs.	33.09	33.50
	GL2-ML	55ºC	48 Hrs.	34.13	34.50
	GL2-HS	85ºC	24 Hrs.	35.00	35.85
	GL2-HL	85ºC	48 Hrs.	36.00	36.00

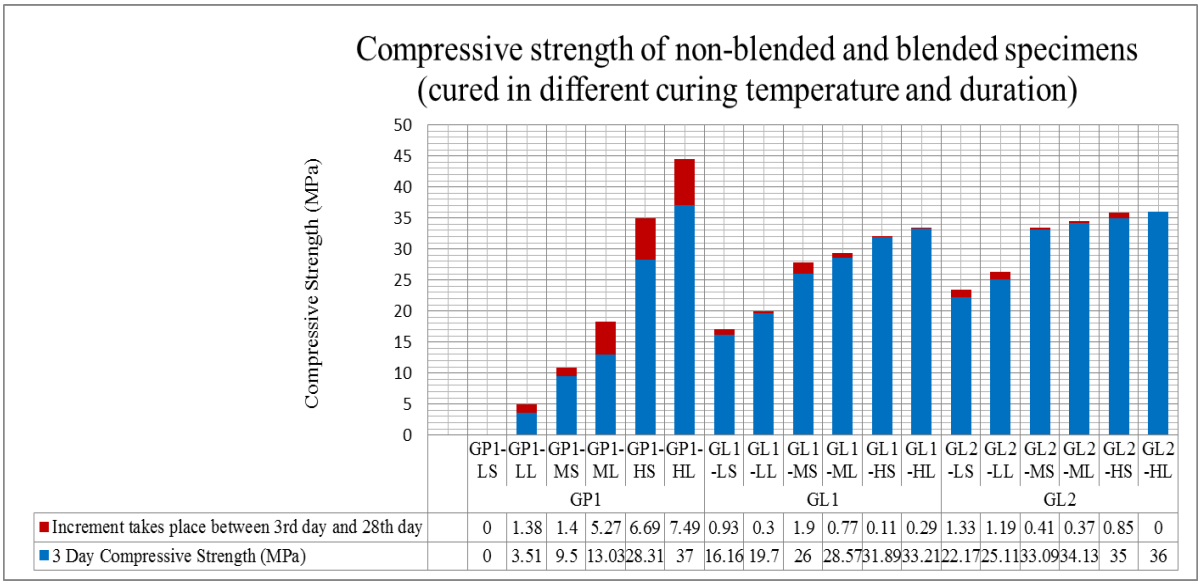

Figure 4.15 Compressive strength at different curing profile for Lime stone dust Blended Fly ash based Geopolymer specimens

4.3.1.2.1.3 Effect of Curing profile on Compressive strength of Fly ash based Geopolymer blended with Slag

Eighteen different series of specimens were studied based on curing temperature and curing duration (Table 4.7). In Table 4.7, the mix id GP1, GB1 and GB2 contain blast furnace slag 0%, 10% and 15% respectively (detail mixing composition is discussed in Chapter-3; Table 3.12). Blending of blast furnace slag increase the presence of calcium content into the geopolymer mix which may accelerate the rate of dissolution silica and aluminium (reactive species). Beside this, secondary amorphous structure (Ca–Al–Si gel) may be developed during geopolymerization in presence supplementary calcium content [48], [78], [79], [82]. Since, stimulation energy is greater for fly ash in compare to slag, the high temperature curing is essential for fly ash [41], [42], [105]. Earlier study [12] noticed that prolonged heat exposure to alkali-activated slag gradually lowers the compressive strength with time. The blending of slag with fly ash may change the role of curing temperature to some extent. Fly ash based geopolymer sample GP1-LL (cured at a temperature of 35ºC for 48 hrs.) provided 3-day compressive strength of 3.51MPa (Table 4.7 and Figure 4.16), whereas, 3-day compressive strength of blended geopolymer GB2-LL (cured at 35ºC temperature for 48 hrs.) was found as 15.01 MPa. Fly ash based geopolymer blended with slag showed higher strength at low curing temperature, compared to non-blended geopolymer. 3-day compressive strength of specimens GP1-MS (cured at 55ºC for 24hrs.) and GP1-HL (cured at 55ºC for 48hrs.) was recorded as 9.5MPa and 37MPa respectively i.e. increased by four times. 3-day compressive strength of sample GB2-MS (cured at 55ºC for 24hrs.) and GB2-HL (cured at 55ºC for

48hrs.) was 23.99 MPa and 41 MPa respectively. The increase in curing temperature (55^{o}C to 85^{o}C) and curing duration (24hrs. to 48hrs.) had much impact on the increment of compressive strength for non-blended specimen rather than blended specimens. Another observation may be noted here that the blended fly ash based geopolymer maintained more or less same strength with age (Table 4.7 and Figure 4.16).

Table 4.7 Compressive strength of Slag Blended Fly ash based Geopolymer specimens with different curing profile (Curing temperature and duration)

Mix ID	Sample ID	Curing Temperature	Curing Duration	Compressive Strength (MPa)	
				After 3 days	After 28 days
GP1	GP1-LS	35^{o}C	24 Hrs.	0.0	0.0
	GP1-LL	35^{o}C	48 Hrs.	3.51	4.89
	GP1-MS	55^{o}C	24 Hrs.	9.50	10.90
	GP1-ML	55^{o}C	48 Hrs.	13.03	18.30
	GP1-HS	85^{o}C	24 Hrs.	28.31	35.00
	GP1-HL	85^{o}C	48 Hrs.	37.00	44.49
GB1	GB1-LS	35^{o}C	24 Hrs.	9.71	10.03
	GB1-LL	35^{o}C	48 Hrs.	12.31	13.00
	GB1-MS	55^{o}C	24 Hrs.	20.54	21.20
	GB1-ML	55^{o}C	48 Hrs.	22.44	23.23
	GB1-HS	85^{o}C	24 Hrs.	37.80	38.46
	GB1-HL	85^{o}C	48 Hrs.	39.00	39.39
GB2	GB2-LS	35^{o}C	24 Hrs.	13.63	13.88
	GB2-LL	35^{o}C	48 Hrs.	15.01	15.47
	GB2-MS	55^{o}C	24 Hrs.	23.99	24.38
	GB2-ML	55^{o}C	48 Hrs.	29.93	26.22
	GB2-HS	85^{o}C	24 Hrs.	39.50	39.71
	GB2-HL	85^{o}C	48 Hrs.	41.00	41.00

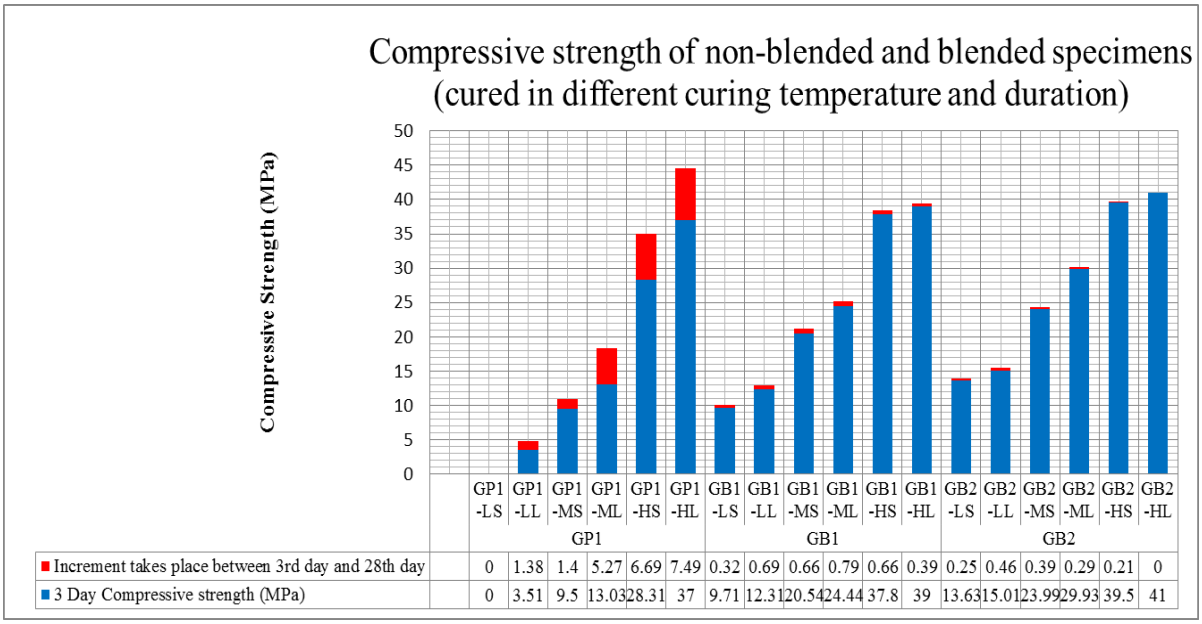

Figure 4.16 Compressive strength at different curing profile for Slag Blended Fly ash based Geopolymer specimens

4.3.1.2.1.4 Effect of Alkali concentration on Compressive strength of Fly ash based Geopolymer blended with Slag

Twelve distinct series of specimens were selected to study the effect of alkali concentration on fly ash based geopolymer blended with slag (discussed in Chapter-3; Table-3.13). The specimens were studied based on alkali concentration (percentage of Na_2O, silicate modulus). 3 day compressive strength were evaluated for non-blended and blended geopolymer with the variation alkali concentration. Further, every series of specimens was subjected to different curing temperature and duration, to find the best combination of alkali and curing profile (as shown in Table 4.8). The effect of Na_2O percentage and silicate modulus on fly ash based geopolymer blended with slag has been studied separately.

Table 4.8 Compressive strength of Fly ash Geopolymer blended with Slag for varying Alkali concentration and Curing profile

Sample ID	Activator		3-day Compressive Strength (MPa)							
			Curing for 24 Hrs. at				Curing for 48 Hrs. at			
	%Na2O	Silicate Modulus	55ºC	65ºC	75ºC	85ºC	55ºC	65ºC	75ºC	85ºC
GP-L	6%	0.5	3.0	6.66	9.83	13.35	4.87	9.89	15.67	18.09
GP	6%	1	6.89	9.39	14.39	20.31	8.68	11.15	19.13	27.66
GP-H	6%	1.5	8.93	9.98	16.03	22.59	10.32	13.01	22.7	29.22
GP1-L	8%	0.5	4.5	8.67	11.37	21.19	7.80	12.35	17.88	26.90

GP1	8%	1	9.5	11.83	16.69	28.31	13.03	15.12	25.09	37.00
GP1-H	8%	1.5	10.11	12.31	19.01	32.33	13.82	15.79	26.50	40.00
GB-L	6%	0.5	17.09	33.29	32.18	31.50	17.62	33.46	32.01	30.73
GB	6%	1	25.23	43.61	42.87	42.08	25.81	43.69	41.60	39.80
GB-H	6%	1.5	29.30	47.09	46.80	46.13	29.56	47.17	46.80	46.09
GB2-L	8%	0.5	15.03	31.65	31.00	31.00	15.89	31.87	30.13	29.65
GB2	8%	1	23.99	40.28	39.90	39.50	25.93	40.63	38.00	41.00
GB2-H	8%	1.5	27.61	42.48	42.09	41.84	28.17	42.70	42.00	40.44

Effect of Na_2O Percentage

Earlier study reported Na_2O percentage of activator (8% to 10% of fly ash) is much suited for fly ash based geopolymer [106]. Slag blended fly ash based geopolymer showed maximum value of compressive strength (Table 4.8 and Figure 4.17), when activated under lower percentage of Na_2O in activator (6% of fly ash plus slag). 3-day compressive strength of specimen GB [15% slag; Activator concentration: 6% Na_2O and Silicate modulus (SM) = 1] was recorded as 43.61 MPa when cured at 65^0C for 24 hrs. Specimens GB2 [15% slag, Activator concentration: 8% Na_2O and Silicate modulus (SM) = 1] attained 40.28 MPa 3day compressive strength under the similar curing condition. The result indicates better compressive strength at 6% Na_2O (in activator) for blended geopolymer, whereas, 3-day compressive strength for non-blended fly ash based geopolymer specimen GP [Activator concentration: 6% Na_2O and Silicate modulus (SM) = 1] was found 27.66 MPa, when cured at 85^0C for 48hrs. Again 3 day compressive strength for another non-blended specimen GP1 [Activator concentration: 8% Na_2O and Silicate modulus (SM) = 1] was found as 37 MPa, under the same curing condition. However, higher percentage of Na_2O (8% in activator), provides higher strength for non-blended geopolymer but for slag blended geopolymer, higher strength can be achieved at lower percentage of Na_2O (6% in activator). Low concentration of Na_2O may give room to the calcium ion for playing the role of charge compensator as depicted by earlier studies [88]. Even slag blended geopolymer under higher percentage of Na_2O may accelerates the precipitation of more amount of C-S-H which is not desirable [108].

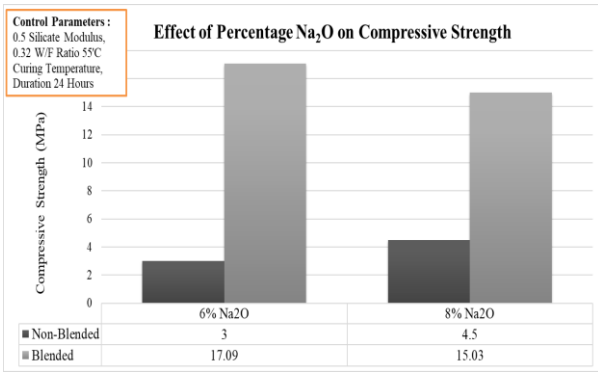
Control Parameters :
0.5 Silicate Modulus,
0.32 W/F Ratio 55'C
Curing Temperature,
Duration 24 Hours
Effect of Percentage Na_2O on Compressive Strength
Compressive Strength (MPa)
6% Na2O
8% Na2O
Non-Blended 3 4.5
Blended 17.09 15.03

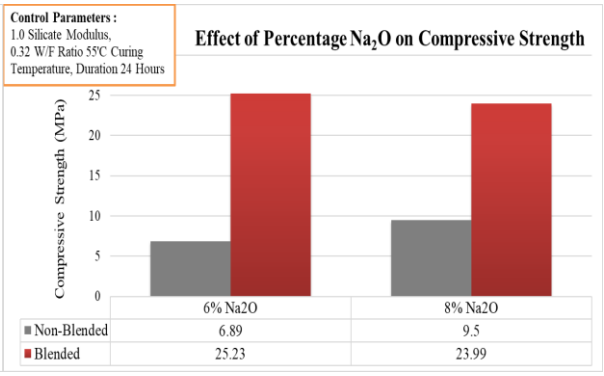
Control Parameters :
1.0 Silicate Modulus,
0.32 W/F Ratio 55'C Curing
Temperature, Duration 24 Hours
Effect of Percentage Na_2O on Compressive Strength
Compressive Strength (MPa)
6% Na2O
8% Na2O
Non-Blended 6.89 9.5
Blended 25.23 23.99

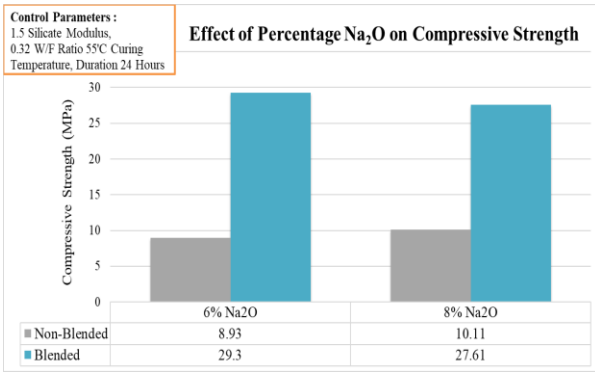
Control Parameters :
1.5 Silicate Modulus,
0.32 W/F Ratio 55'C Curing
Temperature, Duration 24 Hours
Effect of Percentage Na_2O on Compressive Strength
Compressive Strength (MPa)
6% Na2O
8% Na2O
Non-Blended 8.93 10.11
Blended 29.3 27.61

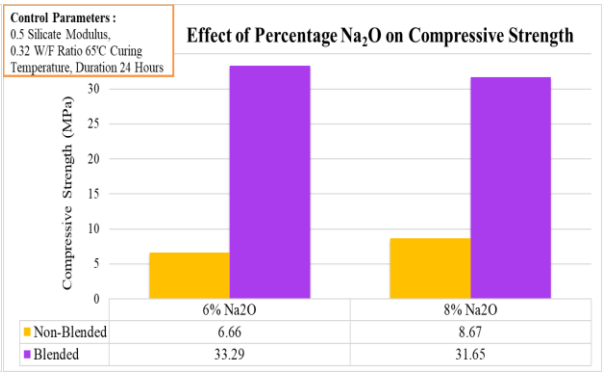
Control Parameters :
0.5 Silicate Modulus,
0.32 W/F Ratio 65'C Curing
Temperature, Duration 24 Hours
Effect of Percentage Na_2O on Compressive Strength
Compressive Strength (MPa)
6% Na2O
8% Na2O
Non-Blended 6.66 8.67
Blended 33.29 31.65

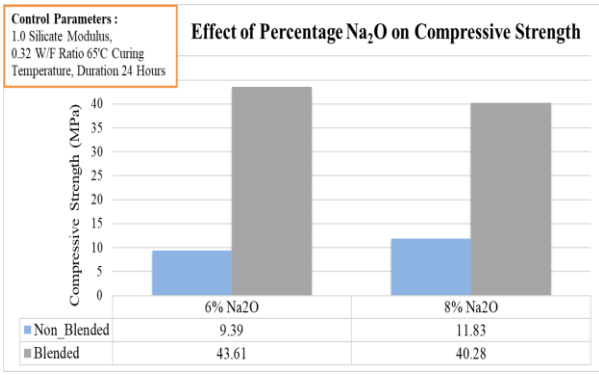
Control Parameters :
1.0 Silicate Modulus,
0.32 W/F Ratio 65'C Curing
Temperature, Duration 24 Hours
Effect of Percentage Na_2O on Compressive Strength
Compressive Strength (MPa)
6% Na2O
8% Na2O
Non_Blended 9.39 11.83
Blended 43.61 40.28

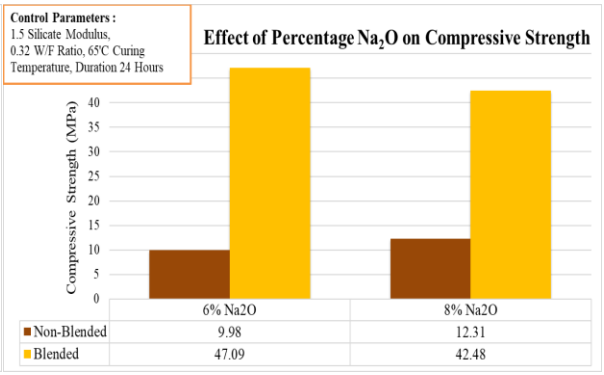
Control Parameters :
1.5 Silicate Modulus,
0.32 W/F Ratio, 65'C Curing
Temperature, Duration 24 Hours
Effect of Percentage Na_2O on Compressive Strength
Compressive Strength (MPa)
6% Na2O
8% Na2O
Non-Blended 9.98 12.31
Blended 47.09 42.48

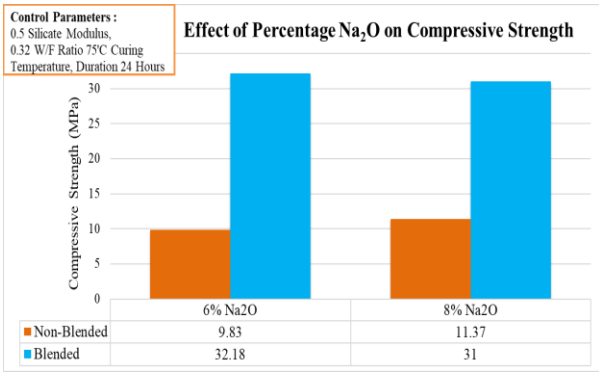
Control Parameters :
0.5 Silicate Modulus,
0.32 W/F Ratio 75'C Curing
Temperature, Duration 24 Hours
Effect of Percentage Na_2O on Compressive Strength
Compressive Strength (MPa)
6% Na2O
8% Na2O
Non-Blended 9.83 11.37
Blended 32.18 31

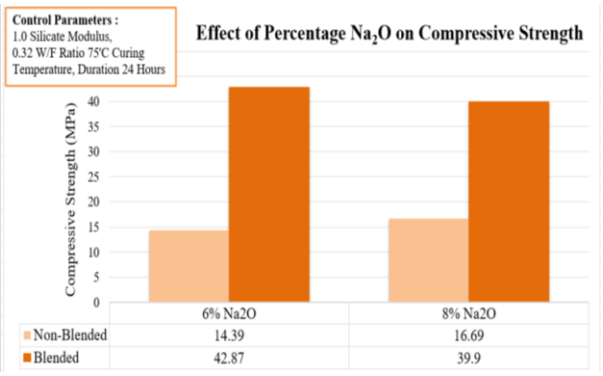
Control Parameters :
1.0 Silicate Modulus,
0.32 W/F Ratio 75'C Curing
Temperature, Duration 24 Hours
Effect of Percentage Na_2O on Compressive Strength
Compressive Strength (MPa)
6% Na2O
8% Na2O
Non-Blended 14.39 16.69
Blended 42.87 39.9

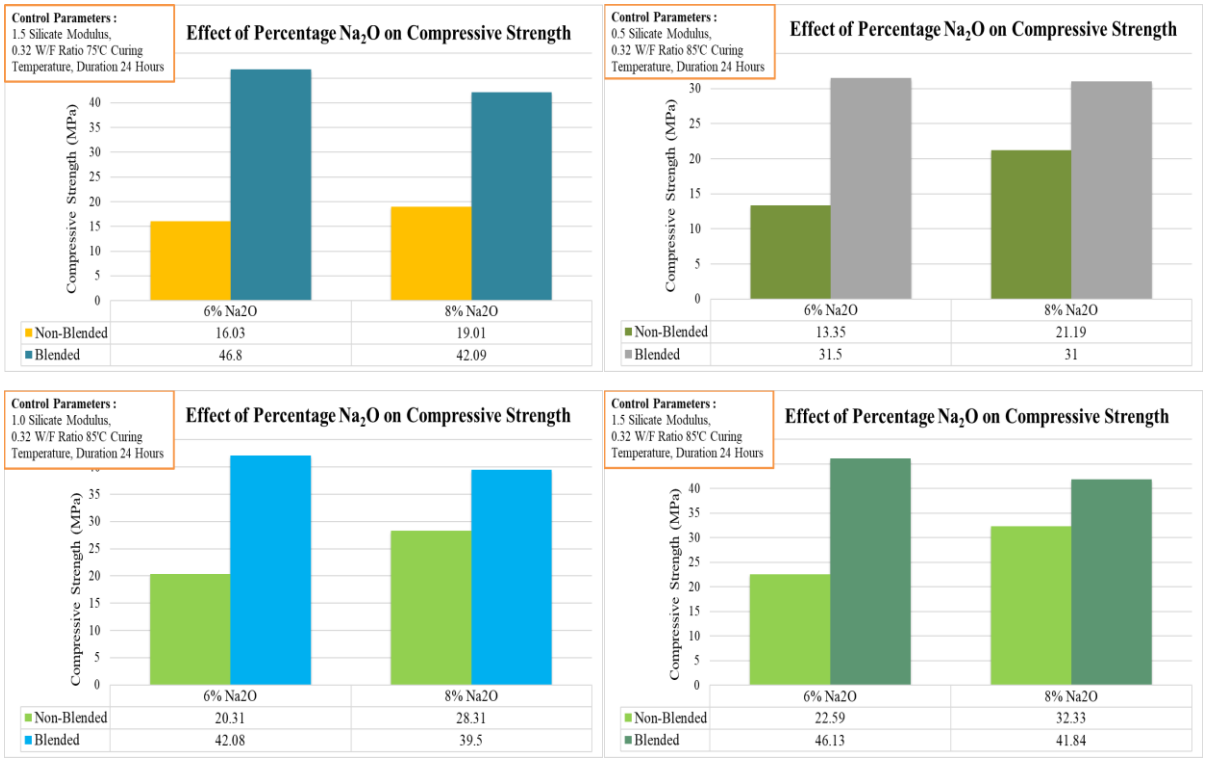

Figure 4.17 Effect of percentage Na_2O on Compressive strength of Slag Blended Fly ash based Geopolymer specimens

Role of Silicate Modulus

The result showed increasing trend of compressive strength with the increase of silicate modulus (0.5 to 1.5) for both the non-blended and blended geopolymer (Table 4.8 and Figure 4.17). But the compressive strength of slag blended fly ash geopolymer specimen was found higher than that of non-blended specimen in every case. Blast furnace slag provides supplementary calcium in the fly ash based geopolymer mix. Due to the higher ionic charges calcium ions may act as a charge balancer of aluminium which increases the dissolution rate of reactive species [88]. The rate of polymerisation has possibility to be increased in presence of calcium in the medium. Higher presence of reactive silica (from sodium silicate) may enhance the poly-condensation for the blended geopolymer. Higher compressive strength was found observed with the increment of silicate modulus for non-blended and blended geopolymer both.

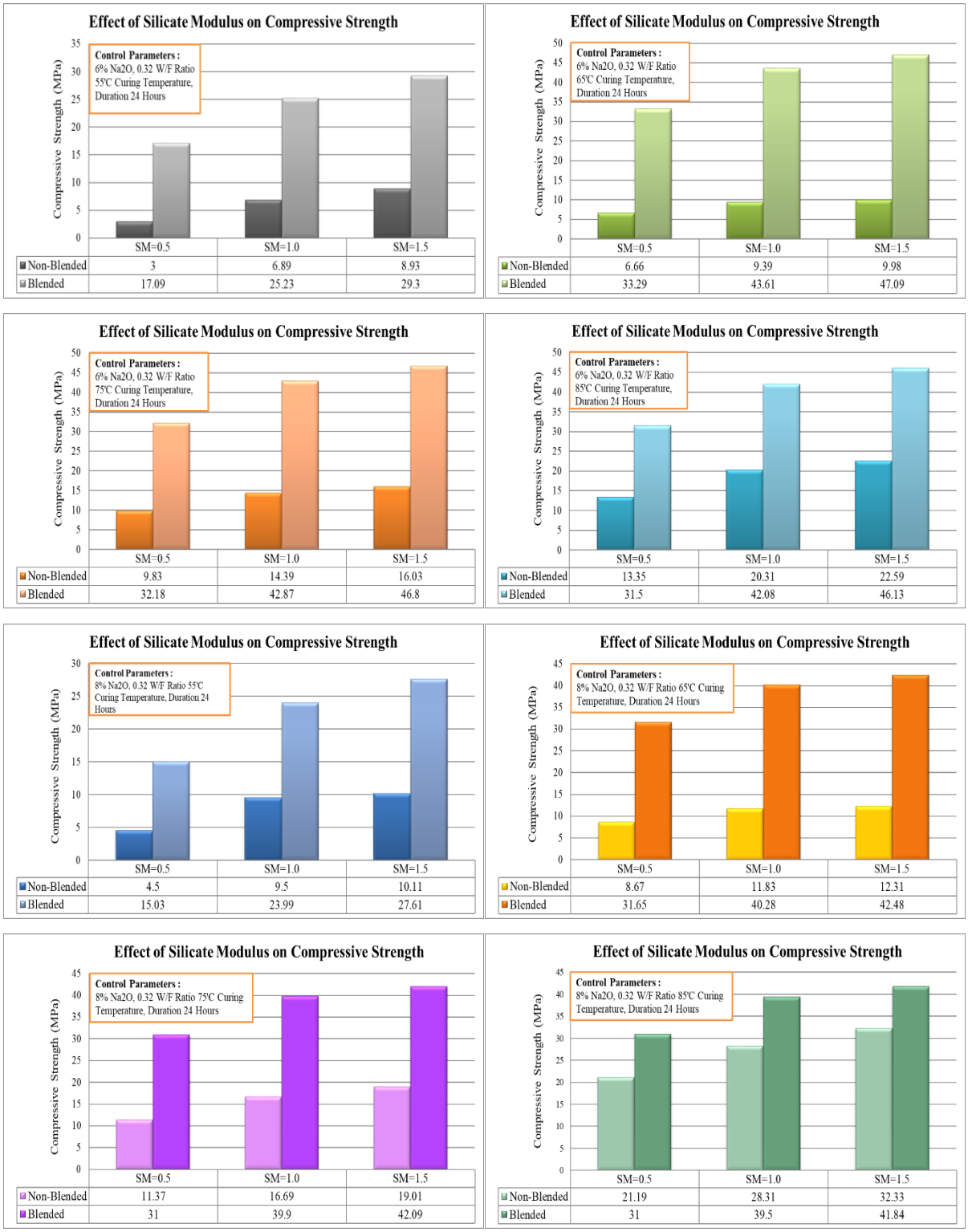

Figure 4.18 Effect of Silicate modulus on Compressive strength of Slag Blended Fly ash based Geopolymer specimens

Combined effect of Alkali concentration and Curing profile

The combined effect of alkali concentration and curing profile (curing temperature and curing duration) on the compressive strength of fly ash based geopolymer blended with slag is presented in Figure 4.19. It was studied to find the right choice of alkali and heat curing profile to achieve maximum compressive strength for fly ash based geopolymer blended with slag. Here, a typical series of fly ash geopolymer blended with slag GB-H [15% slag; Activator concentration: 6% Na_2O and Silicate modulus (SM) = 1.5], was found to provide maximum value of compressive strength, when cured at 65^0C for a duration of 24 hours. A combination like; 6% Na_2O in activator, silicate modulus equal to 1.5 in activator, curing temperature equal to 65^oC and curing duration equal to 24 hours, was observed as the most appropriate for fly ash based geopolymer blended with slag (10% to 15% as supplementary material with fly ash as base material).

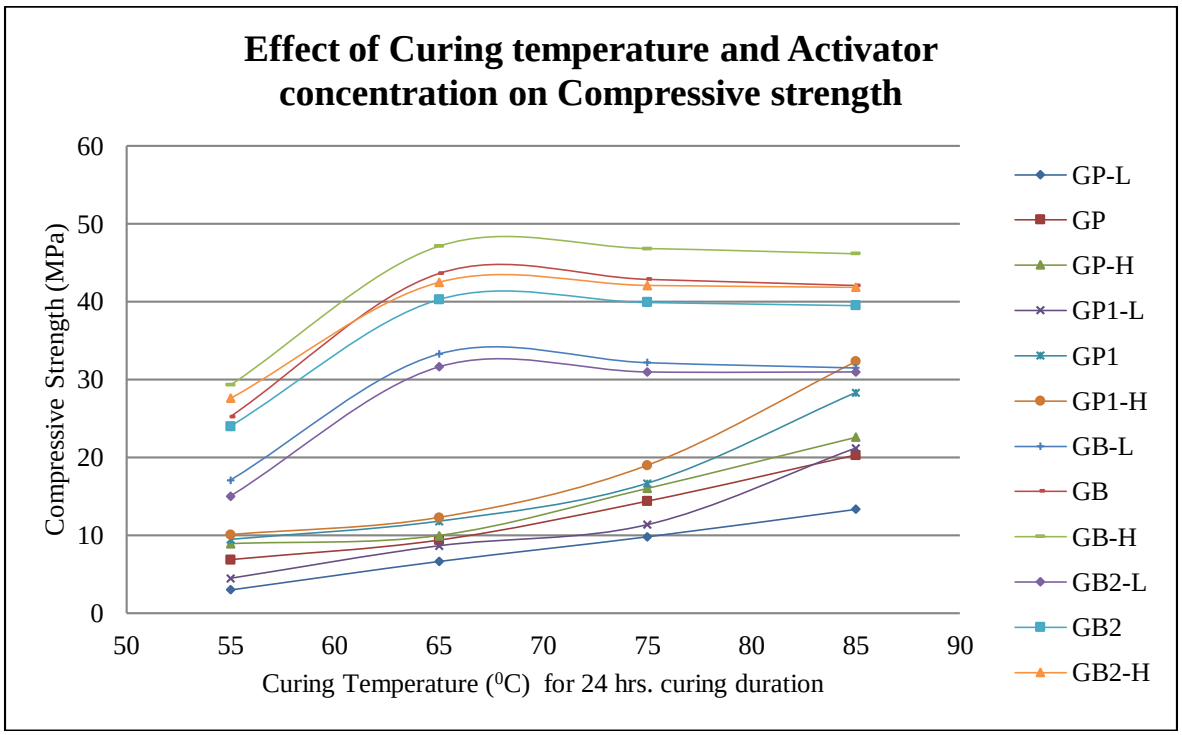

Figure 4.19 Combined effect of Curing temperature and Activator concentration on Compressive strength of Fly ash Geopolymer blended with Slag

4.3.1.2.2 Compressive Strength of Water cured samples

4.3.1.2.2.1 Effect of Rest period on Compressive strength of Alkali activated Fly ash blended with Slag, cured in water

Compressive strength was studied at prefixed interval of time. In this study, the initial chemical composition of every sample was same (mix id: GB; 6% Na_2O in activator and 15 % slag as supplements (Ref. Table 3.16). The specimens were studied based on the rest period (2 to 24 hrs. prior to water curing applied to each cases). Geopolymer specimens subjected to longer rest periods exhibited rapid compressive strength gain subjected to water curing. For example, sample GB_R (24) _WC showed 19 MPa compressive strength after 24 hours of water curing (Figure 4.20a). On the other hand, specimens subjected to shorter rest period exhibited slow strength gain subjected to water curing. For example, GB_R (24)_WC attained around 95% of its strength after 24 hours with respect to 20 day strength i.e. after a water curing of 20 days (Figure 4.20b), whereas GB_R(2)_WC attained only 16% of its strength after 24 hours with respect to 20 day strength (Figure 4.20c). This was due to the fact that when ions dissolve in water, they release energy in the form of heat due to the stabilizing interaction. Somehow this energy may be the summation of lattice energy and heat of hydration due to the dissolution of a portion of the ionic solid. The water molecules oriented themselves in a manner that reduced the localized charge on the ions. The addition of alkali activator to the base material produced a dissolved state. The aqueous state was thermodynamically favorable for the geopolymeric reaction itself. But primary poly-condensation could be initiated with an external source of energy in the form of heat. The post water curing of activated fly ash could incorporate a secondary heat input to enhance the partial polymer formation. These phenomena indicate that the initial rest period had an impact on the chemistry of the reaction, which has been mentioned as a new scope of study in various prior works [27], [133], [76], [101], [96] and [75].

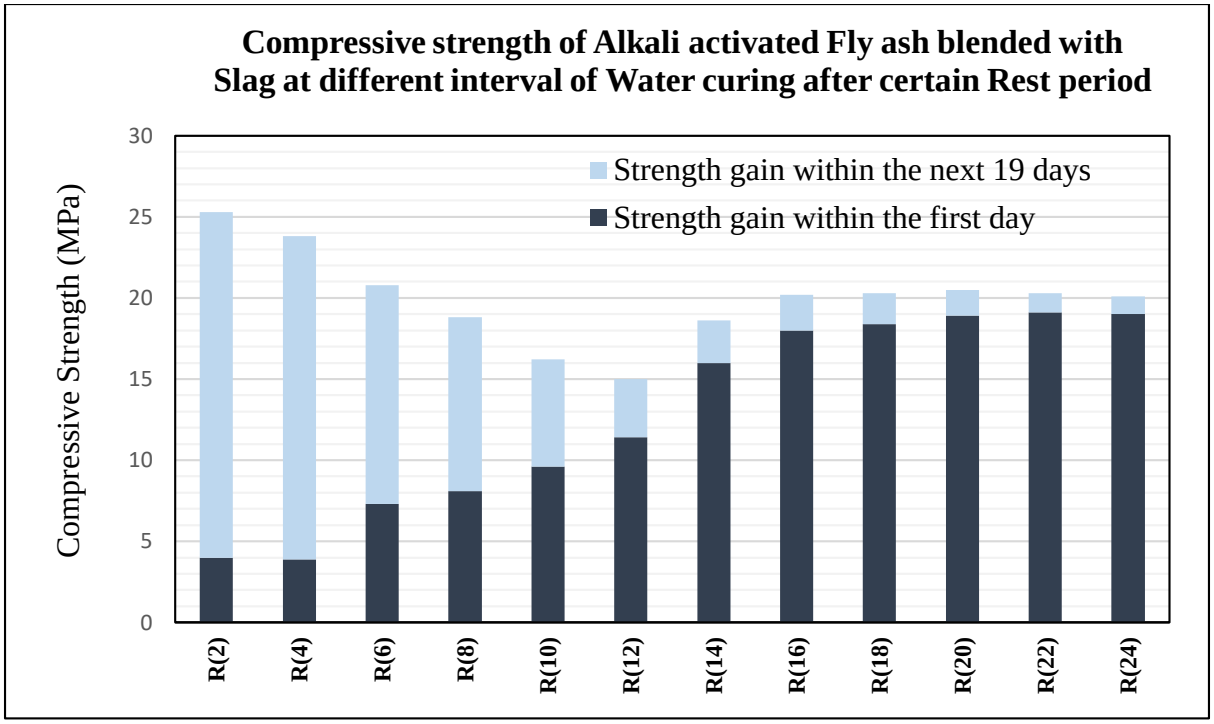

Figure 4.20 (a): 1 and 20 day Compressive strength after curing of specimens (for varying rest periods)

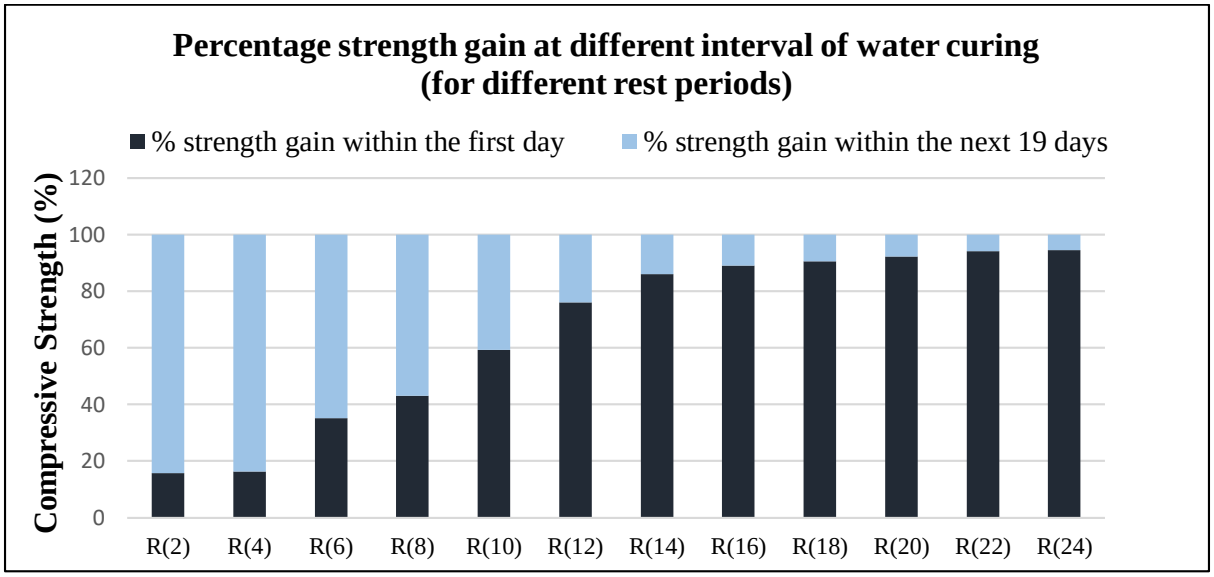

Figure 4.20 (b): 1 and 20 day Compressive strengths (expressed as percentages of 20 day strength) after Water curing of specimens (for different rest periods)

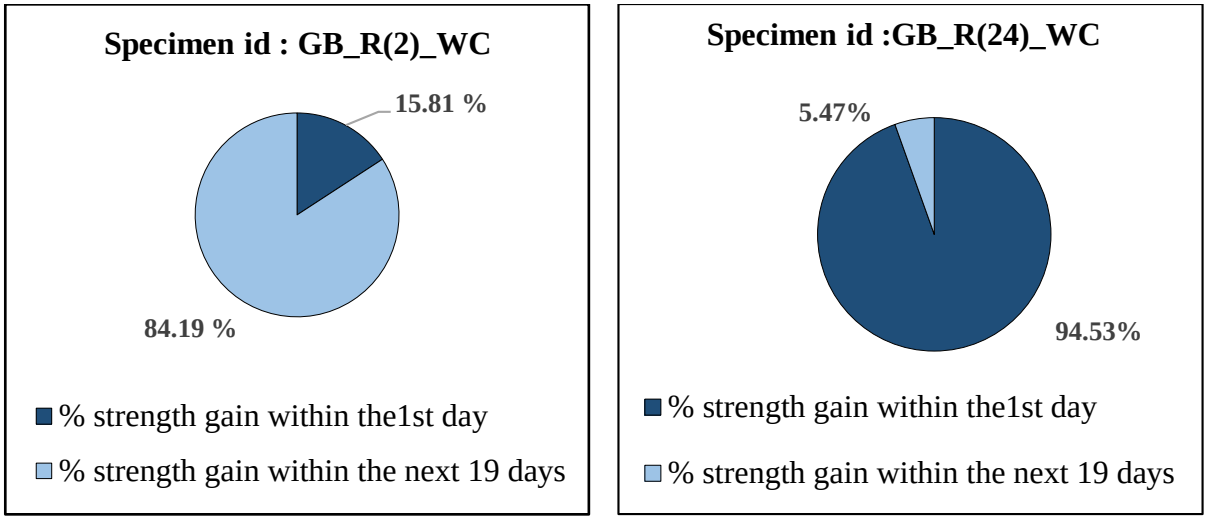

Figure 4.20 (c): Strength gain of Water cured specimens (for varying rest periods)

Table 4.9: Compressive strengths 1 and 20 days after Water curing of Alkali activated Fly ash specimens (for varying rest periods - 2 to 24 hrs.)

Sample ID	Compressive Strength (MPa) after 1st day curing	Compressive Strength (MPa) after 20 days curing	Increment between 2nd day and 20th day	%Compressive strength gain within one day	%Compressive strength gain within next 19 days
GB_R(2)_WC	4	25.3	21.3	15.81	84.19
GB_R(4)_WC	3.9	23.8	19.9	16.39	83.61
GB_R(6)_WC	7.3	20.8	13.5	35.10	64.90
GB_R(8)_WC	8.1	18.8	10.7	43.09	56.91
GB_R(10)_WC	9.6	16.2	6.6	59.26	40.74
GB_R(12)_WC	11.4	15	3.6	76.00	24.00
GB_R(14)_WC	16	18.6	2.6	86.02	13.98
GB_R(16)_WC	18	20.2	2.2	89.11	10.89
GB_R(18)_WC	18.4	20.3	1.9	90.64	9.36
GB_R(20)_WC	18.9	20.5	1.6	92.20	7.80
GB_R(22)_WC	19.1	20.3	1.2	94.09	5.91
GB_R(24)_WC	19	20.1	1.1	94.53	5.47

4.3.1.3 Water absorption and Apparent porosity

4.3.1.3.1 Water absorption and Apparent porosity of Heat cured specimens

4.3.1.3.1.1 Effect of Lime stone dust blending on Apparent porosity and Water absorption of Fly ash based Geopolymer

Three different series of specimens (GP1, GL1 and GL2) were selected to assess the apparent porosity and water absorption (discussed in chapter-3, Table 3.10). These tests were conducted to find the preliminary idea about the permeable pore volume of fly ash based geopolymer when blended with lime stone dust. The selected specimens were subjected to microstructural investigations later on to assess the porosity along with the pore size distribution. Porosity is an important aspect which directly influence on the mechanical performance of fly ash based geopolymer [115]. The apparent porosity and water absorption value were decreased for fly ash based geopolymer with the incorporation of lime stone dust (10% and 15% of (fly ash plus lime stone dust)).The minimum value of apparent porosity and water absorption were found for sample GL2 are 21.7 % and 4.69 % respectively (Figure 4.21 and Figure 4.22). Earlier research indicated that the amorphous sodium aluminosilicate product is achievable in presence of calcium compound in alkaline environment [128].Again, secondary CSH (calcium silicate hydrate) may be formed which can reduce the size of pores [108]. But the tests was carried out for a period of 24 hours (discussed in chapter-3), which may not be sufficient to appreciate the entire permeable pore volume.

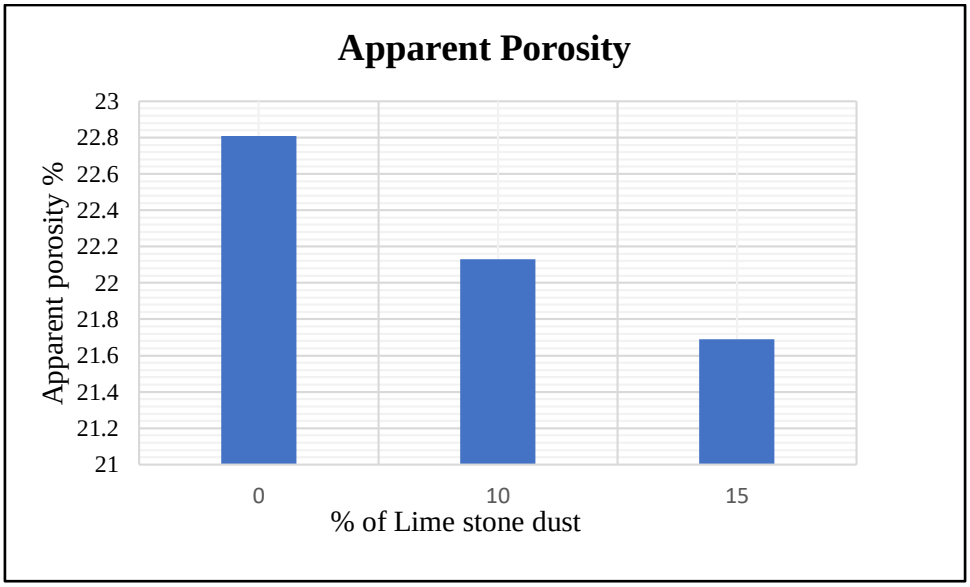

Figure 4.21 Apparent porosity of Fly ash based Geopolymer blended with Slag

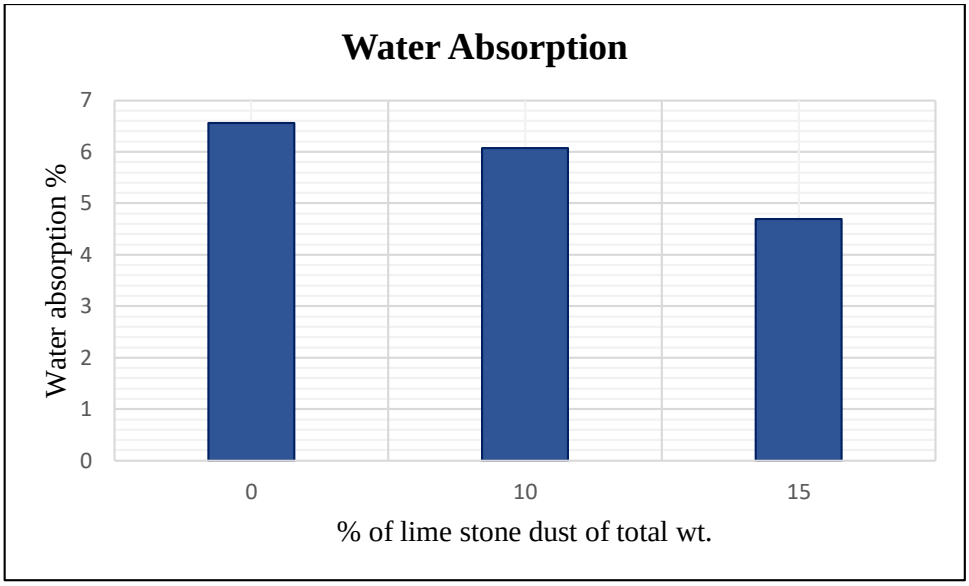

Figure 4.22 Water absorption of Fly ash based Geopolymer blended with Lime stone dust

4.3.1.3.1.2 Effect of Slag blending on Water absorption and Apparent porosity of Fly ash based Geopolymer

GP1, GB1 and GB2 (Chapter-3, Table 3.14) were considered to understand the effect of slag blending with fly ash based geopolymer on apparent porosity and water absorption. The similar impact was found as observed earlier in case of lime stone dust blending. The poly-condensation process is improved in presence calcium ions in the geopolymer mix which may produce better microstructure [44]. Specimen GB2 (fly ash based geopolymer blended with 15 % blast furnace slag) showed minimum values of apparent porosity and water absorption (Figure 4.23 and Figure 4.24). The value of apparent porosity and water absorption for sample GB2 was found 22.93% and 10.89% respectively. The study on the porosity of blended geopolymer may be continued at micro level to study the pore morphology of blended and non-blended fly ash geopolymer.

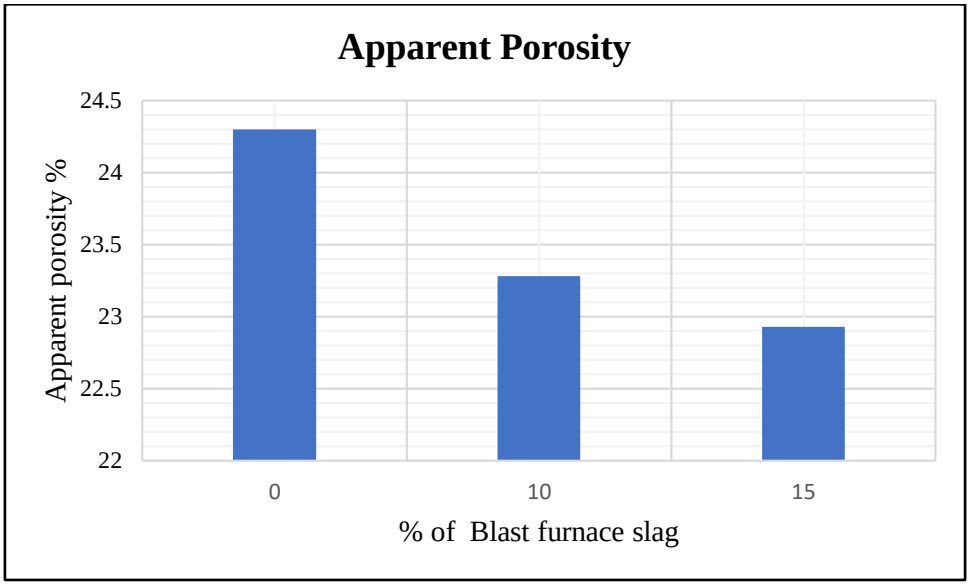

Figure 4.23 Apparent porosity of Fly ash based Geopolymer blended with Slag

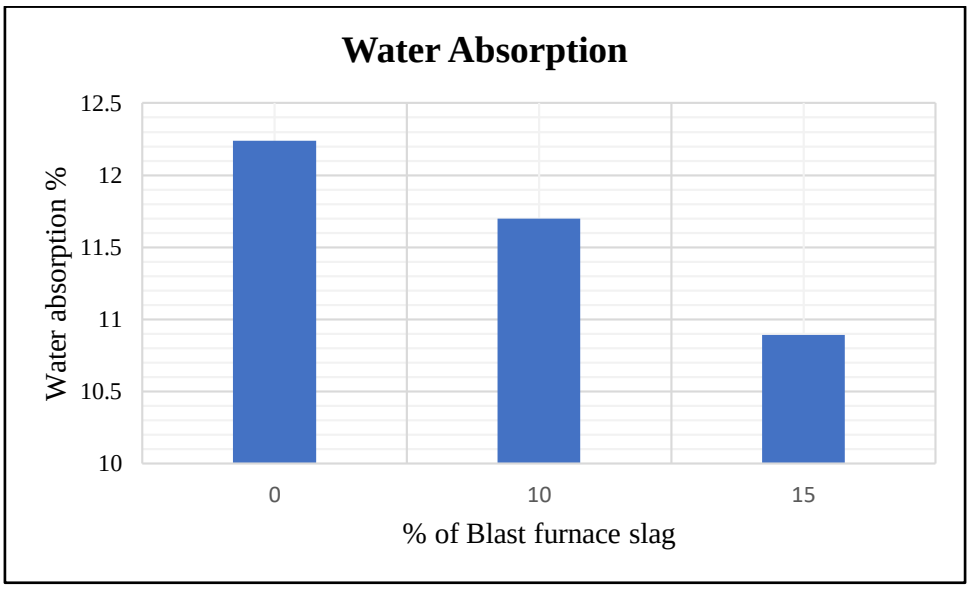

Figure 4.24 Water absorption of Fly ash based Geopolymer blended with Slag

4.3.1.4 Sorptivity

4.3.1.4.1 Sorptivity of Heat cured specimens

4.3.1.4.1.1 Effect of Lime stone blending on Sorptivity of Fly ash Geopolymer

Three series of specimens (GP1, GL1 and GL2) were selected to assess the water sorptivity (discussed in chapter-3, Table 3.10).The procedure of water sorptivity test has been discussed in chapter 3. Some of the literatures has claimed that sorptivity is directly connected to the durability of concrete [116]. Sorptivity is the indication of the flow of water against gravity through a specimen. Unidirectional flow from the bottom surface is only considered for this test. The cumulative absorption of water per unit surface area was plotted with respect to the

square root of time [Figure 4.25(a)]. Trend line on the curve was drawn in a way to find out the slope [Figure 4.25(b)]. The slope of the plot represents the sorptivity (Figure 4.26). The rising initial trend (ref. to Fig. 4.25(a)) of blended geopolymer may be due to the reduction of average pore sizes which may enhance the surface tension and the capillary rise of water through the specimens. However, the total absorption value was less for the blended geopolymer compared to non-blended fly ash based geopolymer. This test clearly indicates the change in pore size and pore volume of different geopolymer specimens with the blending of lime stone dust. This aspect has been further discussed based on MIP results later on.

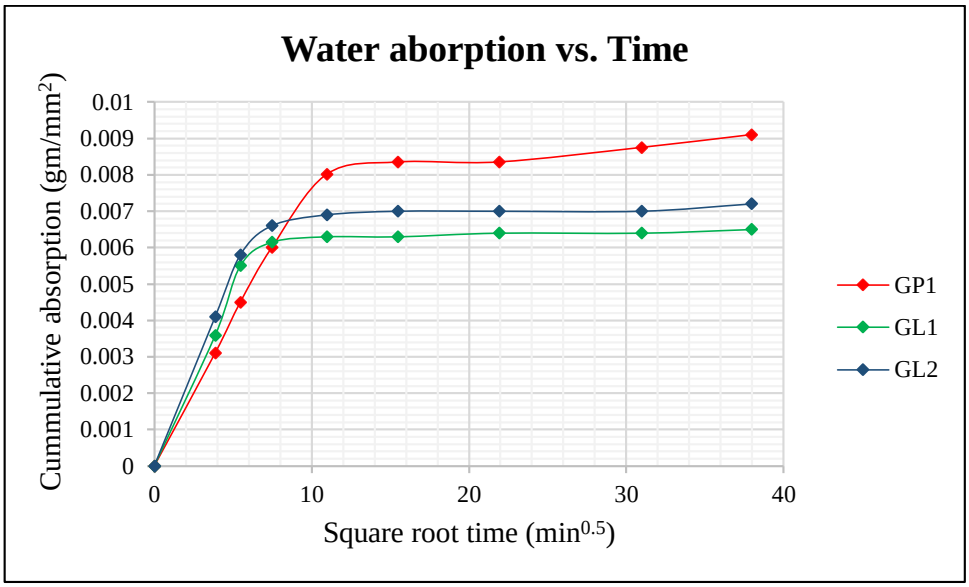

Figure 4.25(a) Trend of cumulative absorption of water for Fly ash based Geopolymer blended with Lime stone dust

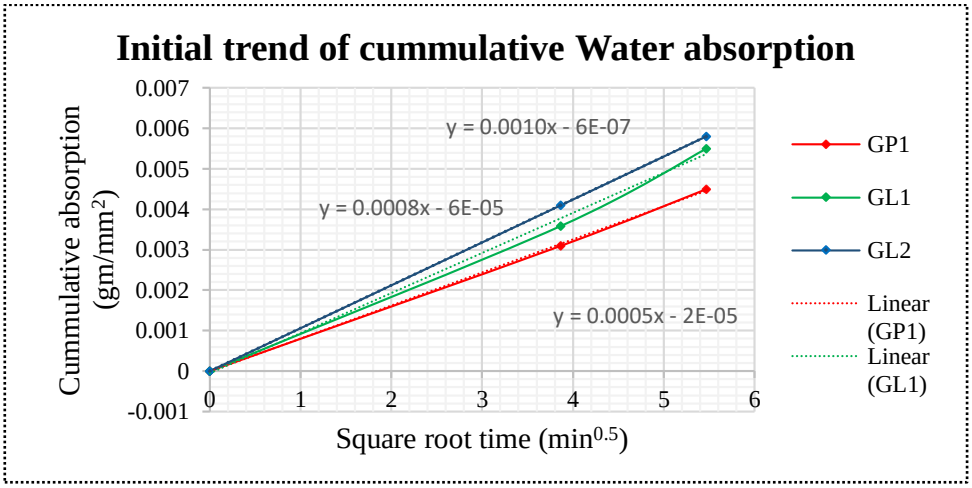

Figure 4.25(b) Initial trend of cumulative absorption of Fly ash based Geopolymer blended with Lime stone dust

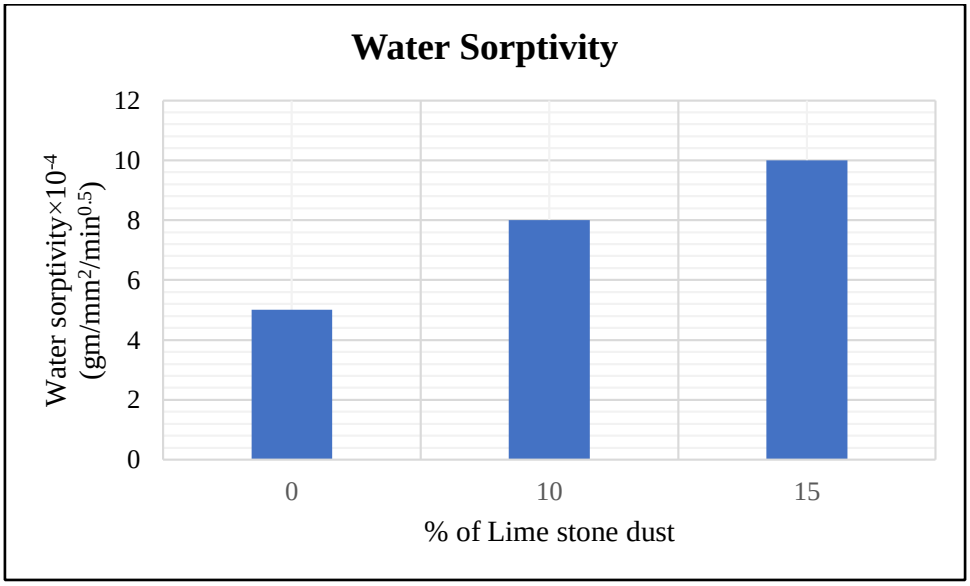

Figure 4.26 Sorptivity of Fly ash based Geopolymer blended with Lime stone dust

4.3.1.4.1.2 Effect of Slag blending on Sorptivity of Fly ash based Geopolymer

In the similar way, GP1, GB1 and GB2 (discussed in chapter-3, Table 3.14) were selected to appreciate the effect of fly ash based geopolymer blended with slag, on sorptivity. Cumulative water absorption with respect to the square root of time has been plotted in Figure 4.27(a). The value of sorptivity for different specimens has been plotted in Figure 4.28. In every cases, all the non-blended and blended specimens showed faster rate of capillary absorption at the initial stage which was drops with time considerably. The highest value of cumulative absorption was observed for the non-blended specimen GP1. But the sorptivity value was quite higher for blended specimens. The sorptivity actually indicates the rate of absorption which is subjected to the capillary surface tension (as discussed earlier). Again, the capillary surface tension is a function of pore sizes. So, the result may be indicated towards the possible reduction in average pore sizes, due to the blending of slag as supplement in fly ash based geopolymer.

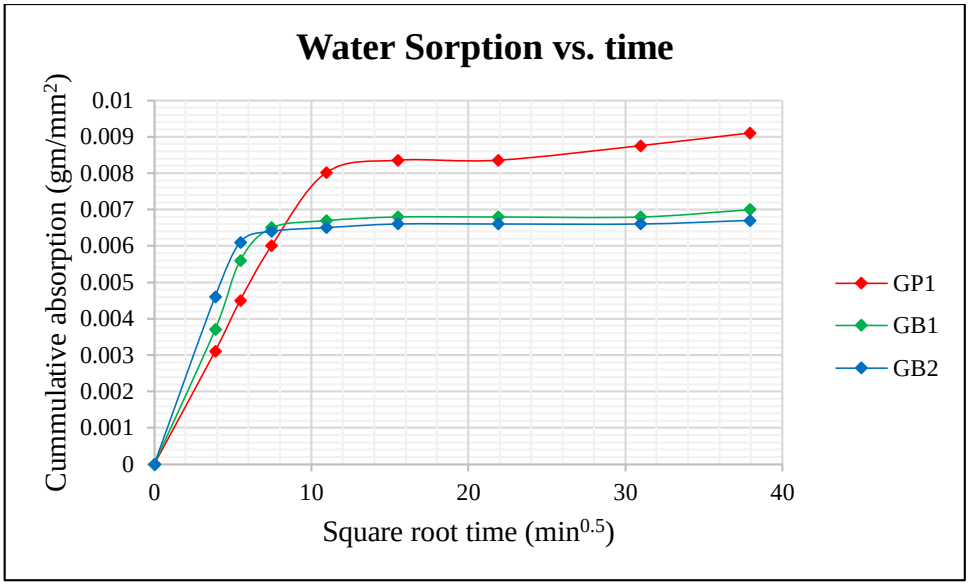

Figure 4.27(a) Cumulative absorption of Fly ash based Geopolymer blended with Slag

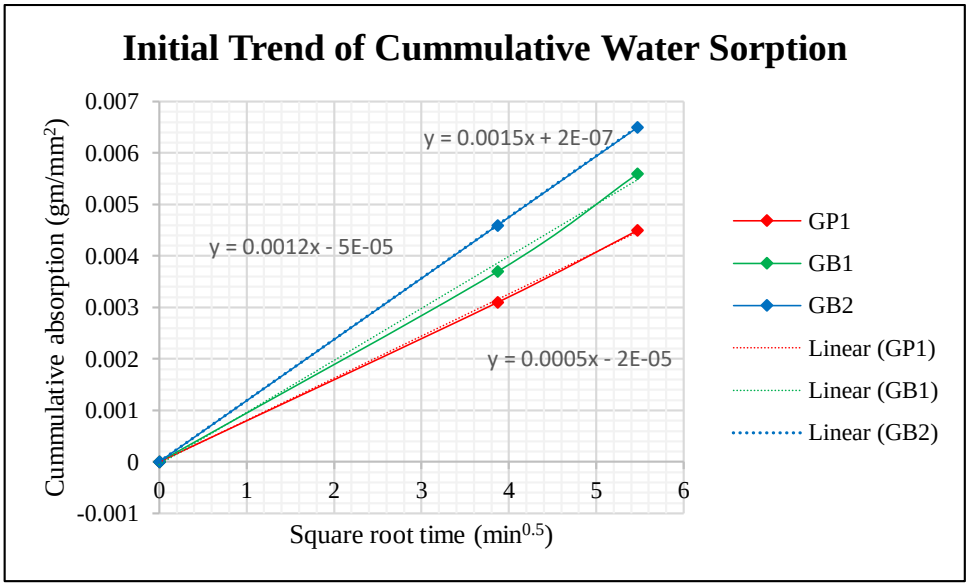

Figure 4.27(b) Initial trend of cumulative absorption of Fly ash based Geopolymer blended with Slag

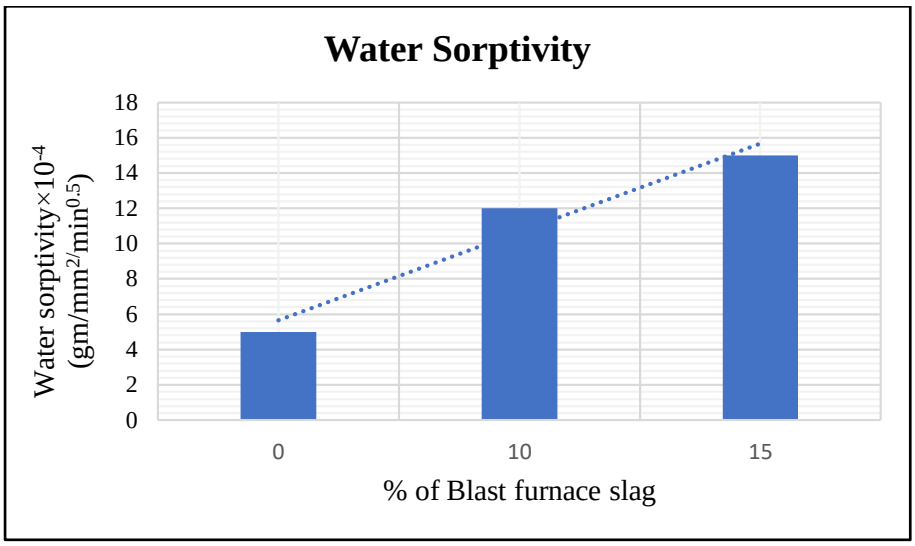

Figure 4.28 Water Sorptivity of Fly ash based Geopolymer blended with Slag

4.3.2 Microstructural Property

4.3.2.1 Microstructural Property of Heat cured specimens

4.3.2.1.1 Microstructural properties analysis by SEM & EDX

4.3.2.1.1.1 Effect of Lime stone dust blending on Microstructural property of Fly ash based Geopolymer

Scanning Electron Microscopy was conducted to find the morphological changes in fly ash based geopolymer with the incorporation of lime stone dust. This test was useful to understand the pore morphology and view the surface texture under higher resolution. In most of the cases, scanning electron microscopy was conducted on particles collected from the inner portion of the geopolymer specimen. Higher extent of porous and rough texture, comprising with some unreacted portion were observed for specimen GP1, whereas less porous and compact surface texture were observed for fly ash based geopolymer blended with lime stone dust, for specimens GL1 and GL2 (discussed in Chapter-3; Table 3.10).The smooth and compact surface indicate the positive effect of blending with lime stone dust. The existence of semi- crystalline and crystalline compound (compound containing water) were found in specimem GP1 under scanning electron microscopy as shown in Figure 4.30. The continuous rise in compressive strength of the fly ash based geopolymer (specimen GP1) with age, may be due to the existence of this non-amorphous product within the amorphous body. But for fly ash based geopolymer blended with lime stone dust (ie. specimens GL1 and GL2) did not show this kind of crystalline compound under scanning electron microscopy. On few selected points EDX spectrums were taken to quantify some basic elements like silicon, aluminium, oxygen, carbon. Sodium and calcium. The element quantity was plotted

as percentage by weight (wt. %). The weight percent of silicon for specimen GP1, GL1 and GL2 were found 15.8 wt. %, 18.18 wt. % and 19.54 wt. % respectively. Similarly, the weight percent of aluminium was recorded as 8.04 wt. %, 10.92 wt. % and 9.12 wt. % respectively. The variation in reacted calcium percentage was observed for GP1, GL1 and GL2 as 0.25 wt. %, 5.22 wt. % and 7.28 wt. % respectively. The earlier studies showed that presence of calcium based compound into the geopolymer mixture, may develop secondary Ca-Al-Si structure in the geopolymer product [48]. The report of EDX analysis indicates the possible presence of secondary Ca-Al-Si structure in the fly ash based geopolymer blended with lime stone dust. The variation in SEM micrographs along with EDX quantification indicates the positive structural changes in fly ash based geopolymer blended with lime stone dust.

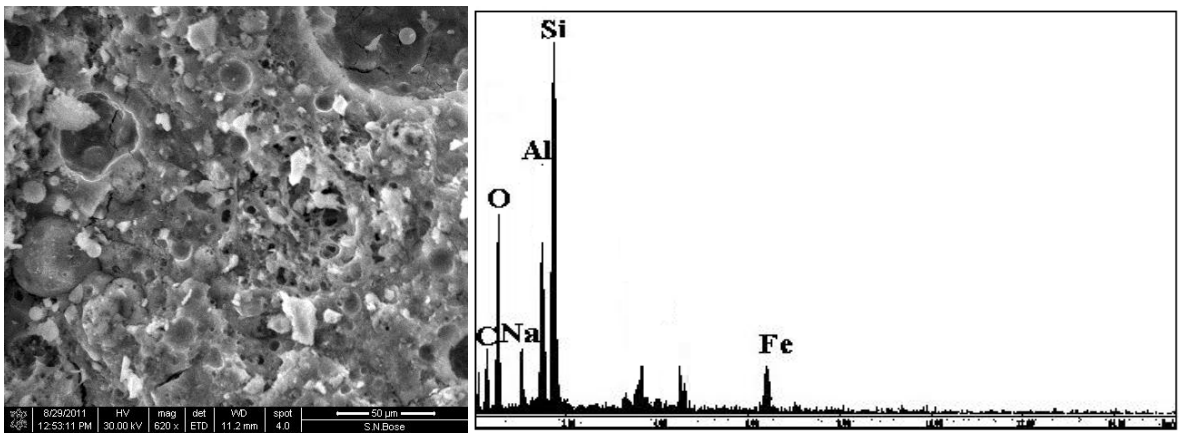

Figure 4.29(a) SEM @ 620x zoom and EDX of specimen GP1

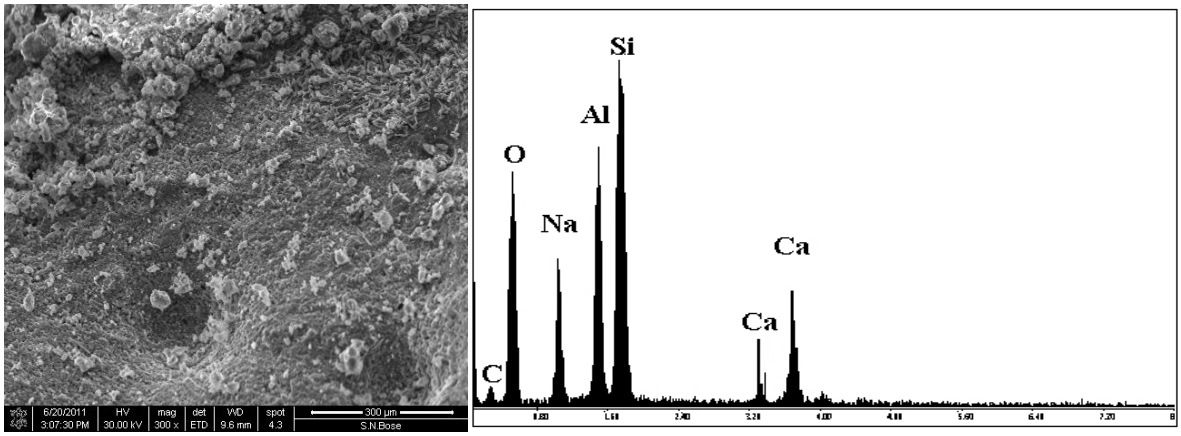

Figure 4.29(b) SEM @ 300x zoom and EDX of specimen GL1

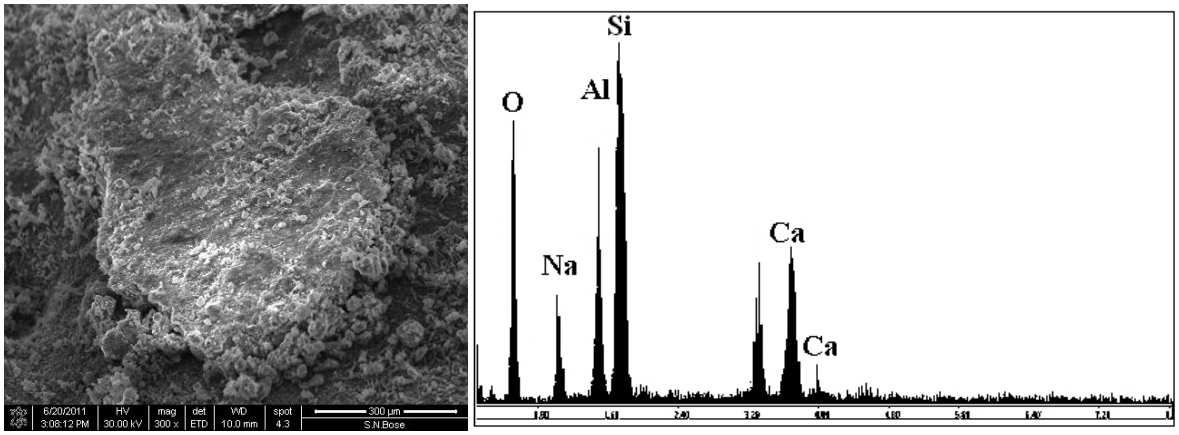

Figure 4.29(c) SEM @ 300x zoom and EDX of specimen GL2

Figure 4.29 SEM micrographs and EDX spectra for Geopolymer paste specimens blended with lime stone dust

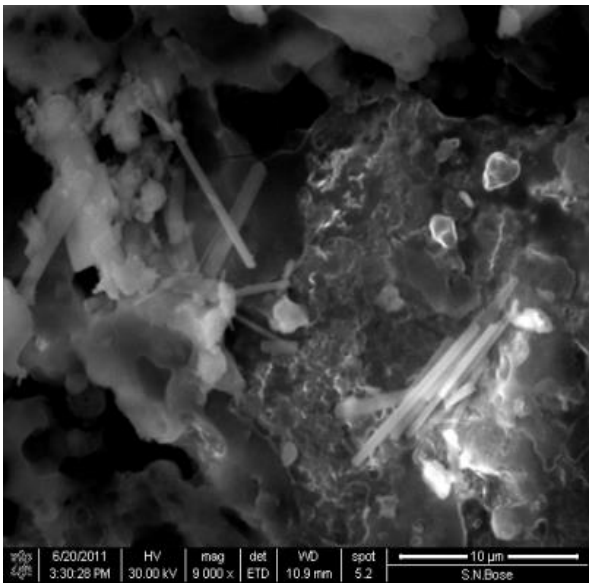

Figure 4.30 SEM @ 9000x zoom; presence water crystal in specimen GP1-HL

4.3.2.1.1.2 Effect of blast furnace slag blending on Microstructural property of Fly ash based Geopolymer

Scanning electron microscopy indicated improved surface texture for fly ash based geopolymer blended with blast furnace slag. The SEM micrographs and EDX spectrums for specimen GP1, GB1 and GB2 (discussed in Chapter-3; Table 3.14) are presented in Figure 4.31(a), 4.31(b) and 4.31(c). All the specimens were undergone to larger magnification of SEM. Under larger magnification of scanning electron microscopy fly ash based geopolymer (specimen GP1) showed the presence of crystalline structure (comprising of water) within the pores, as shown in Figure 4.31(d) to Figure 4.31(i). This crystalline portion may be responsible for the instability of the structure. A crystalline segment with a diameter of 152 nm was observed in specimen GP1 under 50,000 x-zoom as shown in Figure 4.31(i). The EDX spectrum on the crystalline segments indicated the existence of alkali gel associated with sodium, as shown in Figure 4.31(j). Some particles were collected from the inner part of every geopolymer specimens and subjected to scanning electron microscopy. In Figure 4.32, the noted points A, B, C, D for specimen GP1 exhibit few regular crystal structure which may be considered as the non-reacted alkali. This crystal structure may cause volumetric changes with the variation of climatic temperature or make ionic exchange under any aggressive solution exposer [146].The earlier research suggested that the poly-condensation of aluminium and silicon species at the time of gelation may bring complex frameworks comprising with trapped gel [101]. But fly ash based geopolymer blended with slag did not show the existence of crystalline compounds under higher magnification of scanning electron micrographs. Typical variation in connection with elemental weight percentage (wt. %) was observed through EDX spectrum. For example, the weight percentage of silicon, sodium, aluminium, calcium for specimen GP1 were evaluated as 15.95 wt. %, 3.71 wt. %, 8.38 wt.%, and 0.85 wt.% respectively. The important elements for GB1 were reported as Si (19.93 wt. %), Na (4.94 wt. %), Al (9.13 wt. %), Ca (3.32 wt. %). For GB2 the EDX analysis indicated as Si (26.54 wt. %), Na (5.33 wt. %), Al (8.46 wt. %) and Ca (10.52 wt. %). For GB1 & GB2 both the SEM and EDX reports support the existence of CSH and Ca-Al-Si structure which was depicted by earlier research [48, 50]. The fly ash based geopolymer blended with slag was found to be more amorphous. The multi-phase-blended geopolymer was stable enough in connection with strength and age.

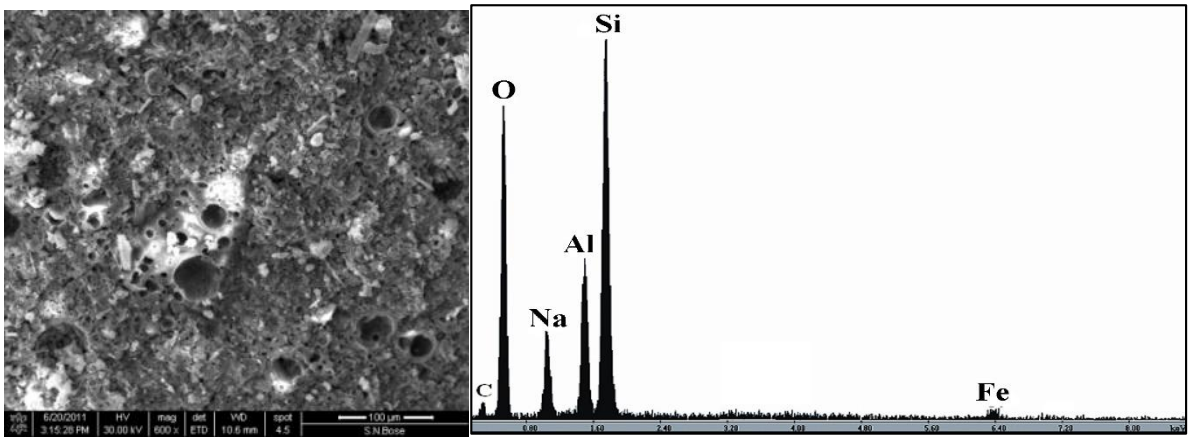

Figure 4.31(a) SEM @ 600x zoom and EDX of specimen GP1

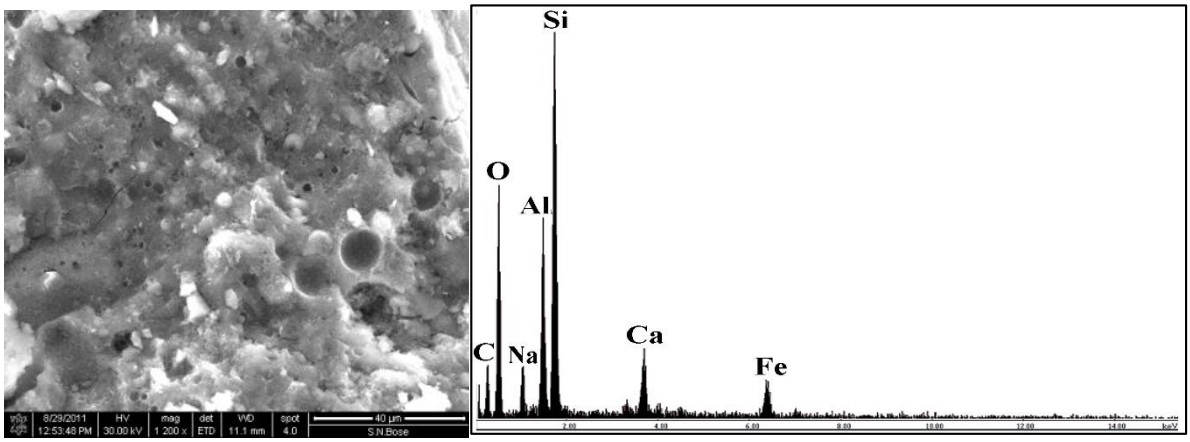

Figure 4.31(b) SEM @ 1200x zoom and EDX of specimen GB1

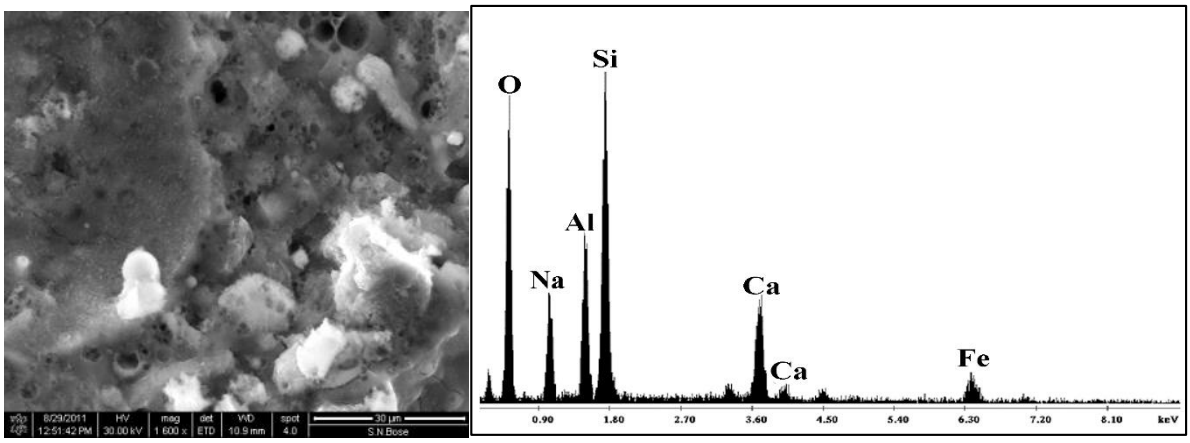

Figure 4.31(c) SEM@ 1600x zoom and EDX of specimen GB2

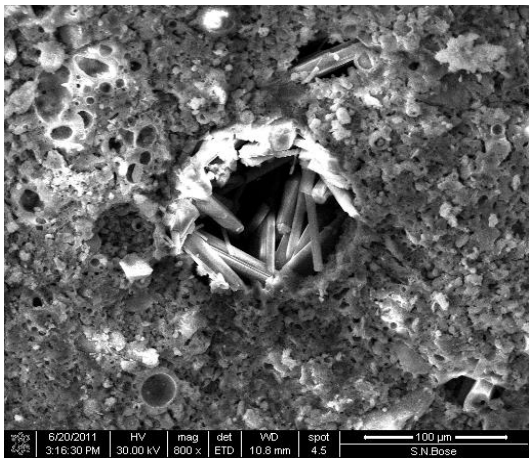

Figure 4.31(d) SEM @ 800x zoom of specimen GP1

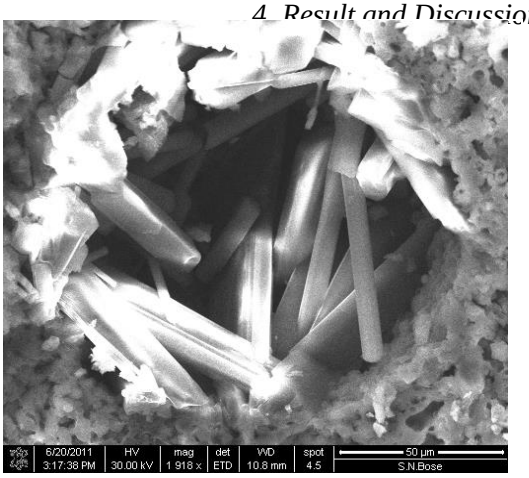

Figure 4.31(e) SEM @1918x zoom of specimen GP1

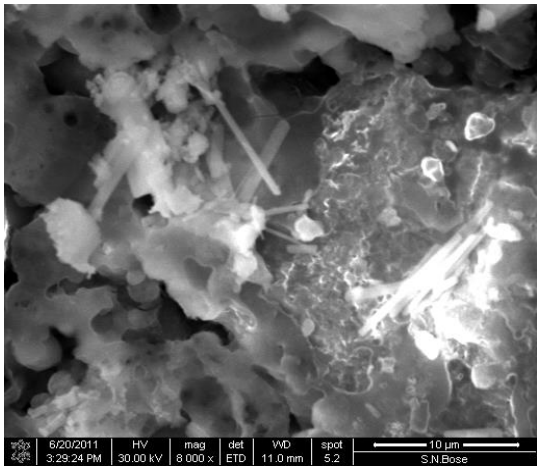

Figure 4.31(f) SEM @ 8000x zoom of specimen GP1

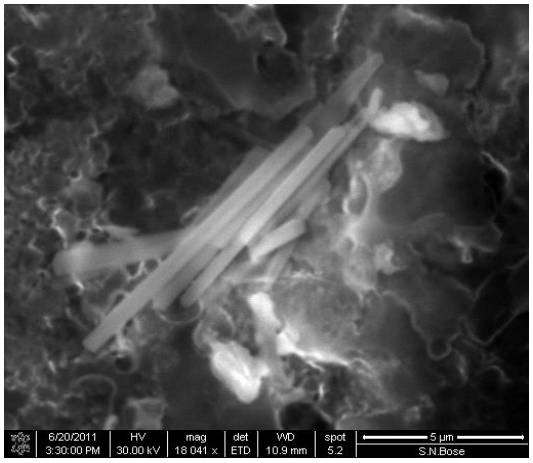

Figure 4.31(g) SEM @ 18041x zoom of specimen GP1

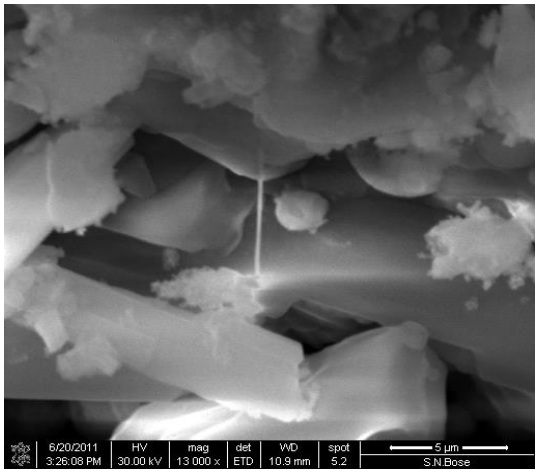

Figure 4.31 (h) SEM @ 13000x zoom of specimen GP1

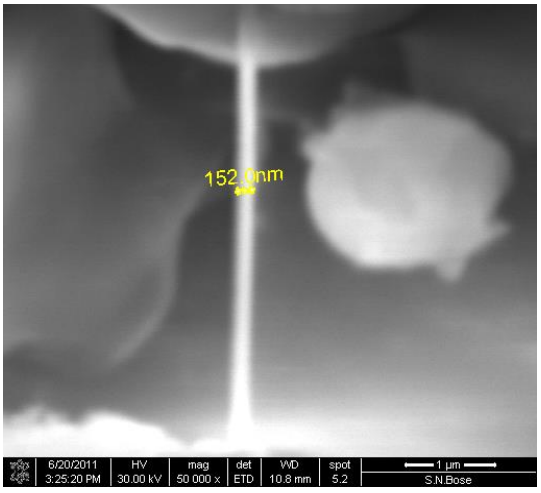

Figure 4.31 (i) SEM @ 50000x zoom of specimen GP1

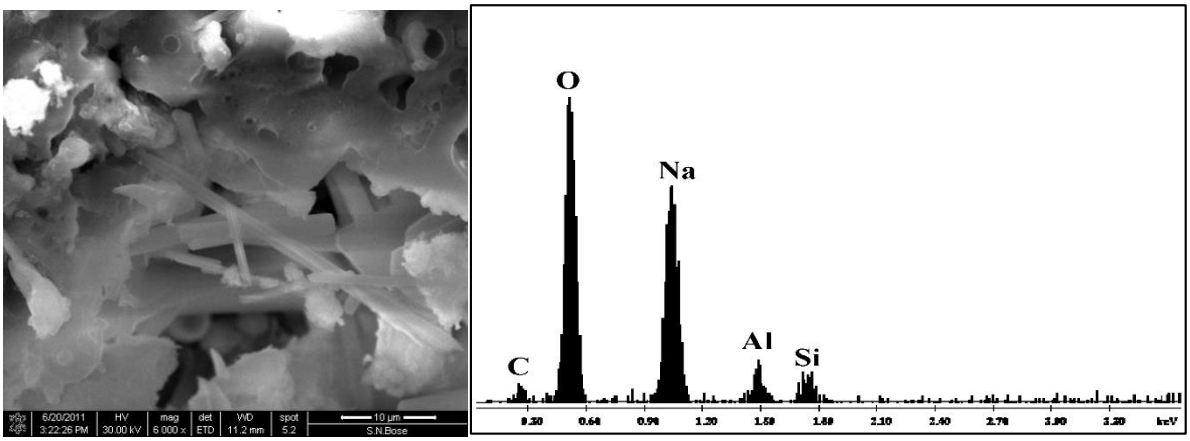

Figure 4.31(j) SEM @ 6000X zoom and EDX of crystalline compound within the pore of specimen

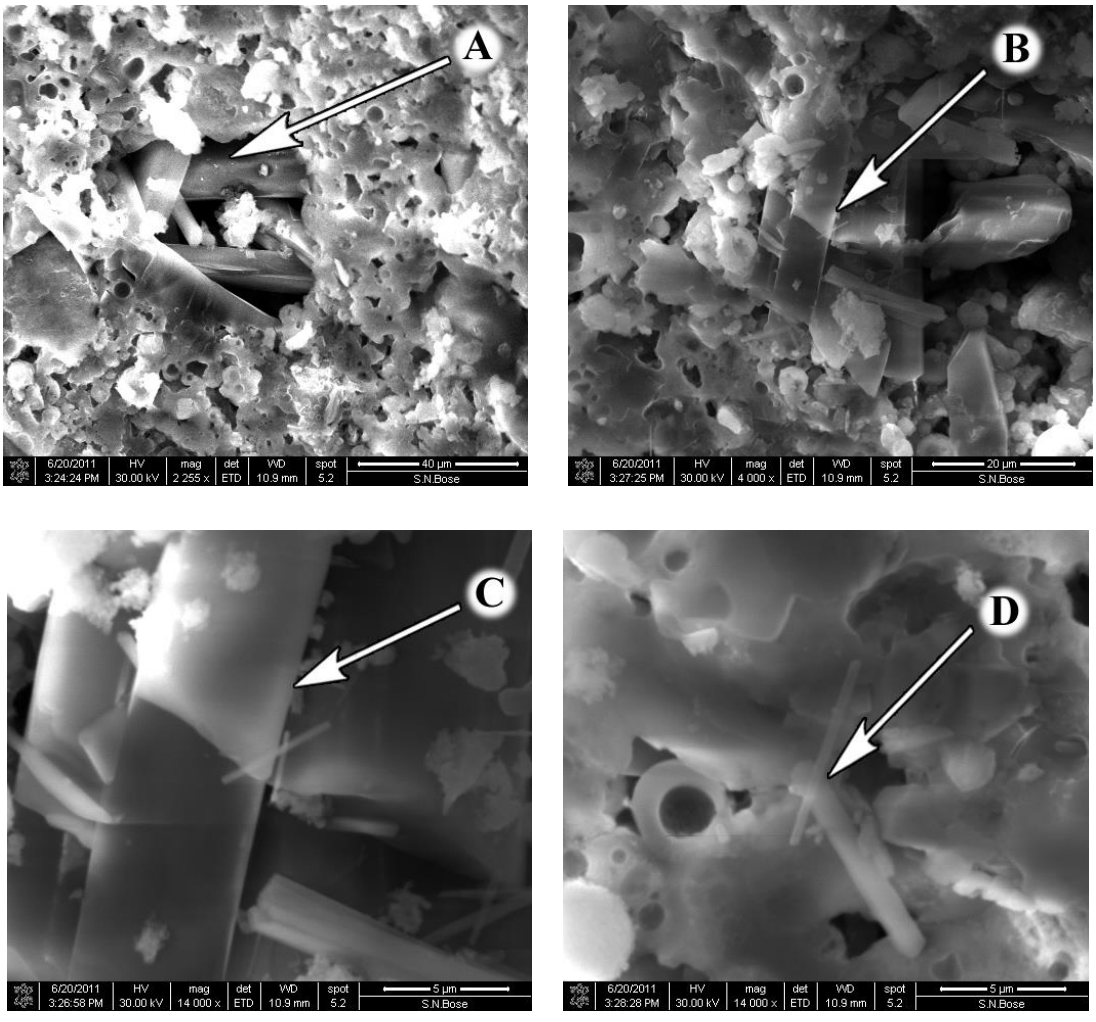

Figure 4.32 SEM of GP1 on typical interior point under progressive zoom
(A) 2255x (B) 4000x (C) 14000x (D) 14000x

4.3.2.1.2 Mercury Intrusion Porosimetry (MIP)

4.3.2.1.2.1 Effect of Lime stone dust blending on Pore distribution of Fly ash Geopolymer

Mercury intrusion porosimetry test was conducted to evaluate the variation in pore characteristics for fly ash based geopolymer blended with lime stone dust. Two distinct specimens (specimen GP1 and specimen GB2) were selected to observe the variation in pore characteristics of fly ash based geopolymer due to the blending of lime stone dust. The mean median pore size, shape, inter-connectivity, permeable pore volume were detected through this MIP test. The intrusion and extrusion pattern of mercury from the permeable pores were different for those specimens. Figure 4.33 and Figure 4.34 represent the typical plotting of MIP curves for specimen GP1 and specimen GB2. The maximum level of mercury intrusion for the fly ash based geopolymer (specimen GP1) was observed within the range of 0.01 to 20 micrometer (pore diameter). The pick intrusion for the specimen was appeared for a pore diameter of 0.1 micrometer. The discontinuity of the mercury extrusion curve (blue line curve in Figure 4.33) indicates the ultimate fracture of specimen GP1 at the time of the extrusion of mercury. Sometime the mercury cannot escape out from the internal pores due to the bottle necked shape of the pores and creates internal pressure. As earlier study depicts that most of the cases larger pores seem like smaller due to its bottle-neck shape [45]. Specimen GB2 showed moderate amount of intrusion within the pore diameters, ranged from 0.005 to 2.0 micrometer. The maximum intrusion was occurred for the pore diameter equal to 0.04 micrometer. Hence, the pore diameter responsible for maximum intrusion under certain pressure is lesser in size for fly ash based geopolymer blended with lime stone dust. This result depicts the reduction in average pore size for fly ash based geopolymer blended with lime stone dust. Bulk density for fly ash based geopolymer was improved by 22% with the incorporation of 15% lime stone dust. In earlier study, the similar research on pore characteristics was conducted by considering typical alkali parameters [39]. The present experimental investigation was focused to the effect of blending by controlling the alkali parameters. The blending of lime stone dust in fly ash increase the calcium content. The calcium ions may participate in poly-condensation of geopolymer as a charge compensator of aluminium and accelerates the development of Ca-Al-Si as secondary filler material [88]. The change in pore characteristics support the improvement of other hardened properties due to the possibility of better reactivity level and bonding of the developed structure.

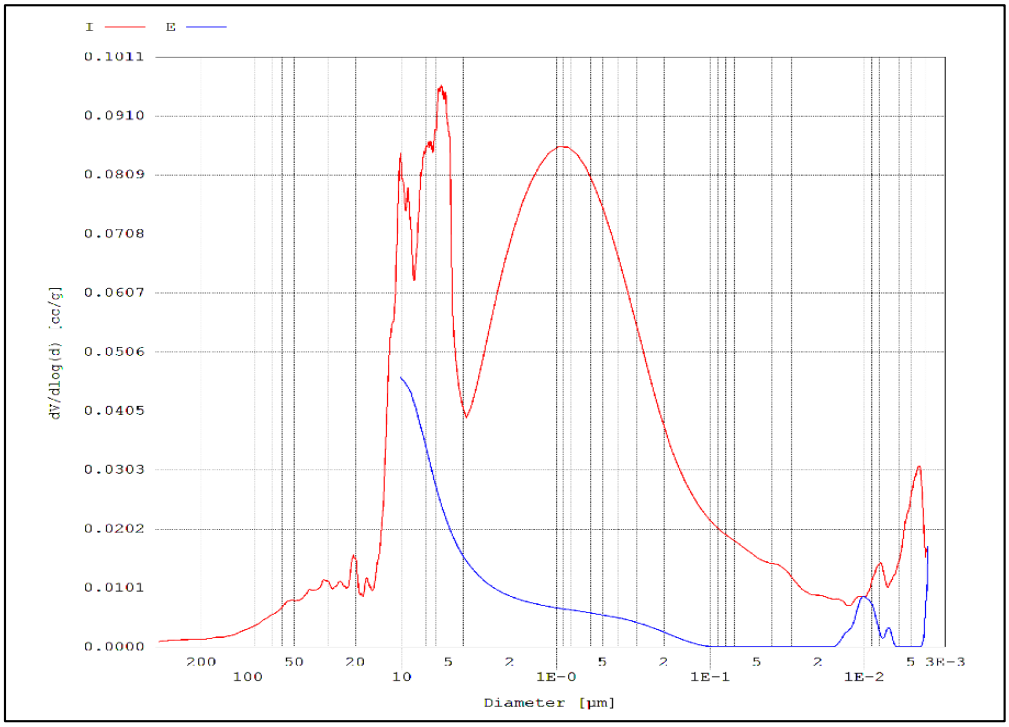

Figure 4.33 Typical plot of MIP analysis of specimen GP1

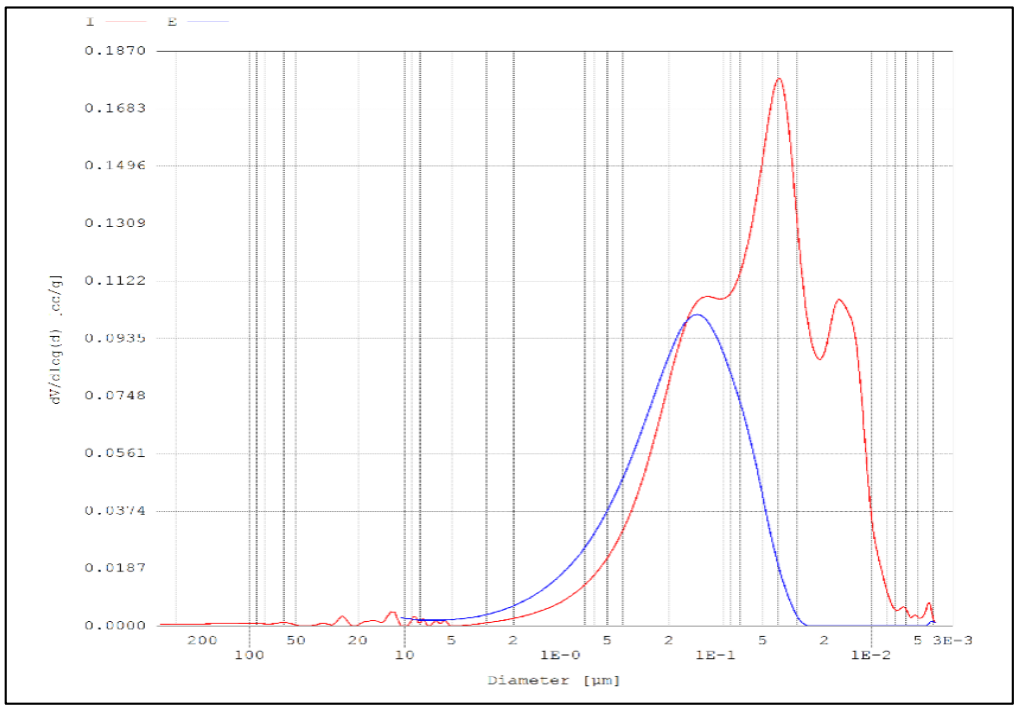

Figure 4.34 Typical plot of MIP analysis of specimen GL2

4.3.2.1.2.2 Effect of Slag Blending on Pore Distribution of Fly Ash based Geopolymer

Blending of slag as supplementary material (15%) with fly ash based geopolymer enhances the pore characteristics by reducing permeable pore volume. Two typical series of specimens; GP1 (only fly ash) and GB2 (fly ash based blended with 15% of slag) were considered. The pore size distribution curves (as shown in Figure 4.35 and Figure 4.36) indicate the notable reduction in the range of pore diameter and permeable pore volume. MIP plot the red and blue curve indicate the intrusion and extrusion of mercury as function of pressure respectively. Again, the return path of mercury is clear enough for blended geopolymer under huge pressure of extrusion. The blue line ie. the return path, indicates the extrusion of mercury with the release of applied pressure was not appeared for specimen GP1.This fact indicates the permanent fracture of the GP1 specimen. The maximum mercury intrusion for specimen GB2 and GP1 were observed at the range of 0.02 to 1.5 micrometre and 0.1 to 10 micrometre of pore diameters respectively. The maximum intrusion was found at a pore diameter of 0.3 and 0.4 micrometre for specimen GP1 and GB2 respectively. The blast furnace slag as a supplementary material in fly ash based geopolymer reduces the average pore size of the blended geopolymer. The improvement of the microstructure of fly ash based geopolymer with the incorporation of blast furnace slag by 15 % was observed.

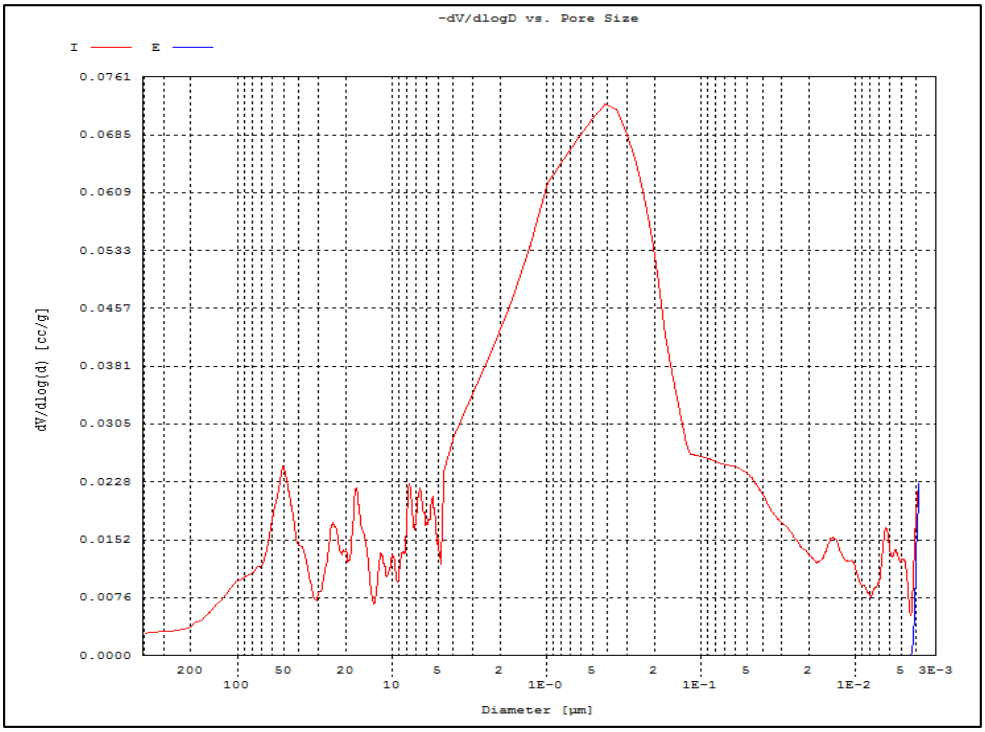

Figure 4.35: Typical plot of MIP analysis for specimen GP1

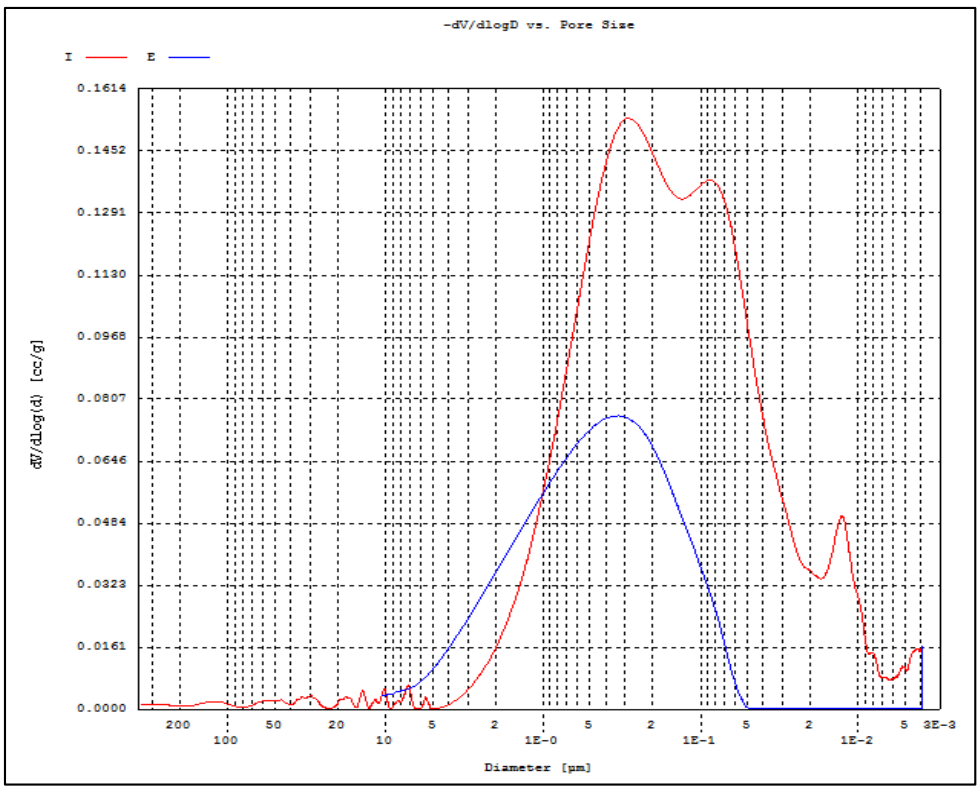

Figure 4.36: Typical plot of MIP analysis for specimen GB1

4.3.2.2 Microstructural Property of Water cured specimens

4.3.2.2.1 Property analyzed by FESEM

4.3.2.2.1.1 Effect of Rest period on the microstructure of Alkali activated Fly ash blended with Slag and cured in water

FESEM images were studied to study the morphological features of various specimens of alkali-activated fly ash (AAFA) blended with slag (mix id GB, Chapter-3; Table 3.16). The research demonstrated the performance of the slag as supplementary material in alkali activated fly ash with the change of rest period after casting before water curing. In every case, some unreacted matrix and partially reacted matrix were observed. In the case of GB_R (24) _WC, a relatively dense phase was identified (Figure 4.37 h;), a great portion of the raw material turned into a well-connected amorphous structure of glassy phase. Distributed particles of various sizes were observed in specimens GB_R (2) _WC, GB_R (8) _WC and GB_R (14) _WC as shown in Figure 4.37(a) to Figure (f). FESEM micrographs of these specimens showed that they contained particles of a wide size range. Earlier research [88] demonstrated that additional calcium contributes to the activation of siliceous material in two ways. Firstly, Ca^{+} primarily acts as a charge balancing agent and secondarily contributes to the formation of CSH gel. Alkali activated fly ash blended with 15 % slag, subjected to the shortest rest period (2 hrs.) before water curing [namely, specimen GB_R (2) _WC] showed certain different types of texture [Figure 4.37(a) and (b)] compared to the other specimens subjected to different rest periods. This particular texture primarily consisted of needle-like structures. It can be assumed that these needle-like projections developed from the development of non-amorphous or crystalline phases. The water curing after rest period might incorporate secondary heat input to enhance the partial polymer formation. The different amorphous and non-amorphous textural developments observed for chemically equivalent materials subjected to different rest periods demonstrated the influence of the rest period as a significant parameter.

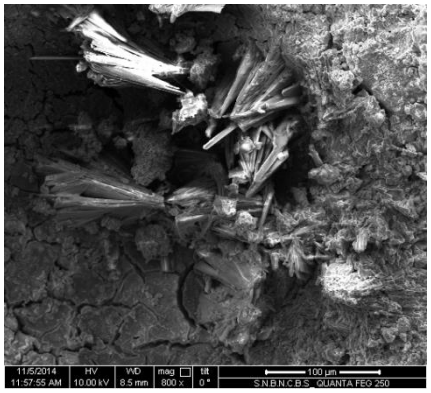

(a)

(b)

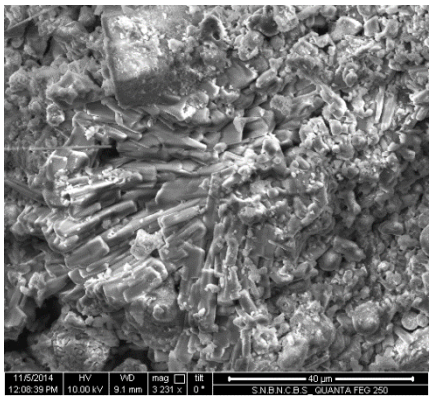

(c)

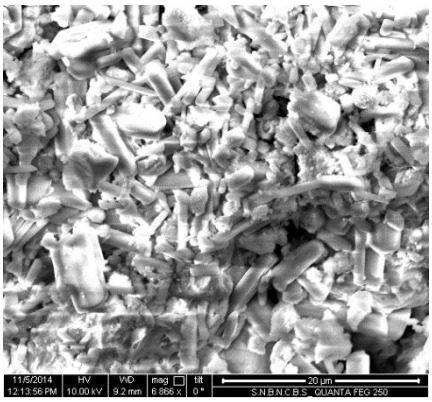

(d)

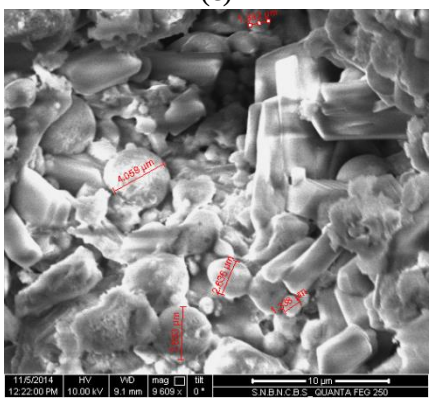

(e)

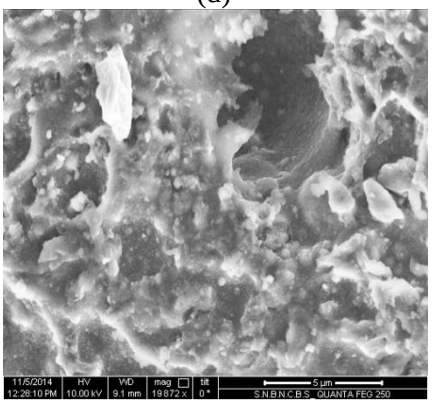

(f)

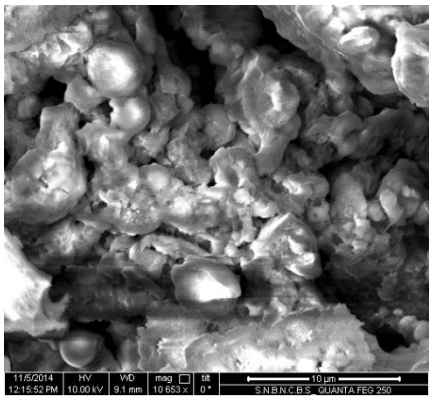

(g)

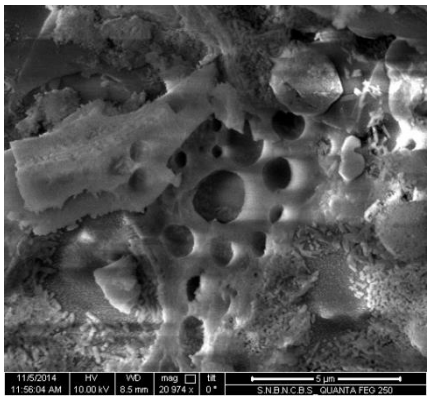

(h)

Figure 4.37 Scanning Electron Microscopy after 20 days of water curing

(a) Specimen GB_R(2)_WC at (800x)

(b) Specimen GB_R(2)_WC at (1524x)

(c) Specimen GB_R(8)_WC at (3231x)

(d) Specimen GB_R(8)_WC at (6866x)

(e) Specimen GB_R(14)_WC at (9609x)

(f) Specimen GB_R(14)_WC at (16479x)

(g) Specimen GB_R(24)_WC at (6866x)

(h) Specimen GB_R(24)_WC at (20974x)

4.3.2.2.2 XRD Analysis to study Mineralogical changes

4.3.2.2.2.1 Effect of Rest period after casting on mineralogical change of Alkali activated Fly ash blended with Slag and cured in water

The effects of rest period on the mineralogical characteristics of AAFA geopolymer pastes cured in water were reflected in XRD patterns (Figure 4.38a to Figure 4.38c). The presence of calcium supplements in alkali-activated fly ash, has been reported to improve mineralogical characteristics [18], but this finding was reported in the context of the use of heat curing. In this context, the alkali-activated specimen was subjected to a rest period after casting, followed by water curing for 20 days. Higher amounts of hydroxyl ions in the mix promote dissociations of silicate and aluminate species to form polymeric structure (Yip *et al.*, 2005) [30]. There was every possibility of the formation of calcium silicate hydrate, calcium aluminum hydrate, and calcium hydroxide, which were supposed to be generated due to the dissolution of calcium species occurring during water exposure of the fly ash. X-ray diffraction analysis was performed over the 2θ scanning range from 5° to 140°. Figure 4.38 plots XRD spectra for geopolymers produced under various rest periods. The presence of multiple inherent crystalline phases, namely quartz and mullite, were recognized by referencing the XRD results for specimen GB_R (2) _WC to the ICSD database (inorganic crystal structure database). Narrower and high-intensity peaks were observed at specific angles in the XRD pattern for specimen GB_R (2) _WC (Figure 4.38a), indicating purely crystalline structure and thus implying that amorphous polymeric phases were largely absent. It was observed from the XRD pattern of specimen GB_R (12) _WC that the crystalline phase having long-range order was converted almost completely into an amorphous phase having only short-range order within the 2θ range of 20° to 40° (Figure 4.38b). The XRD pattern of specimen GB_R (24) _WC indicated a purely amorphous phase throughout the specimen; the pattern had a broad hump in the 2θ range of 5° to 60° (with maximum intensity at 27° to 28°) and reduction in the monoclinic peaks compared to those of specimens R12 and R2 (Figure 4.38c). Referring to the JCPDS database, this phase was identified as Muscovite-3T. The XRD patterns of Figure 4.38a and Figure 4.38b respectively indicate monoclinic and hexagonal crystal systems. The hexagonal structure gave rise to a disordered arrangement of OH^- ions. This might have arised from the enthalpy change associated with the transition from monoclinic to hexagonal phase. Based on the XRD analysis, the study attributed mostly crystalline structure to specimen GB_R(2)_WC and mostly amorphous structure to specimen GB_R(24)_WC. Generally, the amorphous phase exhibited higher reactivity of the polymerization reaction.

Table 4.10 XRD peak list for Water cured blended Alkali activated fly ash

GB_R(2)_WC		GB_R(12)_WC	
2 –Theta Deg.	**Intensity [%]**	**2 –Theta Deg.**	**Intensity [%]**
10.196	0.9	16.356	28
14.668	2.6	20.8	33.6
17.707	6.6	25.937	31.3
20.473	19.0	26.18	37.9
20.638	11.2	26.58	100
23.507	4.1	26.954	17.9
27.195	62.0	27.381	17.5
29.231	12.3	30.89	18
29.583	100.0	33.138	20.6
30.921	40.0	35.185	21.4
33.590	1.3	35.598	13.1
34.688	29.7	36.5	16.4
37.372	13.3	36.918	12.7
38.220	46.5	39.167	13.2
38.930	28	39.408	15.3
42.415	9.3	40.257	12.2
44.321	0.9	40.785	21.2
47.145	5.1	42.452	15.8
49.945	0.5	45.746	11.1
51.634	2.5	48.064	9.2
52.756	1.0	49.383	10
54.996	0.7	50.09	16.9
56.093	6.0	53.369	9.2
56.7	12.0	53.899	10.8
58.269	1.6	54.818	10.1
58.878	20.4	55.264	8.9
61.409	1.5	57.456	10.5
65.011	10.6	58.21	8.9
79.324	4.1	59.904	13.4
80.225	0.9	60.584	14.4
82.075	2.0	63.51	8.9
84.789	4.8	64.47	10.3
88.415	0.3	66.344	7.8
89.339	0.5	67.701	10.3
89.974	0.9	68.158	12.5

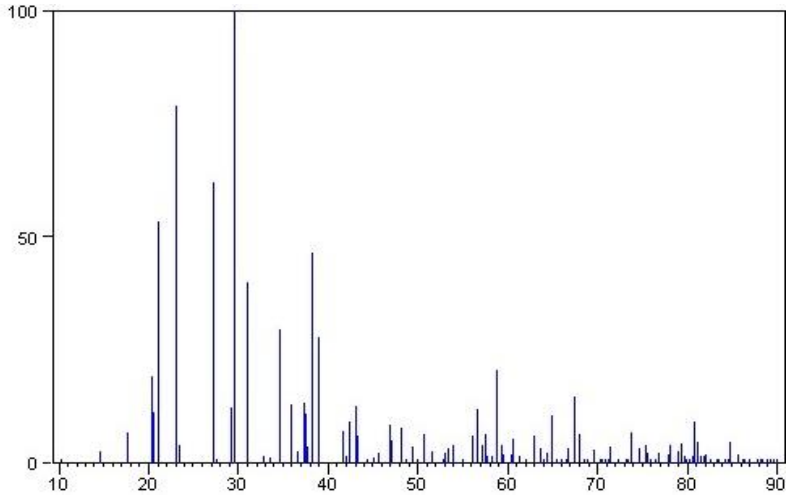

Figure 4.38(a) XRD pattern of specimen GB_R (2) _WC

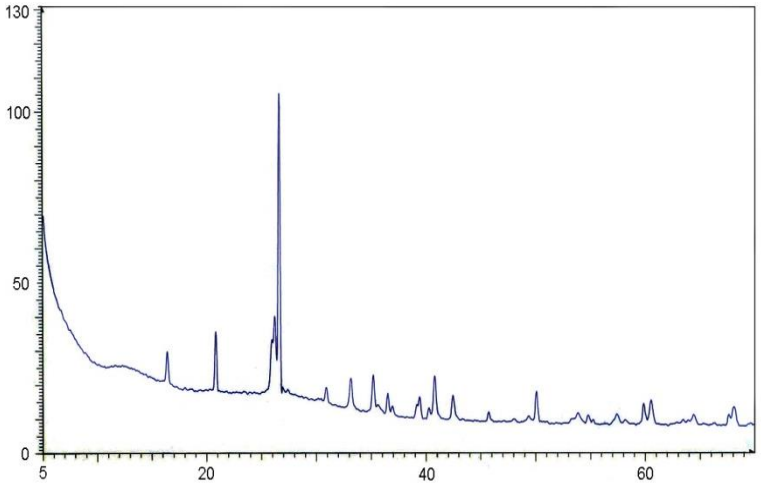

Figure 4.38(b) XRD pattern of specimen GB_R (12) _WC

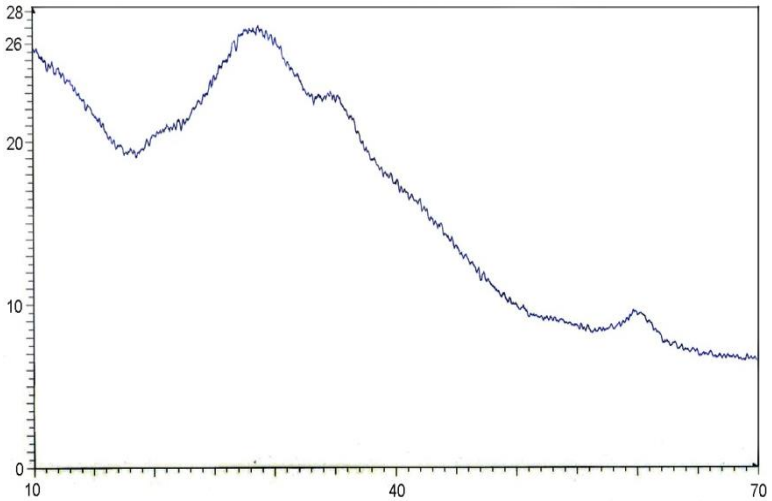

Figure 4.38 (c) XRD pattern of specimen GB_R (24) _WC

4.3.2.2.3 Thermo-Gravimetric Analysis (TGA)

4.3.2.2.3.1 Effect of Rest period on Thermal stability of Alkali activated Fly ash blended with Slag and Cured in water

TGA traces of powdered specimens were collected for specimens GB_R (2)_WC and GB_R (24)_WC. Powdered specimens were used to ensure thermal stability throughout the transient heating (Kong and Sanjayan, 2008) [142]. Figure 4.41 and Figure 4.42 respectively trace the TGA weight losses for specimens GB_R (2)_WC and GB_R (24)_WC. A sharp loss in mass at around 100 °C for specimen GB_R (2)_WC, due to loss of evaporable water (Figure 4.41). An endothermic peak was observed at approximately 70–90 °C in the DTA curve (Figure 4.42), associated with the mass loss from evaporation of free pore water (Duxson *et al.*, 2006) [143]. This temperature range has already been identified and used as an optimized curing temperature (specifically 85 °C) for geopolymer composite preparation in an oven [106]. The rate of weight loss slowed at 100 °C in the analysis and steady weight was observed around 600 °C. The average weight remaining at this stage was 77.71% of initial weight. The TG/DTA pattern of specimen GB_R (24)_WC was dissimilar to that of specimen GB_R (2)_WC; weight loss of only about 2.5% was observed, and occurred between 350 and 600 °C (Figure 4.41). This slight weight change might have occurred from degradation of the isolated organic part. The average total percentage of weight remaining at 600 °C was 97.5%. The thermo-gravimetric results clearly confirmed the more amorphous characteristics of specimen GB_R (24)_WC, which was subjected to a longer rest period, thereby confirming the results as observed in XRD and FESEM analysis discussed earlier.

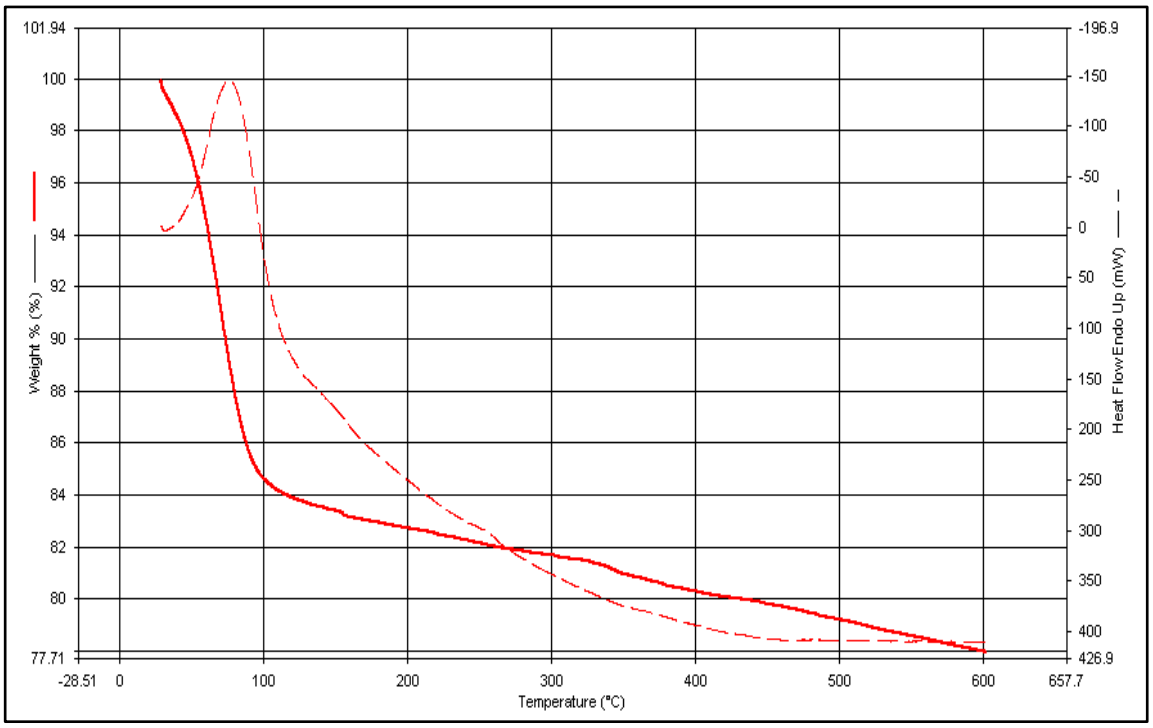

Figure 4.39: TG/DTA Thermo-gram for specimen GB_R (2) _WC

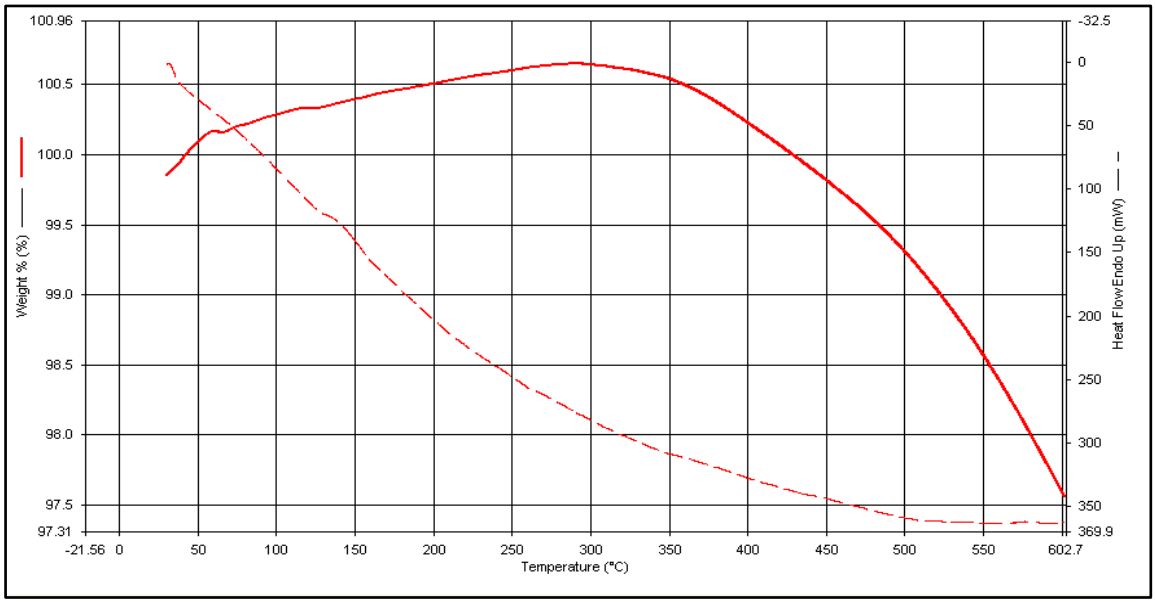

Figure 4.40: TG/DTA Thermo-gram for specimen GB_R (24) _WC

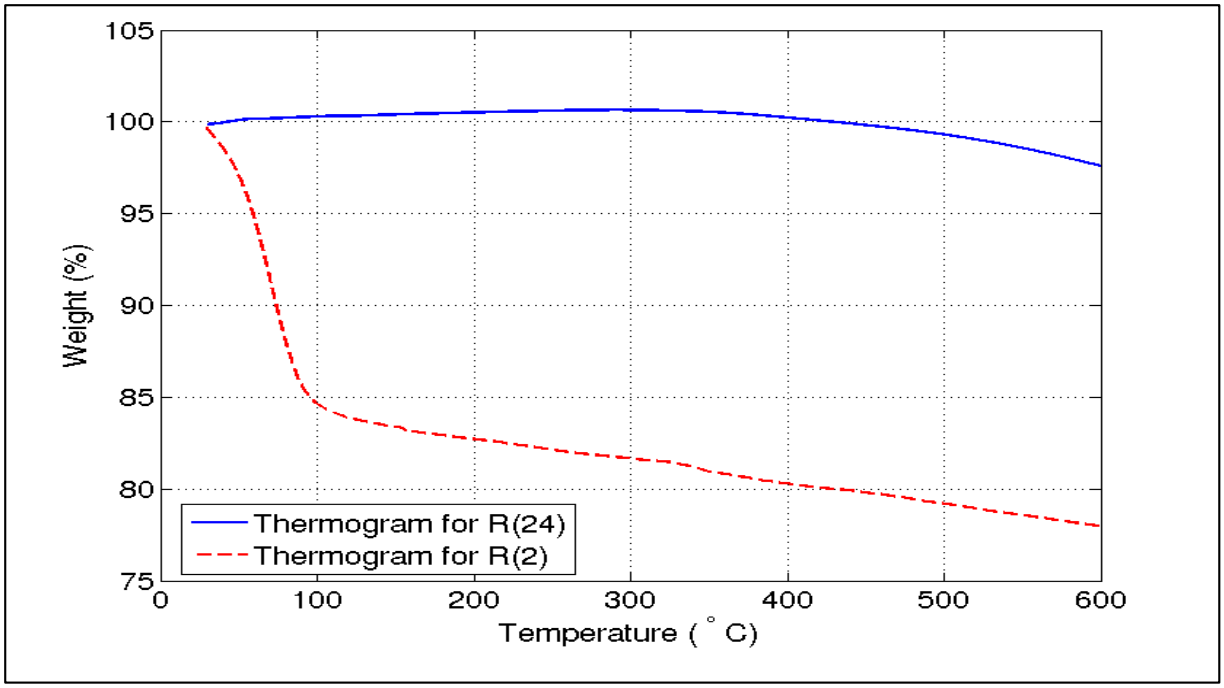

Figure 4.41: Thermo-grams for specimens GB_R (2) _WC and GB_R (24) _WC (indicating remaining weight with the change in temperature)

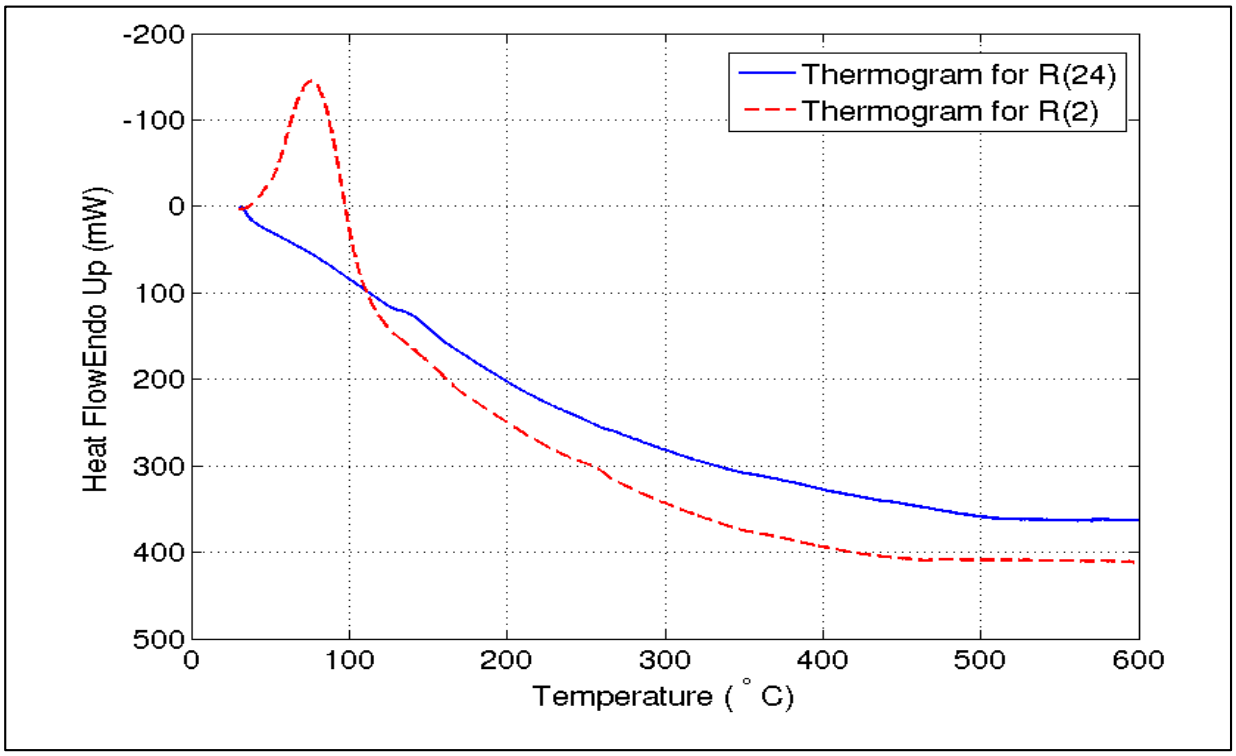

Figure 4.42. Thermo-grams for specimens GB_R (2) _WC and GB_R (24) _WC (indicating heat flow out of each specimen during TGA analysis)

4.3.3 Durability performance

4.3.3.1 Durability performance analysis of Heat cured specimens

4.3.3.1.1 Change in weight under aggressive exposure

4.3.3.1.1.1 Effect of Lime stone dust blending on the Weight change of Fly ash based Geopolymer exposed to 10% Magnesium sulfate solution

The mineralogical and microstructural characterization results obtained in the present study were confirmed by results on the performance of fly ash based geopolymer specimens subjected to aggressive environmental exposure. Three distinct series of specimen GP1, GL1 and GL2 (Chapter -3; Table 3.11) were subjected to 10% Magnesium sulfate exposure (As discussed in Chapter-3).The changes in weight of the three specimen types were dissimilar (Figure 4.43), due to the role of supplementary lime stone dust (calcium based material) in the formation of dissimilar structures with different performance. The specimen GP1 showed the maximum reductions in weight with time during saline exposure, whereas the GL1 and GL2 (fly ash based specimen blended with lime stone dust) showed comparatively good resistance to weight change. Initially, specimen GP1 showed significant increment (16%) in weight seems to be due to the ionic transaction between non-reacted alkali hydroxide within the pores with the magnesium sulfate in solution. The background of this weight loss may be demonstrated by pointing out two sides. Firstly, the permeable pores which allow the intrusion of aggressive solution (such as sulfate) into the structure with the time of exposure. Secondly, the existence of unreacted alkali contents confined within the pores which can make an ionic transaction with exposure solution. In fact, the extrusion of this product is responsible for the drop in weight with time.

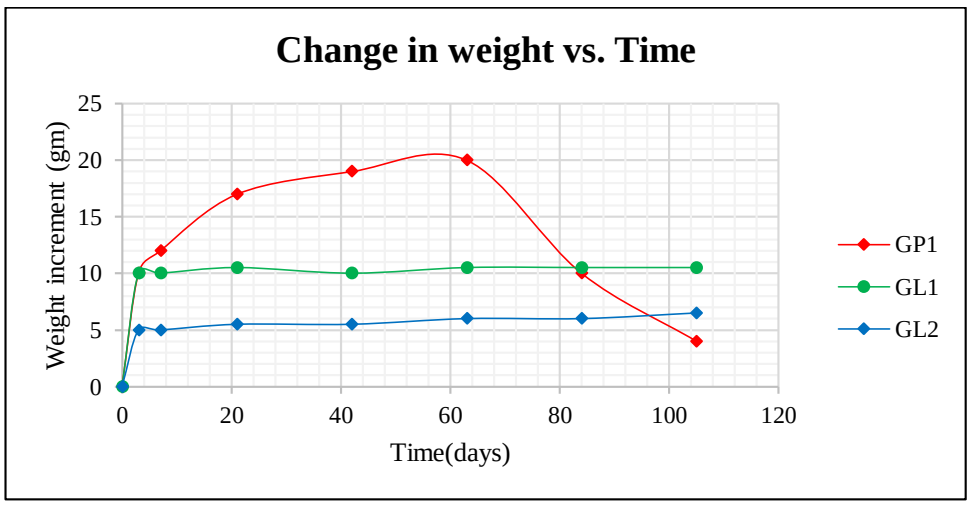

Figure 4.43: Weight changes for Lime stone dust blended Geopolymer paste specimens

4.3.3.1.1.2 Effect of Slag blending on the Weight change of Fly ash based Geopolymer exposed to 10% Magnesium sulfate solution

Three distinct series of specimen GP1, GB1 and GB2 (as discussed in Chapter -3; Table 3.15) were exposed to 10% Magnesium sulfate solution (procedure elaborated in Chapter-3; Figure 3.15). The changes in weight of the specimen types were dissimilar (Figure 4.44), due to the effect of slag (calcium based) as supplementary material in the formation of dissimilar structures with better performance. The fly ash based geopolymer specimens showed comparatively good resistance to weight change with the incorporation of blast furnace slag up to 15% by weight of total (fly ash plus slag). Specimen GP1 showed the maximum increment after 70 days of exposure, seems to be due to the ionic transaction between non-reacted alkali hydroxide within the pores with the magnesium sulfate in solution. There may be an ionic exchange between the entrapped non reacted gel within the internal pores of geopolymer and the sulfate solution; as suggested by earlier researchers [114]. The sudden drop in weight may be due to the extrusion of the reacted product from the pores with the progression of exposure. Specimen GP1showed remarkable weight loss after 15 days of exposure. Almost no further weight loss or gain was observed for specimen GB1 and GB2 (fly ash based geopolymer blended with slag). This observation could be attributed to the fact that the blending of slag in fact promoted the formation of a more intact, less porous, amorphous polymeric structure, promoting the resistance in sulfate exposure.

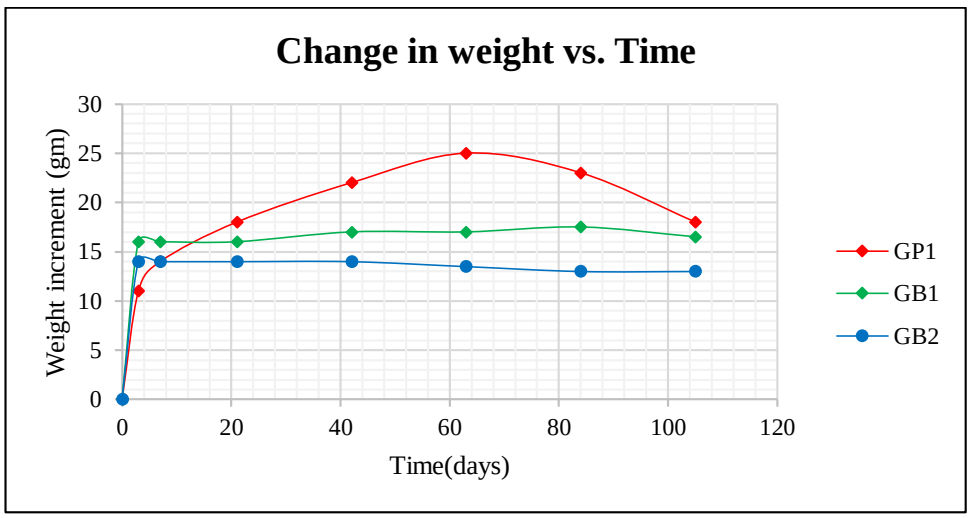

Figure 4.44 Weight changes for Slag blended Geopolymer paste specimens

4.3.3.1.1.3 Effect of Slag blending on the Weight change of Fly ash based Geopolymer under cyclic Freezing thawing exposed to 20% Magnesium sulfate solution

Two series of specimen GP1 and specimen GB2 (Chapter -3; Table 3.15) were subjected to cyclic freezing and thawing in 20% Magnesium sulfate exposure (Chapter-3; Figure 3.15 and Figure 3.16). Typical cylinder and cube specimens were used for the test. The results are given in Table 4.11 and Figure 4.45. The change in weight for GP1 specimens were differed a lot in contrast with GB2 specimens. In each case, the weight was decreased except the data obtained after 3 months for GP1. The notable increment of GP1 material may be due to the ionic transaction between the entrapped alkali within the internal pores and the Magnesium Sulfate solution. The weight of specimen GP1 was significantly dropped by 10.89% and 44.63% after 6 months and 9 months of exposure respectively. The noticeable weight gains observed for these specimens (GP1) may have occurred due to ionic transfer under saline exposure. The volumetric increment of entrapped pore water was the basic cause of creating more internal pressure within the structure lead to development of micro-cracks. Consequently more solution was absorbed by the GP1 specimens through the micro-cracks and accelerates the water percolation further and due to which the GP1 structure was totally distorted after 12 months. But the change in weight for GB2 (fly ash based geopolymer blended with 15% slag) varied between -1.09% to -4.08%; measured after 3 months to 12 months. This phenomenon indicates compact and impervious nature of GB2 specimens.

Table 4.11 Change in Weight after different immersion time of specimens GP1 and GB2

Specimen	Shape	Temperature of Exposure	Immersion period	Change in Weight (%) after			
				3 months	6 months	9 months	12 months
GP1	Cubical	Cool (8°C)	3 months (Oct-Dec)	12.43	-	-	-
	Cylindrical						
GB2	Cubical			-1.09	-	-	-
	Cylindrical						
GP1	Cubical	Chill (-20°C)	3 months (Jan-Mar)	-	-10.89	-	-
	Cylindrical						
GB2	Cubical			-	-1.5	-	-
	Cylindrical						
GP1	Cubical	Cool (8°C)	3 Months (April-Jun)	-	-	-14.63	-
	Cylindrical						
GB2	Cubical			-	-	-3.5	-
	Cylindrical						
GP1	Cubical	Chill (-20°C)	3 months (Jul-Sep)	-	-	-	*
	Cylindrical						
GB2	Cubical			-	-	-	-4.08
	Cylindrical						

*complete fracture of specimen

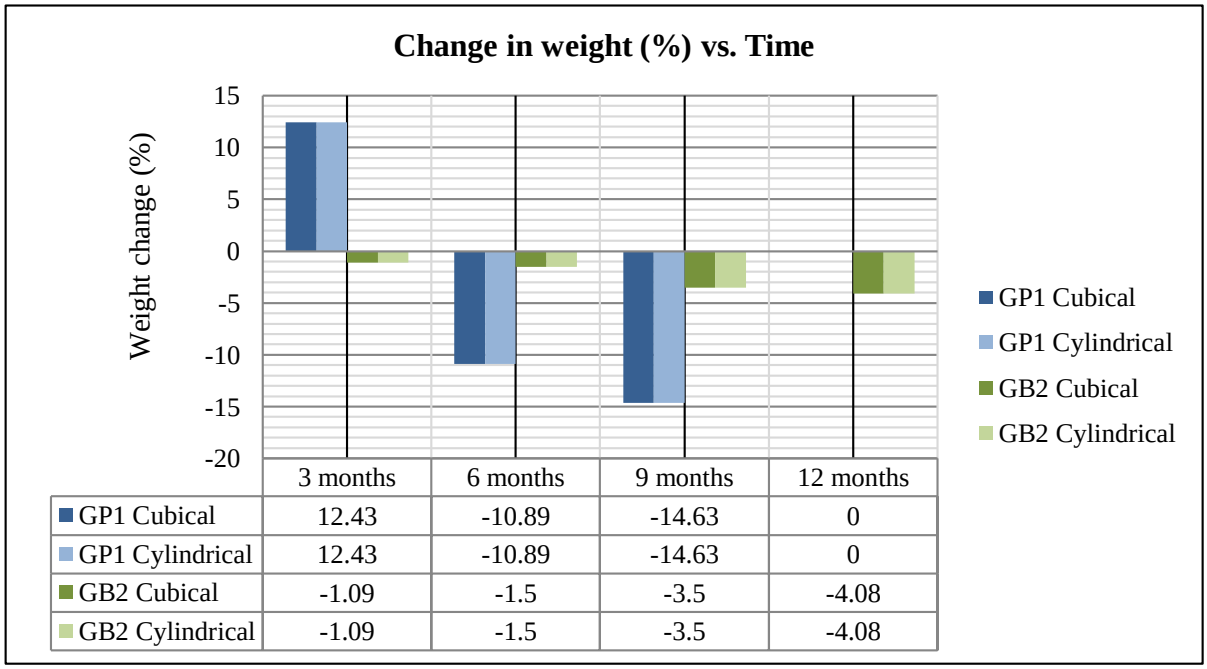

Figure 4.45: Change in weight after different immersion time of GP1 & GB2 specimens

4.3.3.1.2 Residual strength under aggressive exposure

4.3.3.1.2.1 Effect of Lime stone dust blending on the Residual strength of Fly ash based Geopolymer exposed to 10% Magnesium sulfate solution

Three different specimens GP1, GL1 and GL2 (Chapter -3; Table 3.11) were exposed to 10% Magnesium sulfate solution (As discussed in Chapter-3). Residual strength is the parameter representing the final strength after exposure as a fraction of initial strength. Here initial strength is defined as the primary strength before exposure. Figure 4.46 presents the dissimilar residual compressive strength for different specimens exposed to magnesium sulfate solution of 10% concentration. Bakharev [13] at al. recognise the migration of alkalis from the geopolymer as the prime cause of the reduction in strength. The specimen GP1, GL1 and GL2 exhibited a residual strength of 65.34%, 98.12% and 99.2% respectively after an exposure of fifteen weeks (as shown in Figure 4.46).

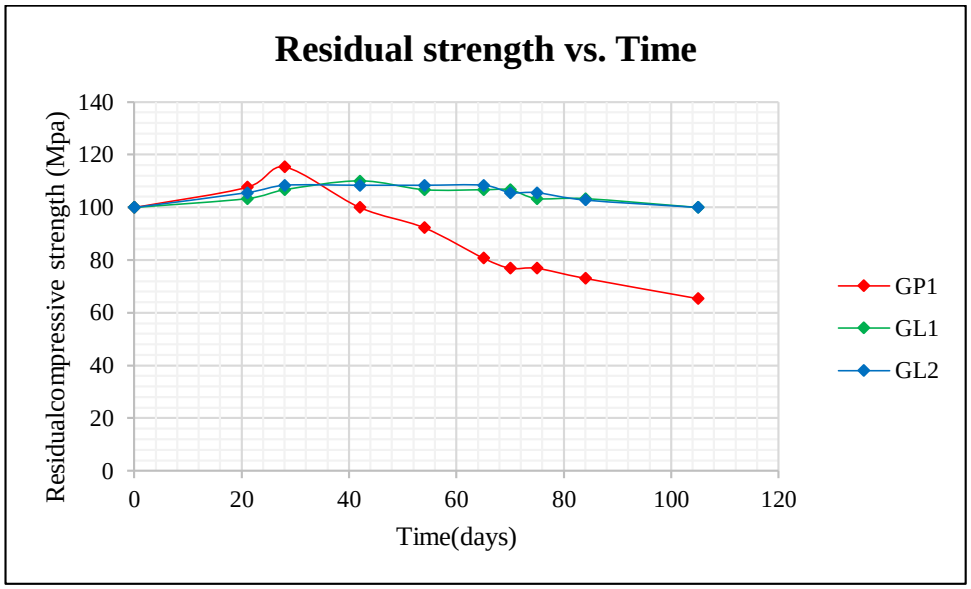

Figure 4.46: Residual strength of Lime stone dust blended Geopolymer paste

4.3.3.1.2.2 Effect of Slag blending on the Residual strength of Fly ash based Geopolymer exposed to 10% Magnesium sulfate solution

The strength change of GB1 and GB2 (ref. to Chapter-3; Figure 3.15) was quite less (exposed to 10% magnesium sulfate solution) than that of GP1. Figure 4.47 presents the change in residual compressive strength for fly ash based geopolymer under the exposure of 10% magnesium sulfate solution as well as for fly ash based geopolymer blended with slag. The trend of residual strength was similar that of fly ash geopolymer blended with lime stone dust. Similar kind of performance was found for blended specimen. No reduction of strength

have been observed in case of specimens GB1 and GB2 even after 15weeks of sulfate exposure. Presence of Ca^{+} ions in mixture not only promote the secondary input C-S-H but also play a crucial role to the faster reactivity [88]. These dual effects of calcium (presence in supplementary calcium based material; such as blast furnace slag) in the mix made the structure of fly ash based geopolymer more compact and dense and results in higher performance level of blended geopolymer.

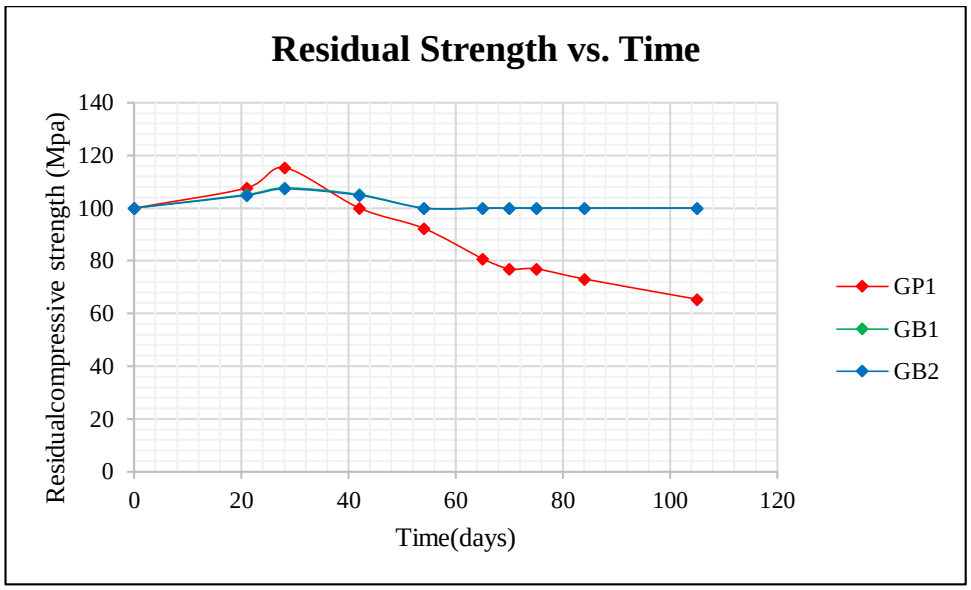

Figure 4.47 Residual strength of Slag blended Geopolymer paste

4.3.3.1.2.3 Effect of Slag blending on the Residual strength of Fly ash based Geopolymer under cyclic Freezing thawing exposed to 20% Magnesium sulfate solution

Two series of specimen GP1 and specimen GB2 (Chapter -3; Table 3.15) were subjected to cyclic freezing and thawing simultaneously exposed to 20% Magnesium sulfate solution (Chapter-3; Figure 3.15 and Figure 3.16).Typical cylinder and cube specimens were used for the test. The residual strength was decreased significantly for GP1 (Fly ash based geopolymer without blending) specimen after 6 months. The results are given in Table 4.12 and Figure 4.48. Beside the concentration of sulphate solution (20% Magnesium sulfate solution), remarkable impact has been observed due to freezing-thawing which reduced the residual strength of every specimen. After the second cycle of freezing the GP1 specimens were completely distorted. But positive result was observed for fly ash based geopolymer blended with 15% slag (specimen GB2) which showed residual strength up to 95.5%. The residual strength of the two specimen types were dissimilar (Figure 4.48), confirming the merit of the calcium based compound (blast furnace slag) as a supplementary material in alkali activated fly ash, due to the formation of dissimilar structures which influences the performance.

Table 4.12 Residual strength after different immersion times for GP1 and GB2 Specimens

Specimen	Shape	Temperature of Exposure	Immersion period	Residual Strength (%) after			
				3 months	6 months	9 months	12 months
GP1	Cubical	Cool (8°C)	3 months (Oct-Dec)	97.35	-	-	-
	Cylindrical			96.38	-	-	-
GB2	Cubical			99.98	-	-	-
	Cylindrical			99.00	-	-	-
GP1	Cubical	Chill (-20°C)	3 months (Jan-Mar)	-	67.00	-	-
	Cylindrical			-	65.83	-	-
GB2	Cubical			-	97.98	-	-
	Cylindrical			-	97.28	-	-
GP1	Cubical	Cool (8°C)	3 Months (April-Jun)	-	-	45.40	-
	Cylindrical			-	-	43.61	-
GB2	Cubical			-	-	97.33	-
	Cylindrical			-	-	96.84	-
GP1	Cubical	Chill (-20°C)	3 months (Jul-Sep)	-	-	-	*
	Cylindrical			-	-	-	*
GB2	Cubical	-	-	-		96.60	
	Cylindrical	-	-	-		95.50	

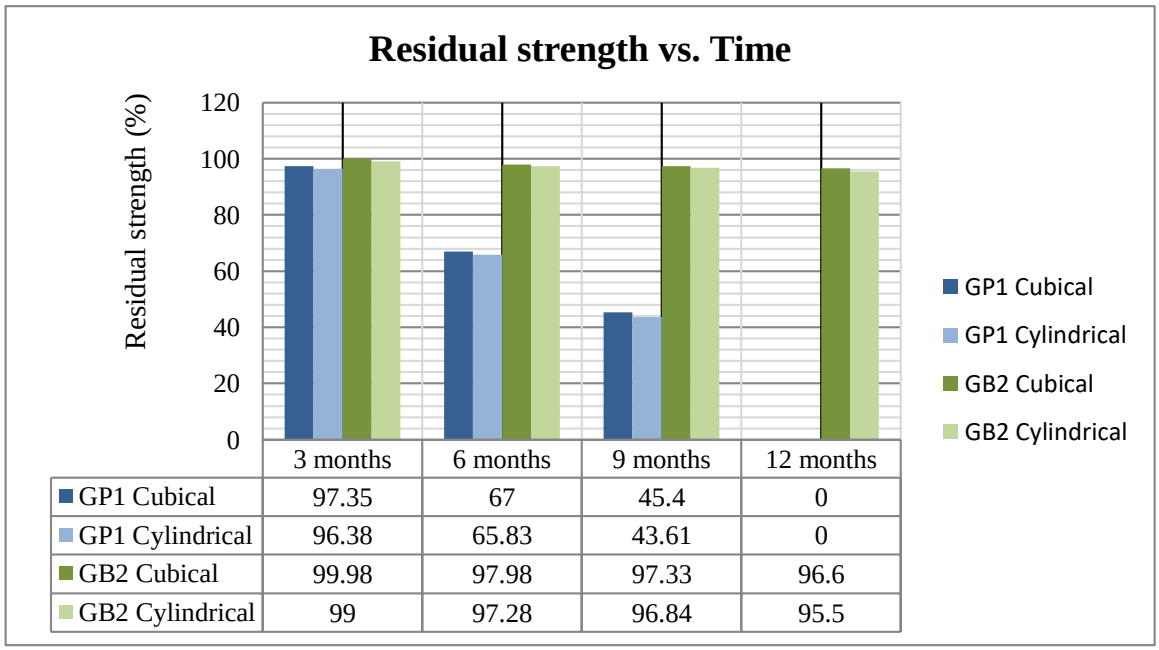

	3 months	6 months	9 months	12 months
GP1 Cubical	97.35	67	45.4	0
GP1 Cylindrical	96.38	65.83	43.61	0
GB2 Cubical	99.98	97.98	97.33	96.6
GB2 Cylindrical	99	97.28	96.84	95.5

Figure 4.48: Residual strength after different immersion times for GP1 & GB2 Specimens

4.3.3.1.3 Physical change in appearance

4.3.3.1.3.1 Effect of Lime Stone dust blending on the Physical appearance of Fly ash based Geopolymer under 10% Magnesium sulfate solution exposure

Three different specimen GP1, GL1 and GL2 (Chapter -3; Table 3.11) were subjected to 10% Magnesium sulfate exposure (As discussed in Chapter-3). The surface deposit of geopolymer specimen exposed to sulfate solution has two aspects. Firstly, the permeable pores which allow the intrusion of aggressive solution (such as sulfate) into the specimen with the time of exposure. Secondly, the existence of unreacted alkali contents within the pores, may undergo an ionic transaction with exposure solution and compounds coming out and deposited on the surface (white deposit in this case). No deposit on the surface observed (periodical observation made using optical microscopy (WF 10X; C&D Micro Services Ltd., UK as discussed in chapter 3) on blended fly ash based geopolymer. After six weeks of observation, blended fly ash based geopolymer specimens showed sufficient white deposits on the surface. Scanning electron microscopy and the elemental quantification [as shown in Figure 4.49(d)] indicated the possible chances of the formation of magnesium alumina silicate as reported by other researchers [2], [38], [112] . The typical surface condition for specimen GP1, GL1 and GL2 are presented in Figure 4.49(a), 4.49(b) and 4.49(c) respectively.

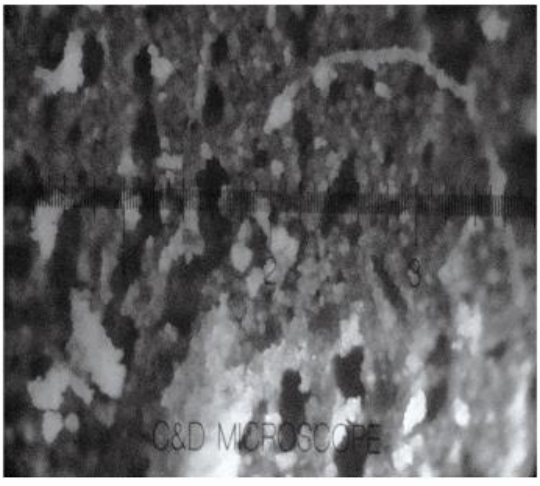

Figure 4.49 (a): Geopolymer paste specimen GP1, after 6 weeks in 10% Magnesium sulfate solution

Figure 4.49 (b) Geopolymer paste specimen GL1, after 6 weeks in 10% Magnesium sulfate solution

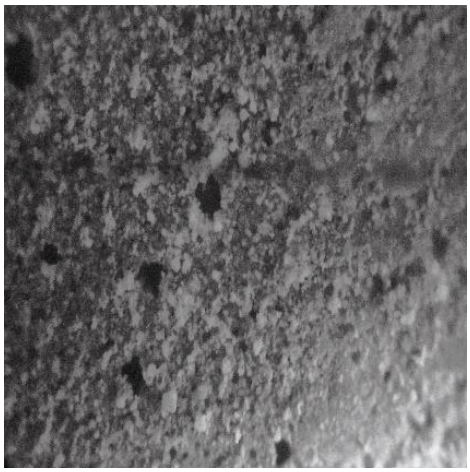

Figure 4.49 (c) Geopolymer paste specimens GL2, after 6 weeks in 10% Magnesium sulfate solution

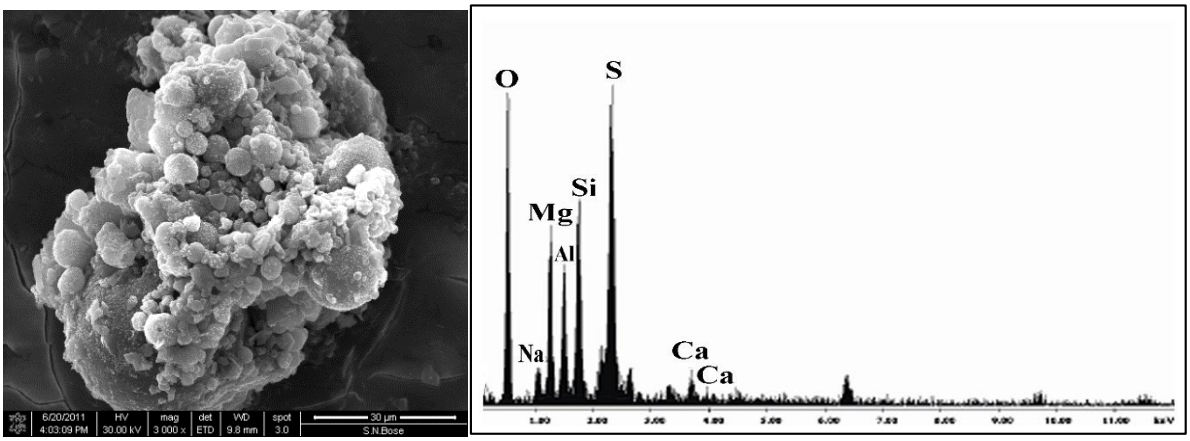

Figure 4.49 (d) SEM @ 3000x zoom and EDX of white deposit on the surface of specimen after exposure

4.3.3.1.3.2 Effect of Slag blending on the Physical appearance of Fly ash based Geopolymer under 10% Magnesium sulfate solution exposure

Three different specimens GP1, GB1 and GB2 (Chapter -3; Table 3.15) were subjected to 10% Magnesium sulfate exposure as discussed earlier. The compact, less porous and less permeable fly ash based geopolymer blended with blast furnace slag, exhibited better performance. The white deposits, expelled from the interior part of exposed geopolymer specimen was observed only for specimen GP1 (as shown in Figure 4.50a). Optical microscope was used periodically to observe the change of surface texture (magnified image), deposits etc. Soft and powdery deposits was observed for GP1 specimens (fly ash geopolymer without blending). This white deposits was identified as magnesium alumina silicate by the other researchers [38], [112]. The SEM images and EDX analysis supported the presence of magnesium, silicon, aluminium; as shown in figure 4.50(d). The fly ash geopolymer blended with slag did not show any surface deposit with time.

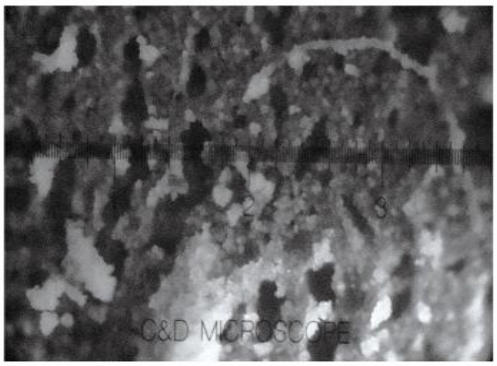

Figure 4.50(a) Geopolymer paste specimens GP1, after 6 weeks in 10% Magnesium sulfate solution

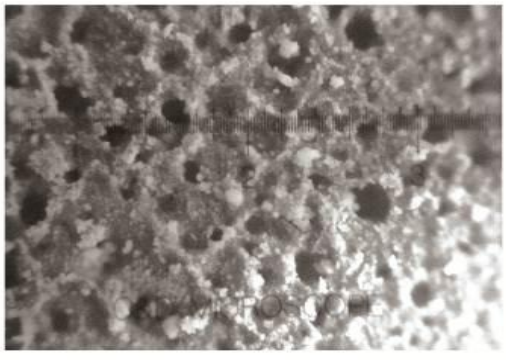

Figure 4.50(b) Geopolymer paste specimens, GB1 after 6 weeks in 10% Magnesium sulfate solution

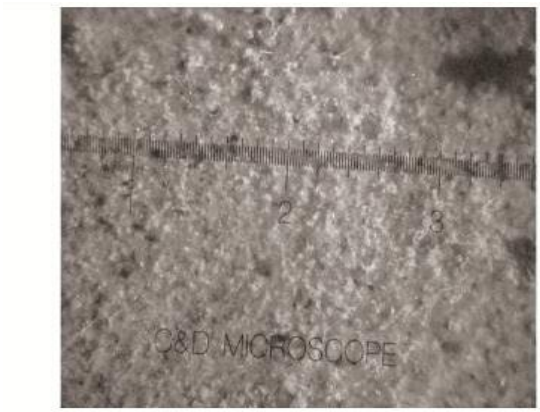

Figure 4.50(c) Geopolymer paste specimens, GB after 6 weeks in 10% Magnesium sulfate solution

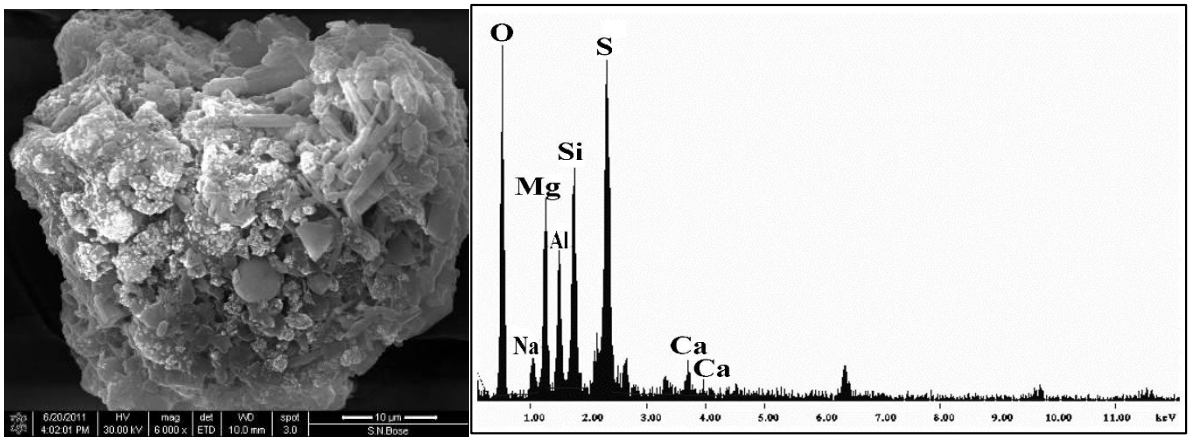

Figure 4.50(d): SEM @ 400x zoom and EDX of white deposit on the surface of specimen after exposure

4.3.3.1.3.3 Effect of Slag blending on the Physical appearance of Fly ash based Geopolymer under cyclic Freezing thawing and exposed to 20% Magnesium sulfate solution

Two series of specimens GP1 and GB2 were subjected to cyclic freezing and thawing exposed to 20% Magnesium sulfate solution (Chapter-3; Figure 3.15 and Figure 3.16). Crack was observed in fly ash based geopolymer specimens GP1; as shown in in Figure 4.51.The experiment supports the eligibility of GB2 materials for typical sulphate exposure in frost environment. The volumetric increment of entrapped pore water was the basic cause of creating pressure leading to developed of micro-cracks. More solution was absorbed by the GP1 specimens because of these mico-cracks which accelerates the water percolation further. The source of the pore water indicates primarily the water entrapped within the pore at the time of geopolymer formation and due to the percolated water after immersion. The experiment supports the compact and less porous structure for specimen GB2 (fly ash based geopolymer blended with 15% slag) with minimum presence of pore water.

Figure 4.51 (a) Cylinder specimens, (b) Crack in the GP1 specimen

4.3.3.2 Durability performance analysis of Water cured specimens

4.3.3.2.1 Change in weight for specimens exposed to Aggressive exposure

4.3.3.2.1.1 Effect of Rest period on Weight change of Alkali activated Fly ash blended with Slag and Water cured, under cyclic Freezing-thawing exposed to 20% Magnesium sulfate exposure

Including supplementary cementing materials such as GGBS in geopolymers avoids the durability issues by making geopolymers more durable against extreme environmental exposures and chemical attacks (Mohammadreza and Riding, 2015) [149]. The mineralogical and microstructural characterization results obtained in the present study, confirmed the performance of blended and non-blended alkali-activated specimens subjected to aggressive exposure. Two series of specimen GB_R (24) _WC and specimen GB_R (2) _WC were subjected to cyclic freezing and thawing exposed to 20% Magnesium sulfate solution (Chapter-3; Figure 3.15 and Figure 3.16). The changes in weight of the two types of specimens were dissimilar (Figure 4.52a), confirming the importance of the rest period in the formation of dissimilar structures having different performance. The GB_R (2) _WC specimens showed the greatest reductions in weight and strength during sulphate exposure, whereas the GB_R (24) _WC specimens showed comparatively good resistance to weight change. GB_R (24) _WC specimens showed a small increment in weight (1.78%) but GB_R (2) _WC specimens showed the maximum increment (27.94%), possibly due to the ionic transaction between unreacted alkali hydroxide within the pores with the magnesium sulfate in solution.

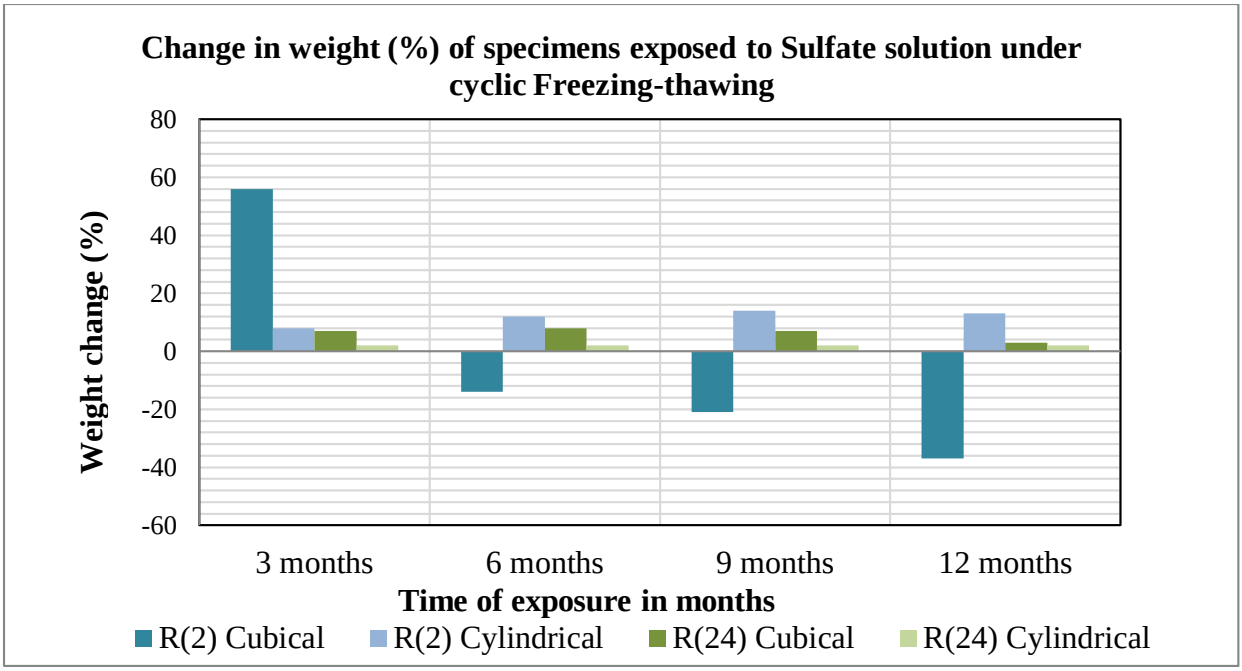

Figure 4.52(a): Change in Weight after different immersion times for specimens GB_R(24) _WC and GB_R (2) _WC Specimens

4.3.3.2.2 Residual strength for specimens exposed to Aggressive exposure

4.3.3.2.2.1 Effect of Rest period on Residual strength of Alkali activated Fly ash blended with Slag and Water cured, subjected to cyclic Freezing-thawing exposed to 20% Magnesium sulfate solution

In exposure to cyclic freezing and thawing in sulfate solution (Chapter-3; Figure 3.15 and Figure 3.16), the strength changes of GB_R (24) _WC was quite less than that of GB_R (2) _WC (Figure 4.52b). The residual strength dropped remarkably for GB_R (2) _WC after the second cycle of freezing. The residual strength of GB_R (2) _WC specimens dropped by 52% relative to their initial values after 6 months of exposure, whereas GB_R (24) _WC specimens retained 79.21% of their initial strengths at this time. This was similar to the performance trends observed for cement paste specimens under sulphate exposure. After 1 year of sulphate exposure under cyclic freezing and thawing, specimen GB_R (24) _WC exhibited 70.93% residual strength but the GB_R (2) _WC specimen showed zero strength under loading. The role of the rest period thus affected the mineralogical characteristics, microstructural characteristics, and mechanical performance as well.

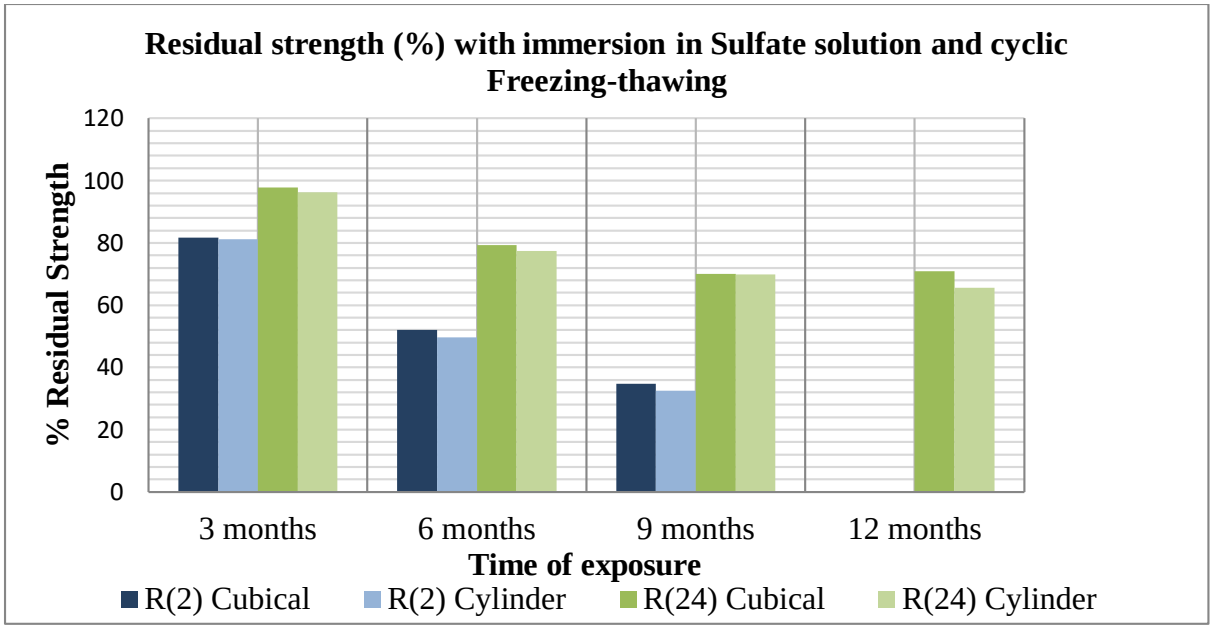

Figure 4.52(b): Residual strength after different immersion times of specimens GB_R (24)_WC and GB_R_(2)_WC Specimens

4.3.3.2.3 Physical change in appearance

4.3.3.2.3.1 Effect of Rest period on Efflorescence of Alkali activated Fly ash blended with Slag and Water cured under ambient environment

Efflorescence occurred on some of the AAFA based geopolymers. In these highly alkaline geopolymers, the charge compensator alkali hydroxide was ejected as the synthesis progressed in terms of the formation of Si–O–Al bonds. In alkali activation of fly ash, the alkali metal hydroxide acts as a catalyst and almost all the hydroxide added during synthesis subsequently leaches out from the structure [1-7]. Previous reports on alkali-activated fly ash subjected to heat curing have noted that it tends to form complete amorphous geopolymers, but in scenarios completely different in the present study. In the present study, each specimen was initially kept at room temperature, after which it was water cured. Mild leaching was observed in specimens subjected to longer rest periods of 12 hours and more. Specifically, specimens GB_R (16) _WC and GB_R (24)_WC showed mild efflorescence under optical microscopy whereas the specimen subjected to the shortest rest period [i.e. GB_R (2)_WC] did not show the same kind of efflorescence (Figure 5). This observation could be attributed to the fact that longer rest periods in fact promoted the formation of a more amorphous polymeric structure, promoting the ejection of alkali from the geopolymer matrix.

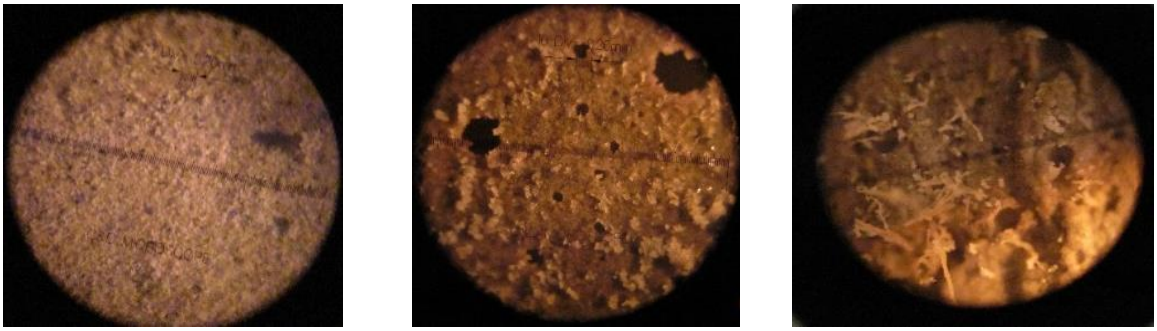

(a) (b) (c)

Figure 4.53: (a) Efflorescence in specimen GB_R (2) _WC after 3 months from casting
(b) Efflorescence in specimen GB_R (16) _WC after 3 months from casting
(c) Efflorescence in specimen GB_R (24) _WC after 3 months from casting

4.4 Fly ash based Geopolymer blended with Supplementary Silica compound

4.4.1 Physical property

4.4.1.1 Workability

4.4.1.1.1 Effect of Silica fume blending in Fly ash based Geopolymer in presence of Murram

14 individual series of blended fly ash based geopolymer specimens (Chapter-3; Table 3.18), studied based on percentage of blending of silica fume, percentage blending of murram, percentage of K_2O, silicate modulus and water to solid ratio, were subjected to the workability test at fresh state. The workability test data for blended and non-blended specimens at fresh state are furnished in Table- 4.13. The compensation of the charge of aluminium by potassium ions may accelerates the rate of poly-condensation. For example, the non-blended specimen GPC (fly ash based specimen activated with 6% K_2O, Silicate modulus=1), showed good workability even at lower K_2O percentage. In absence of sodium silicate the non- blended fly ash based geopolymer GPC1-N (fly ash based geopolymer activated with 8% K_2O and silicate modulus=0) and GPC-N (fly ash based geopolymer activated with 6% K_2O and silicate modulus =0) were failed to form gel [as shown in Figure 4.54(f) and Figure 4.54(g)]. In absence of sodium silicate the initiation of polymerization may not be possible for fly ash based geopolymer [68] .But addition of silica fume in fly ash based geopolymer showed improved workability at every cases (even in absence of sodium silicate in mix i.e. silicate modulus equal =0). But presence of higher reactive silica (supplementary silica fume by 10%) in fly ash based geopolymer mix, increases the Si/Al ratio. The higher value of Si /Al may enhance the formation of chain structure (Si-O-Si) rather than tetrahedral framework structure [28]. Due to which higher value of workability was recorded for fly ash

based geopolymer blended with silica fume only. Like GSC1 (fly ash based geopolymer blended with 10% silica fume, activated by 6% K_2O and silicate modulus equal =1), showed abrupt increase in workability (area factor = 36). To reduce the value of Si/Al in silica fume blended fly ash based geopolymer mix to some extent, another supplementary material comprising of alumina (Murram) may be incorporated. In this research, the Murram was chosen as an alternative source of aluminium to bring the Si/Al ratio to an appreciable level. Considerable workability was achieved for every fly ash based specimen blended with silica fume (10%) and Murrum (2.5%) as supplementary material. Every blended fly ash based geopolymer specimens like GSC1R, GSC1R-N, GSCR and GSCR-N, showed better workability in compared to non-blended specimens. Appreciable workability was also found for some blended specimen like GSC1R1 and GSCR1 at lower value of water content in mix (25% of the total of fly ash, silica fume and Murram).

Table 4.13 Results of Workability test of the Geopolymer paste

Specimen Id	Initial Diameter (d_1) (cm)	Final Equivalent Diameter (d_2) (cm)	Initial Area (a_1) (cm^2)	Final Area After Flow (a_2) (cm^2)	Area Factor $=a_2/a_1$
GPC-1	6	24	28.26	452.16	16.0
GPC1-N	6	6	28.26	28.26	1.0
GPC	6	20	28.26	314	11.1
GPC-N	-	-	-	-	-
GSC1	6	36	28.26	1017.36	36.0
GSC1-N	6	15	28.26	176.63	6.25
GSC	6	33	28.26	854.87	30.3
GSC-N	6	11	28.26	95	3.4
GSC1R	6	34	28.26	907.46	32.1
GSC1R-N	6	31	28.26	754.39	26.7
GSCR	6	30	28.26	706.5	25.0
GSCR-N	6	27	28.26	572.265	20.3
GSC1R1	6	28	28.26	615.44	21.8
GSCR1	6	31	28.26	754.385	26.7

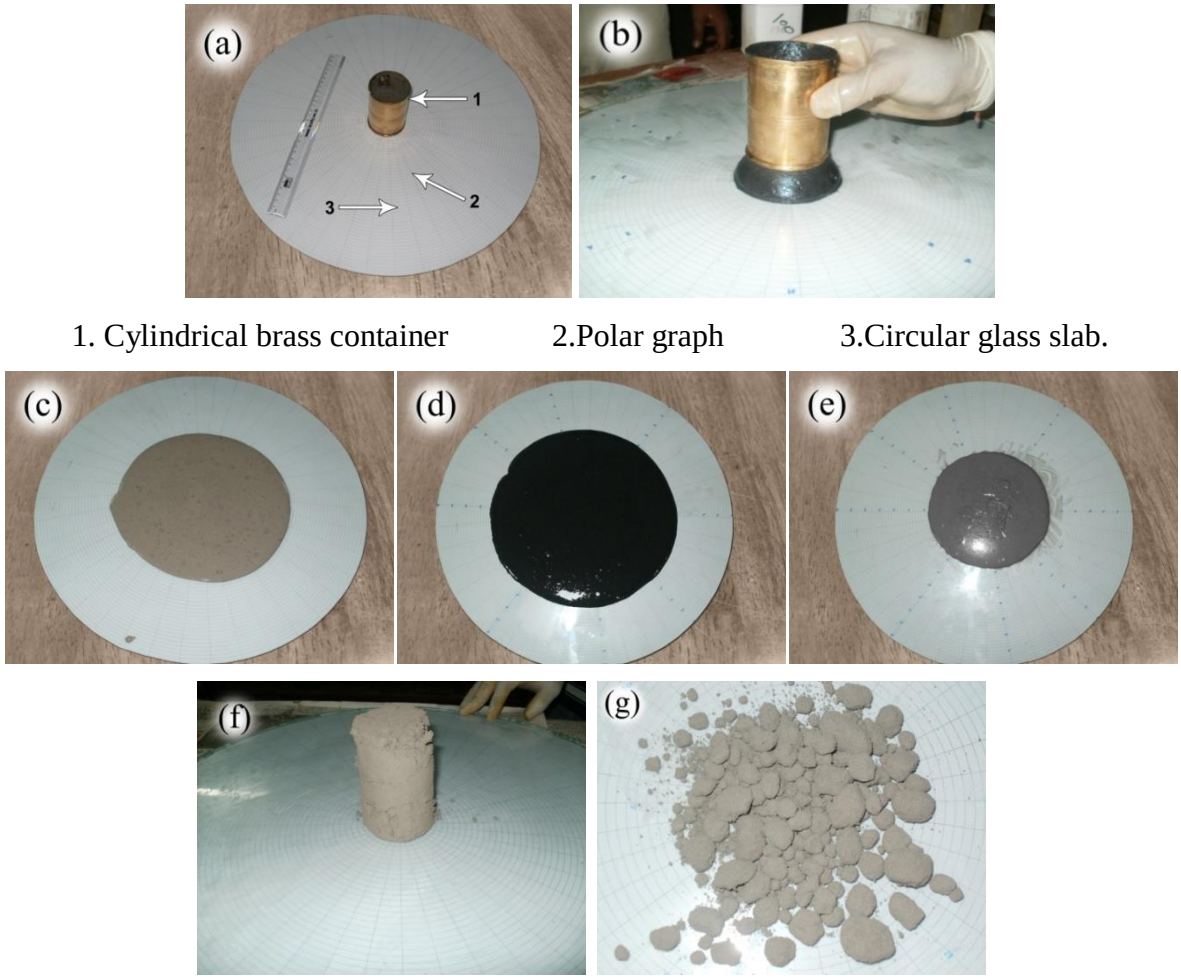

1. Cylindrical brass container 2.Polar graph 3.Circular glass slab.

Figure 4.54 (a) Workability set up (b) Raising of cylinder (c) Specimen GPC-1 (d) Specimen GSC1R-N (e) Specimen GPC (f) Specimen GPC1-N (g) Specimen GPC-N

4.4.1.2 Compressive strength

4.4.1.2.1 Effect of Silica fume blending in Fly ash based Geopolymer in presence of Borax on Compressive strength

Table 4.14 presents 3-day compressive strength of the six different series of non-blended and blended fly ash based geopolymer (silica fume by 5% ,7.5% ,10% and borax by 2.5% , 5.0% as supplementary material) specimens (as discussed in chapter-3;Table 3.17). Borax, comprising of boron (as an alternative of aluminium) was incorporated along with silica fume in fly ash based geopolymer. Increase in compressive strength was observed with the incorporation of silica fume (up to 10%) and borax (up to 5%) in the blended fly ash based geopolymer. For example, non-blended specimen GPC-M (fly ash activated by 6% K_2O with silicate modulus = 0.1) was failed to form geopolymer gel, due to lower value sodium silicate in the mix. Figure 4.54(h) shows the disintegrated part of partially reacted fly ash of GPC-M,

whereas, 3-day compressive strength for blended fly ash geopolymer specimen GSCB2-M (blended with 5% silica fume,5% borax; activated by 6% K_2O with silicate modulus = 0.1) was recorded a compressive strength of 28MPa. Alkali activation of fly ash based geopolymer could be initiate without sufficient amount of sodium silicate which initiate the polymerization in earlier stage [29]. But for blended geopolymer the scenario was different. Silica fume may initiate the polymerization process by the formation of in-situ inorganic foam itself at the initial stage of activation [36]. Tremendous volumetric increment was observed for the blended fly ash based specimen GSC (blended with 10% silica fume only). Due to this volumetric increment compressive test could not be conducted. Fly ash activation in the presence of external Silica fume and Borax sources provided a better geopolymer. The lowering of sodium silicate in activator had little or no effect on compressive strength of fly ash based geopolymer blended with silica fume in presence of borax. Maximum compressive strength was obtained for blended specimen GSCB2 i.e. 29.05 MPa.

Table 4.14: 3 day Compressive strength of non-blended and blended specimen

Specimen mkd.	3 day Compressive strength (MPa),
GPC	14.25
GPC-M	0.0
GSC	--
GSCB1	18.62
GSCB2	29.05
GSCB2-M	28

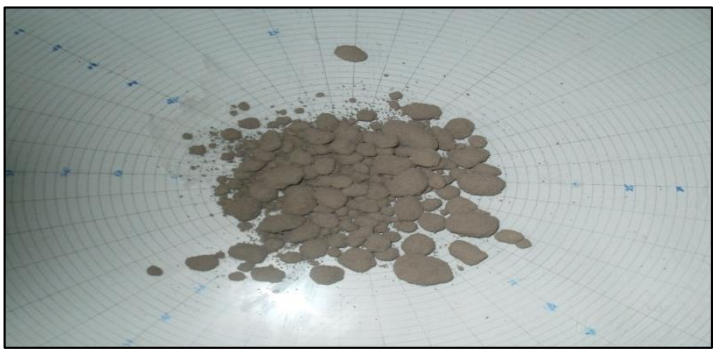

Figure 4.54(h) Specimen GPC-M (failed to form normal specimen)

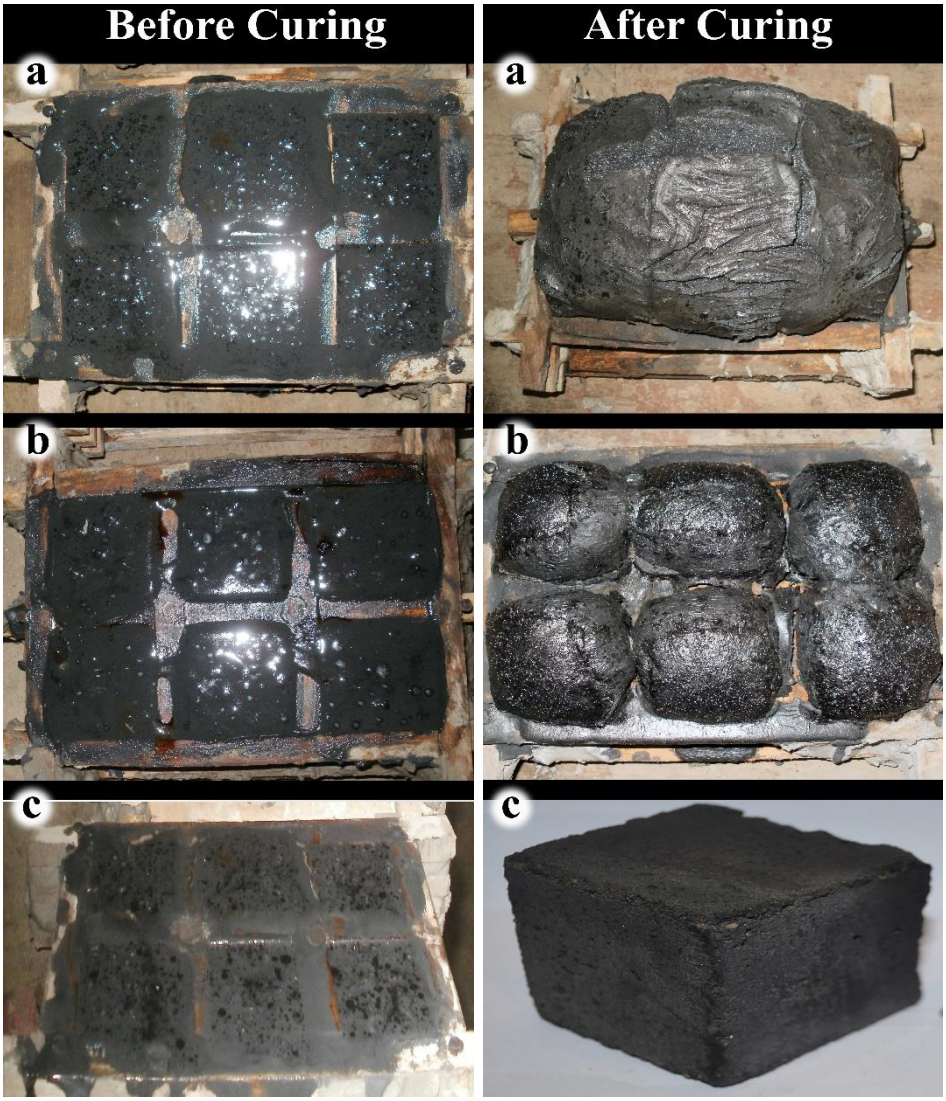

Figure 4.55 Specimens (a) GSC, (b) GSCB1 and (c) GSCB2 at different phase of Manufacturing

4.4.1.2.2 Effect of Silica fume blending in Fly ash based Geopolymer in presence of Murram on Compressive strength

Fourteen different series of non-blended and blended specimens were tested for compressive strength test (specimen details are given in Table 3.18; Chapter-3). Fourteen mix/specimen were studied based on percentage of blending of silica fume, percentage blending of Murram, percentage of K_2O, silicate modulus and water to solid ratio etc. 3-day compressive strength value for every series of specimens are furnished in Table 4.15.

Table 4.15 Compressive strength of Geopolymer paste specimen (Fly ash +Silica fume +Murram)

Specimen	3-day Compressive strength (MPa)
GPC-1	27.1
GPC1-N	3.9
GPC	14.3
GPC-N	-
GSC1	-
GSC1-N	15.8
GSC	-
GSC-N	8.11
GSC1R	34.2
GSC1R-N	18.1
GSCR	22.5
GSCR-N	10.0
GSC1R1	39.1
GSCR1	27.2

The blending of silica fume (10 %) and Murram (2.5%) as supplementary material, showed noteworthy improvement in compressive strength of blended fly ash based geopolymer. 3-day compressive strength of non-blended specimen GPC-1 (fly ash based geopolymer activated by 8% K_2O with silicate modulus equal = 1) and specimen GPC (fly ash based geopolymer activated by 6% K_2O with silicate modulus=1) was recorded as 27.1MPa and 14.3 MPa whereas, 3-day compressive strength of specimen GSC1R and GSCR was found 34.2 MPa and 22.5 MPa. The results indicate that the blending of silica fume (10%) and Murram (2.5%) mix recorded higher compressive strength by 26.25% and 58.03%, compared to non-blended specimens. Again, blended specimen like GSC1R-N activated in absence of silicate solution (silicate modulus=0) recorded a 3-day compressive strength of 18.1 MPa. 3-day compressive strength of blended specimen GSC1R was recorded as 39 MPa. The increment in compressive strength due to the blending of silica fume (by 10%) and Murram (by 2.5%) was recorded up to 90.2%.

4.4.2 Microstructural Property

4.4.2.1 Scanning Electron Microscopy (SEM) & Energy Dispersive X-ray(EDX)

4.4.2.1.1 SEM and EDX report on the effect of Silica fume blending

4.4.2.1.1.1 Report on the effect of Silica fume blending in the presence of Borax in Fly ash based Geopolymer

Non-blended specimen GPC and blended specimen GSCB2 (as discussed in chapter-3, Table 3.17) were selected for scanning electron microscopy test. The change in microstructural morphology of blended and non-blended specimen at different age were investigated. Excessive erupted outcome was observed under scanning electron microscopy for non-blended specimen GPC after 60 days. Figure 4.56(a), 4.56(b) and 4.56(c) represent the SEM image of specimen GPC after 3, 30 and 60 days of manufacturing. The specimen GSCB2 did not show enough leachates on the outer surface after the same period. Figure 4.57(a), 4.57(b) and 4.57(c) showed compact and intact surface. Strong alkali silicate reaction product was observed [as pointed as - '**A'** in Figure 4.57(a)].

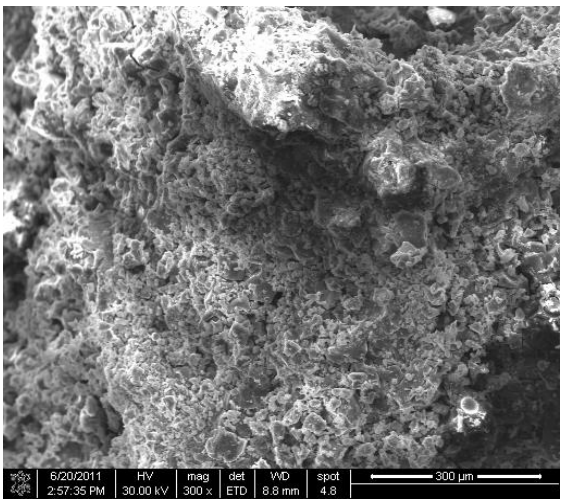

Figure 4.56(a) SEM @ 300x zoom on surface of specimen GPC after 3 days of manufacturing

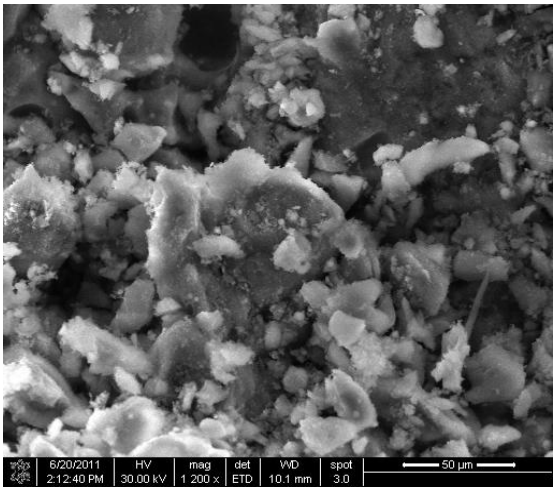

Figure 4.56(b) SEM @ 1200x zoom on surfaces of specimen GPC after 30 days of manufacturing

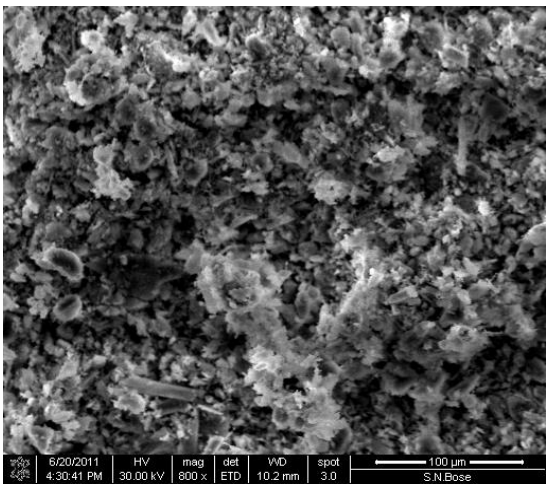

Figure 4.56(c) SEM @ 800x zoom on surfaces of specimen GPC after 60 days of manufacturing

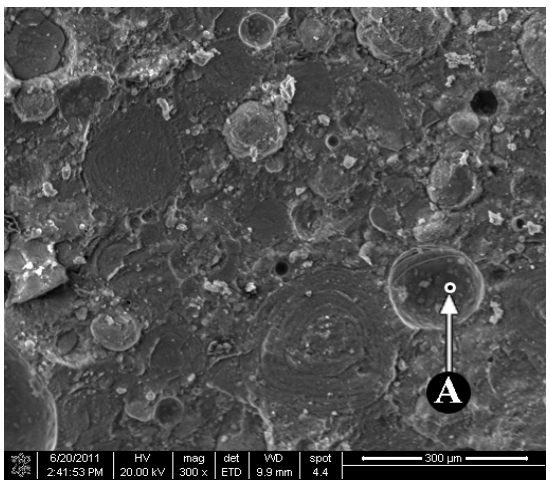

Figure 4.57(a) SEM @ 300x zoom on surface of specimen GSCB2 after 3 days of manufacturing

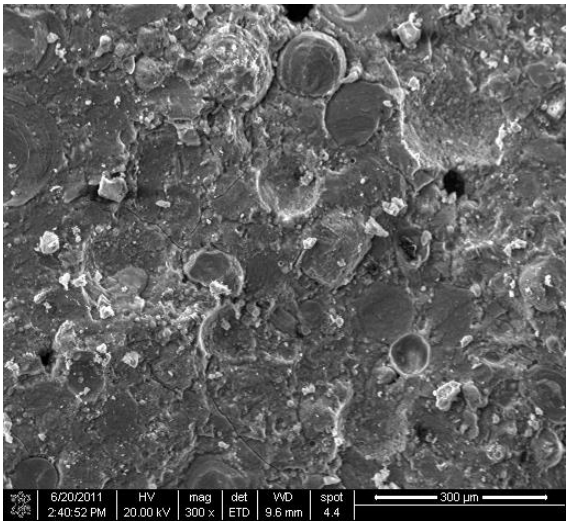

Figure 4.57(b) SEM @ 1500x zoom on surfaces of specimen GSCB2 after 30 days of manufacturing

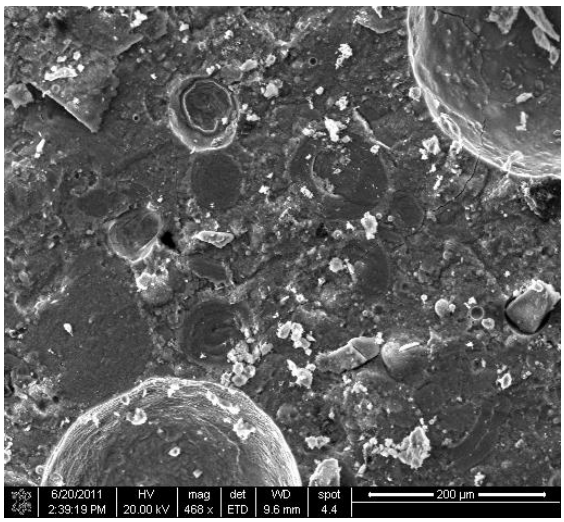

Figure 4.57(c) SEM @ 1200x zoom outer surfaces for specimen GSCB2 after 60 days of Manufacturing

4.4.2.1.1.2 Report on the effect of Silica fume blending in presence of Murram in Fly ash based Geopolymer

Scanning Electron Microscopy of non-blended and blended geopolymer specimens (as discussed in chapter-3; Table 3.18) was conducted. The possibility of development of fly ash based geopolymer in absence of silicate solution and in presence of lower percentage of alkali oxide (6% K_2O) was explored and observations were furnished. For blended geopolymer specimen GSC1R-N (prepared in absence of silicate solution), mostly compacted and less porous morphology was observed [as shown in Figure 4.59(d)]. Similarly, Figure 4.59(a) and Figure 4.59(b) represent a better pore morphology for specimen GSCR and GSCR-N respectively. For specimen GSC1-N, the microstructure showed the presence of

interconnected pores [Fig. 4.59 (c)]. These pores were responsible for the reduction of compressive strength. Higher existence of reactive silica may accelerate the Si-O-Si chain structure due to rising value Si/Al in the geopolymer mixture [28]. These differential pore morphology may be considered as the main cause behind the difference in strength characteristics [101]. The incorporation of silica fume and Murram in fly ash based geopolymer improves the pore morphology remarkably, as observed for different blended specimens (GSC1R, GSC1R-N). It may be reported that better micro-structure of fly ash geopolymer can be developed even with low alkalinity. Use of sodium silicate may be omitted with the incorporation of silica fume to have better development of geopolymeric structure.

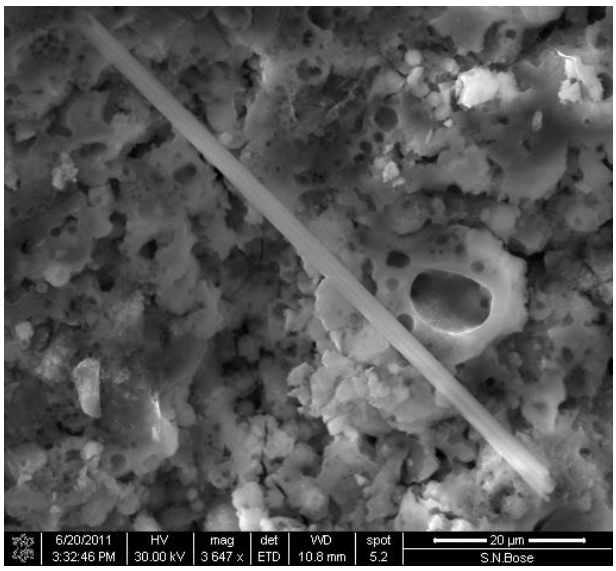

Figure 4.58(a) SEM @ 3647x zoom of specimen GPC-1

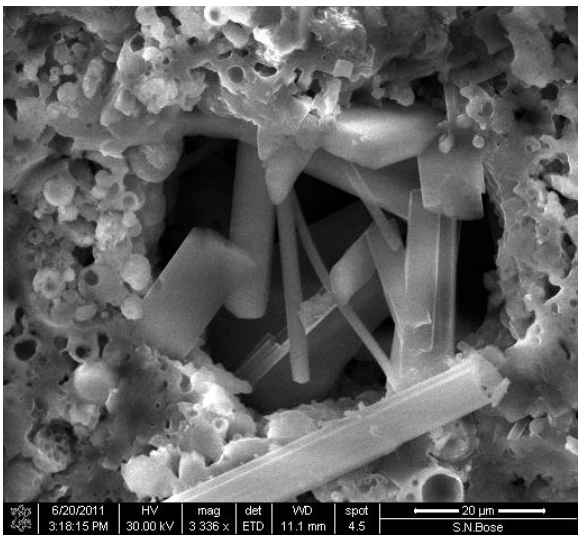

Figure 4.58(b) SEM @ 3336x zoom of specimen GPC-1

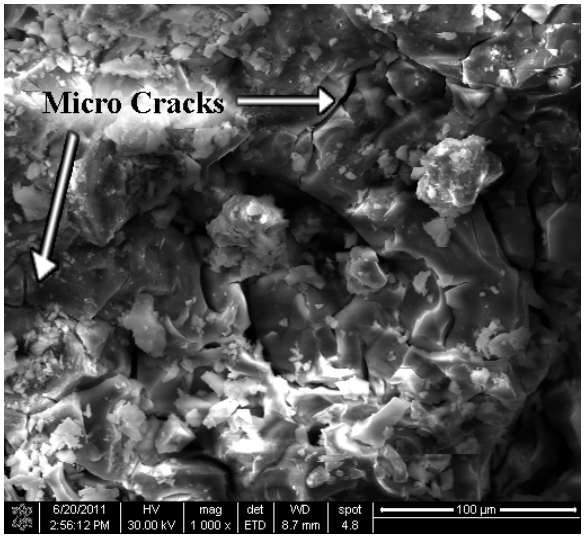

Figure 4.58(c) SEM @ 3526x zoom of specimen GSC1R

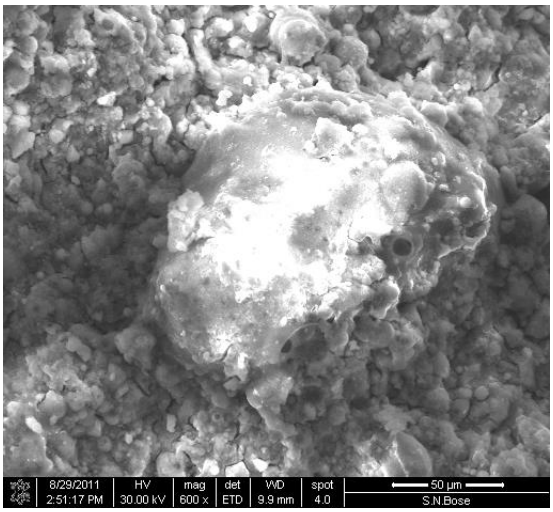

Figure 4.59(a) SEM @ 600x zoom of specimen GSCR

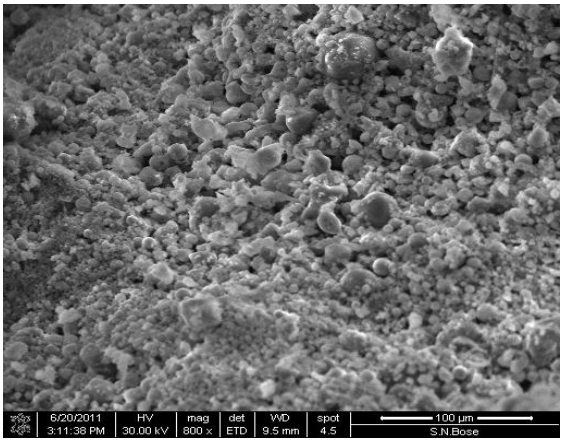

Figure 4.59(b) SEM @ 800x zoom of specimen GSCR-N

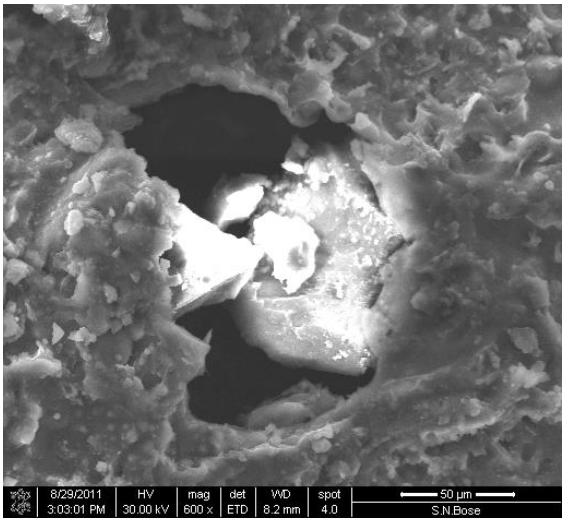

Figure 4.59(c) SEM @ 600x zoom of specimen GSC1-N

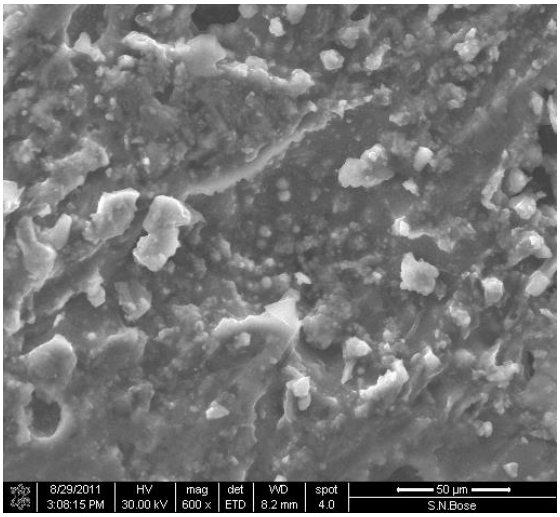

Figure 4.59(d) SEM @ 600x zoom of specimen GSC1R-N

The results of EDX analysis of three different specimens are shown in Figure 4.60(a), 4.60(b), 4.60(c).Three different specimens GPC-1 (only fly ash), GSC1(fly ash blended with 10% silica fume), GSC1R (fly ash blended with 10% silica fume and 2.5 % Murram) were subjected to EDX analysis. The blending of only silica fume primarily indicates the increase in the content of silicon in the product of the reaction (Figure 4.60b). This results expected to indicate the increment in Si/Al ratio by the blending of silica fume only. EDX analysis of GSC1R showed the presence of comparatively higher quantity in potassium and aluminum [Figure 4.60(c)]. This may be because of the better stabilization of Si-O-Al (amorphous structure) in presence of supplementary silicon and aluminium. Fly ash based geopolymer blended with silica fume and murram, is expected to have better development of geopolymeric structure.

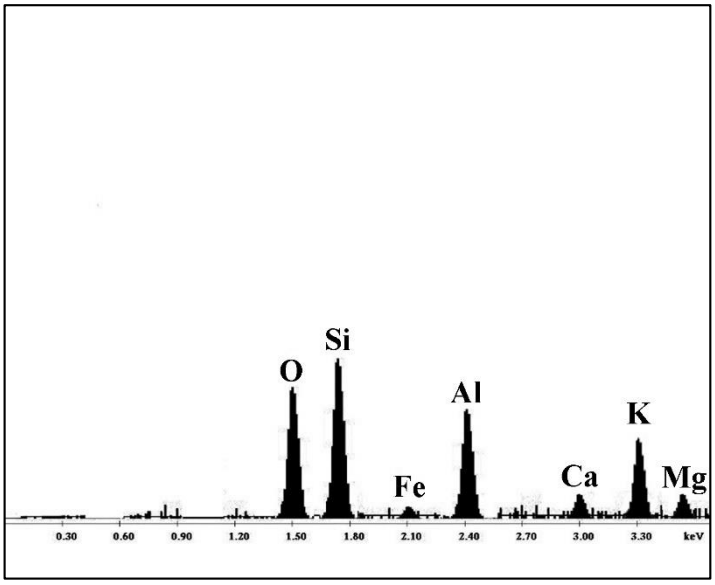

Figure 4.60(a) EDX of specimen GPC-1

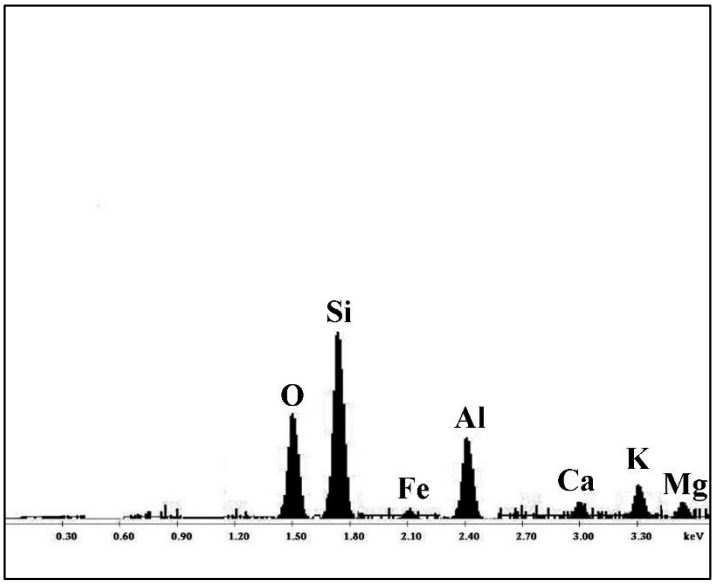

Figure 4.60(b) EDX of specimen GSC1

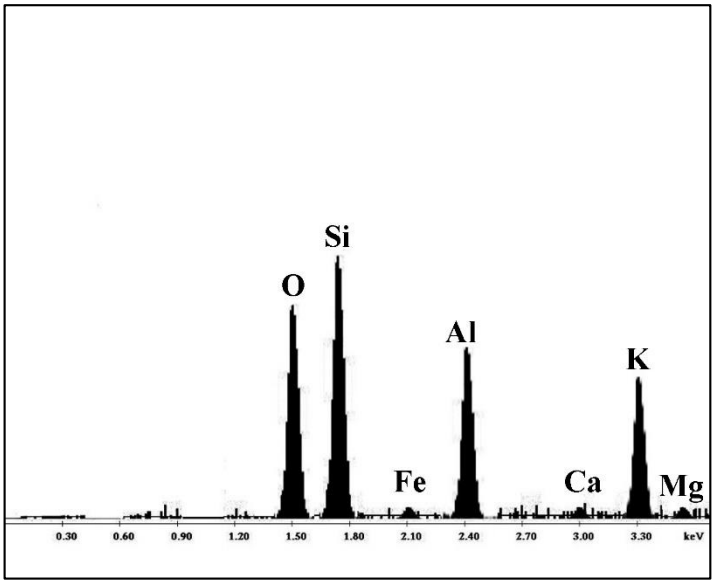

Figure 4.60(c) EDX of specimen GSC1R

4.4.2.2 Mercury Intrusion Porosimetry (MIP)

4.4.2.2.1 Effect of Silica fume blending on the pore characteristics of Fly ash based Geopolymer in the presence of Murram

MIP test was performed on two specimens, non-blended GPC-1 (fly ash activated with 8% K_2O) and blended GSC1R (fly ash blended with 10% silica fume and 2.5% Murram; activated with 8% K_2O). Integration of silica fume and Murram in fly ash based geopolymer reduce the average pore size and the total porosity. Earlier literature found some limitations in MIP in connection with proper information regarding pore characteristics [127]. But, MIP test was performed to make a comparative study between non-blended and blended fly ash based geopolymer specimen in in regard to total porosity, pore size and pore distribution. The pick applied pressure at the time of mercury intrusion were measured as 53194.551 psi and 53228.703 psi for specimen GPC-1 and specimen GSC1R, respectively. The MIP curve of specimen GPC-1 and specimen GSC1R have been shown in Figure 4.61(a) and Figure 4.61(b). The geopolymer specimen GPC-1 showed noteworthy intrusion within a diameter, range of 5 micrometer to 0.2 micrometer. The pick intrusion was appeared corresponding to 2 micrometer. The specimen GSC1R showed significant intrusion of mercury for a range within 2 to 0.009 micrometer. In these case, the pick intrusion value was attained for 0.075 micrometer. This result clearly indicates the lowering in mean median pore sizes for the blended specimen GSC1R. Breakage of the extrusion curve was observed for specimen GPC-1 (as shown by blue line in Figure 4.61 (a). It may be due to the breakage of the specimen under internal pore pressure, developed at the time of mercury extrusion with the release of

pressure. Complete extrusion curve was observed for blended geopolymer which may indicate the better integrity of fly ash geopolymer blended with Silica fume and Murram simultaneously.

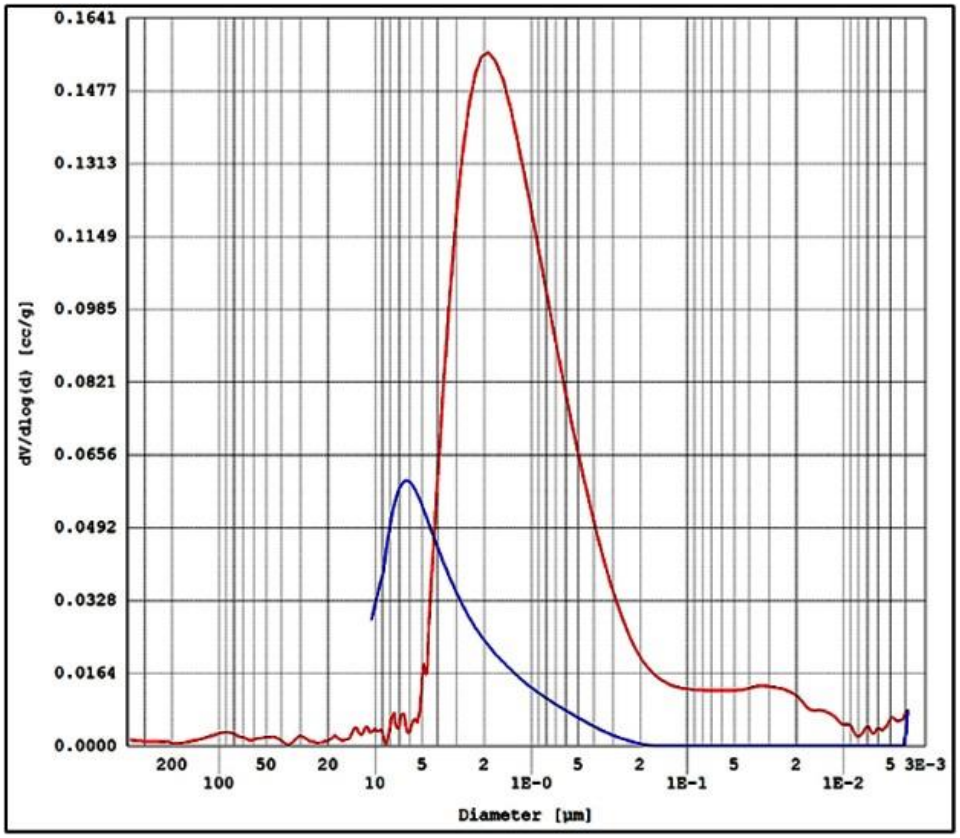

Figure 4.61(a) MIP curve for specimen GPC-1

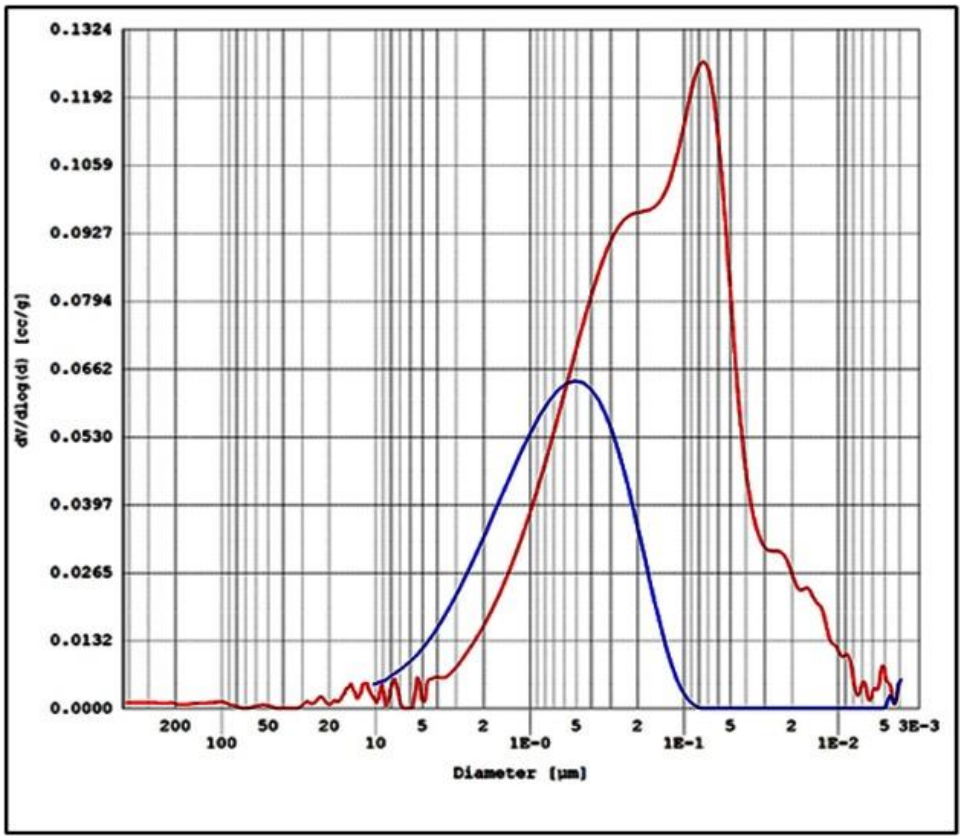

Figure 4.61(b) MIP curve for specimen GSC1R

4.4.2.2.2 Effect of Silica fume blending on the pore characteristics of Fly ash based Geopolymer in the presence of Borax

The MIP test was performed on four typical fly ash based specimen GPC (non-blended), GSC (blended with 10% silica fume), GSCB1 (blended with 7.5% silica fume, 2.5% borax) and GSCB2 (blended with 5% silica fume and 5% borax) geopolymer specimens (chapter -3; Table 3.17). The volumetric intrusion with time are shown in Figure 4.62, Figure 4.63, Figure 4.64 and Figure 4.65. The volume intrusion down to 1 micro meter was indicated for specimen GSCB2 (blended specimen). The results of volume intrusion of four different specimens clearly indicates the change in microstructure and pore characteristics of fly ash based geopolymer with the blending of silica fume and borax. Reactive silica fume in fly ash based geopolymer significantly produced higher percentage of larger pores with a lower limit greater than 10 micrometer (Figure 4.63 and Figure 4.64) specimens- GSC and GSCB1). Based on the Si/Al atomic ratio, the geopolymeric aluminosilicate structure diverges in different families from amorphous to semicrystalline frameworks like polysialate type (Si–O–Al–O–), polysialate-siloxo type (Si–O–Al–O–Si–O–), and polysialatedisiloxo type (Si–O–Al–O–Si–O–Si–O–) [28]. For specimens GSC and GSCB1, the excessive rise in Si/Al ratio (due to the incorporation of reactive silica supplements) may insist the possible formation of

Si–O–Si chain structure rather than any framework structure. However, specimen GSCB2 again tends to form framework structure because of the presence of borax containing boron (B). Here, the role of aluminium (Al) is compensated by boron (another fourfold). The difference in pore morphology must signify the change in structural formation. Figure 4.65 illustrates the curve located within a small area for GSCB2. This indicates that the silica fume-blended geopolymers in the presence of borax reduces the mean pore size. Also, the threshold volume intruded values for the non-blended geopolymer GPC are larger than other silica blended specimens. Thus, the reduced total volume of porosity and better pore size distribution contribute to the strength development.

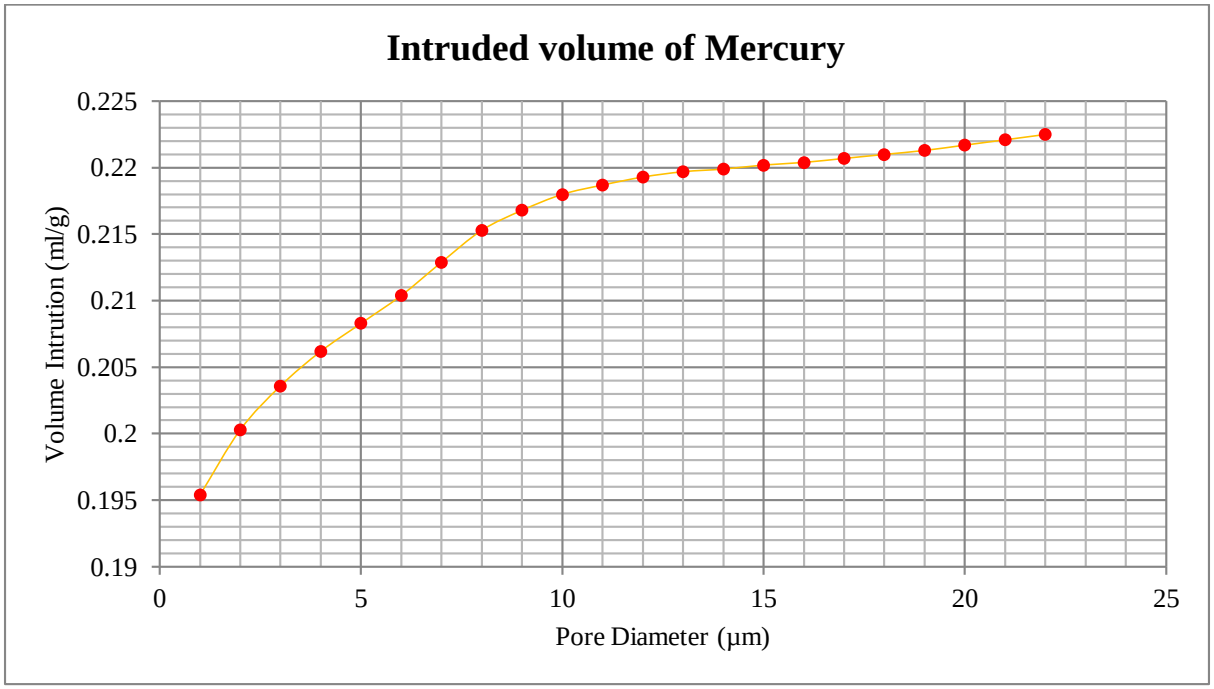

Figure 4.62 Intruded volume of Mercury for Geopolymer specimen GPC

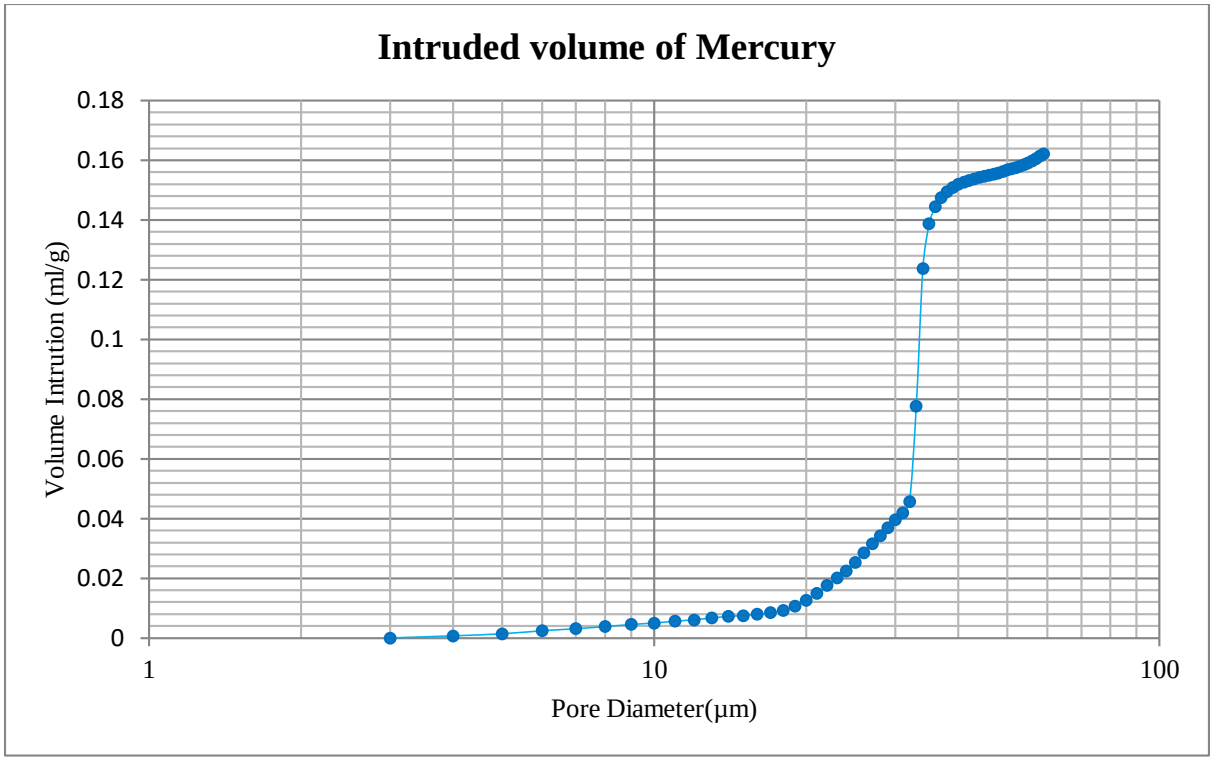

Figure 4.63 Intruded volume of Mercury for Geopolymer specimen GSC

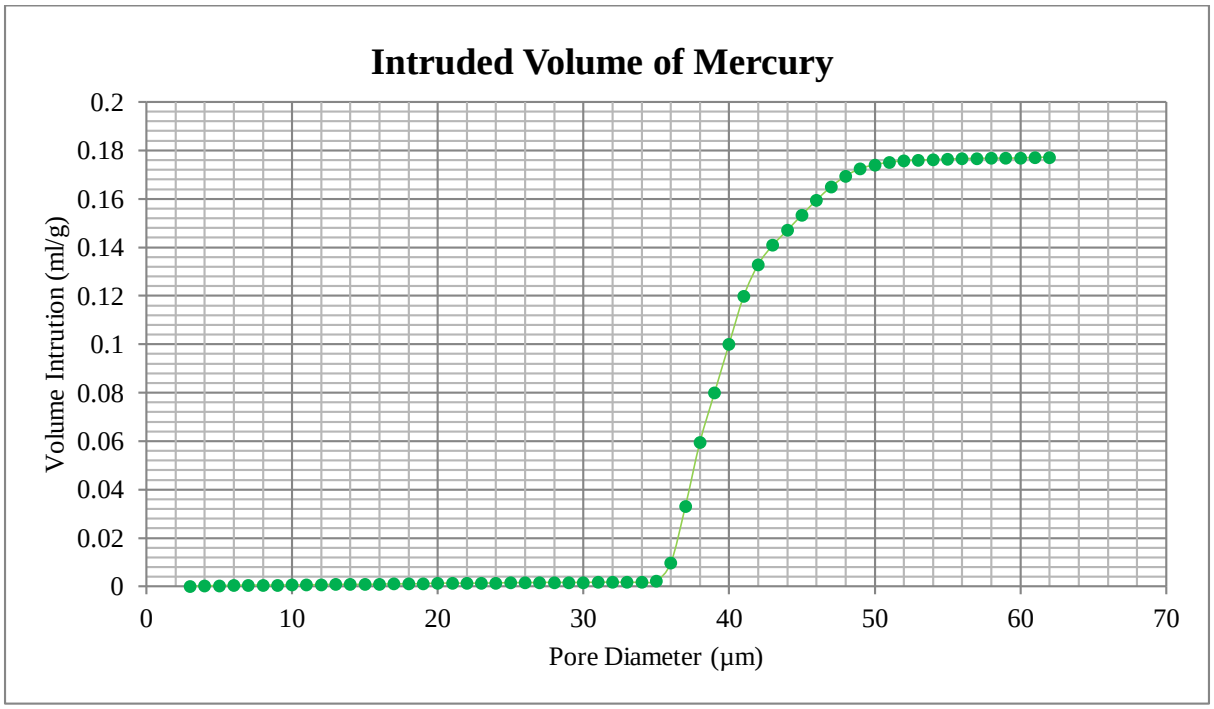

Figure 4.64 Intruded volume of Mercury for Geopolymer specimen GSCB1

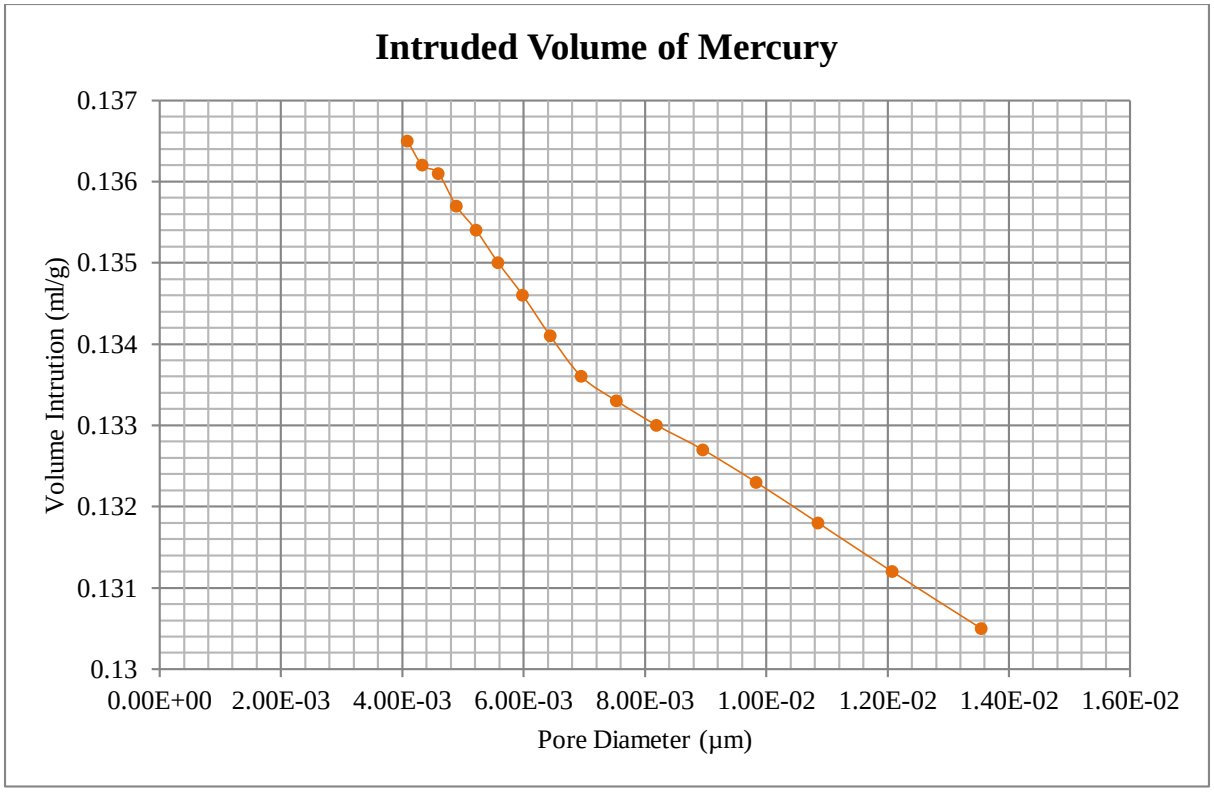

Figure 4.65 Intruded volume of Mercury for Geopolymer specimen GSCB2

4.4.3 Durability performance in Aggressive and Room exposure

4.4.3.1 Effect of Silica fume and Borax in Fly ash Geopolymer on Efflorescence in room exposure

Geopolymer efflorescence is the deposits on the geopolymer specimen. The deposits are highly alkaline. The charge compensator alkali hydroxide basically extrudes from the process of synthesis or the formation of Si-O-Al. Basically alkali metal hydroxide acts as catalyst but almost same amount which was added during synthesis is leached out from the hardened structure [130]. Slight leaching was observed for fly ash based geopolymer activated with potassium hydroxide as activator, under optical microscopy [as shown in Figure 4.66(a)]. But silica fume blended geopolymer did not exhibit such characteristics [as shown in Figure 4.66(b)]. It is because of the presence of silica fume which possess very reactive complex and compact structure further. Again, application of sodium silicate initializes the primary polymerization but for the blended mix this role might be taken by the reactive silica fume [81].

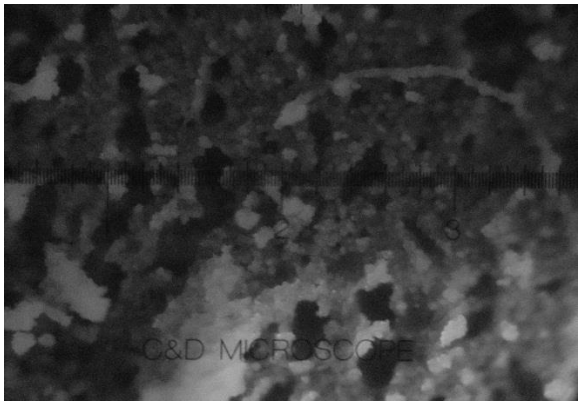

Figure 4.66(a) Specimen GPC after 30 days of manufacturing

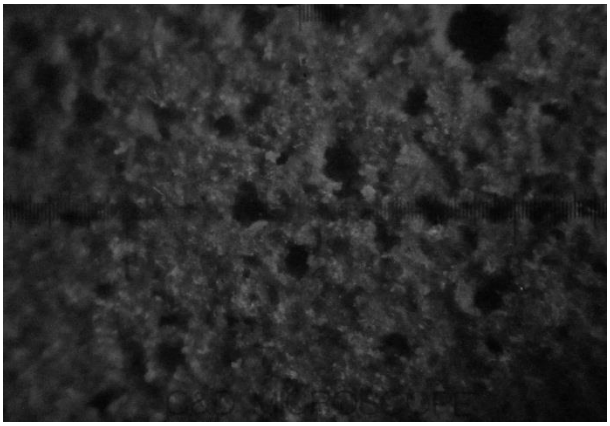

Figure 4.66(b) Specimen GSCB2 after 30 days manufacturing

4.4.3.2 Effect of Silica fume and Borax blending on the durability performance Fly ash Geopolymer under Sulfate exposure (10% concentration)

4.4.3.2.1 Change in Physical appearance (Micro and Macro Level)

Specimen GPC, GSC, GSCB1, GSCB2 (discuss in chapter-3, Table 3.17) were subjected to 10% magnesium sulfate solution for 12 months. The methodology was same as followed by earlier studies [114]. At prefixed interval of time, the physical appearance of geopolymer specimens were examined. Elongated needle like crystal formation began appearing on the surfaces of the non-blended specimen GPC, after few weeks [as shown in Figure 4.67(a)]. These images of surfaces for specimens were observed under optical microscope with a magnification of 10x. After 12 weeks of exposure in 10% magnesium sulfate solution specimen GPC showed needle like elongated crystal formation. It is due to the reaction between alkali hydroxide and magnesium sulfate which forms less soluble magnesium hydroxide with precipitation of alkali sulfate. White precipitation in larger quantity was observed for specimen GPC after 6 months [as shown in Figure 4.67(b)] which may be magnesium hydroxide with sodium sulfate.

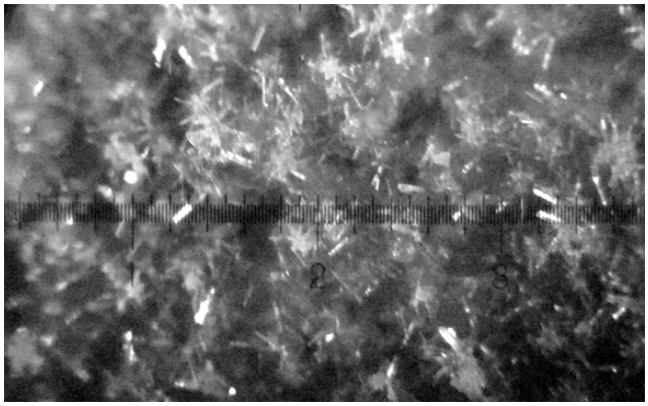

Figure 4.67(a) Specimen GPC showing needle like structure after 1 month exposure to 10% Magnesium sulfate solution

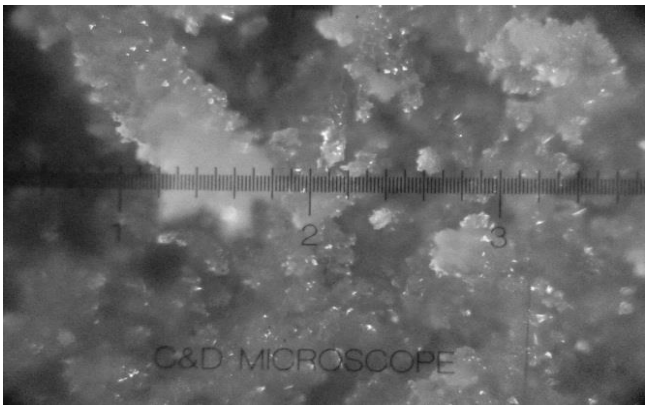

Figure 4.67(b) Specimen GPC showing white precipitant after 6 months exposure to 10% Magnesium sulfate solution

Scanning electron microscopy as shown in and EDX analysis Figure 4.68(a) and Figure 4.68(b) support the existence of that outcome. This deposits are the basic cause behind the drop in weight and strength after 9 months for non-blended specimen GPC. Bakharev [123] reported that drop of strength is due to immigration of alkalis from the geopolymer structure and subsequent diffusion nearby the surface region. But blended specimen GSCB2 and GSCB2-M did not show any formation at the outer surface with the time under sulfate exposure [as shown in Figure 4.69(a) and Figure 4.69(b)].

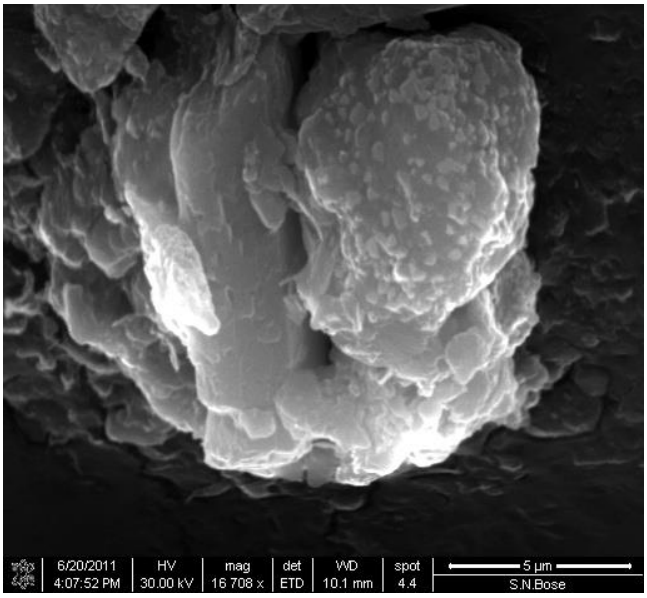

Figure 4.68(a) SEM @ 16708x zoom of the white deposit on specimen GPC

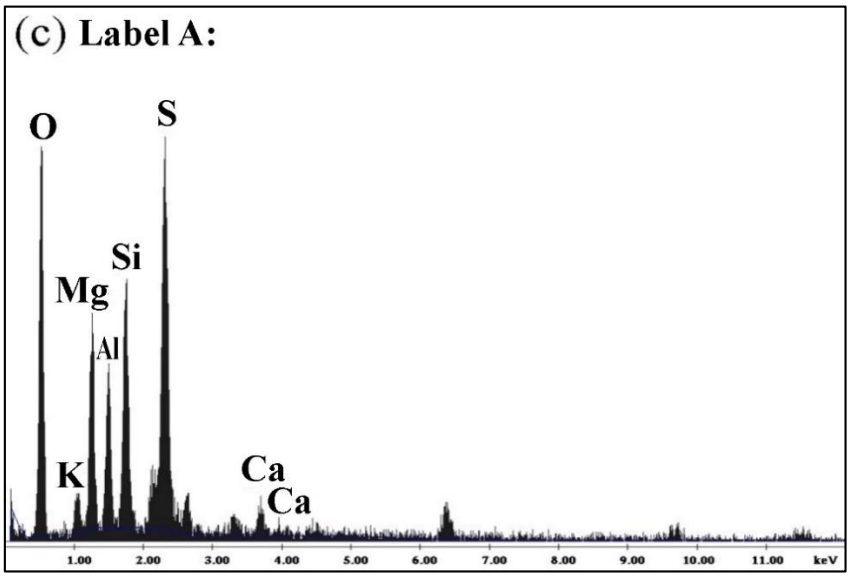

Figure 4.68(b) EDX of white precipitant on specimen GPC

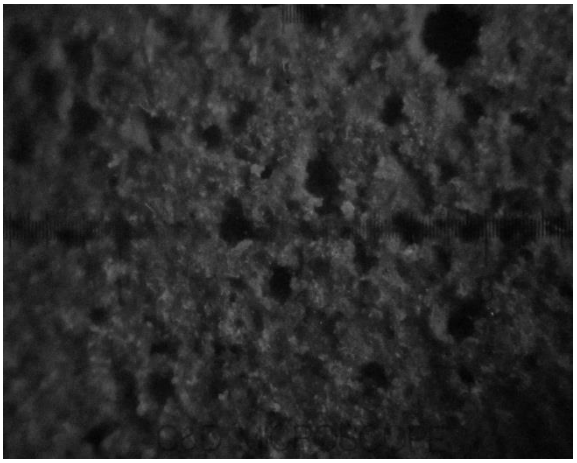

Figure 4.69(a) Specimen GSCB2 showing fresh surface after 1 month exposure to Magnesium sulfate solution

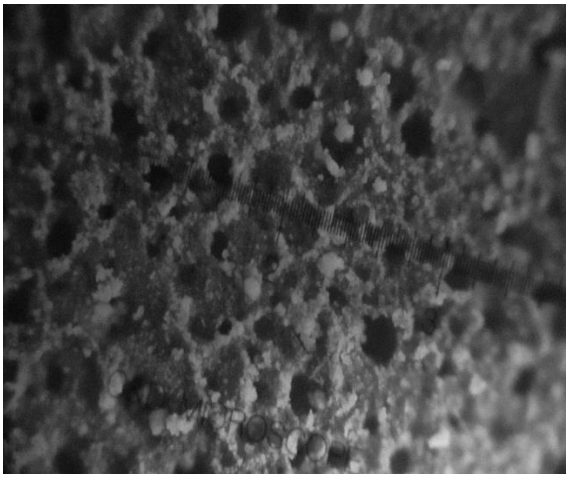

Figure 4.69(b) Specimen GSCB2 showing very little precipitants on surface after 6 months exposure to Magnesium sulfate solution

4.4.3.2.2 Changes in Weight and Strength exposed to 10% concentrated sulfate exposure

Result shows remarkable increment in the weight of non-blended specimens exposed in magnesium sulfate solution at room temperature up to 3 months [Figure 4.71(a)]. The similar trend was observed for the change of compressive strength [Figure 4.71 (b)]. But material blended with silica fume and borax did not show any remarkable change in connection with weight and strength change. The entrapped alkali within the pores of geopolymer (as shown in Figure 4.70(a) expected to participate in the ionic transaction in presence of magnesium sulfate. Increment in weight was exhibited as a result of this phenomenon. Again, the volumetric change enhances a pore pressure within the geopolymer structure. This may be treated as the initial cause of strength increment. But later on this continuous change in volume (compound within the pore) deteriorates the polymer structure as shown in Figure 4.70 (b). Due to lack of presence of untreated hydroxide within the pore, silica fume blended geopolymer did not exhibit in this manner. The detail regarding change in weight and strength at different time of exposure in sulfate solution (as a percentage of primary value) is plotted in Figure 4.71(a) and Figure 4.71(b) respectively. The figures indicate a noticeable drop from the primary values in connection with weight and strength for non-blended specimen GPC specimen mainly. The drop in compressive strength for non-blended specimen GPC was around 37.26%. Minimum change in weight and strength were observed for blended geopolymer specimen GSCB2 (fly ash + silica fume + borax).

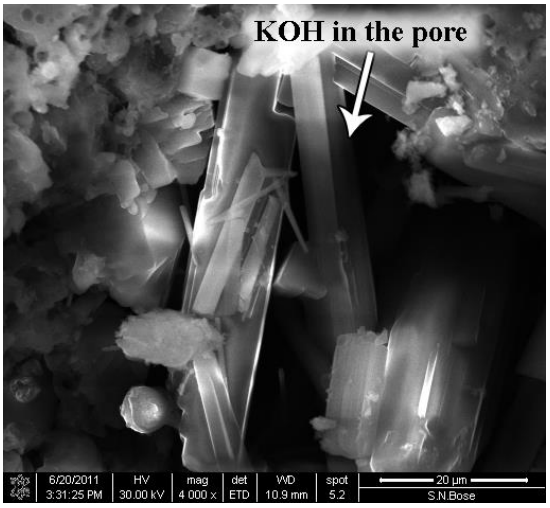

Figure 4.70 (a) SEM @ 4000x zoom of specimen GPC shows crystal structure

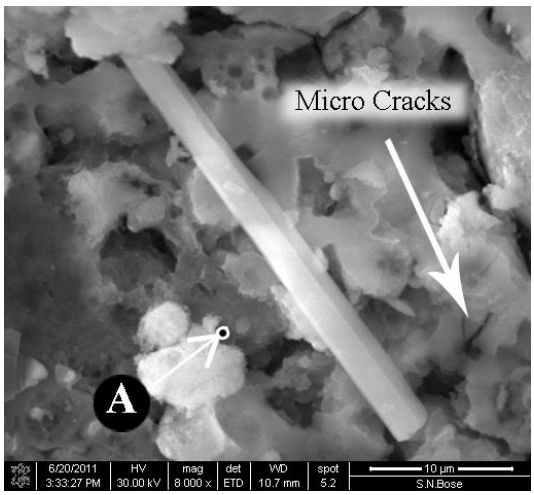

Figure 4.70 (b) SEM @ 8000x zoom of specimen GPC, showed micro crack

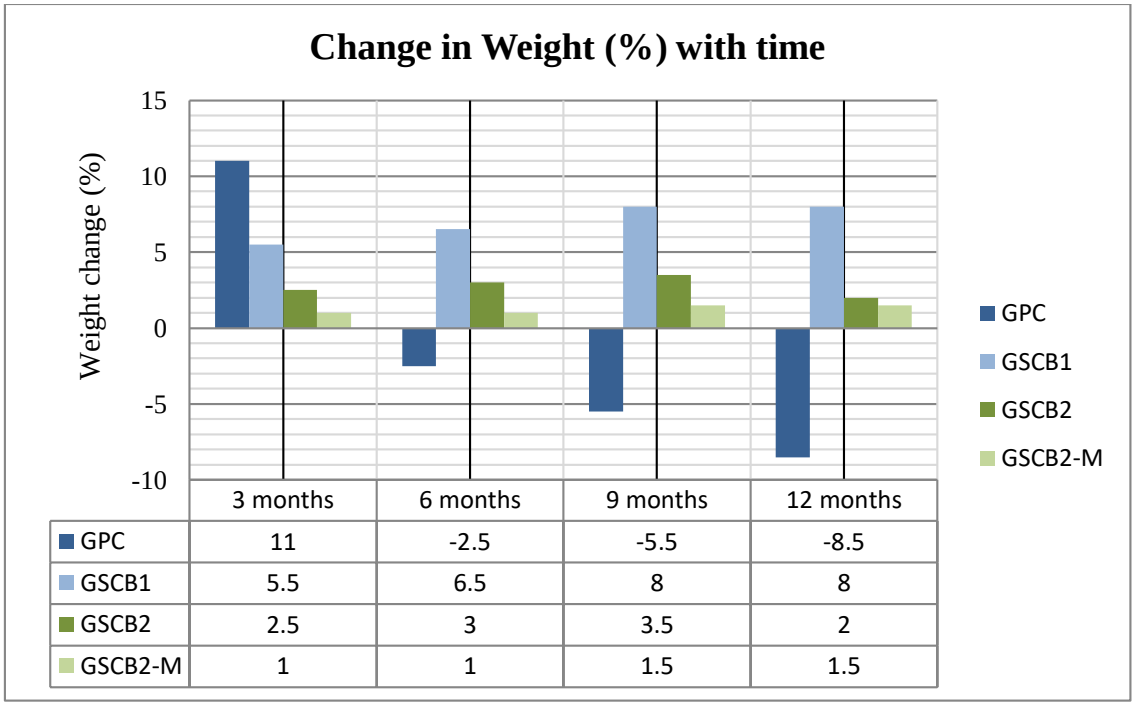

	3 months	6 months	9 months	12 months
GPC	11	-2.5	-5.5	-8.5
GSCB1	5.5	6.5	8	8
GSCB2	2.5	3	3.5	2
GSCB2-M	1	1	1.5	1.5

Figure 4.71 (a) Percentage gain or loss in weight with time of exposure to magnesium sulfate solution

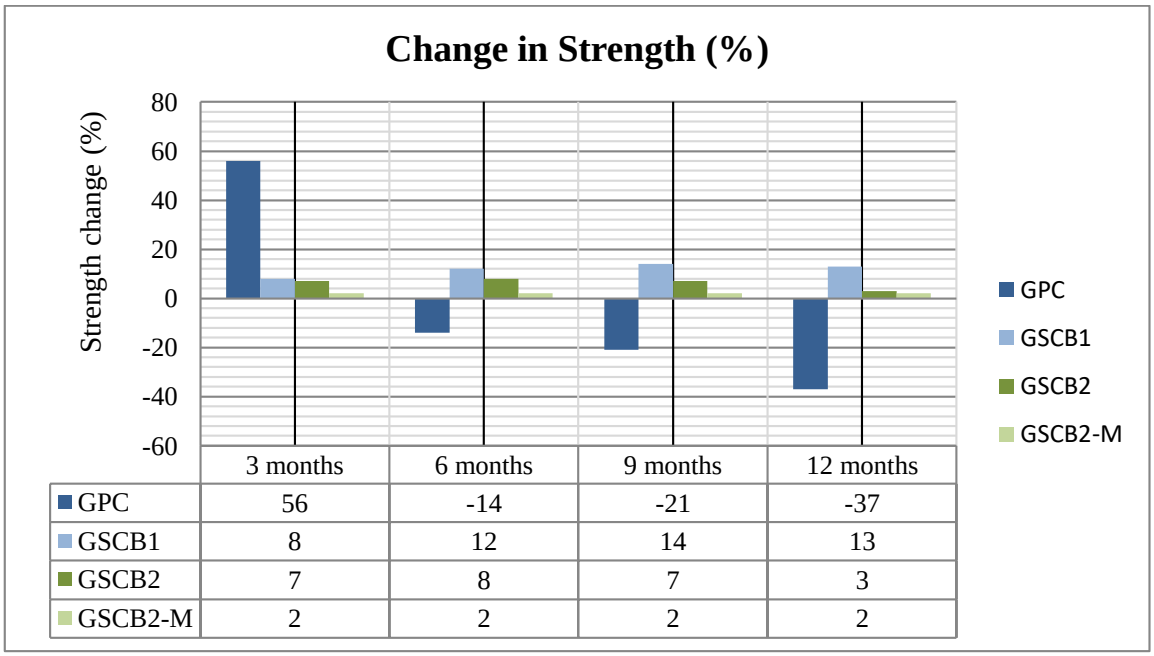

	3 months	6 months	9 months	12 months
GPC	56	-14	-21	-37
GSCB1	8	12	14	13
GSCB2	7	8	7	3
GSCB2-M	2	2	2	2

Figure 4.71 (b) Percentage gain or loss in strength with time of exposure to magnesium sulfate solution.

5. CONCLUSION

5.1 Preamble

Drawbacks of fly ash based geopolymer like hardening characteristics, cracking with age, efflorescence, low reactivity level etc. were appreciated and then present research scope was decided. Water cured fly ash based geopolymers, has not received proper attention in the past and it is included in the present study. It is observed that dissolution of sodium hydroxide in lower ambient temperature (in winter) is very low. The optimization of temperature level of activator prior mixing has been done to overcome this problem and have a considerably better geopolymer. Again, the rate of poly-condensation is dependent on the choice of oxide/combination of oxides in activator solution for different base and supplementary material/additives. Slow synthesis may provide an amorphous structure but partly crystalline. The sequential development of crystallized compound within the pores affects the product performance. An investigation on the pre-mixing and post-mixing performance of different combination of activators, have been undertaken. The scope of supplementary reactive silica (like silica fume) as an alternative of sodium silicate was investigated. Most of the research is confined with the effect of supplements added to the base material, concerning strength and durability properties. A systematic parametric study have been made on blended fly ash based geopolymer considering the influence of silicate modulus, oxide/combination of oxides in activator solution, curing regime on synthesis etc.. Fly ash was blended with Calcium / Silicon intensive supplementary materials like lime stone dust, blast furnace slag, silica fumes etc. New measurement procedure to assess workability has been introduced. The concept, dealing with the typical alkali activated and water cured new blended product has been investigated. A systematic study has been done to evaluate performance of blended geopolymer with less permeable pores in severe exposure to assess long term performance.

Present study was inclined towards the long term performance of geopolymer, optimization of strength, suitable parameter for measuring workability, choice of supplementary materials, choice of oxide/combination of oxides in activator solution, choice of curing profile etc. Present research deals with the incorporation of supplementary materials to improve the performance of fly ash based geopolymer .The entire research work was divided into three different aspects. Firstly, use of oxide/combination of oxides in activator solution, to study the performance of fly ash based non blended/ blended geopolymer. Secondly, the impact of supplementary materials on the performance of fly ash based non blended/ blended geopolymer at fresh and hardened state. Lastly, on water cured fly ash based blended geopolymer. Performance of potassium hydroxide, sodium hydroxide or combination of

oxides in activator solution, was examined with non-blended (only fly ash) and blended base material. This research has provided pathway to produce high performance fly ash based non blended and blended geopolymers in different forms overcoming present drawbacks as discussed earlier. Following conclusions can be made for better understanding of the subject.

5.1.1 Study on Activator parameter and its Impact on Non-Blended Fly Ash Geopolymer

5.1.1.1 Level of temperature induced on Activator (pre heating) prior to use to manufacture Geopolymer

Imposing temperature on activator prior mixing affects different parameters of the alkali activated product like workability, compressive strength and structural morphology significantly. In fact the state of reactivity of alkaline activator is greatly influenced with the temperature of activator which has impact on the performance of the alkali activated products.

Temperature of activator around 45^0C has got maximum impact in gaining compressive strength of fly ash geopolymer **[Ref. Figure 4.5].** Structural morphology shows better texture also. Scanning Electron Microscopy shows better structural integrity when activator temperature was around 45^0C. **[Ref. Figure 4.7]**

Workability of geopolymer at fresh state is found maximum if temperature of activator is near to 45^0C. **[Ref. Table 4.1]**

5.1.1.2 Combination of oxides in activator

Combination of Potassium hydroxide and Sodium silicate as activator has higher reactivity level with fly ash particles at higher content of Sodium silicate. For Silicate Modulus equal to one, fly ash based geopolymer paste exhibits better workability and strength with the choice of Potassium hydroxide as an alkali hydroxide results in 8% $X_2O(Na_2O+K_2O)$ in activator. **[Ref. Figure 4.6 and Table 4.2]**

Sodium hydroxide plus Sodium silicate showed higher reactivity level at lower value of Silicate modulus. Sodium hydroxide as an activator with sodium silicate showed better performance when the silicate modulus and % X_2O in the activator are 0.5 and 8% respectively. In this case X_2O is nothing but Na_2O. **[Ref. Figure 4.6 and Table 4.2].**

It is indicated smooth and compact micro structure. **[Ref. Table 4.3 and Figure 4.8]**

The long term physical study shows that specimen prepared with sodium hydroxide gains compressive strength with age but cracking occurs after particular age. Cracking can be avoided if potassium hydroxide and sodium silicate are used in combination.

5.1.2 Study on Fly ash Geopolymer blended with Supplementary Calcium compound

5.1.2.1 Study on Workability

Quicker rate of polymerization and development of secondary Ca-Al-Si amorphous structure due to the presence of calcium ions brings the early setting behavior for geopolymer specimen blended with calcium. Lime stone dust as supplements is responsible for low workability which is indicated by the drop in area factor **[Ref. Table 4.4 and Figure 4.10].**Similarly, incorporation of blast furnace slag is liable for the reduction in workability indicated by area factors. The presence of calcium in slag accelerates the charge balancing of aluminium which minimize the setting duration **[Ref. Table 4.5 and Figure 4.12].**

The typical workability set up explains the rapid setting of calcium blended geopolymer. Area factor reduces with time. The value of area factor is reaches to 1.00 after around 35-40 minutes, which indicates end of plastic state. This time will reduce to 2-3 minutes and 3-4 minutes for blended fly ash geopolymer with lime stone dust and slag respectively.

This setting problem is severe if the supplementary material (lime stone dust / Slag) is more than 18 wt. %. **[Ref. Table 4.5.1]**

5.1.2.2 Study on Heat cured specimens

5.1.2.2.1 Study on Compressive strength

5.1.2.2.1.1 Effect of Aging on Compressive strength

Every non-blended fly ash based geopolymer exhibits micro-structural changes with age which directly affects the compressive strength. After few weeks, more than 50% non-blended specimens showed hair cracks which lead to zero strength value in few cases. A well-stabilized polymeric structure was developed with the blending of blast furnace slag/ lime stone dust in fly ash based geopolymer. The compressive strength is not changing to a great extent with age for the blended geopolymer **[Ref. Figure 4.14].**

5.1.2.2.1.2 Effect of Curing temperature on Compressive strength

Curing temperature controls the gaining of strength at initial level for non-blended fly ash based geopolymer. However, the calcium compound as supplements favors the dissolution of reactive species and lead to faster strength gaining. Increase in curing temperature beyond a particular value has less effect on strength gaining of calcium blended fly ash based geopolymer. Geopolymer blended with lime stone dust/slag shows highest compressive strength at curing temperature of $65^oC \pm 5^oC$ **[Figure 4.15, Ref. Table 4.6, Figure 4.16 and Table 4.7].** Only 5.5% increment in compressive strength is observed for lime stone dust blended specimen with the rise in curing temperature from 55^0C to 85^0C. But compressive

strength is increased by 184% for non-blended specimen for the change in curing temperature from 55^0C to 85^0C. **[Ref. Table 4.6 and Figure 4.15]**.Curing even at very low temperature (< 35^0C) shows sufficient compressive strength value for fly ash based geopolymer blended with lime stone dust/slag **[Ref. Table 4.6; Figure 4.15 and Table 4.7; Figure 4.16].** However**,** higher curing temperature has less impact on further strength improvement of geopolymer specimens blended with slag **[Ref. Figure 4.16].**

5.1.2.2.1.3 Effect of Curing duration on Compressive strength

The curing duration has considerable effect on strength gaining of fly ash based geopolymer. But the change in compressive strength with duration of curing is almost negligible for fly ash based geopolymer blended with slag/lime stone dust **[Ref. Table 4.6; Figure 4.15 and Table 4.7; Figure 4.16].**Slag blended geopolymer specimen shows very small percentage of increment in compressive strength for longer curing duration for a curing temperature up to 65^0C, but at any case this increment is not greater than 1%. Furthermore, a curing duration of 48 hours with a curing temperature greater than 65^0C gives lesser compressive strength for the blended specimens **[Ref. Table 4.7 and Figure 4.16].** The blended geopolymer showed higher compressive strength in shorter time period of curing. Maximum compressive strength (47.09 MPa) is observed for slag blended geopolymer specimens subjected to 65^0C curing temperature for 24 hours. **[Ref. Table 4.7 and Figure 4.16].** Incorporation of lime stone dust up to 15wt. %, compressive strength increases up to 44% **[Ref. Figure 4.15]**.

5.1.2.2.1.4 Effect of Alkali concentration on Compressive strength

Higher percentage of Na_2O is not suitable for fly ash based geopolymer blended with lime stone dust/ blast furnace slag. In fact, lower percentage of Na_2O gives higher strength of fly ash based geopolymer blended with slag. At lower alkali concentration (%Na_2O) calcium ions play the role of charge balancer of aluminum to a great extent. The compressive strength of blended geopolymer specimens activated with 6% Na_2O concentration is higher than that obtain under 8% Na_2O concentration of activator. The result is completely opposite for non-blended geopolymer specimens. **[Ref. Figure 4.17].** Higher silicate modulus provides higher compressive strength of non-blended and blended geopolymer both but the magnitude of compressive strength of slag blended specimen is far high than the non-blended specimen **[Ref. Figure 4.18].**

5.1.2.2.1.5 Study on Microstructure

Existence of crystal-like compound (regular shaped structure comprising water) is observed for non-blended fly ash based geopolymer under scanning electron microscopy. This pore water is responsible for the increase in internal pressure with age which generates micro-cracks **[Ref. Figure 4.31(d-j) and Figure 4.32].** Scanning electron microscopy showed better surface texture with the incorporation of external calcium sources like blast furnace slag/lime stone dust in fly ash based geopolymer **[Ref. Figure 4.29, Figure 4.31(a-c)].** Results of Mercury intrusion porosimetry indicated the reduction in mean-median sizes of pores with the incorporation of lime stone dust / slag in fly ash based geopolymer. This has a positive effect on microstructure which lead to better pore distribution and higher compressive strength. **[Ref. Figure 4.33; Figure 4.34 and Figure 4.35; Figure 4.36]**. Blending of lime stone dust/slag in fly ash geopolymer showed reduction in apparent porosity and water absorption. **[Ref. Figure 4.21 ; Figure 4.22 and Figure 4.23 ; Figure 4.24].**The rate of absorption of water through the surface was slightly higher for the fly ash based geopolymer blended with slag/lime stone dust, due to the drop in average pore sizes. But the total absorption of water was lower for the blended geopolymer specimens **[Ref. Figure 4.25(a-c); Figure 4.26 and Figure 4.27(a-c) ; Figure 4.28].**

5.1.2.2.1.6 Study on Durability performance

Fly ash based Geopolymer blended with lime stone dust/slag as supplements showed better performance under magnesium sulfate exposure. Geopolymer blended with slag/lime stone dust showed higher residual strength and lesser weight change compared to non-blended fly ash based geopolymer. The drop in weight for non-blended specimens, seems to be due to the ionic transaction between excess alkali hydroxide within the pore and magnesium sulfate solution. **[Ref. Figure 4.43, Figure 4.44, Figure 4.46 and Figure 4.47].**The optical microscopic images clearly revealed the existence of surface deposits mainly for non-blended specimen under sulfate exposure, which was not observed for the blended geopolymer specimens. The SEM images and EDX analysis supported the presence of deposits on the non-blended specimens, with the existence of Mg, Si, and Al. **[Ref. Figure 4.49 and Figure 4.50].** Slag blended specimens did not exhibit any remarkable drop in tensile and compressive strength after an exposure to cyclic freezing–thawing for one year**.** But cyclic freezing and thawing showed noteworthy change in weight and strength of non-blended geopolymer specimens **[Ref. Table 4.11 and Figure 4.44].**

5.1.2.3 Study on Water cured specimens

5.1.2.3.1 Study on Compressive strength

The rest period (delayed curing) played a crucial role in regard to compressive strength of blended fly ash based geopolymer paste. Fly ash based geopolymer paste specimens subjected to longer rest periods showed rapid early strength gaining under water curing compared to those subjected to shorter rest periods. **[Ref: Table 4.9 and Figure 4.20 (a-c)].**

5.1.2.3.2 Study on Mineralogical and Microstructural properties

A specific crystalline texture consisting of needle-like structures was observed for shorter rest period. This indicates that the length of the rest period influenced the development of amorphous or non-amorphous texture. Huge portion of raw material was turned into well connected structure with glassy phase for 24 hours rest period before water curing of 20 days **[Ref: Figure 4.37 (a-h)].** Multiple inherent crystalline phases, namely quartz and mullite, were recognized in XRD patterns in water cured blended geopolymer. Longer rest period influence the development of completely amorphous phase, with a broad hump in the XRD pattern whereas, attenuated monoclinic peaks were observed for shorter rest period. **[Ref: Table 4.10 and Figure 4.38 (a-c)].**Dissimilar weight losses during heating takes place due to different rest period which was observed in TG/DTA test. **[Ref: Figure 4.39, Figure 4.40, Figure 4.41, Figure 4.42].**Leaching was observed for specimens subjected to longer rest periods of 12 hours and more. Longer rest periods brought about the formation of more amorphous polymeric structure, which promoted the ejection of alkali from the geopolymer matrix **[Ref: Figure 4.53].**

5.1.2.3.3 Study on Durability performance

The strength loss occurs due to shorter rest period. After 12 months of sulphate exposure with cyclic freezing and thawing, showed good higher resistance for longer rest periods showed. **[Ref: Figure 4.52 (a-b)].**

5.1.3 Study on Fly ash Geopolymer blended with supplementary Silica compound

5.1.3.1 General observation

Blending of silica fume along with Murram / Borax in fly ash based geopolymer showed better strength, workability and micro-structure, even at lower alkalinity level and lesser water content. It can be resolved that fly ash based geopolymer blended with silica fume leads to new trend which appears to be more amorphous. Silica fume is likely to enhance initial polymerization even in absence of sodium silicate. Although addition of only silica fume reduces the mechanical properties of geopolymer due to lesser formation of three dimensional geopolymeric aluminosilicate network. But the effect of silica fume is found to

be favouarble in the presence of Murram /Borax. Excessive rise in Si/Al ratio (due to the incorporation of reactive silica supplements) may insist the possible formation of Si-O-Si chain-structure rather than any frame-work structure. Addition of Murram / Borax tends to form frame-work structure because of the presence of Aluminium / Boron (another four fold). Murram/Borax can compensate the additional requirement of alumina to balance the Si/Al ratio in the mix.

5.1.3.2 Study on Workability

Geopolymer blended with silica fume provides higher workability. Even at lower water content and lower alkalinity, the blended geopolymer shows reasonably higher workability **[Ref: Table 4.13].**

5.1.3.3 Study on Compressive Strength

A high strength fly ash based geopolymer blended with silica fume in presence of Murram/borax was successfully made even at lower water content. **[Ref: Table 4.15]**. Compressive strength was increased by 102% with the incorporation of silica fume and borax as aluminium compensator for fly ash based geopolymer. **[Ref. Table 4.14]**

5.1.3.4 Study on Micro-structure

The MIP results indicated better micro-structure of fly ash based geopolymer blended with Silica fume and Murram, showing lower permeable volume and lower pore sizes **[Ref: Figure 4.61(a-b)]**. Again, the lower threshold values of the intruded volume, pore sizes and distribution indicates dense microstructure for silica fume and borax incorporated fly ash based geopolymer. **[Ref. Figure 4.65]**. Better morphology and compact texture was observed under scanning electron microscopy for fly ash geopolymer blended with silica fume and aluminium compensator (Murram or Borax). **[Ref. Figure 4.57 (a-c)]**

5.1.3.5 Study on Durability

The presence of the unreacted alkaline solution in fly ash based geopolymer caused by partial dissolution of the fly ash spheres was found to be absent for specimens blended with Silica fume and Murram. This reflects the increment in dissolution rate of fly ash, which is favourable in the reduction of efflorescence **[Ref: Figure 4.56]**. Almost no efflorescence was observed for specimen blended with silica fume in presence of borax. Excessive leaching was observed under scanning electron microscopy for non-blended specimen with age. The blended specimen did not show enough leachates on the outer surface with age. Compact and intact structure with strong alkali silicate reaction product was observed in microscopic study.

[Ref: Figure 4.66].Long term exposure in sulfate solution showed white deposits both on the outer surface and inner surface of non- blended specimen which was found as the unreacted alkali, extruded from the specimen. **[Ref:4.67, Ref:4.68 and Ref: 4.69]**.The resistance to sulfate attack for fly ash based geopolymer blended with silica fume in presence of Murram / Borax was observed far better compared to non-blended specimen. The minimum change in weight and strength was observed for the blended geopolymer specimen exposed to sulfate solutions. **[Ref. Figure 4.71]**

5.2 Scope of future study

The geopolymer diversities may be stretched from simple-phase composite to multi-phase composite with an objective to get a high performance geopolymer is the need of the day. Many areas may be explored in future as listed below

1. Durability of water cured fly ash geopolymer blended with calcium compound in different acid and salt solution including cyclic freezing and thawing.
2. Ductility of non-blended and blended fly ash geopolymer.
3. Shrinkage and Creep behavior of blended fly ash based Geopolymers.
4. Slag based Geopolymer blended with silica fume.
5. Longer duration study on carbonation of fly ash Geopolymer blended with Calcium.
6. Fly ash based geopolymer from naturally available alkaline sludge.
7. Effect of different acids and salt of different concentration on blended geopolymer

REFERENCE

[1] **Buchwald, A., Dombrowski, K. and Weil, M.** (2005) "The influence of calcium content on the performance of geopolymeric binder especially resistance against acids", *4th international conference on geopolymers*, 29.6.-1.07.05, st. Quentin, France

[2] **Allahverdi, A., and Skvara, F.** (2005), "Sulfuric acid attack on hardened Paste of geopolymeric cements part 1, Mechanism of corrosion at relatively high concentrations", *Ceramics-Silikaty*, 49 (4), pp. 225-229.

[3] **Fernandez-Jimenez, A. and Palomo, A.** (2005), "Composition and microstructure of alkali activated fly ash binder: effect of activator", *Cement and Concrete Research*, 35, pp. 1984–1992.

[4] **Palomo, A., Alonso, S., Fernandez-Jimenez, A., Sobrados, I. and Sanz, J.** (2004), "Alkaline Activation of Fly Ashes. An NMR Study of the Reaction Products", *Journal of American Ceramic Society*, 87, pp. 1141–1145.

[5] **Palomo, A., Blanco-Varela, M.T., Granizo, M.L., Puertas, F., Vazquez, T. and Grutzeck, M.W.** (1999), "Chemical stability of cementitious materials based on metakaolin", *Cement and Concrete Research*, 29, pp. 997–1004.

[6] **Palomo, A., Grutzeck, M.W. and Blanco, M.T.,** (1999), "Alkali activated fly ashes. A cement for the future," *Cement and Concrete Research*, 29, pp: 1323-1329.

[7] **ASTM C 109/C 109M-02**: Standard Test Method for Compressive Strength of Hydraulic Cement Mortars using 50 mm Cube specimens.

[8] **ASTM C 1437-01**: Standard Test Method for Flow of Hydraulic Cement Mortar.

[9] **ASTM C 230/230M-03**: Standard Specification for Flow Table for Use in Tests in Hydraulic Cement.

[10] **Latella, B.A., Perera, D.S., Durce, D., Mehrtens, E. G. and Davis, J.** (2008), "Mechanical properties of metakaolin-based geopolymers with molar ratios of Si/Al ≈ 2 and Na/Al ≈1", *J Mater Sci*, 43, pp. 2693–2699.

[11] **Bakharev, T.** (2005), "Geopolymeric materials prepared using class Fly ash and elevated temperature curing", *Cement and Concrete Research*, 35, pp. 1224-1232.

[12] **Bakharev, T., Sanjayan, J. and Cheny, Y.B.** (1999), "Alkali-activation of Australian slag cements", *Cement and Concrete Research*, 29, pp. 113-120.

[13] **Bakharev, T., Sanjayan, J. and Cheny, Y.B.** (2003), "Resistance of alkali-activated slag concrete to acid attack", *Cement and Concrete Research*, 33 (10), pp. 1607–1611.

[14] **Brooks, J.J.** (2002), "Prediction of Setting Time of Fly Ash Concrete", *ACI Material Journal*, 99 (6), pp. 591-597.

[15] **Brough, A.R. and Atkinson, A.** (2002), "Sodium silicate-based alkali-activated slag mortars. Part I. Strength, hydration and microstructure". *Cement & Concrete Research*, 32, pp. 865-879.

[16] **Yip, C. K. and Van Deventer, J.S.J.** (2003), "Microanalysis of calcium silicate hydrate gel formed within a geopolymeric binder". *J Mater Sci.*, 38(18), pp: 3851–3860.

[17] **Chotetanorm, C., Chindaprasirt, P., Sata, V., Rukzon, S. and Sathonsaowaphak, A.** (2013), "High-Calcium Bottom Ash Geopolymer: Sorptivity, Pore Size, and Resistance to Sodium Sulpate Attack" *J. Mater. Civ. Eng.*, 25, pp. 105-111.

[18] **Yip, C. K., Lukey, G.C. and Van Deventer, J.S.J.** (2005), "The coexistence of geopolymeric gel and calcium silicate hydrate at early stage of alkaline activation", *Cement and Concrete Research*, 35, pp. 1688–1697.

[19] **Camarim, G.** (1995), "Thermal curing performance of blast furnace slag and portland cement mixtures". *PhD Thesis University of Sao Paulo*; [only in Portuguese].

[20] **Rees, Catherine A., Provis, John L, Lukey, Grant C. and Van Deventer, J.S.J.** (2008), "The mechanism of geopolymer gel formation investigated through seeded nucleation", *Colloids and Surfaces A Physicochemical and Engineering Aspects*, 318, pp. 97–105

[21] **Chanh, N.V** (2008), "Recent Research Geopolymer Concrete", *The 3rd ACF International Conference-ACF/VCA*, Faculty of Civil Engineering-University of Technology HCM City, Vietnam. pp. 235-241.

[22] **Classie, P. A., Elsayad, H. I. and Shabban, I. G.** (1997) "Absorption and sorptivity of cover concrete", *Journal of Materials in Civil Engineering*, 9(3), pp. 105-110.

[23] **Collins, F. and Sanjayan, J.** (2001), "Micro-cracking and strength development of alkali-activated slag concrete", *Cement and Concrete Research*, 23, pp. 345-352.

[24] **Collins, F. and Sanjayan, J.** (1999), "Strength and shrinkage properties of alkali-activated slag concrete placed into a large column", *Cement and Concrete Research*, 29, pp. 659-666.

[25] **Criado, M., Palomo, A. and Fernandez-Jimenez, A** (2005), "Alkali activation of fly ashes. Part 1: Effect of curing conditions on the carbonation of the reaction products", *Fuel*, 84(16), pp. 2048 .54.

[26] **Cullity, B.D.** (1978), "Elements of x-ray diffraction". Second Edition. Reading, *Massachusetts: Addison-Wesley*, Reading, MA, pp. 102.

[27] **Breck, D.W.** (1974), "Zeolite Molecular Sieves: Structure, Chemistry and Use", *John Wiley & Sons*, New York.

[28] **Davitovits J.** (1991), "Geopolymers: Inorganic polymeric new materials", *Journal of Thermal Analysis*, 37(8). pp. 1633-1656.

[29] **Dutta, D., Chakrabarty, S., Bose, C. and Ghosh, S.** (2012), "Comparative Study of Geopolymer Paste Prepared from Different Activators", *STM Journals*, 2, pp. 1-10.

[30] **Dutta, D. and Ghosh, S.** (2014), "Microstructure of Fly Ash Geopolymer Paste with Blast Furnace Slag", CACE Volume 2, Issue 3, *American V-King Scientific Publishing*, pp. 95-101.

[31] **Dutta, D. and Ghosh, S.** (2014), "Parametric Study of Geopolymer Paste with the Different Combination of Activators", *International Journal of Engineering Innovation & Research Volume*, 3, Issue 6, pp.787-793.

[32] **Diaz, E. I., Allouche, E. N. and Eklund, S.** (2010), "Factors affecting the suitability of fly ash as source material for geopolymers", *Fuel*, 89 (5), pp. 992–996.

[33] **Khale, D. and Chaudhary, R.** (2007), "Mechanism of geopolymerization and factors influencing its development: a review", *Journal of Material Science*, 42 (3), pp. 729-746.

[34] **Duxson, P., Provis, J. L., Lukey, G.C. and Van Deventer, J.S.J** (2007), "The role of inorganic polymer technology in the development of 'green concrete'", *Cement and Concrete Research*, 37(12), pp. 1590–1597.

[35] **Kontori, E., Panagiotopoulou, Ch., Perraki, Th. and Kakali, G.** (2007), "Dissolution of aluminosilicate minerals and by-products in alkaline media", *Journal of Material Science*, 42, pp. 2967–2973.

[36] **Prud'homme, E., Michaud, P., Joussein, E., Peyratout, C., Smith, A., Arrii Clacens, S., Clacens, J.M. and Rossignol, S.** (2010), "Silica fume as porogent agent in geo-materials at low temperature", *Journal of the European Ceramic Society*, 30(7), pp. 1641-1646.

[37] **Obonyo, E., Kamseu, E., Melo, Uphie C. and Leonelli, C.** (2011), "Advancing the Use of Secondary Inputs in Geopolymer Binders for Sustainable Cementitious Composites: A Review", *Sustainability*, 3, pp. 410-423,

[38] **Rendell, F. and Jauberthie, R.** (1999), "The deterioration of Paste in sulfate environments", *Cement & Concrete Research*, 13, pp. 321-327.

[39] **Skvara, F., Kopecky, L., Nemecek, J. and Bittnar Z.** (2006), "Microstructure of Geopolymer Materials based on fly ash", *Ceramics-Silikaty*, 50 (4), pp. 208-215.

[40] **Memon, F.A., Nuruddin, M.F. and Shafiq N.** (2013), "Effect of silica fume on the fresh and hardened properties of fly ash-based self-compacting geopolymer concrete", *International Journal of Minerals, Metallurgy, and Materials*, 20(2), pp. 205-213.

[41] **Fernandez-Jimenez, A., Palomo, J.G. and Puertas, F.** (1999), "Alkali activated slag mortars: Mechanical strength behavior", *Cement & Concrete Research*, 29(8), pp. 1313-1321.

[42] **Fernandez-Jimenez, A. and Puertas, F.** (1997), "Alkali activated slag cements: kinetic studies", *Cement & Concrete Research*, 27(3), pp. 359-368.

[43] **Fernandez-Jimenez, A., Garcia-Lodeiro, I. and Palomo, A.** (2007), "Durability of alkali activated fly ash cementitious materials", *J. Mater Sci.*, 42, pp. 3055-3065.

[44] **Pacheco-Torgal, F., Castro-Gomes J. and Jalali, S.** (2008), "Alkali-activated binders: A review Part 1. Historical background, terminology, reaction mechanisms and hydration products", Construction and Building Materials, 22 (7), pp. 1305–1314.

[45] **Skvara, F., Jilek, T. and Kopecky, L.** (2005), "Geopolymer Materials Based on Fly Ash", *Ceramics-Silikaty*, 49(3), pp. 195-204.

[46] **Glukhovsky, V.D., Zaitsev, Y. and Pakhomov, V.** (1983), "Slag-alkaline cements and concrete structure, properties, technological and economical aspects of use", *Silic Ind*, 10, pp.197-200.

[47] **Gopalan, M. K.** (1996), "Sorptivity of fly ashes", *Cement and Concrete Research*, 26(8), pp. 1189-1197.

[48] **Xu, H. and Van Deventer, J.S.J.** (2002), "Geopolymerisation of multiple minerals.", *Mineral Engineering*, 15, pp. 1131–1139.

[49] **Djwantoro, H. and Rangan, B.V.** (2006), "Development and properties of low-calcium fly ash-based geopolymer concrete", *Geopolymer Institute*, France.

[50] **Khater, H. M.** (2012), "Effect of Calcium on Geopolymerization of Aluminosilicate Waste", *J. Mater. Civ. Engg.*, 24(92), pp. 92-101.

[51] **Xu, H. and Van Deventer, J.S.J.** (2003), "The Effect of Alkali Metals on the Formation of Geopolymeric Gels from Alkali-Feldspars", *Colloids and Surfaces A: Physicochem. Eng. Aspects*, 00, pp. 1-18

[52] **Hall, C.** (1989). "Water sorptivity of mortars and concrete: a review", *Magazine of Concrete Research*, 41(147), pp. 51-61.

[53] **Hardjito, D., Wallah, S.E., Sumajouw, D.M.J. and Rangan, B.V.** (2004), "On the development of fly ash-based geopolymer concrete", *ACI Materials Journal-American Concrete Institute*, 101(6), pp. 467-472

[54] **Hardjito, D., Wallah, S.E., Sumajouw, D.M.J. and Rangan, B.V.** (2003), "Brief review of development of geopolymer concrete", *George Hoff Symposium*, ACI, Las Vegas USA.

[55] **Hendricks, W. M., Bell, A. T. and Radke, C.J.** (1991), "Effect of organic and alkali metal cations on the distribution of silicate anions in aqueous solutions", *J. Phys., Chem.*, 95, pp. 9513-9518.

[56] **Hermann, E., Kunze, C. and Gatzweiler, R.** (1999), "Proceedings of Geopolymers*"*. pp. 211.

[57] **Hu, M., Zhu, X. and Long, F.** (2009), "Alkali-activated fly ash-based geopolymers with zeolite or bentonite as additives", *Cement and Concrete Composites*, 31(10), pp. 762-768.

[58] **IS 13311:** Methods of non-destructive testing of concrete, part 1 – Ultrasonic pulse velocity, Bureau of Indian Standard, New Delhi, India, 1992.

[59] **IS 1727:** Methods of Tests for Pozzolanic Materials, Bureau of Indian Standard, New Delhi, India, 1967.

[60] **IS 3812** (Part-1), Pulverized Fuel ash Specifications, Part-1, For Use as Pozzolans in Cement, Cement Mortar and Concrete, Bureau of Indian Standard, New Delhi, India, 2003.

[61] **IS 3812** (Part-2), Pulverized Fuel ash Specifications, Part-2, For Use as Admixtures in Cement, Cement Mortar and Concrete, Bureau of Indian Standard, New Delhi, India, 2003.

[62] **IS 383**: Specification for coarse and fine aggregates from natural sources for concrete, Bureau of Indian Standard, New Delhi, India, 1970.

[63] **IS 4031:** Methods of Physical tests for hydraulic cement, Bureau of Indian Standard, New Delhi, India, 1988.

[64] **IS 4305:** Glossary of terms related to Pozzolana, Bureau of Indian Standard, New Delhi, India, 1967.

[65] **IS 519:** Methods of test for strength of concrete, Bureau of Indian Standard, New Delhi, India, 1959.

[66] **IS 6491:** Methods of Sampling Fly ash, Bureau of Indian Standard, New Delhi,

[67] **Temuujin, J., Van Riessen, A. and Williams, R.** (2009), "Influence of calcium compounds on the mechanical properties of fly ash geopolymer pastes", *Journal of Hazardous Materials*, 167(1–3), pp. 82–88.

[68] **Temuujin, J., Van Riessen, A. and Williams, R.** (2009), "Effect of mechanical activation of fly ash on the properties of geopolymer cured at ambient temperature", *Journal of Materials Processing Technology*, 209, pp. 5276-5280.

[69] **Bear, J. and Bachmat, Y.** (1990), "Introduction to Modeling and Transport Phenomena in Porous Media", *Theory and Applications of Transport in Porous Media*, 4, Kluwer, Dodrecht.

[70] **Swanepoel, J. C. and Strydom, C. A.** (2002), "Utilisation of fly ash in a geopolymeric material," *Applied Geochemistry*,17, pp. 1143-1148.

[71] **Davidovits, J., Buzzi, L., Rocher, P., Gimeno, D., Marini, C. and Atocco, S.** (1999), "Geopolymeric Cement based on low Cast Geologic Materials", *Results from the European Research Project GEOCISTEM*, pp.83-96.

[72] **Davidovits, J.** (1994), "Properties of geopolymer cements. Proceedings," *First International Conference on Alkaline Cements and Concretes, Scientific Research Institute on Binders and Materials*, Kiev State Technical University, 9, pp: 131- 149.

[73] **Davidovits, J.** (1994), "Geopolymer: Man-made Rock Geosynthesis and the Resulting Development of Very Early High Strength Cement," *Journal of Materials Education*, 16 (2-3), pp. 91-137.

[74] **Van Brakel, J.** (1981), "A special Issue Devoted to Mercury Porosimetry", *Powder Tech*, 29(1), pp. 1-209.

[75] **LaRosa, J. L., Kwan, S. and Crutzeck, M.W.** (1992), "Zeolite formation in class F fly ash blended cement pastes", *Journal of the American Ceramic Society*, 75 (6) pp. 1574–1580.

[76] **Provis, J.L., Lukey, G.C. and Van Deventer, J.S.J.** (2005), "Do geopolymers actually contain nanocrystalline zeolites? A re-examination of existing results", *Chemistry of Materials*, 17, pp. 3075–3085.

[77] **Van Jaarsveld, J.G.S., Van Deventer, J.S.J. and Lukey, G.C.** (2002), "The effect of composition and temperature on the properties of fly ash and kaolinite based geopolymers", *Chemical Engineering Journal*, 89 (63), pp.73.

[78] **Van Jaarsveld, J.G.S., Van Deventer, J.S.J. and Lukey, G.C.** (2003), "The characterisation ofsource materials in fly ash-based geopolymers." *Materials Letters*, 12, pp. 72–80.

[79] **Van Jaarsveld, J.G.S., Van Deventer, J.S.J. and Lorenzen, L.** (1998) "Factors affecting the immobilisation of metals in geopolymerised fly ash", *Metall Mater Trans B*, 29, pp. 283–291.

[80] **Jimenez, A.F. and Palomo, A.** (2003), "Alkali-activated fly ashes: properties and characteristics", *Fuel*, 82, pp. 2259-2265

[81] **Gourley, J.T.** (2003), "Geopolymers; Opportunities for Environmentally Friendly Construction Materials", *Materials 2003 Conference: Adaptive materials for a modern society*, October 2003, Sydney.

[82] **Wang., K, Shah, S.P. and Mishulovich, A.** (2004), "Effects of curing temperature and NaOH addition on hydration and strength development of clinker-free CKD-fly ash binder", *Cement Concrete Research*, 34, pp. 299–309.

[83] **Katz, A.** (1998), "Microscopic study of alkali-activation fly ash", *Cement Concrete Research*, 28 (2), pp.197-208.

[84] **Khalil, M. and Merz., E.,** (1994), "Immobilization of intermediate-level waste in geopolymers", *J Nucl. Mater*, (211), pp.141.

[85] **V. Kirschner, A. and Harmuth, H.** (2004), "Investigation of geopolymer binders with respect to their application for building materials", *Ceram.-Silikáty*, 48, pp. 117-120.

[86] **Kriven, W.M. and Bell, J.L.** (2008), "Effect of Alkali Choice on Geopolymer Properties", *28th International Conference on Advanced Ceramics and Composites*

B: Ceramic Engineering and Science Proceedings, 25 (4), (EDITED by- Lara-Curzio, E. and Readey, M. J.), John Wiley & Sons, Inc., Hoboken, NJ, USA

[87] Le Chatelier's principle, Wikipedia-the free encyclopedia, available at http://en.wikipedia.org/ wiki/Le_Chatelier%27s_principle, accessed on January 2012.

[88] **Lee, W.K.W. and Van Deventer, J.S.J.,** (2002), "The effect of ionic contaminants on the early-age properties of alkali-activated fly ash-based cements", *Cement and Concrete Research*, 32, pp. 577–584.

[89] **Inada, M., Eguchi, Y., Enomote, N. and Hojo, J.** (2005), "Synthesis of zeolite from coal fly ashes with different silica-alumina composition", *Fuel*, 84, pp. 299-304.

[90] **Marinho, E. P.** (2004), "Desenvolvimento de pastas geopoliméricas para cimentação de postos de petr´oleo", Ph.D. thesis, Universidade Federal do Rio Grande do Norte, Brasil.

[91] **McCormick, A.V., Bell, A.T. and Radke, C.J** (1989), "Evidence from alkali metal NMR spectroscopy for ion pairing in alkaline silicate solution", *J .Phys Chem.*, 93(5), pp. 1733-1737.

[92] **McCarter, W. J.** (1993), "Influence of surface finish on sorptivity on concrete", *Journal of Materials in Civil Engineering*, 5(1), pp. 130-136.

[93] **McCarter, W. J., Ezirim, H. and Emerson, M.** (1992), "Absorption of water and chlorideinto concrete", *Magazine of Concrete Research*, 44(158): pp. 31-37.

[94] **Qureshi, Mohd. N. and Ghosh, S.** (2013), "Workability and Setting Time of Alkali Activated Blast Furnace Slag Paste", *Advances in Civil Engineering Materials*, 2 (1), pp. 62-77.

[95] **Micheline, Moranville- Regourd** (1998), "Cements made from blast furnace slag", *Lea's Chemistry of cement and concrete. Ed. Peter C. Hewlett.*, Fourth Edition, London, England: Arnold, pp. 633-674.

[96] **Murayama, N., Yamamoto, H. and Shibata, J.** (2002), "Mechanism of zeolite synthesis from coal fly ash by alkali hydrothermal reaction", *International Journal of Mineral Processing*, 64, pp. 1–17.

[97] **Duxson., P., Fernandez-Jimenez, A., Provis, J.L., Lukey, G.C., Palomo, A. and Van Deventer, J.S.J.** (2007), "Geopolymer technology: The current state of the art.", *Journal of Material Science*, 42, pp. 2917-2933.

[98] **Palomo, A., Grutzeck, M.W. and Blanco, M.T.** (1999), "Alkali-activated fly ashes: a cement for the future", *Cement and concrete research*, 29(8), pp. 1323-1329.

[99] **Palomo, A. and Glasser, F.P.** (1992), "Chemically-Bonded Cementitiousn Material Based on Metakaolin", *Journal of British Ceramic Transactions*, 91, pp. 107–112.

[100] **H. R. Borges, P., F. Fonseca, L., A. Nunes, V., H. Panzera, Tulio and C. Martuscelli, C.** (2014), "Andreasen Particle Packing Method on the Development of Geopolymer Concrete for Civil Engineering", *ASCE J. Mater. Civ. Engg*, 26, pp. 692-697.

[101] **Duxson P., Provis, J.L., Lukey, G.C., W. Mallicoat, S., M. Kriven, W. and Van Deventer, J.S.J.** (2005), "Understanding the relationship between geopolymer composition, microstructure and mechanical properties", *Colloids and Surfaces A: Physicochem. Eng. Aspects*, 269, pp. 47–58.

[102] **Pinto A.T.** (2004), "Alkali-activated metakaolin based binders. PhD Thesis. University of Minho.

[103] **De Silva, P.**, "Medium-term phase stability of $Na_2O–Al_2O_3–SiO_2–H_2O$ geopolymer systems", *Kwesi Sagoe-Crenstil CSIRO Manufacturing & Materials Technology*, 14 Julius Avenue, Riverside Corporate Park, North Ryde, NSW 2113, Australia, pp. 01.

[104] **De Silva, P.**, Kwesi Sagoe Crenstil, (2008), "Medium-term phase stability of $Na_2O–Al_2O_3–SiO_2–H_2O$ geopolymer systems", *Cement and Concrete Research*, Volume 38, Issue 6, pp. 870–876.

[105] **Puertas, F., Martinez-Ramirez, S, Alonso, S. and Vasquez, T.** (2000), "Alkali-activated fly ash/slag cement. Strength behaviour and hydration products", *Cement and Concrete Research*, 30, pp. 1625-1632.

[106] **Thakur, R. N. and Ghosh, S.** (2009), "Effect of mix composition on compressive strength and microstructure of fly ash based geopolymer composites", *ARPN Journal of Engineering and Applied Sciences*, 6, pp. 70-71.

[107] **Fletcher, R.A., MacKenzie, J.D., Nicholson, C.L. and Shimada, S.** (2005), "The composition range of aluminosilicate geopolymers", *Journal of the European Ceramic Society*, 25, pp. 1471–1477.

[108] **Thakur, R. and Ghosh, S.** (2007), "Fly ash based geopolymer composites",10^{th} NCB International seminar on cement and building materials, New Delhi, India, pp. 442-451.

[109] **Rovnanik, P.** (2010), "Effect of curing temperature on the development of hard structure of metakaolin based geopolymer", *Construction and Building Materials*, 24(7) pp. 1176-1183.

[110] **Palomo, A. and Alonso, S.** (2001), "Calorimetric study of alkaline activation of calcium hydroxide–metakaolin solid mixtures", *Cement and Concrete Research*, 31, pp. 25– 30.

[111] **Palomo, A. and Alonso, S.** (2001), "Alkaline activation of metakaolin and calcium hydroxide mixtures: influence of temperature, activator concentration and solids ratio", *Mater. Lett.*, 47, pp. 55– 62.

[112] **Thokchom, S., Ghosh, P. and Ghosh, S.**, "Influence of alkali content on performance of geopolymer Pastes in magnesium sulfate" Arabian J. for Science and Engineering, Accepted for publication.

[113] **Wallah, S.E. and Rangan B.V.,** (2006), "Low calcium fly ash based geopolymer concrete: Long term properties, Research report GL2", Curtin University of Technology, Australia.

[114] **Thokchom, S., Dutta, D. and Ghosh, S.** (2011), "Effect of Incorporating Silica Fume in Fly Ash Geopolymers", *World Academy of Science, Engineering and Technology*, 60, pp. 243-247

[115] **Thokchom, S., Ghosh, P. and Ghosh, S.** (2009), "Porosity and sorptivity on performance of fly ash based geopolymer Pastes in Nitric acid", *Int. J Applied Engg. Research*, 4(11), pp. 2065-2092.

[116] **Sabir, B.B., Wild, S. and O'Farrel, M.**, (1998), "A water sorptivity test for Paste and concrete", Materials and Structures, 31, pp.568-574.

[117] **Silva M.G. and Agopyan., V.** (1998), "Hydration of blast furnace slag cements; Influence of temperature". *Technical magazine BT/PCC/204.,* University of Sao Paulo.

[118] **Silva M.G.** (1998) "Thermal curing of pastes and mortars using blast furnace slag". PhD Thesis. University of Sao Paulo.

[119] **Song, X.J., Marosszeky, M., Brungs, M. and Munn, R.** (2005), "Durability of fly ash based Geopolymer concrete against sulfuric acid attack", 10 DBMC *International Conferences on Durability of Building Materials and Components*, Lyon, France.

[120] **Thokchom, S., Ghosh, P. and Ghosh, S.** (2011), "Durability of Fly Ash Geopolymer Mortars in Nitric Acid–effect of Alkali (Na2o) Content", *Journal of Civil Engineering and Management*, 17 (3), pp. 393-399.

[121] **Swaddle, T.W., Salerno, J. and Tregloan, P.A.** (1994). "Aqueous aluminates, silicates and aluminosilicates", *Chem. Soc. Rev*. pp. 319- 325.

[122] **Swanepoel, J.C. and Strydom, C.A.** (2002) "Utilisation of fly ash in a geopolymeric material". *Appl. Geochem*, 17, pp. 1143-1148.

[123] **Bakharev, T.** (2005), "Durability of geopolymer materials in sodium and magnesium sulfate solutions",*Cement and Concrete Research*, 35, pp.1233-1246.

[124] **Bakharev, T.**, (2005), "Resistance of geopolymer materials to acid attack", *Cement and Concrete Research*, 35, pp. 658-670.

[125] **Bakharev, T. and Sanjayan, J.G.** (2002), "Alkali-activated slag concrete: Durability in aggressive Environment Geopolymer" Melbourne, Australia .

[126] **Terzano, R., Spagnuolo, M., Medicu, L., Vekemans, B., Vincze, L., Janssens. K and Ruggiero, P.** (2005), "Copper stabilization by zeolite synthesis in polluted soils treated with coal fly ash", *Environ Sci. Tech.,* 39, pp.6280

[127] **Brakel, V., Modry, S. and Svata, M.** (1981), "A Special Issue Devoted to Mercury Porosimetry", *Powder Technology*, 29, pp. 201-209.

[128] **Van Jaarsveld, J.G.S, Van Deventer, J.S.J. and Lorenzen, L.** (1997). "The potential use of geopolymeric materials to immobilize toxic metals: Part I". Theory and applications Minerals Engineering, 10, pp. 659-669.

[129] **Van Jaarsveld, J.G.S., Van Deventer, J.S.J. and Lukey, G.C.** (2003), "The Characterization of source material in fly ash based geopolymer", *Mater Let.*, 57, pp.1272

[130] **Van Jaarsveld, J.G.S., Van Deventer, J.S.J. and Lorenzen, L.** (1998), "Factors affecting the immobilization of metals in geopolymerized fly ash", *Metallurgical and Materials Transactions*, B, 29 (1), pp. 283-291.

[131] **Van Jaarsveld, J.G.S., Van Deventer, J.S.J. and Lukey, G.C.** (2002), "The effect of composition and temperature on the properties of fly ash- and kaolinite-based geopolymers", *Chemical Engineering Journal*, 89(1-3): pp. 63-73.

[132] **Lee, W.K.W. and Van Jaarsveld, J.G.S.** (2002), "Structural reorganisation of class F fly ash in alkaline silicate solutions. Colloids and Surfaces" A*: Physicochemical engineering Aspects*, 211(1), pp 49-66.

[133] **Kriven, W.M., Gordon, M. and Bell J.L.** (2004), "Geopolymers: nanoparticulate, nanoporous ceramics made under ambient conditions, Microscopy and Microanalysis" '04, Proc. *62nd Annual Meeting of the Microscopy Society of America*, vol. 10, pp. 404–405.

[134] **Wang, K., Shah, S.P. and Mishulovich, A.** (2004), "Effects of curing temperature and NaOH addition on hydration and strength development of clinker-free CKD-fly ash binders", *Cement Concrete Research*, 34, pp. 299

[135] **Wang., S.D., Scrivener, K. and Pratt, P.** (1994), "Factors affecting the strength of alkali-activated slag", *Cement Concrete Research*, 24, pp. 1033-43.

[136] **Guo, X., Shi H. and A. Dick, Warren** (2010), "Compressive strength and microstructural characteristics of class C fly ash geopolymer", *Cement & Concrete Composites*, 32, pp. 142-147.

[137] **Xu, H. and Van Deventer, J.S.J.** (2000), "The geopolymerisation of aluminosilicate minerals", *International Journal of Mineral Processing*, 59 (3), pp. 247-266.

[138] **Yip, C.K. and Van Deventer, J.S.J** (2001), "Effect of granulated blast furnace slag on geopolymerisation", *6th World Congress of Chemical Engineering*, Melbourne, Australia.

[139] **Li, Z. and Liu, S.** (2007), "Influence of slag as additive on compressive strength of fly ash based geopolymer", *J. Mater. Civil. Engg*. 19 (6), pp. 470–474.

[140] **Zuhua Z., Xiao Y., Huajun Z. and Yue C.** (2009), "Role of water in the synthesis of calcined kaolin-based geopolymer", *Applied Clay Science*, 43 (2), pp. 218–223.

[141] **Rashad, A. M.** (2013), "Properties of alkali-activated fly ash concrete blended with slag", *Iran. J. Mater. Sci. Engg*, 10(1) (2013), pp. 57-64.

[142] **Kong, D.L.Y. and Sanjayan, J.G.** (2008), "Damage behavior of geopolymer composites exposed to elevated temperatures", *Cement and Concrete Composites*, Volume 30, Issue 10, Nov. (2008), pp. 986-991.

[143] **Duxson, P., Lukey, G.C. and Van Deventer, J.S.J.** (2006), "Thermal evolution of metakaolin geopolymers: Part Physical evolution", *Journal of Non-Crystalline Solids*, 352, pp.,5541-5555.

[144] **IUPAC-NIST** Solubility Database, Version 1.1, NIST Standard Reference Database 106.

[145] **Nath, P. and Sarker, P.K.** (2014), "Effect of GGBFS on setting, workability and early strength properties of fly ash geopolymer concrete cured in ambient condition", *Construction and Building Materials*, 66, pp. 163–171.

[146] **Kuenzel, C., Vandeperre, L.J., Donatello, S., Boccaccini, A.R. and Cheeseman, C.** (2012), "Ambient temperature drying shrinkage and cracking in metakaolin-based geopolymers", *J. Am. Ceram. Soc.*, 95, pp. 3270–3277.

[147] **Ferone, C., Colangelo, F., Roviello, G., Asprone, D., Menna, C., Balsamo, A., Prota, A., Cioffi, R. and Manfredi, G.** (2013), "Application-oriented chemical optimization of a metakaolin based geopolymer", *Mater*,6, pp.1583-1598.

[148] **Ghosh, K. and Ghosh, P.** (2018), "Effect of variation of slag content on chemical, engineering and microstructural properties of thermally cured fly ash-slag based geopolymer composites", *Rasayan J. Chem.*, 11, pp. 426-439.

APPENDIX-I

CALCULATION FOR CONSTITUENT PROPORTION OF ACTIVATOR AND GEOPOLYMER PASTE

A1: CALCULATION FOR CONSTITUENTS OF ACTIVATOR SOLUTION ($NaOH$ & Na_2SiO_3)

For Activator solution having Na_2O of 8% by weight of total material (base material and supplementary material) and silicate modulus (SiO_2/Na_2O) equals to 1.0 (Refer Table 3.7)

[A] Reaction equation of Sodium Hydroxide (NaOH)

	Na_2O	+	H_2O	=	2NaOH
Molar weight	$(23\times2)+16$		$(1\times2)+1$		$2(23+16+1)$
=	62		18		80 (in gm.)

[B] Composition of Sodium Silicate (Na_2SiO_3) solution as per test report

Na_2O = 8 %

SiO_2 = 26.6 %

Water (H_2O) = 65.5 %

[C] Required quantity of Na_2O for 1000 gm. of total material

Na_2O = 8 % of weight of total material

$= \frac{8\times1000}{100}$ = 80 gm.

[D] Since, Silicate Modulus, SiO_2/Na_2O = 1

Requirement quantity of SiO_2 = 1 × Na_2O quantity

= 1 × 80

= 80 gm.

[E] Quantity of Na_2SiO_3 required to get 80 gm. SiO_2

$= \frac{80\times100}{26.5}$ = 301.88 gm. Say; 302 gm

[F] Quantity of Na_2O available in Na_2SiO_3

$= \frac{302\times8}{100}$ = 24.16 gm

[G] Quantity of Na_2O required from NaOH

= (Total Na_2O required) – (Na_2O obtained from Na_2SiO_3)

= 80- 24.16

= 55.84 gm.

[H] Quantity of NaOH required to get 55.54 gm. Na_2O

$= \frac{80\times55.84}{62}$ = 72.05 gm

[I] Required quantity of NaOH pellets with 98% purity

$$= \frac{100 \times 72.05}{98} = 73.52 \text{ gm} \quad \text{say } 74 \text{ gm}$$

[J] Water available in NaOH pellets and Na_2SiO_3 solution

$$= \frac{18 \times 74}{80} + \frac{65.5 \times 302}{100} = 214.46 \text{ gm}$$

[K] Total water required per 1000 gm. of total material

Water to total material ratio = 0.33

Hence total quantity of water required = 0.33 × 1000

= 330 gm.

[L] Free water to be added

= Total water required – Water available in NaOH pellets and Na_2SiO_3 solution

= 330 – 214.46

= 115.54 gm. Say; 116 gm.

[M] Summary of Activator solution constituents for 1000 gm. of total material

NaOH pellets = 74 gm.

Na_2SiO_3 solution = 302 gm.

Free Water = 116 gm.

A2: CALCULATION FOR CONSTITUENTS OF ACTIVATOR SOLUTION KOH & Na_2SiO_3

For Activator solution having X_2O of 8% by weight of total material (base material and supplementary material) and Equivalent silicate modulus (SiO_2/X_2O) equals to 1.0

(Refer Table 3.8)

Here X refers to alkali Cation. X_2O indicates combination of Na_2O & K_2O. The term activator solution indicates combination of Sodium Silicate & Alkali Hydroxide.

[A] Reaction equation of Potassium Hydroxide

	K_2O	+	H_2O	=	2KOH	
Molar weight	(39×2) +16		(1×2) +16		2(39+16+1)	
=	94		18		112	(in gm.)

[B] Required quantity of X_2O for 1000 gm. total material

X_2O = 8 % by weight of total material

$$= \frac{8 \times 1000}{100} = 80 \text{ gm.}$$

[C] Since, Equivalent Silicate Modulus, $SiO_2/X_2O = 1$

Quantity of $SiO_2 = 1 \times X_2O$

$= 1 \times 80$

$= 80$ gm.

[D] Quantity of Na_2SiO_3 required to get 80 gm. SiO_2

$= \frac{80 \times 100}{26.5} = 301.88$ gm. Say; 302 gm.

[E] Quantity of Na_2O available in Na_2SiO_3

$= \frac{302 \times 8}{100} = 24.16$ gm.

[F] Quantity of K_2O required from KOH

= (Total X_2O required) – (Na_2O obtained from Na_2SiO_3)

= 80- 24.16

= 55.84 gm.

[G] Quantity of KOH required to get 55.54 gm. K_2O

$= \frac{112 \times 55.84}{94} = 66.53$ gm.

[H] Required quantity of KOH pellets with 84% purity

$= \frac{100 \times 66.53}{84} = 79.20$ gm. Say; 79 gm.

[I] Water available in KOH pellets and Na_2SiO_3 solution

$= \frac{18 \times 79}{112} + \frac{65.5 \times 302}{100} = 210.5$ gm.

[J] Total water required per 1000 gm. of total material

Water to total material ratio = 0.33

Hence total quantity of water required = 0.33×1000

$= 330$ gm.

[K] Free water to be added

= Total water required – Water available in NaOH pellets and Na_2SiO_3 solution

= 330 – 210.50

= 119.50 gm. Say; 120 gm.

[L] Summary of Activator solution constituents for 1000 gm. total material

KOH pellets = 79 gm.

Na_2SiO_3 solution = 302 gm.

Free Water = 120 gm.

A3: CALCULATION FOR CONSTITUENT PROPORTION OF GEOPOLYMER PASTE Fly ash + NaOH + Na_2SiO_3

For Geopolymer paste specimen GP1 (Refer Table 3.9)

[A] Activator solution composition

Na_2O = 8%

Silicate modulus (SiO_2/Na_2O) = 1.0

[B] Mix proportion for 1000 gm. of total material

In absence of supplementary material, total material equal to base material (fly ash).

Fly ash = 1000 gm.

NaOH pellets = 74 gm.

Sodium silicate solution = 302 gm.

Free water = 116 gm.

A4: CALCULATION FOR CONSTITUENT PROPORTION OF GEOPOLYMER PASTE Fly ash + NaOH + Na_2SiO_3 + supplementary material (lime stone dust)

For Geopolymer paste specimen GL1 (Refer Table 3.9)

[A] Activator solution composition

Na_2O = 8%

Silicate modulus (SiO_2/Na_2O) = 1.0

[B] Required amount of lime stone dust (supplementary material)

= 10 % of total material

$= \frac{10 \times 1000}{100}$ = 100 gm.

[C] Required amount of fly ash (base material)

= total material – supplementary material

= 1000 – 100 = 900 gm.

[D] Mix proportion for 1000gm of total material

Fly ash = 900 gm.

Lime stone dust = 100 gm.

NaOH pellets = 74 gm.

Sodium silicate solution = 302 gm.

Free water = 116 gm.

A5: CALCULATION FOR CONSTITUENT PROPORTION OF GEOPOLYMER PASTE Fly ash + NaOH + Na_2SiO_3 + supplementary material (blast furnace slag)

For Geopolymer paste specimen GB1 (Refer Table 3.12)

[A] Activator solution composition

Na_2O = 8%

Silicate modulus (SiO_2/Na_2O) = 1.0

[B] Required amount of blast furnace slag (supplementary material)

= 10 % of total material

$= \frac{10 \times 1000}{100}$ = 100 gm.

[C] Required amount of fly ash (base material)

= total material – supplementary material

= 1000 – 100 = 900 gm.

[C] Mix proportion for 1000gm of total material

Fly ash = 900 gm.

Blast furnace slag = 100 gm.

NaOH pellets = 74 gm.

Sodium silicate solution = 302 gm.

Free water = 116 gm.

A6: CALCULATION FOR CONSTITUENT PROPORTION OF GEOPOLYMER PASTE Fly ash + KOH + Na_2SiO_3

For Geopolymer paste specimen GPX1 (Refer Table 3.8)

[A] Activator solution composition

X_2O = 8%

Equivalent Silicate modulus (SiO_2/X_2O) = 1.0

[B] Mix proportion for 1000gm of total material

In absence of supplementary material, in this case total material equal to base material which is fly ash.

Fly ash = 1000 gm.

KOH pellets = 79 gm.

Sodium silicate solution = 302 gm.

Free water = 120 gm.

A7: CALCULATION FOR CONSTITUENT PROPORTION OF GEOPOLYMER PASTE
Fly ash + KOH + Na_2SiO_3 + supplementary material (Silica fume and Murram)

Geopolymer paste specimen GSC1R (Refer Table 3.18)

For Activator solution having K_2O of 8% by weight of total material (base material and supplementary material) and silicate modulus (SiO_2/K_2O) equals to 1.0

[A] Reaction equation of Potassium Hydroxide (KOH)

$$K_2O + H_2O = 2KOH$$

Molar weight $(39\times2)+16$ $(1\times2)+16$ $2(39+16+1)$

$= 94 \quad 18 \quad 112$ (in gm.)

[B] Required quantity of K_2O for 1000 gm. total material

K_2O = 8 % by weight of total material

$= \frac{8\times1000}{100} = 80$ gm.

[C] Since, Silicate Modulus, $SiO_2/K_2O = 1$

Quantity of $SiO_2 = 1 \times K_2O$

$= 1 \times 80$

$= 80$ gm.

[D] Quantity of Na_2SiO_3 required to get 80 gm. SiO_2

$= \frac{80\times100}{26.5} = 301.89$ gm. Say; 302 gm.

[E] Quantity of KOH required to get 80 gm. K_2O

$= \frac{112\times80}{94} = 95.32$ gm.

[F] Required quantity of KOH pellets with 84% purity

$= \frac{100\times95.32}{84} = 113$ gm.

[G] Water available in KOH pellets and Na_2SiO_3 solution

$= \frac{18\times113}{112} + \frac{65.5\times302}{100} = 216$ gm.

[H] Total water required per 1000 gm. of total material

Water to total material ratio = 0.33

Hence total quantity of water required = 0.33×1000

$= 330$ gm.

[I] Free water to be added

= Total water required – Water available in KOH pellets and Na_2SiO_3 solution

= 330 – 216

= 114 gm.

[J] Mix proportion for 1000 gm. of total material

Fly ash = 875 gm.

Silica fume = 100 gm.

Murram = 25 gm.

KOH pellets = 113 gm.

Sodium silicate solution = 302 gm.

Free water = 114 gm.

A8: CALCULATION FOR CONSTITUENT PROPORTION OF GEOPOLYMER PASTE
Fly ash + KOH + Na_2SiO_3 + supplementary material (Silica fume and Borax)

Geopolymer paste specimen GSCB2 (Refer Table 3.17)

For Activator solution having K_2O of 8% by weight of total material (base material and supplementary material) and silicate modulus (SiO_2/K_2O) equals to 1.0

[A] Reaction equation of Potassium Hydroxide (KOH)

	K_2O	+	H_2O	=	2KOH	
Molar weight	$(39\times2)+16$		$(1\times2)+16$		$2(39+16+1)$	
	= 94		18		112	(in gm.)

[B] Required quantity of K_2O for 1000 gm. total material

K_2O = 6 % of weight of total material

$= \frac{6\times1000}{100}$ = 60 gm.

[C] Since, Silicate Modulus, SiO_2/K_2O = 1

Quantity of $SiO_2 = 1 \times K_2O$

$= 1 \times 60$

= 60 gm.

[D] Quantity of Na_2SiO_3 required to get 60 gm. SiO_2

$= \frac{60\times100}{26.5}$ = 226 gm.

[E] Quantity of KOH required to get 80 gm. K_2O

$$= \frac{112 \times 60}{94} = 71.48 \text{ gm.}$$

[F] Required quantity of KOH pellets with 84% purity

$$= \frac{100 \times 71.48}{84} = 85 \text{ gm.}$$

[G] Water available in KOH pellets and Na_2SiO_3 solution

$$= \frac{18 \times 85}{112} + \frac{65.5 \times 226}{100} = 162 \text{ gm.}$$

[H] Total water required per 1000 gm. of total material

Water to total material ratio = 0.33

Hence total quantity of water required = 0.33 × 1000

= 330 gm.

[I] Free water to be added

= Total water required – Water available in KOH pellets and Na_2SiO_3 solution

= 330 – 162

= 168 gm.

[B] Mix proportion for 1000gm of total material

Fly ash = 900 gm.

Silica fume = 50 gm.

Borax = 50 gm.

KOH pellets = 85 gm.

Sodium silicate solution = 226 gm.

Free water = 168 gm.

APPENDIX-II

REPRINTS OF SOME PUBLISHED PAPERS

Hindawi
Advances in Civil Engineering
Volume 2018, Article ID 2940169, 12 pages
https://doi.org/10.1155/2018/2940169

Research Article

Comparative Study on the Performance of Blended and Nonblended Fly Ash Geopolymer Composites as Durable Construction Materials

Debabrata Dutta and Somnath Ghosh

Department of Civil Engineering, Jadavpur University, 188 Raja S.C. Mallick Road, Kolkata 700032, India

Correspondence should be addressed to Debabrata Dutta; ddebabrata83@gmail.com

Received 20 August 2017; Accepted 27 December 2017; Published 19 February 2018

Academic Editor: Robert Černý

This article represents that the mechanical and microstructural properties and durability of fly ash-based geopolymers blended with silica fume and borax are better than those of conventional fly ash-based geopolymers. Fly ash itself contains the sources of silica and alumina which are required for geopolymerisation. But a sufficient amount of high-reactive silica is able to rapidly initiate geopolymerisation with activation. Pure potassium hydroxide pellets and sodium silicate solution were used for preparation of alkaline activator solution. Fly ash geopolymer paste exhibited better mechanical properties in the presence of silica fume with slight portion of borax. The effect of silica fume-blended geopolymer paste on temperature fluctuation (heating and cooling cycle at certain temperatures) showed better performance than nonblended fly ash-based specimens. Durability property was evaluated by immersion of geopolymer specimens in 10% magnesium sulfate solution for a period of one year. The change in weight, strength, and microstructure was studied and compared. In the magnesium sulfate solution, a significant drop of strength to around 37.26% occurred after one year for nonblended fly ash-based specimens. It is evident that specimens prepared incorporating silica fume had the best performance in terms of their properties.

1. Introduction

Numerous studies have already been done on fly ash-based geopolymers, as fly ash contains large amounts of silica and alumina. It is also clear that the reaction process basically involves alkaline activation of the source material by alkali hydroxide and sodium silicate solution followed by heat curing [1]. Again, this material exhibits good strength and durability when compared to conventional concrete [2]. The geopolymer chemistry elaborates the formation of 3D polymeric chain by Si–O–Al–O bond during the reaction between the source material rich in silica and alumina [3]. But the chemistry of geopolymers is altered for different combinations of raw material and alkalis [4]. The higher viscosity of the activator interferes with the rheological characteristics of the geopolymers. Thus, the porosity of geopolymers increases for finer precursor materials [5]. Inclination is needed towards several disposals over fly ash as the supplemental material in geopolymers like silica fume. Silica fume is a very fine material (particle size ranging from 1 μm to 15 μm). The basic problem in using silica fume as a base material for geopolymers is the absence of aluminium (trivalent in character). This phenomenon may be overcome with two different alternatives. The primary one is the choice of an activator, and the second one is the intrusion of secondary material. The choice of an activator is subjected to specific chemistry. Higher presence of monomers and dimers which exists during dissolution of Al–Si appreciates sodium hydroxide for better stabilization. Again, for larger silicate oligomers, potassium hydroxide is preferred for better coordination [6]. Latest research exhibits typical geopolymer varieties from simple to multiple phases. In the present research, silica fume was incorporated in fly ash-based geopolymers. Commercial borax (like substitute of aluminium) was used as another secondary input in the mixture. Borax arises in nature as evaporated dump formed by the continual evaporation of seasonal lakes. The effectiveness of

the pioneer composite was studied by comparing typical parameters like strength and durability with traditional fly ash-based geopolymers.

2. Chemistry of the Study

Fly ash activated with sodium hydroxide sometimes creates cracks with aging [7]. It is because of continuous pore pressure developed within the hardened composite by the late precipitated alkali compound [7]. However, at the initial level, it shows successive strength gaining for the time being [7]. On the contrary, potassium hydroxide is better for developing stable structures only under higher concentration of sodium silicate [8]. Earlier studies depict that despite having the same electric charges, the Na^+ and K^+ act in a different way because of dissimilar size. The smaller cation favors the ion-pair reaction with the smaller silicate oligomers, like silicate monomers, dimers, and trimers [9–11]. Xu et al. observed that the smaller silicate oligomers like monomers and dimer are better stabilized by Na^+ (sodium ion) and result in higher extent of dissolution, whereas more silicate solution emphasizes larger silicate oligomers which can be better coordinated by K^+ cation of larger size [6]. The previous study showed stable compressive strength for fly ash-based geopolymers activated with potassium hydroxide with higher concentration of sodium silicate [12]. The major drawback of this geopolymer composite is the rise in water content in the mixture. The higher amount of sodium silicate in fact allows the presence of additional water embedded within it. Consecutively, additional water makes the structure more porous, lesser in weight, and mainly permeable to some extent. Based on the discussed theory, a suitable compensator of sodium silicate has been evaluated in this study where silica fume has been introduced as the primary source of reactive silica to initiate the faster reaction. The presence of a higher oligomer in the chemical environment is favorable for the purpose of using potassium as the charge compensator or system stabilizer. Geopolymer is a Si–O–Al–O tetrahedral frame structure. But rise in the ratio of Si to Al may insist the formation of a chain-like structure over frame structure. So, another secondary input borax (B) has been typically applied in a manner to maintain the Si/X ratio, where X = Al or B, considering that both have three valence electrons. Another cause of choosing borax in this study is specifically to enhance the X content without allowing further incorporation of additional silica.

3. Experimental Procedure

3.1. Materials. The materials used in this research were class F fly ash (ASTM C618) produced by Kolaghat Thermal Power Plant, India; silica fume supplied by Oriental Trexim Pvt. Ltd., India; and commercial borax collected from DRD Educational & Consultancy Pvt. Ltd., India. In fly ash, 78% of the particles were finer than 45 microns with Blaine's specific surface area equal to 380 m^2/kg. The BET surface area of silica fume was 18,900 m^2/kg. Commercial borax had specific gravity and BET surface area equal to 1.7 and 557 m^2/kg, respectively. Potassium hydroxide pellets and sodium silicate solution were collected from Loba Chemie Limited, India.

3.2. Specimen Preparation. Alkaline activator was prepared by dissolving potassium hydroxide pellets directly into water. The dissolved hydroxide pellets were left at room temperature for 24 hrs. After that, predetermined quantity of sodium silicate solution was added 3 hours before being used for mixing as done earlier [13]. In the activator solution, the K_2O content was maintained at 6% of the total base material plus supplementary material (fly ash, silica fume, and borax). Apparent silicate modulus (SiO_2/K_2O) was kept as 1 and 0.1. Originally, silicate modulus in the activator has to be calculated from the formulation ($SiO_2/(K_2O + Na_2O)$). In this case, apparent silicate modulus is taken earlier for easier calculation. It is already described that Na^+ is essentially required to promote monomers, dimers, and trimers in the starting of activation. Here, a slight amount of sodium silicate solution was added in some cases only to confirm the presence of Na^+ in the mixture. The mixture was prepared in the model P660 Hobart mixer of capacity 600 cc and speed 60 cps. Fly ash with activator solution was mixed for 5 minutes. For blended mixtures, fly ash with supplementary material was mixed with activator solution for 5 minutes. The mixture was then transferred into a cubical mould and subjected to a table vibration for 2 minutes to expel entrapped air. After 60 minutes of rest period in open air, the cubes were cured in a hot air oven for a period of 48 hours at 85°C and allowed to cool inside the oven after that. The scanning electron micrographs and chemical composition of fly ash, silica fume, and borax are represented in Figure 1 and Table 1, respectively. The mix proportions of six sample mixes are elaborated in Table 2.

3.3. Test Details

3.3.1. Strength Test. Compressive strength of the specimens was tested by digital compression testing machine of model number EM500 supplied by Enkay Enterprise. The least count was 0.001 kN. The compressive strength of cube specimens was done as per ASTM C109.

3.3.2. Exposure Test in Sulfate Solution. Experimental setup was prepared to investigate the performance of blended and non-blended fly ash-based geopolymer samples in 10% concentration of magnesium sulfate solutions for one year. The test specimens (cubical) were immersed vertically in a glass pan. After immersion, the water level was maintained at 4 cm-5 cm over specimens. Throughout the exposure, regular investigations on physical appearance, residual strength, and weight changes were monitored at preselected intervals.

3.3.3. Physical Changes and Optical Microscopy. At preset intervals, the exposed geopolymer specimens were removed from the solutions and observed for any remarkable changes in its physical appearance. A crack detection microscope WF 10x, manufactured by C&D (Micro services) Ltd. (U.K.) was

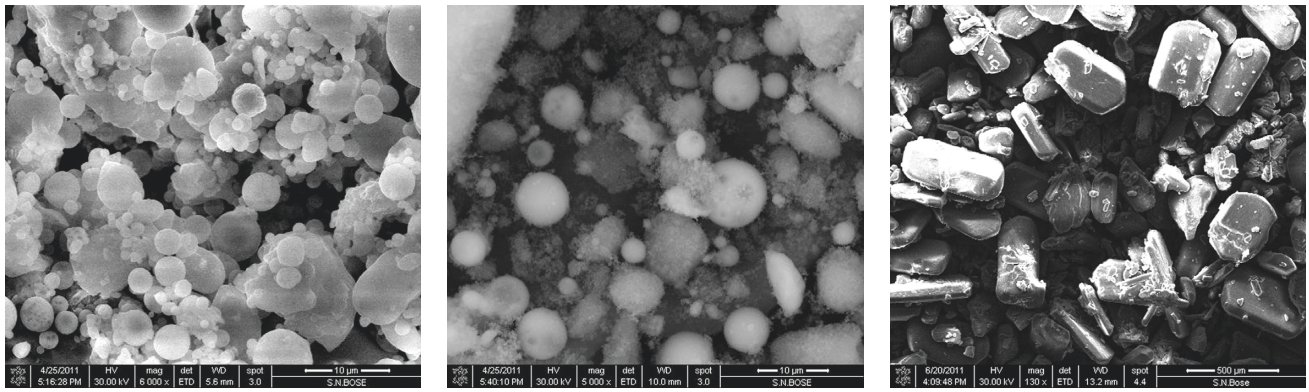

(a) (b) (c)

Figure 1: Scanning electron microscopic images of (a) fly ash, (b) silica fume, and (c) borax.

Table 1: Chemical composition of different raw materials (quantity in %).

Chemical composition	SiO_2	Al_2O_3	Fe_2O_3	TiO_2	CaO	MgO	K_2O	Na_2O	SO_3	P_2O_5	B_2O_3	LOI (%)
Fly ash	56.01	29.8	3.58	1.75	2.36	0.30	0.73	0.61	Nil	0.44	Nil	0.44
Silica fume	92.00	0.46	1.60	Nil	0.29	0.28	0.61	0.51	0.19	Nil	Nil	1.00
Borax	Nil	Nil	1.0	Nil	Nil	Nil	Nil	17.0	1.0	Nil	59.00	22.08

Table 2: Mix proportions of geopolymer mixes.

Sample ID	Fly ash* (%)	Silica fume* (%)	Borax* (%)	K_2O content in activator (%)	SiO_2 content in activator (%)	Water* (%)
SMF1	100	0	0	6	6	33
SMF2	100	0	0	6	0.6	33
SMS1	90	10	0	6	6	33
SMSB1	90	7.5	2.5	6	6	33
SMSB2	90	5.0	5.0	6	6	33
SMSB3	90	5.0	5.0	6	0.6	33

*This is the percentage amount with respect to the total weight of fly ash, silica fume, and borax. Calculated as the % of (fly ash + silica fume + borax); measured by weight.

used to detect the surface changes of the specimens at preset intervals throughout the exposure period. Observations on unexposed samples were conducted for making comparison with exposed samples.

3.3.4. Change in Weight. Before immersion in saline water, every specimen was kept submerged in potable water for 1 hour. After that, the samples were taken out and weighed. This measured weight value was indicated as the primary weight for individual. Specimens were weighed after every preselected interval. Before weighing, the specimens were clothed and brushed out to remove the free water and needle-like outcome (if any). Here, simple scrub brushes and cotton cloth were used for cleaning. Every specimen was brought to a saturated surface dry condition by applying mild airflow over the specimens for 5 minutes. Digital electronic balance of least count equal to 0.001 gm was used to conduct weighing. Change in weight indicates the percentage change (increment or decrement) with respect to the primary data at different intervals.

3.3.5. Change in Strength and Residual Strength. The average strength of any defined series of sample before the first immersion in the setup was treated as the primary strength value for specimens. A set of ten samples of different series were subjected to strength test at preselected intervals. Before testing, the specimens were kept at room temperature under airflow for 24 hrs. Digital electronic balance of least count equal to 0.001 gm was used to conduct weighing. The percentage change in strength (+/−) with respect to the primary strength value at different intervals is evaluated. The residual strength indicates the percentage of strength achieved at different intervals to the primary strength value. The residual strength at any interval is expressed as "100 − percentage change in strength."

3.3.6. Thermal Fluctuation Setup. A chest freezer of Model No. VT3-NUCAB 400L with glass-top configuration supplied by Hindustan Unilever, India, has been used in this study. The temperature fluctuating domain is limited from 8°C to −20°C. Each specimen was subjected to 20 consecutive

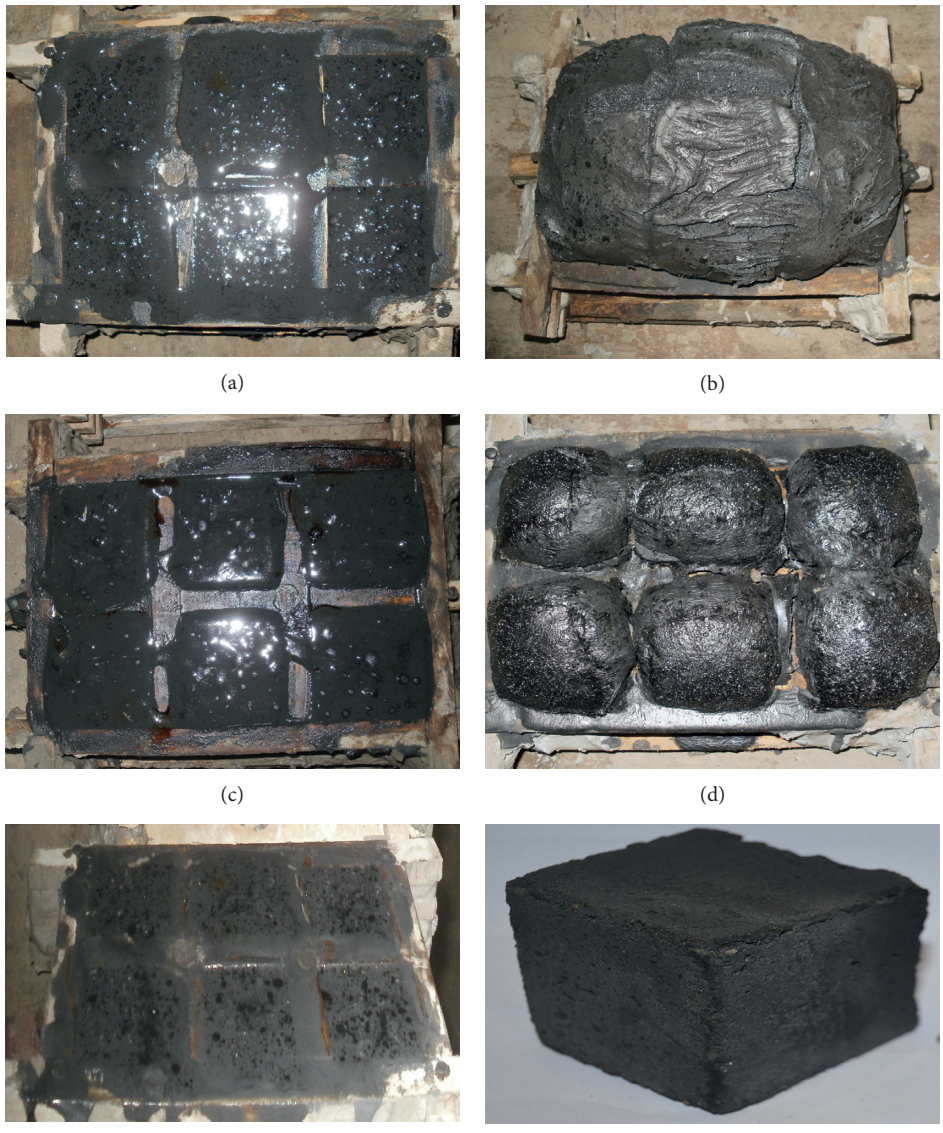

Figure 2: Physical appearance of the samples: (a, b) SMS1, (c, d) SMSB1, and (e, f) SMSB2.

cycles for a program of almost 85 hours. At the initial phase, the specimens were allowed to cool at 8°C for 2 hours. After that, it was brought to −20°C for the immediate next 2 hours. The temperature change rate was reported almost as 2°C/minute.

3.3.7. Scanning Electron Microscopy. Scanning electron microscopy was conducted by QUANTA 2000 with a capacity of 2.4 nm at 30 kV at high vacuum condition. The geopolymer sample was collected as a small scrap form to conduct this study. Samples with irregular shape were collected at the time of crushing. For the research, scraps were collected from the inner part of the specimen under consideration. No further grinding or polishing was done for SEM analysis.

3.3.8. Mercury Intrusion Porosimetry. MIP samples were made by cutting a cylinder of ¼ in. diameter to ½ in. height, having a bulk sample volume of 1.00 cc, which were tested on Micromeritics Autopore II (Central Glass and Ceramic, India) from 0 to 60,000 psi, with Hg surface tension 480.00 erg/cm^2 and contact angles (I) 140.00° and (E) 140.00°. MIP was used to examine a statistical comparison of the tested samples in terms of mean and median pore size, pore distribution, total porosity, bulk density, and apparent density. The bulk volume of each test specimen was 1 cc, and the maximum applied intrusion pressure during the test was about 53,500 psi. In this method, mercury is intruded under pressure in an evacuated sample, and volume of intruded mercury is monitored against pressure. In the feature of this very test, the pore volume distribution over pore diameter is presented as a distribution function $F = -dV/d \log D$, where V is the collective pore volume and D the diameter of pores. It indicates that the part under

Table 3: Compressive strength at 3 days after heat curing.

Number	Sample ID	Compressive strength (MPa) at 3 days after heat curing
1	SMF1	14.25
2	SMF2	0.0
3	SMS1	—
4	SMSB1	18.62
5	SMSB2	29.05
6	SMSB3	28

a function of any pore diameter range capitulates pore volume of pores in that range.

3.3.9. Energy Dispersive X-Ray Analysis. Energy dispersive X-ray analysis was carried on a point of selected samples for SEM under QUANTA FEG 250. The geopolymer sample was collected as a small scrap form to conduct this study.

4. Results and Discussion

4.1. Physical Appearance. Excessive volumetric increment was observed for sample SMS1 (Figure 2). As silica fume is very reactive, it emphasizes the formation of dihydrogen by oxidation of free silicon by water of alkaline medium during synthesis [14]. In alkali-activated fly ash-based geopolymers, the purpose of sodium silicate is to start the polymerization at the earlier stage [13]. But, for blended geopolymers, silica fume helps the formation of in situ inorganic foam itself at the initial stage [14]. The volumetric enlargement of SMS1 was due to the increment in dihydrogen production by water in the presence of reactive silica fume. Further, the addition of external borax can better stabilize the structure macroscopically. Borax can play the role of alumina in a similar manner to compensate the additional requirement of alumina due to the presence of much reactive silica from silica fume.

4.2. Compressive Strength. At hardened state, compressive strength is considered as the characteristic material value for the identification of the structural feature. Table 3 presents the mean compressive strength of the six samples measured in digital compressive strength testing equipment. In this study, the noticeable feature was visualized in absence of sodium silicate for fly ash-based geopolymer SMF2. Figure 3 shows the disintegrated part of partially reacted geopolymer SMF2. Sample SMSB1 had almost a shape of fungus mushroom, where a swelled top has risen upon the perfect cube base. The swelled portion was cut out by using an electrically operated low-speed concrete saw cutter to obtain a perfect cube. Excessive swelling was observed for sample SMS1. Extrication of any right cubical unit from the honeycombed, asymmetrical, and distorted outcome of sample SMS1 was not possible. Because of that, sample SMS1 was not supportive for the measurement of compressive strength in test setup.

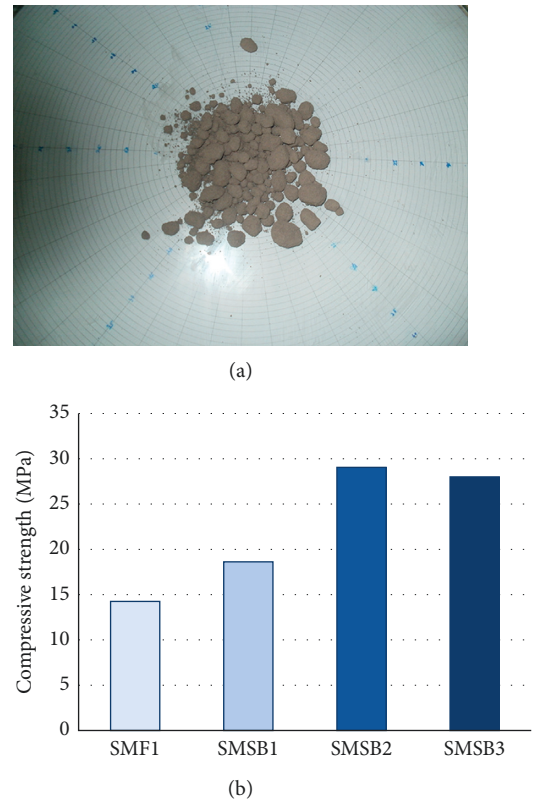

Figure 3: (a) Sample SMF2 after mixing and (b) compressive strength at the third day after curing.

Fly ash activation in the presence of external silica fume and borax sources yields a better geopolymer. Successive betterment in compressive strength was observed with the incorporation of silica fume and borax in certain percentage in the composition. Another important finding was that lowering of sodium silicate in mixing had little to no effect in polymerization or condensation process of silica fume-blended geopolymers (as treated for SMSB3). Maximum compressive strength was obtained for SMSB2 (29.05 MPa).

4.3. Thermal Fluctuation Effect. For a hardened geopolymer, it can be assumed that the most thermal sensitive part within the geopolymer composite is the crystalline alkali precipitation. In Figures 4(a) and 4(b), the regular crystal structure within the pore indicates the presence of alkali. Point A indicates alkaline surplus within the pores of the geopolymer body for fly ash-based geopolymers. In Figure 5, EDAX shows the existence of sodium-based alkaline precipitation, at point A. This entrapped crystal compound is basically due to the late and less reaction. In fact, alkali hydroxide is essential for the dissolution of silica and alumina. The metallic cations (Na, K, and others) maintain the structure neutrality as aluminium has fourfold coordination. But, alkali metal hydroxide which acts as a catalyst expelled out during the hardening of the gel phase with the progression of reaction [15]. In this research, it is supposed that incorporation of

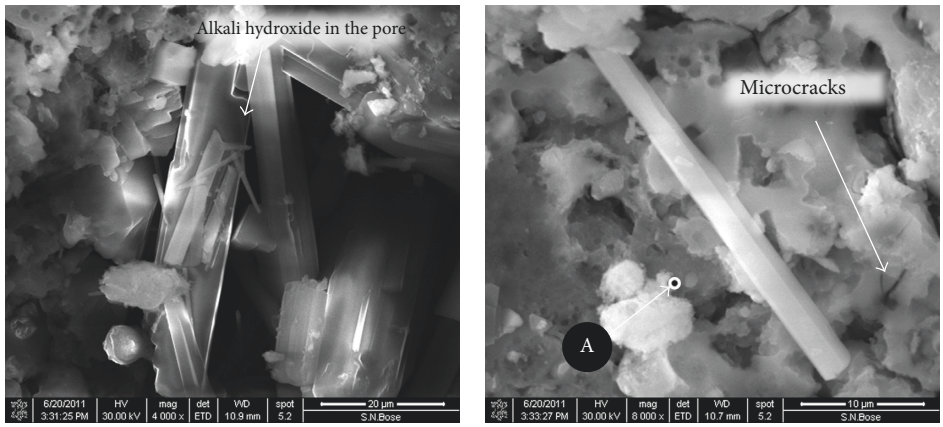

(a) (b)

Figure 4: (a) Crystal structure within SMF1. (b) After fatigue exposure, microcracks in SMF1.

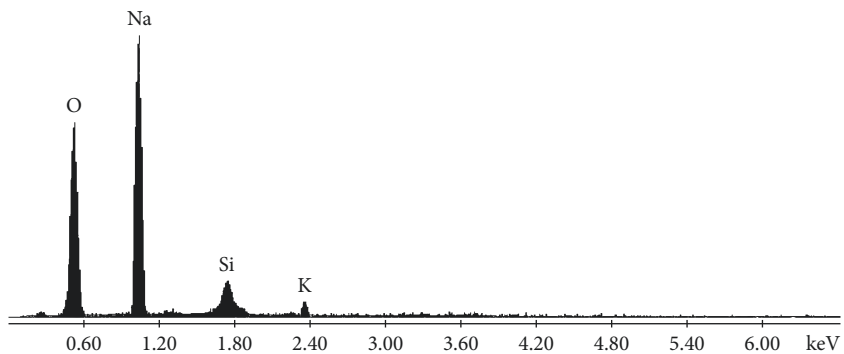

Figure 5: EDAX analysis at the position near A.

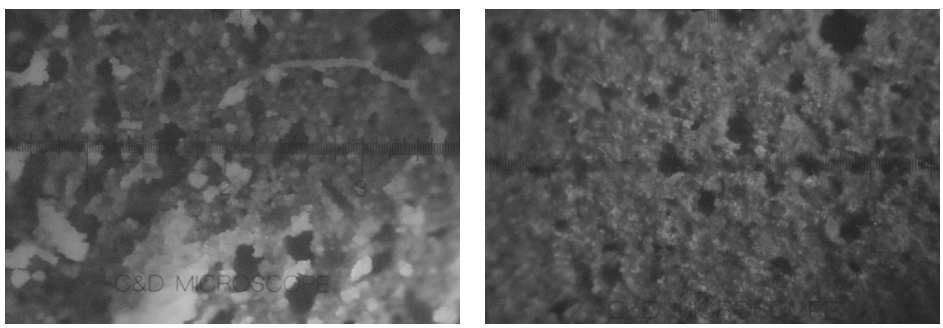

(a) (b)

Figure 6: Optical microscopy (10x magnification). Sample SMF1 (a) and sample SMSB2 (b) after 30 days.

silica fume emphasizes the speed of reaction which allows the expulsion of metal hydroxide instantaneously. The existence of the entrapped alkaline entity in the nonblended composites after hardening possibly resulted from the slower rate of reaction. Now, the temperature fluctuation affects the volumetric change of alkali solution within the pore. This can cause remarkable fatigue on the geopolymer skeleton and successive crack formation (as shown in Figure 4(b)). The result shows failure for sample SMF1 at the end of temperature fluctuating cycles.

4.4. Efflorescence Behavior (Study at Micro- and Macrolevel). Geopolymer efflorescence is the outcome from the geopolymer body which is highly alkaline. The charge compensator alkali hydroxide basically extrudes from the pores with the process of synthesis or the formation of Si–O–Al. Basically, alkali metal hydroxide acts as a catalyst, but almost the same amount which is added during synthesis is leached out from the hardened structure [15]. Moderate amount of late leaching was noticeable for sample SMF1 under optical microscopy (as shown in Figure 6(a)). But silica

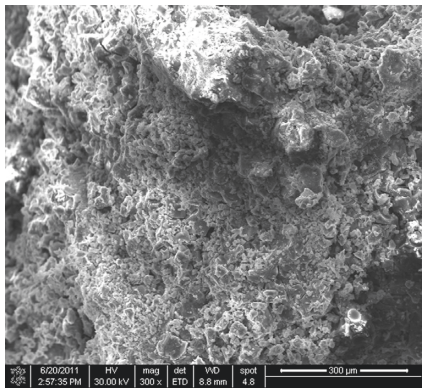

(a)

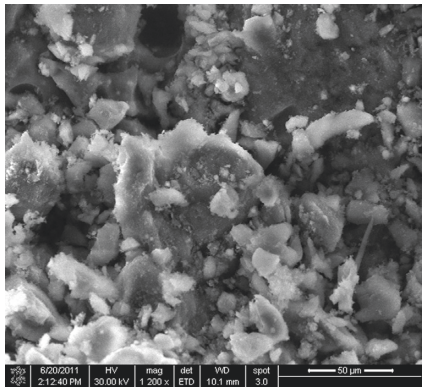

(b)

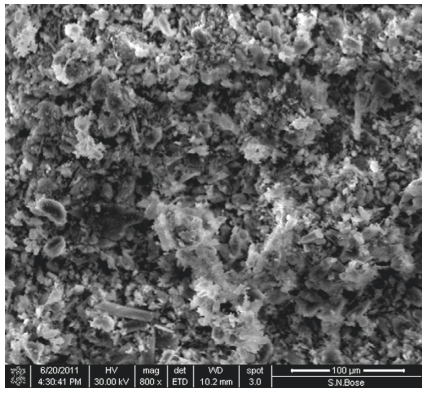

(c)

Figure 7: (a) Outer surfaces of sample SMF1 at 3 days (a), 30 days (b), and 60 days (c) from the end of heat curing.

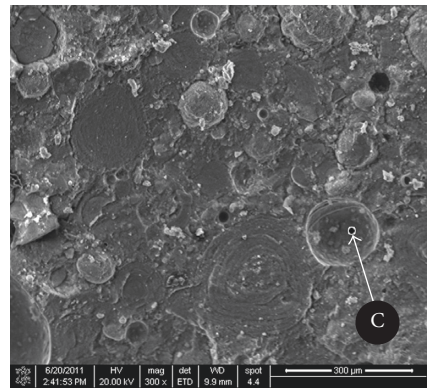

(a)

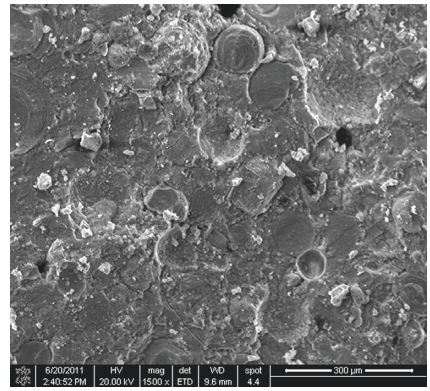

(b)

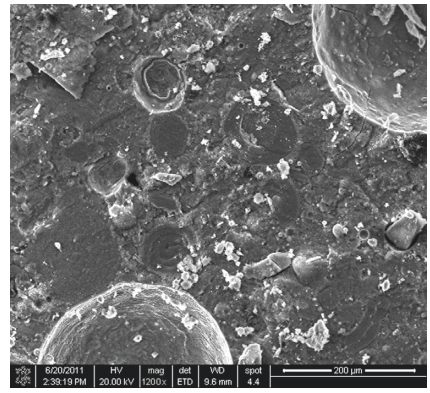

(c)

Figure 8: (a) Outer surfaces of sample SMSB2 at 3 days (a), 30 days (b), and 60 days (c) from the end of heat curing.

fume-blended geopolymers did not exhibit such characteristics (as shown in Figure 6(b)). It is because of the presence of silica fume which makes a very reactive complex and compact structure. Generally, the application of sodium silicate initializes the primary polymerization, but for the blended mix, this role is almost taken by the reactive silica fume [16]. Excessive leaching was observed under scanning electron microscopy for sample SMF1 with aging. Figures 7(a)–7(c) represent the SEM images of sample SMF1 at the age of 3, 30, and 60 days. The sample SMSB2 did not show excessive leaching with aging. Figures 8(a)–8(c) show compact and intact structure supporting strong alkali silicate reaction product as defined by point *C* in Figure 8(a).

4.5. Durability Study in Magnesium Sulfate Exposure. Samples SMF1, SMS1, SMSB1, SMSB2, and SMSB3 were immersed in 10% magnesium sulfate solution for 12 months. The methodology was the same as Thokchom et al. taken earlier [17]. At a preselected interval, the physical appearance of geopolymer specimens was examined. Elongated needle-like crystal formation began appearing on the surfaces of sample SMF1 after few weeks (as shown in Figure 9(a)).

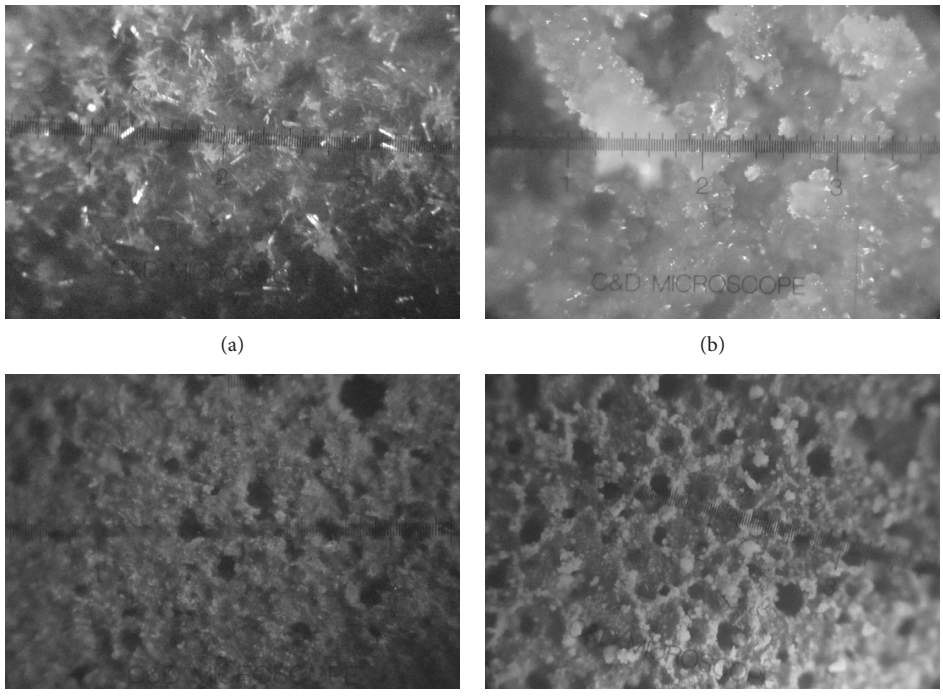

Figure 9: (a) Sample SMF1 showing a needle-like structure after 1 month of exposure to magnesium sulfate solution (optical microscope at 10x magnification). (b) Sample SMF1 showing white precipitant after 6 months of exposure to magnesium sulfate solution (optical microscope at 10x magnification). (c) Sample SMSB2 showing the fresh surface after 1 month of exposure to magnesium sulfate solution (optical microscope at 10x magnification). (d) Sample SMSB2 showing very little precipitants on the surface after 6 months of exposure to magnesium sulfate solution (optical microscope at 10x magnification).

These images of surfaces of the specimens were observed under an optical microscope with a magnification of 10x. After 12 weeks of exposure in 10% magnesium sulfate solution, sample SMF1 showed needle-like elongated crystal formation. It is due to the reaction of alkali hydroxide (within the pores) with magnesium sulfate, which forms less-soluble magnesium hydroxide with precipitation of alkali sulfate. White precipitant in larger quantity was observed for sample SMF1 after 6 months (as shown in Figure 9(b)), which may be magnesium hydroxide with sodium sulfate. Again, it was confirmed through scanning electron microscopy (as shown in Figures 10(a) and 10(b)) and EDAX analysis (as shown in Figure 10(c)) of scrap taken from the inner part of the sample. This outcome was the basic cause behind the drop in weight and strength after 9 months for sample SMF1. Bakharev [18] reported that the loss of strength is due to the migration of alkalis from the specimens and also due to the diffusion of calcium and sulfur near the surface region. But samples SMSB2 and SMSB3 did not show any formation at the outer surface for the time being during sulfate exposure (as shown in Figures 9(c) and 9(d)).

4.6. Change in Weight and Residual Strength. The result shows a remarkable increment in the weight of the non-blended samples exposed to magnesium sulfate solution at room temperature up to 3 months (Figure 11(a)). The similar trend was observed for compressive strength (Figure 11(b)). But materials blended with silica fume and borax did not show any remarkable change in connection with weight and strength. As mentioned earlier, the entrapped alkali within the pores of geopolymers participates in the ionic transaction in the presence of magnesium sulfate. This phenomenon has a great impact on the change in weight and strength for the time being during sulfate exposure. Again, the volumetric change within the pores enhances the pore pressure. This may be treated as the initial cause of strength increment. But later on, this continuous change in volume (compound within the pore) deteriorates the polymer structure. Due to the lack of the presence of the untreated hydroxide within the pore, silica fume-based geopolymers did not exhibit in this manner. The drop in compressive strength of sample SMF1 was around 37.26%. But there was almost no such change for SMSB2. The detail of change in weight and strength at different times of exposure to sulfate solution (as a percentage of primary value) is plotted in Figures 11(a) and 11(b), respectively. The figures indicate a noticeable drop from the primary values in connection with weight and strength for the SMF1 specimen.

The results of volume intrusion of the MIP of geopolymers are shown in Figure 12. The volume intrusion down to 1 micrometer was indicated for sample SMSB2. The results of volume intrusion of samples clearly reflect the change in chemistry with the change in the constituent materials. The

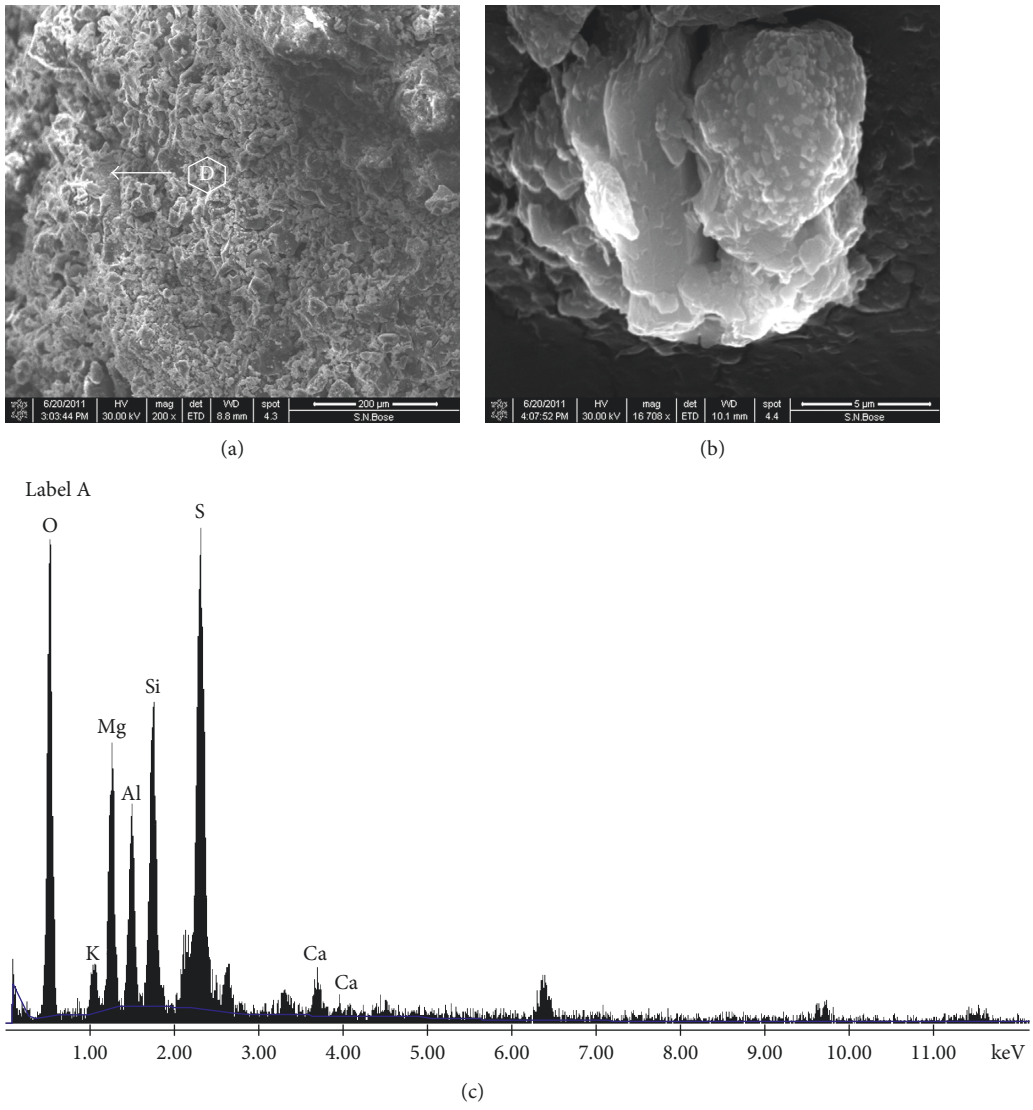

Figure 10: (a) Sample SMF1 showing white precipitant at the inner surface after 3 months at 200x magnifications. (b) SEM analysis near point D at 16708x magnification. (c) EDAX analysis at point D.

fine silica fume with high surface area eased the dissolution of silica which resulted in higher rate of reaction and produced denser matrix with higher compressive strength. Reactive silica fume significantly produced higher percentage of larger pores with a lower limit greater than 10 micrometers (the specimens SMS1 and SMSB1). The study reveals that geopolymer is a tetrahedral aluminosilicate structure. This structure (Al–O–Si) consisting of aluminium and silica is interlinked tetrahedrally by allotting alternate oxygen atoms. But based on the Si/Al atomic ratio, the geopolymeric aluminosilicate structure diverges in different families from amorphous to semicrystalline frameworks like polysialate type (Si–O–Al–O–), polysialate-siloxo type (Si–O–Al–O–Si–O–), and polysialate-disiloxo type (Si–O–Al–O–Si–O–Si–O–) [19]. For samples SMS1 and SMSB1, the excessive rise in Si/Al ratio (due to the incorporation of reactive silica supplements) may insist the possible formation of Si–O–Si chain structure rather than any framework structure. However, sample SMSB2 again tends to form framework structure because of the presence of borax containing boron (B). Here, the role of aluminium (Al) is compensated by boron (another fourfold). The difference in pore morphology must signify the change in structural formation.

Figure 12(d) illustrates the curve located within a small area for SMSB2. This indicates that the silica fume-blended geopolymers in the presence of borax reduces the mean pore size. Also, the threshold volume intruded values for the nonblended geopolymer SMF1 are larger than other silica-blended specimens. Thus, the reduced total volume of porosity and better pore size distribution contribute to the strength development.

5. Conclusions

Based on the experimental investigation, it is concluded that silica fume-blended fly ash-based geopolymers leads

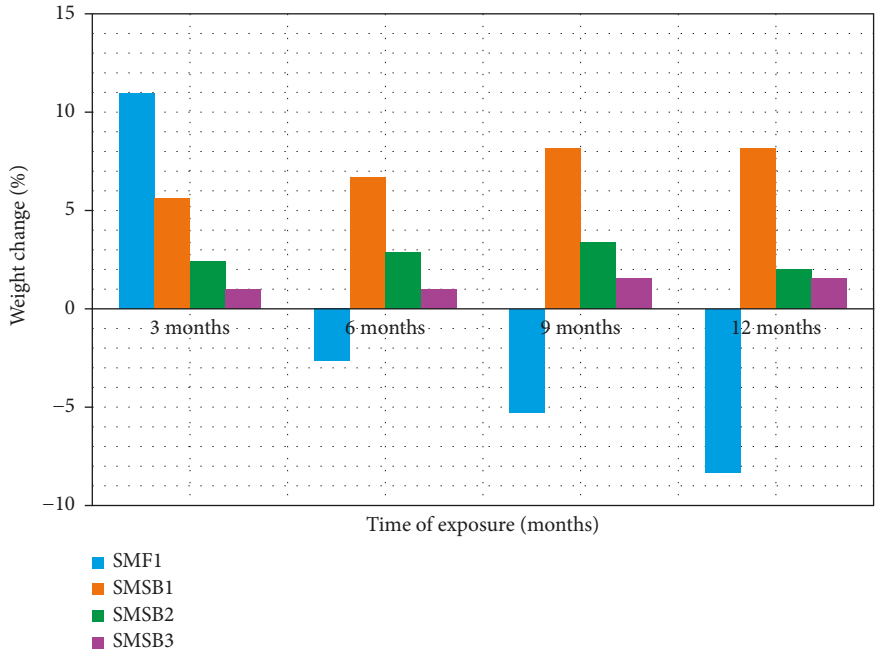

(a)

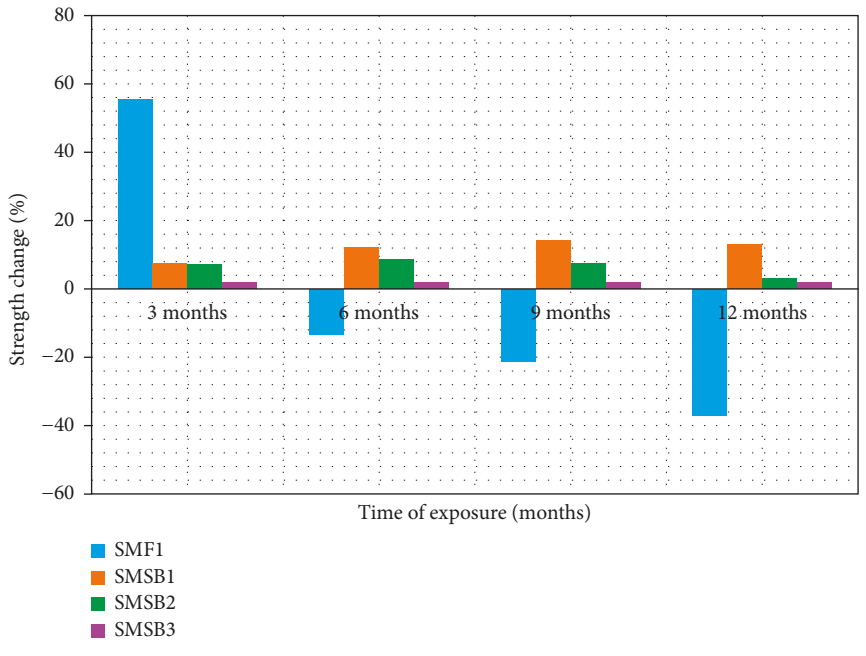

(b)

Figure 11: Percentage gain or loss in (a) weight and (b) strength with time of exposure to magnesium sulfate.

to a new trend which appears to generate more amorphous products and accelerates the rate of reaction in lower alkalinity. Sample SMSB3 (activated with very low value of sodium silicate) showed the compressive strength of 28 MPa after just 3 days, which is 96.49% greater than the compressive strength of sample SMF1. The maximum compressive strength (29.05 MPa) was obtained for SMSB2 (90% fly ash, 10% silica fume, and 5% borax-made specimens). Almost no efflorescence was observed for sample blended with silica fume in the presence of borax. Temperature fluctuation has little to no effect in microstructure and mechanical properties of silica fume and borax-blended geopolymers when compared to the geopolymer produced from only fly ash. The resistance to sulfate attack for silica fume and borax-blended geopolymers was excellent and almost stable in connection with weight and strength change. The threshold values of the intruded volume pore sizes and distribution confirm dense

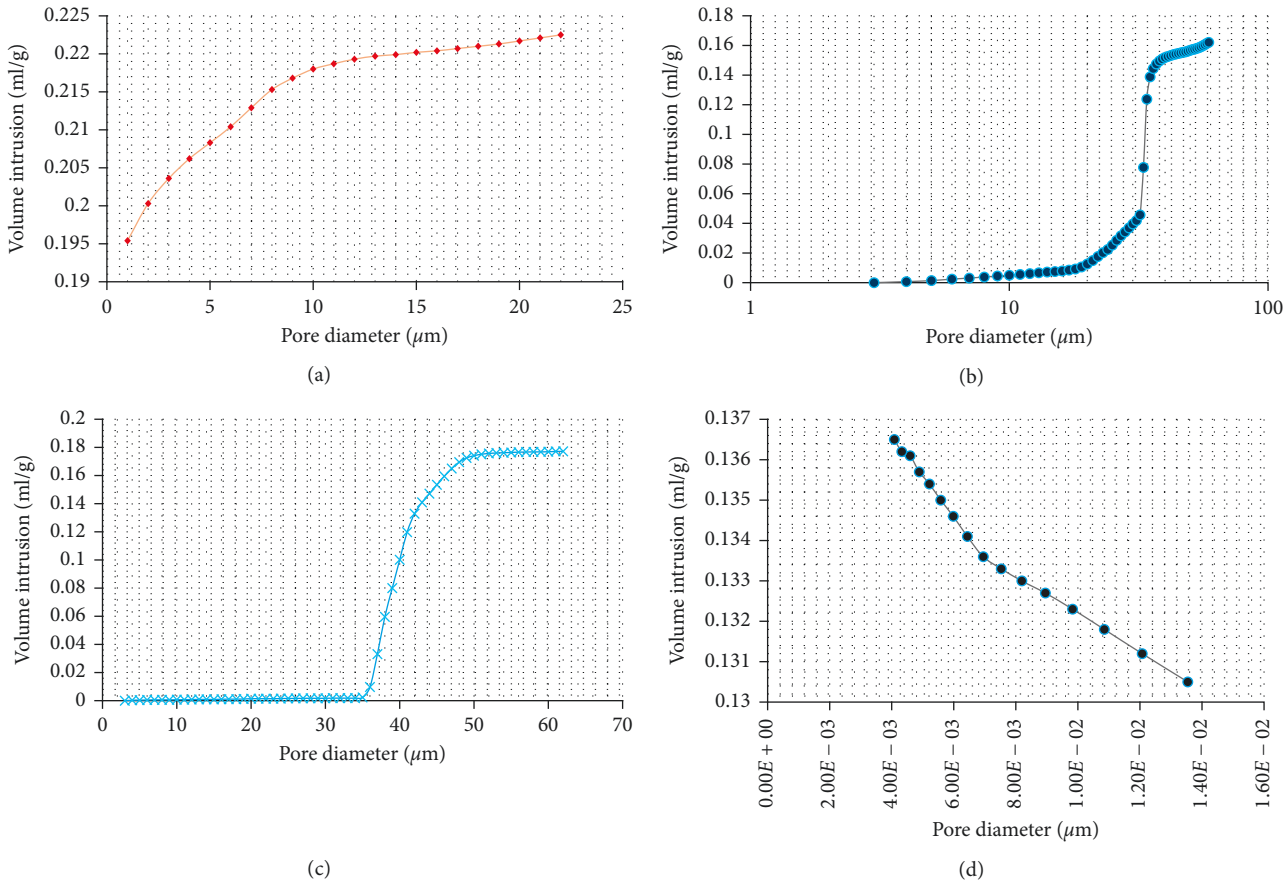

Figure 12: Intruded volume of MIP of geopolymers. (a) Sample SMF1, (b) sample SMS1, (c) sample SMSB1, and (d) sample SMSB2.

microstructure for silica fume and borax-incorporated fly ash-based geopolymers.

Conflicts of Interest

The authors declare that they have no conflicts of interest.

References

[1] J. G. S. van Jaarsveld, J. S. J. van Deventer, and G. C. Lukey, "The effect of composition and temperature on the properties of fly ash- and kaolinite-based geopolymers," *Chemical Engineering Journal*, vol. 89, no. 1–3, pp. 63–73, 2002.

[2] T. Bakharev, J. G. Sanjayan, and Y. B. Cheng, "Resistance of alkali-activated slag concrete to acid attack," *Cement and Concrete Research*, vol. 33, no. 10, pp. 1607–1611, 2003.

[3] E. I. Diaz, E. N. Allouche, and S. Eklund, "Factors affecting the suitability of fly ash as source material for geopolymers," *Fuel*, vol. 89, no. 5, pp. 992–996, 2010.

[4] E. P. Marinho, *Desenvolvimento de Pastas Geopoliméricas Para Cimentação de Postos de Petr´oleo*, Universidade Federal do Rio Grande do Norte, BrazilUniversidade Federal do Rio Grande do Norte, 2004 Ph.D. thesis, Thesis.

[5] P. H. R. Borges, L. F. Fonseca, V. A. Nunes, T. H. Panzera, and C. C. Martuscelli, "Andreasen particle packing method on the development of geopolymer concrete for civil engineering," *Journal of Materials in Civil Engineering*, vol. 26, no. 4, pp. 692–697, 2014.

[6] H. Xu and J. S. J. van Deventer, "The geopolymerisation of aluminosilicate minerals," *International Journal of Mineral Processing*, vol. 59, no. 3, pp. 247–266, 2000.

[7] D. Dutta and S. Ghosh, "Microstructure of fly ash geopolymer paste with blast furnace slag," *Current Advances in Civil Engineering*, vol. 2, no. 3, pp. 95–101, 2014.

[8] D. Dutta and S. Ghosh, "Parametric study of geopolymer paste with the different combination of activators," *International Journal of Engineering Innovation & Research*, vol. 3, no. 6, pp. 786–793, 2014.

[9] A. V. Mc Cormick, A. T. Bell, and C. J. Radke, "Evidence from alkali metal NMR spectroscopy for ion pairing in alkaline silicate solution," *Journal of Physical Chemistry*, vol. 93, no. 5, pp. 1733–1737, 1989.

[10] W. M. Hendricks, A. T. Bell, and C. J. Radke, "Effect of organic and alkali metal cations on the distribution of silicate anions in aqueous solutions," *Journal of Physical Chemistry*, vol. 95, no. 23, pp. 9513–9518, 1991.

[11] T. W. Swaddle, J. Salerno, and P. A. Tregloan, "Aqueous aluminates, silicates and aluminosilicates," *Chemical Society Reviews*, vol. 23, no. 5, pp. 319–325, 1994.

[12] D. Dutta, S. Chakrabarty, C. Bose, and S. Ghosh, "Comparative study of geo-polymer paste prepared from different activators," *STM Journals*, vol. 2, pp. 1–10, 2012.

[13] S. Thokchom, P. Ghosh, and S. Ghosh, "Durability of fly ash geopolymer mortars in nitric acid–effect of alkali (Na_2O) content," *Journal of Civil Engineering and Management*, vol. 17, no. 3, pp. 395–399, 2011.

[14] E. Prud'homme, P. Michaud, E. Joussein et al., "Silica fume as porogent agent in geo-materials at low temperature," *Journal of the European Ceramic Society*, vol. 30, no. 7, pp. 1641–1648, 2010.

[15] J. S. G. van Jaarsveld, J. S. J. van Deventer, and L. Lorenzen, "Factors affecting the immobilization of metals in geopolymerized fly ash," *Metallurgical and Materials Transactions, B*, vol. 29, no. 1, pp. 283–291, 1998.

[16] J. T. Gourley, "Geopolymers, opportunities for environmentally friendly construction materials," in *Proceedings of Conferenc in adaptive materials for a modern society*, vol. 49, 15–26, pp. 1455–1461, Institute of Materials Engineering Australia, Sydney, Australia, October 2003.

[17] S. Thokchom, D. Dutta, and S. Ghosh, "Effect of incorporating silica fume in fly ash geopolymers," *World Academy of Science, Engineering and Technology*, vol. 60, pp. 245–247, 2011.

[18] T. Bakharev, "Durability of geopolymer materials in sodium and magnesium sulfate solutions," *Paste and Concrete Research*, vol. 35, no. 6, pp. 1233–1246, 2005.

[19] J. Davitovits, "Geopolymers: inorganic polymeric new materials," *Journal of Thermal Analysis*, vol. 37, no. 8, pp. 1633–1656, 1991.

THE ROLE OF DELAYED WATER CURING IN IMPROVING THE MECHANICAL AND MICROSTRUCTURAL PROPERTIES OF ALKALI ACTIVATED FLY ASH BASED GEOPOLYMER PASTE BLENDED WITH SLAG

Journal:	*World Journal of Engineering*
Manuscript ID	WJE-03-2018-0103.R6
Manuscript Type:	Research Paper
Keywords:	GGBS, Fly Ash, Water curing, Microstructure, Aging period, Geopolymer

World Journal of Engineering

Decision Letter (WJE-03-2018-0103.R6)

From: syz@hebeu.edu.cn

To: ddebabrata83@gmail.com, dduttaddutta@gmail.com

CC:

Subject: World Journal of Engineering - Decision on Manuscript ID WJE-03-2018-0103.R6

Body: 21-Jun-2018

Dear Mr. Dutta:

It is a pleasure to accept your manuscript entitled "THE ROLE OF DELAYED WATER CURING IN IMPROVING THE MECHANICAL AND MICROSTRUCTURAL PROPERTIES OF ALKALI ACTIVATED FLY ASH BASED GEOPOLYMER PASTE BLENDED WITH SLAG" in its current form for publication in World Journal of Engineering. The comments of the reviewer(s) who reviewed your manuscript are included at the foot of this letter.

By publishing in this journal, your work will benefit from Emerald EarlyCite. This is a pre-publication service which allows your paper to be published online earlier, and so read by users and, potentially, cited earlier.

Please note, EarlyCite is not a proofing service. Emerald operates a 'right first time' policy, which means that the final version of the article which has been accepted by the Editor will be the published version. We cannot allow further changes to the article once it has been accepted.

Please go to your Author Centre on Manuscript Central (Manuscripts with Decisions/Manuscripts I have co-authored) to complete the copyright assignment form. We cannot publish your paper without the copyright form. Only the submitting author need complete the form, however, all authors are advised to complete the form and to input their full contact details, to ensure that a complimentary author pack can be despatched upon publication. If any of the information is incorrect please contact the journal Publisher immediately.

If you would like more information about Emerald’s copyright policy please visit the Information & Forms section in the Resources section of your Author Centre.

Thank you for your contribution. On behalf of the Editors of World Journal of Engineering, we look forward to your continued contributions to the Journal.

Sincerely,
Dr. Yuzhuang Sun
Editor, World Journal of Engineering
syz@hebeu.edu.cn

Reviewer(s)' and Associate Editor Comments to Author:

Associate Editor
Comments to the Author:
(There are no comments.)

Date Sent: 21-Jun-2018

Close Window

Role of delayed water curing in improving mechanical and microstructural properties of geopolymer paste based on alkali-activated fly ash blended with slag

Abstract

Purpose: This paper aims to investigate the effect of delayed water curing upon the mechanical and microstructural properties of geopolymer paste based on alkali-activated fly ash blended with ground granulated blast furnace slag (GGBS).

Design/methodology/approach: The blended geopolymer paste was composed of GGBS (15% of total weight) and the base material, fly ash (FA). The blended mix was activated using an activator solution (sodium hydroxide and sodium silicate) containing 6% Na_2O relative to the total base material. The effect of delayed water curing was studied by subjecting samples to various aging periods (rest periods) from 2 to 24 h prior to water curing, and studying the resulting geopolymer structure and performance. Addition of alkali activator into the base material produces an aqueous state that is thermodynamically favorable for the geopolymeric reaction. However, an external source of energy in the form of heat is needed to initiate the primary polycondensation reactions. To analyze the mechanical and microstructural properties of the resultant blended geopolymer paste, compressive strength testing and FESEM and XRD analyses were carried out. Moreover, to evaluate the durability of the designed sustainable geopolymer paste, a long-term durability test was performed including exposure to sulfate under cyclic freezing and thawing.

Findings: The present study shows that delayed water curing is accompanied by a secondary heat input that enhances the partial polymer formation and the formation of CSH. Samples subjected to 2 and 24 h rest periods and 1 d of subsequent water curing respectively exhibited compressive strengths of 4 and 19 MPa. Final strength of around 95% was achieved by subjecting samples to a 24 h rest period and then curing them for 1 d. After 1 year of severe environmental exposure, this material retained 70% of its initial strength.

Originality/Value: To the best of the authors' knowledge, the effect of delayed water curing on the mechanical and microstructural properties of geopolymer paste based upon alkali-activated fly ash blended with slag has not been studied before.

Keywords: GGBS, fly ash, activator solution, aging period, water curing, compressive strength, microstructure

1. Introduction

Recently, geopolymers have attracted considerable research interest among environmentalists and material scientists as replacement building materials for ordinary Portland cement (OPC), as a means of reducing the associated emissions of greenhouse gases, which are considered to be a key contributor to global warming (Huntzinger and Eatmon, 2009). Geopolymer concrete is considered to be a greener alternative to cement concrete, having less associated health hazards and pollution (Feely *et al.*, 2004). Moreover, extensive studies of geopolymer

concrete have proven that it has remarkable advantages over conventional cement concrete in terms of durability and sustainability (Mehta and Burrows, 2001; Castel and Foster, 2015; Ganesan *et al.*, 2014).

Geopolymers are correlated aluminum silicate structures in which alkaline cations play the role of charge balancer. Geopolymers have amorphous structure, in contrast to zeolites which have fine crystalline structure (De Silva and Sagoe-Crenstil, 2008). The pozzolanic reactions of geopolymerization involving silica and alumina in alkaline solution can be described by the following steps: surface dissolution of Al and Si in highly alkaline solution; diffusion of dissolved species through the solution; polycondensation of Al and Si complexes with the added silicate solution; and formation and hardening of a gel to form the final geopolymer. Zeolites are generally synthesized from gels consisting of an insoluble solid phase and a trapped liquid phase that contains an equilibrium distribution of silicate and aluminosilicate anions, the supply of which is maintained by dissolution of the solid phase (Provis *et al.*, 2005; Palomo *et al.*, 1999). The existence of nanocrystalline particles (i.e. zeolitic structure) within the body of geopolymeric structure has been found in most studies on alkali-activated fly ash (Provis *et al.*, 2005; Palomo *et al.*, 1999; Fletcher *et al.*, 2005). The geopolymer synthesis conditions greatly impact the degree of crystallization (Provis *et al.*, 2005). Again, the formation of amorphous as opposed to crystalline structure depends on several factors such as curing temperature, aging time (i.e. time lag between mixing and curing), type and concentration of the alkaline activator, composition of the source material, presence of free water, and environmental coverage (Breck, 1974; Fernández-Jiménez and Palomo, 2005; Kriven *et al.*, 2004; Provis *et al.*, 2005; Palomo *et al.*, 1999; Murayama *et al.*, 2002; Inada *et al.*, 2005; LaRosa *et al.*, 1992). In the alkali-activated fly ash (AAFA) system, hydroxide activators have a greater tendency to produce crystals than silicate activators; also, zeolite phase formation is favored by the presence of sodium ions rather than potassium ions (Provis *et al.*, 2005; Murayama *et al.*, 2002; Inada *et al.*, 2005). It is also evident that using more free water in mixing emphasizes the synthesis of zeolites (Breck, 1974). Increasing the curing temperature from 45 to 65 °C is associated with a five-fold increase in the rate of strength gain, and a ten-fold increase has been noted between 65 and 85 °C (Palomo *et al.*, 2004). Mild curing temperatures promote the formation of zeolitic phases in the AAFA system (Fernández-Jiménez and Palomo, 2005). When the fly ash in a geopolymer is exposed to alkaline medium, its vitreous component rapidly dissolves, as sufficient time and space is not available for the formation of a well crystallized structure (Khale and Chaudhary, 2007; Fernández-Jiménez *et al.*, 2007; Terzano *et al.*, 2005). But a zeolite phase may crystallize from a dilute aqueous solution, in which case the precursor species likely has enough time and space to grow in the proper orientation and alignment to form a crystal structure (Khale and Chaudhary, 2007). Slag has a high percentage of CaO, and as the aluminosilicate network of the material starts decomposing under the attack of the highly alkaline solution, Ca^{2+} moves within the solution and precipitates as $Ca(OH)_2$, allowing the formation of calcium silicate hydrate (CSH) phases (Panagiotopoulou *et al.*, 2007). In the presence of highly alkaline solution, the base material metakaolin produces amorphous aluminosilicate, even in the presence of calcium compounds (Alonso and Palomo, 2001a, Alonso and Palomo, 2001b). The occurrence of this phenomenon supports the conclusion that CSH is formed in the basic geopolymeric structure when soluble calcium and silicate species are present in a

neutral to mild pH environment (Yip, C.K. *et al.*, 2005). The concept of a geopolymer as consisting of an agglomeration of nanocrystalline zeolitic phases bound together by an aluminosilicate gel has been broadly highlighted from a chemical thermodynamic and mechanistic standpoint (Provis *et al.*, 2005). The primary product of the polymerization process is amorphous Na–Al–Si phase(s), which progressively transform into crystalline phase(s) during prolonged curing (De Silva and Sagoe-Crenstil, 2008). Geopolymers can be formed by the polymerization of individual aluminate and silicate species that are dissolved from their sources at low pH in the presence of external calcium sources, and then subjected to heat curing. In these processes calcium cations, not the alkali cations, act as the initial charge compensators of aluminum ions.

The concept of improving the properties of AAFA without heat curing by blending them with other supplementary cementitious materials (SCMs) is comparatively new. The effects of blending ground granulated blast furnace slag (GGBS) with class F fly ash in the binder of geopolymer concrete cured at ambient temperature have been experimentally studied by Nath and Sarker (2014), who found that the workability of geopolymer concrete decreased with increasing GGBS content, whereas compressive strength at all ages up to 180 d increased with increasing slag content. These studies justify the choice of GGBS as a SCM in AAFA-based geopolymer concretes.

However, there have been few studies in the literature regarding water curing of fly ash–based blended geopolymer paste. This paper attempts to fill this gap in the literature. This paper deals with the new construction product prepared by means of alkali activation followed by water curing of fly ash with GGBS. The formation of geopolymeric versus zeolite phases is studied by varying the influencing parameters of curing profile and aging time. This detailed study dealing with typical alkali-activated and post-water-cured products will be very useful to judge the feasibility of using these materials as cast-in-situ building products.

2. Materials and methods

2.1 Materials

2.1.1 GGBS

GGBS, a byproduct of iron making in blast furnaces, was obtained from Tata Metallic, Kharagpur, West Bengal, India. GGBS was used in a powdered form having specific gravity 2.8 and density 1236 kg·m^{-3}. The average particle size ranged between 35 and 65 μm. Table 1 lists the composition of the GGBS sample according to X-ray fluorescence analysis; notably, a relatively high amount of calcium was found to be present.

2.1.2 Fly ash

Class F fly ash satisfying ASTMC 618 was supplied by Kolaghat Thermal Power Plant (Mecheda, India); 75% or more of the fly ash particles were finer than 45 μm. The Blaine surface area of the fly ash was 380 $m^2 \cdot kg^{-1}$. Table 1 lists the composition of the fly ash used.

Table 1. Chemical compositions of fly ash and blast furnace slag

Material/Chemical Component	SiO_2	Al_2O_3	Fe_2O_3	TiO_2	CaO	MgO	MnO	K_2O	Na_2O	SO_3	P_2O_5	LOI*
Fly ash	56.01%	29.8%	3.58%	1.75%	2.36%	0.30%	—	0.73%	0.61%	—	0.44%	0.40%
Blast furnace slag	30.26%	15.18%	1.87%	—	39.07%	8.95%	0.44%	—	—	—	—	0.04%

*LOI: loss on ignition

2.1.3 Alkali activator

Laboratory-grade sodium hydroxide in pellet form (97% pure) and sodium silicate solution (Na_2O, 8%; SiO_2, 26.5%; H_2O, 65.5%) of silicate modulus 3.3 and bulk density 1410 $kg \cdot m^{-3}$ were obtained from Loba Chemie Ltd., India. To prepare the alkaline activator solution, sodium hydroxide pellets were dissolved into water in the required quantity and the solution was held at 35 °C for 24 h. Then, a predetermined quantity of sodium silicate solution was added 3 h before mixing (Fernández-Jiménez and Palomo, 2005). The activator solutions had Na_2O content equal to 6 wt% of the fly ash content. The SiO_2/Na_2O ratio of the activator solution was maintained at 1.0; this ratio is known as the silicate modulus. Sodium silicate was used as the SiO_2 source in the activator solution.

2.1.4 Mixing and pouring

A mixer having a capacity of 600 cm^3 and speed of 60 cycles per second (Hobart p660) was used for mixing the raw materials. First, the fly ash and GGBS were well mixed in completely dry conditions in the mixer. Then, a predetermined quantity of activator solution was added into the dry mix. The fly ash and GGBS mixture was mixed with the activator solution for around 5 min. Then the mix was poured into cubic and cylindrical molds, which were then subjected to table vibration for 2 min to remove entrapped air. Table 2a lists details on the composition of the resulting geopolymer paste. Table 2b describes the weights of the ingredients used in a typical mixing.

Table 2a. Geopolymer specimen shapes and geopolymer paste compositions

Specimen Type	Specimen Shape	Specimen Size	Na_2O content of activator [wt%]*	SiO_2 content of activator [wt%]*	Blast furnace slag [wt%]*	Water to Fly ash Ratio
Paste	Cubic	50 mm × 50 mm × 50 mm	6	6	15	0.33
	Cylindrical	50 mm (diameter) × 100 mm (length)				

*Content relative to the combined weight of fly ash and slag

Table 2b. Detailed report on a typical GPC sample mixing

Component/Parameter	Quantity
Fly ash	850 g
Blast furnace slag	150 g
Na_2O as proportion of total base material	6 wt%
Na_2O required (in activator)	60 g
Silicate modulus	1
SiO_2 required (in activator)	60 g
Sodium silicate (SS) required	226.42 g
Na_2O from SS	18.18 g
NaOH required	53.96 g
Water from SS	148.30 g
Water from NaOH	12.14 g
Impure NaOH	55.04 g
Water/base material ratio	0.33
Water required	330 g
Free water required	169.56 g

2.1.5 Curing

Immediately after casting, the geopolymer specimens were covered with plastic sheets to control the water evaporation. The specimens were allowed to rest at a controlled temperature of 27 °C in an incubator (Figure 1) for predetermined resting periods; samples are hereinafter designated as R2, R4, etc. for resting periods of 2 h, 4 h, etc. After the resting period, each specimen was cured in a water basin. The program schedule was monitored to ensure that each specimen was water-cured for 20 d after its selected rest period.

Figure 1. Incubator used for sample resting (IIC Industrial Corporation)

2.2 Test setups

2.2.1 Workability in green state

Workability testing was carried out on the geopolymer paste in the green state. A typical experimental setup was used for workability determination (Figure 3a), comprising a brass cylindrical container (6 cm diameter, 8 cm height) and a circular glass slab (50 cm diameter, 7 mm thickness). A polar graph with 50 concentric circles (with the *n*th circle having diameter *n* cm) and 40 equiangular radial lines was placed under the glass. This segmentation allowed measurement of the areal extent of the geopolymer paste slump. The brass cylinder was placed exactly at the center of the polar graph, filled with a paste sample, allowed to stand for a 60 s retention period, and then raised vertically to allow the paste to flow. A reading of the outermost periphery of the flow was taken after the end of flow (>1 min). The change in phase with time was reflected by the workability. Workability was expressed in terms of the area factor, namely, the ratio of the area of the unconfined paste to that of the confined paste. This measurement procedure was taken from an earlier study (Dutta and Ghosh, 2014; Dutta *et al.*, 2012). Paste samples were collected at 9 distinct times, immediately after mixing for 5 to 45 min, in 5 min intervals. Testing the samples collected in this manner was useful for determining the changes in phase over time.

2.2.2 Strength testing

Compressive strength testing was conducted using a digital compressive strength testing machine (model EM500; Enkay Enterprises), which was calibrated and determined to have the accuracy of ±1%. The compressive strengths of geopolymer cubes were tested in accordance with ASTM C109. The final compressive strength was determined as the average value of ten specimens. Split tensile strengths of cylindrical specimens (see Figure 2) were calculated using the formula $\sigma_t = \frac{2P}{\pi dl}$ where P is the compressive load at failure, l is the length of the cylinder, and d is the diameter of the cylinder as per ASTM C496.

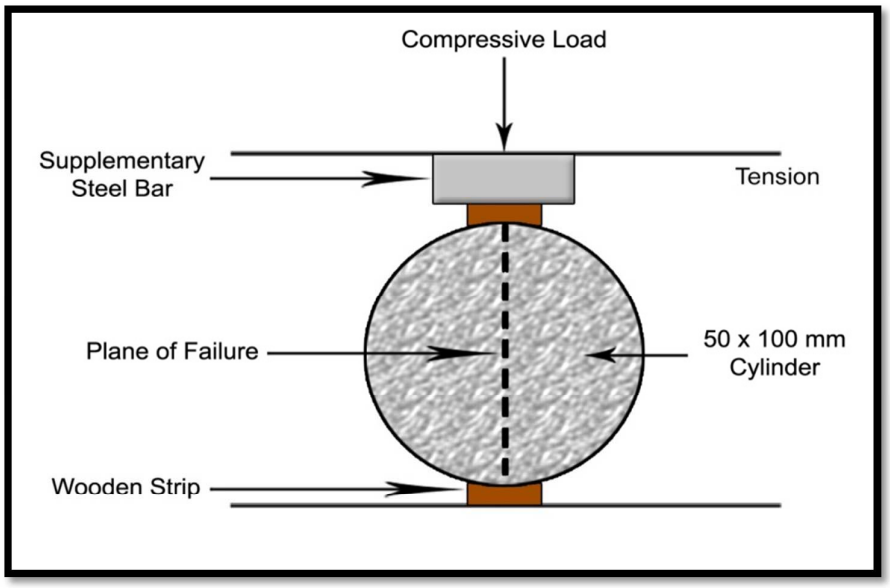

Figure 2. Schematic diagram of tensile strength testing setup

2.2.3 X-ray diffraction analysis

To acquire mineralogical information, X-ray diffractograms of hardened paste samples in powdered form were collected over the 2θ range of 5° to 140° using an XRD instrument (Panalytical X'Pert Pro) equipped with a Cu Kα source (wavelength 1.54 Å).

2.2.4 Field emission scanning electron microscopy (FESEM)

FESEM was conducted using a Quanta FEG 250 instrument (FEI Company) equipped with energy-dispersive X-ray spectroscopy detectors. The testing focused on microstructural imaging and analysis. Hardened samples for this analysis were collected as small scraps of dimensions not greater than 100 mm.

2.2.5 Thermogravimetric analysis (TGA)

Thermogravimetric analysis was performed using a thermogravimetric/differential thermal analyzer (Diamond TG/DTA; Perkin Elmer). The goal of TGA testing was to determine the structural water content under the variations of weight and heat energy arising during phase transitions in the temperature range of 30 to 1000 °C.

2.2.6 Environmental exposure testing

Samples were exposed to severe conditions to test their changes in physical and mechanical properties. Samples were immersed in 20 wt% magnesium sulfate solution and subjected to cyclical freezing and thawing. To carry out the freeze/thaw cycling, the assembly was

cyclically alternated between the temperatures of +8 °C and −20 °C in a chest freezer with a glass top (Model No. VT3-NUCAB 400L; Hindustan Unilever, India).

Test specimens of both cylindrical and cubic type were immersed vertically in saline water within the chest freezer. The water level above the specimen was maintained between 4 and 5 cm. In each cycle, the immersed samples were first held at +8 °C for 2 h, cooled to −20 °C, held at this temperature for 2 h, and then heated to +8 °C. Each specimen was exposed to 20 freeze/thaw cycles over a period of approximately 85 h. The samples were removed at 3 month intervals and tested to determine their physical appearance, weight, and strength according to the procedures given in the following subsections.

2.2.7 Changes in physical appearance

Specimens removed from exposure were visually inspected for any notable changes in physical appearance. Specimens were then subjected to optical microscopy using a crack detection microscope (WF 10X; C&D Micro Services Ltd., UK) was used to microscopically observe the physical changes at exposed surfaces.

2.2.8 Changes in weight

Prior to environmental exposure testing, each specimen was submerged in tap water for 1 h and then weighed; subsequent weight loss was determined with reference to this weight measurement. Samples were removed from exposure periodically and weighed. Simple scrub brushes and cotton cloth were respectively used to clean the samples and remove free water before weighing. Each specimen was brought to a saturated surface dry condition before weighing. Weights were measured with a digital electronic balance of least count 0.001 g.

2.2.9 Changes in strength

Initial specimen strengths were determined as the average strengths during testing conducted prior to immersion. Samples were prepared for subsequent strength tests by removing them from exposure and holding them at room temperature overnight. Changes in strength (either positive or negative) were calculated simply as percentage changes with respect to the initial strength. The residual strength at a given time was taken as unity minus the change in strength.

3. Results and discussion

3.1 Workability

The geopolymers based upon AAFA blended with GGBS exhibited quick setting. The area factor fell rapidly with time after mixing. Earlier studies showed that blending of slag

incorporates calcium into the mixture, which hastens the formation of Ca–Al–Si structure (Van Jaarsveld *et al.*, 2003; Xu and Van Deventer, 2002; Wang *et al.*, 2004). Additionally, there have been reports that the presence of calcium during the synthesis of fly ash–based geopolymers brings about the possibility of forming compounds like calcium silicates and calcium aluminate hydrates (Yip, C.K. and Van Deventer, 2003). It has also been suggested that the workability of fresh AAFA composites decreases with increasing slag content (Rashad, 2013). Table 3 lists the workability results, which demonstrate the rapid setting of the blended geopolymer. The area factor reached unity between 35 and 40 min; an area factor of unity is considered to correspond to the end of the plastic state.

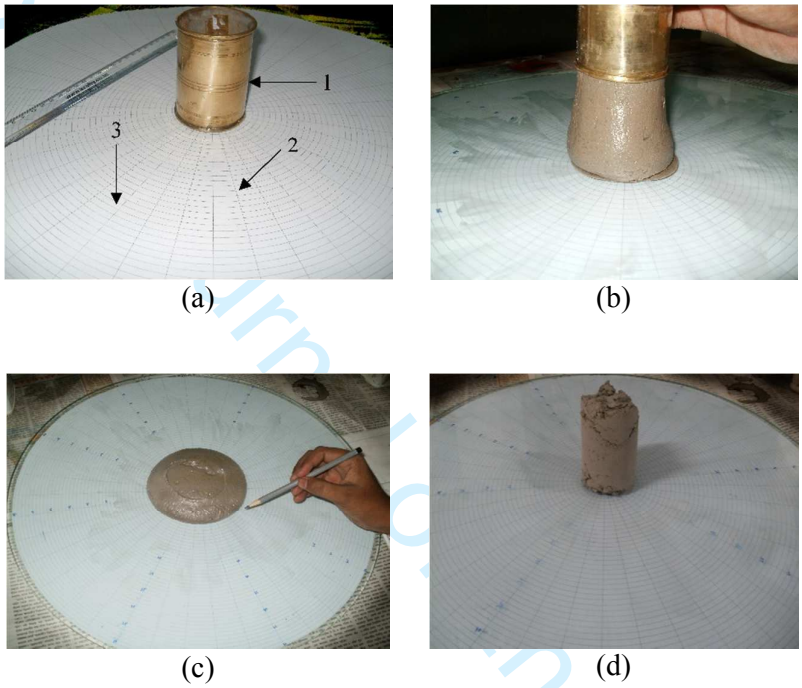

Figure 3. Workability testing. (a) Test setup (1: cylindrical brass container; 2: polar graph; 3. circular glass slab); (b) raising of cylinder; (c, d) flow measurements conducted (c) 5 and (d) 40 min after mixing

Table 3. Results of workability testing of blended geopolymers

Time elapsed after mixing [min]	Initial diameter (D1) [cm]	Final equivalent diameter (D2) [cm]	Initial area (A1) [cm^2]	Final area after flow (A2) [cm^2]	Area factor (A2/A1)
5	6	20	28.26	314.2857	11.12122
10	6	19	28.26	283.6429	10.0369
15	6	16	28.26	201.1429	7.117583
20	6	15	28.26	176.7857	6.255686
25	6	15	28.26	176.7857	6.255686
30	6	12	28.26	113.1429	4.003641
35	6	10	28.26	78.5714	2.780304
40	6	6	28.26	28.26	1.00

45	6	6	28.26	28.26	1.00

3.2 Compressive strength

Compressive strength was evaluated at preselected intervals. In this study, the initial chemical composition of every sample was the same. The samples were differentiated based on the rest period applied to each. Geopolymer samples subjected to longer rest periods exhibited rapid compressive strength gain upon water curing. For example, sample R24 showed 19 MPa strength under compression after 1 d of water curing (Figure 4a). Contrastingly, samples subjected to shorter rest periods exhibited slow strength gain upon water curing. For example, R24 attained around 95% of its final cured strength after 1 d of the 20 d water curing period (Figure 4b), whereas R2 attained only 16% of its final strength after the first day (Figure 4c). This was due to the fact that when ions dissolve in water, they release energy in the form of heat due to the stabilizing interaction. Somehow this energy might be the summation of lattice energy and heat of hydration due to the dissolution of a portion of the ionic solid. The water molecules oriented themselves in a manner that reduced the localized charge on the ions. The addition of alkali activator to the base material produced a dissolved state. The aqueous state was thermodynamically favorable for the geopolymeric reaction itself. But primary polycondensation could be initiated with an external source of energy in the form of heat. The post water curing of activated fly ash could incorporate a secondary heat input to enhance the partial polymer formation. These phenomena indicate that the initial rest period had an impact on the chemistry of the reaction, which has been mentioned as a new scope of study in various prior works (Breck, 1974; Fernández-Jiménez and Palomo, 2005; Kriven *et al.*, 2004; Provis *et al.*, 2005; Palomo *et al.*, 1999; Murayama *et al.*, 2002; Inada *et al.*, 2005; LaRosa *et al*., 1992).

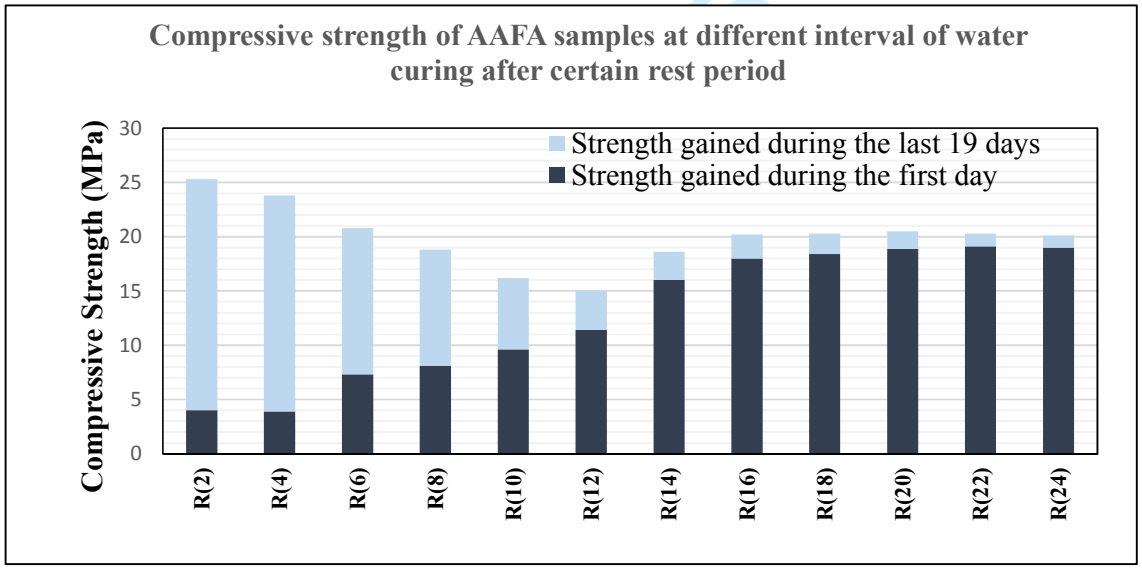

Figure 4a. Compressive strengths 1 and 20 days after curing of samples previously subjected to various rest periods

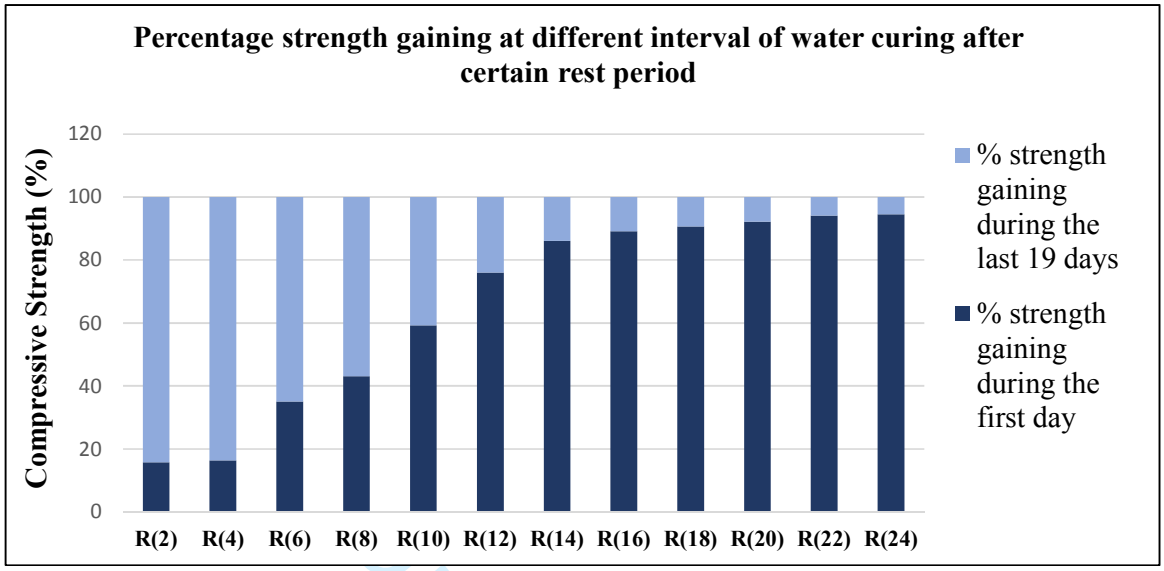

Figure 4b. Compressive strengths (as percentages of final strength) 1 and 20 days after curing of samples previously subjected to various rest periods

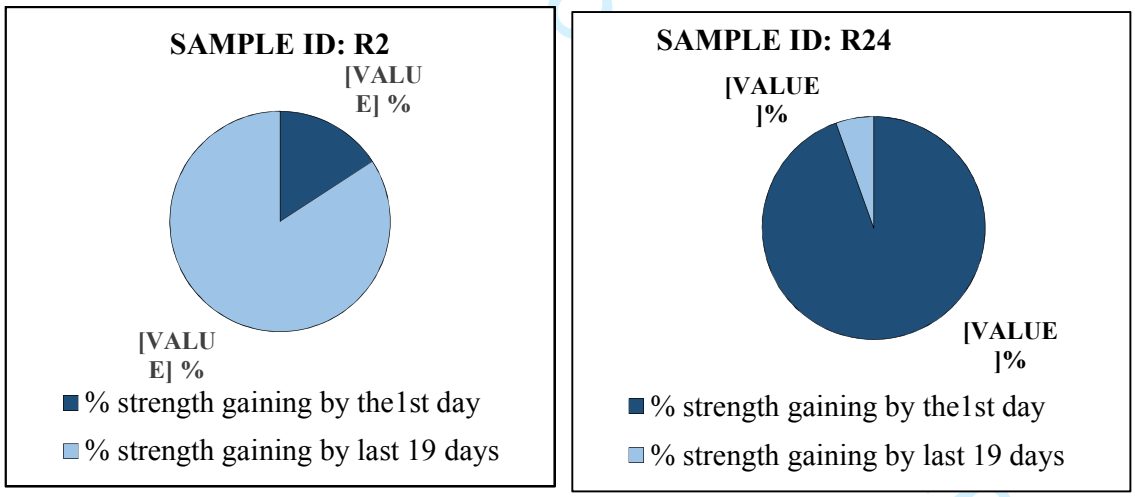

Figure 4c. Strength gain profiles of two samples subjected to different rest periods.

3.3 Efflorescence behavior at micro and macro levels

Efflorescence occurred on some of the AAFA-based geopolymers. In these highly alkaline geopolymers, the charge compensator alkali hydroxide was ejected as the synthesis progressed in terms of the formation of Si–O–Al bonds. In alkali activation of fly ash, the

alkali metal hydroxide acts as a catalyst and almost all the hydroxide added during synthesis subsequently leaches out from the structure (Van Jaarsveld *et al.*, 1998). Previous reports on alkali-activated fly ash subjected to heat curing have noted that it tends to form complete amorphous geopolymers, but in scenarios completely different from that of the present study. In the present work, each sample was initially held at room temperature, after which it was water cured. Mild leaching was observed in samples subjected to longer rest periods of 12 h and more. Specifically, samples R16 and R24 showed mild efflorescence under optical microscopy whereas the sample subjected to the shortest rest period (i.e. R2) did not (Figure 5). This observation could be attributed to the fact that longer rest periods in fact promoted the formation of a more amorphous polymeric structure, promoting the ejection of alkali from the geopolymer matrix.

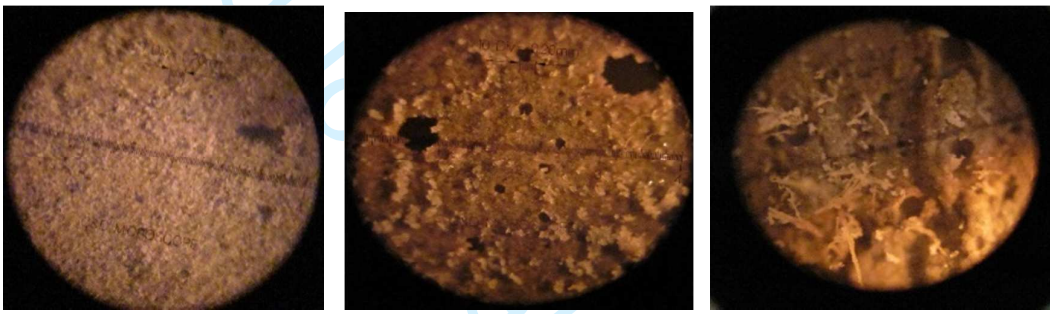

(a) **(b)** **(c)**

Figure 5. Efflorescence 3 months after sample preparation in (a) R2; (b) R16; (c) R24

3.4 FESEM analysis

FESEM images were studied to elucidate the morphological features of various samples of alkali-activated paste. In every case, some unreacted matrix and partially reacted matrix were observed. In the case of R24, a relatively dense phase was identified (Figure 6h;) in this sample, a great portion of the raw material turned into a well-connected structure of glassy phase. Distributed particles of various sizes were observed in samples R2, R8, and R14. FESEM micrographs of these samples showed that they contained particles of a wide size range. Earlier research (Dutta and Ghosh, 2014) demonstrated that additional calcium contributes to the activation of siliceous material in two ways: Ca^{+} primarily acts as a charge balancing agent and secondarily contributes to the formation of CSH gel. The present research demonstrated the performance of the calcium compound given the proper regulation of rest period before water curing. AAFA blended with 15 wt% GGBS subjected to the shortest rest period studied before exposure to water curing (namely, sample R2) showed certain different types of texture (Figure 6a and b) from the other samples. This particular texture consisted primarily of needle-like structures. It can be assumed that these needle-like projections arose simply from the development of non-amorphous or crystalline phases. The different amorphous and non-amorphous textural developments observed for chemically

equivalent materials subjected to different rest periods demonstrated the influence of the rest period as a significant parameter.


(a)

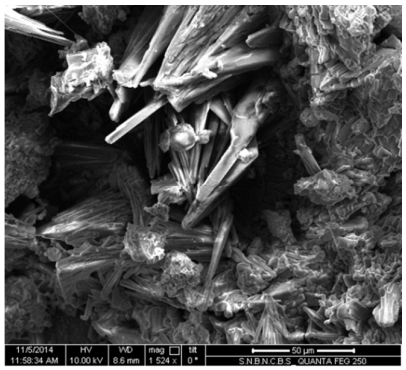
(b)

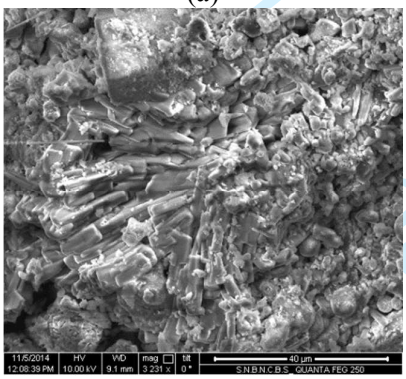
(c)

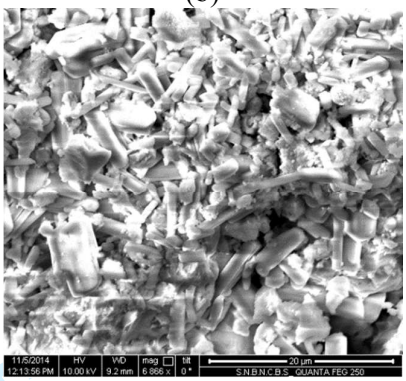
(d)

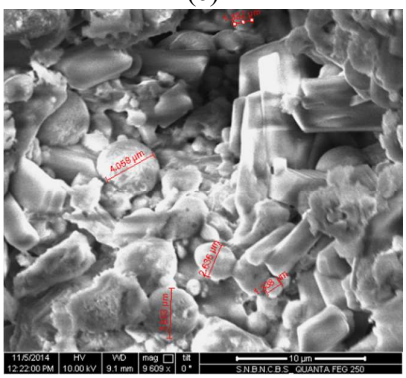
(e)

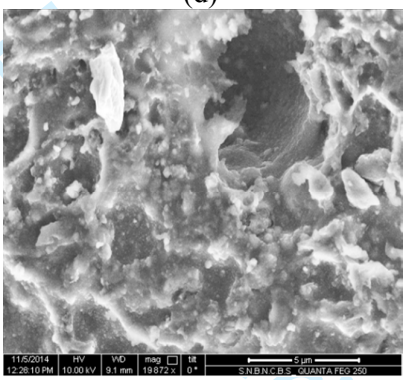
(f)

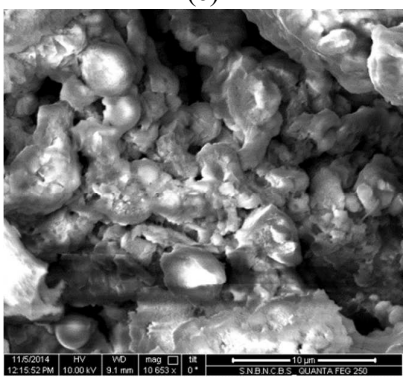
(g)

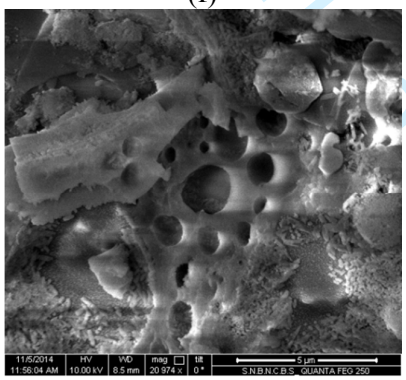
(h)

Figure 6. SEM micrographs collected after 20 d of water curing of samples (a, b) R2 (a: 800× magnification; b: 1524×); (c, d) R8 (c: 3231×; d: 6866×); (e, f) R14 (e: 9609×; f: 16,479×); (g, h) R24 (g: 6866×; h: 20,974×)

3.5 XRD analysis

The effects of rest period upon the mineralogical characteristics of AAFA-based geopolymer pastes cured in water were reflected in XRD patterns (Figure 7). The presence of calcium supplements in alkali-activated fly ash has been reported to improve mineralogical characteristics (Dutta and Ghosh, 2014), but this finding was reported in the context of the use of hot curing. In the present study, the alkali-activated sample was subjected to a rest period after casting, followed by water curing. Higher amounts of hydroxyl ions in the mix promote dissociations of silicate and aluminate species to form polymeric structure (Yip *et al.*, 2005). There was every possibility of the formation of calcium silicate hydrate, calcium aluminum hydrate, and calcium hydroxide, which were supposed to be generated due to the dissolution of calcium species occurring during water exposure of the fly ash.

X-ray diffraction analysis was performed over the 2θ scanning range from 5° to 140°. Figure 7 plots XRD spectra for geopolymers produced under various rest periods. The presence of multiple inherent crystalline phases, namely quartz and mullite, were recognized by referencing the XRD results for sample R2 to the Inorganic Crystal Structure Database. Narrower and high-intensity peaks were observed at specific angles in the XRD pattern for sample R2, indicating purely crystalline structure and thus implying that amorphous polymeric phases were largely absent. It was observed from the XRD pattern of sample R12 that the crystalline phase having long-range order was converted almost completely into an amorphous phase having only short-range order within the 2θ range of 20° to 40° (Figure 7b). The XRD pattern of sample R24 indicated a purely amorphous phase throughout the sample; the pattern had a broad hump in the 2θ range of 5° to 60° (with maximum intensity at 27° to 28°) and reduction in the monoclinic peaks compared to those of samples R12 and R2 (Figure 7c). With reference to the JCPDS database, this phase was identified as Muscovite-3T. The XRD patterns of Figure 7a and Figure 7b respectively indicate monoclinic and hexagonal crystal systems. The hexagonal structure gave rise to a disordered arrangement of OH^- ions. This might have arisen from the enthalpy change associated with the transition from monoclinic to hexagonal phase. Based on the XRD analysis, we attributed mostly crystalline structure to sample R2 and mostly amorphous structure to sample R24. Generally, the amorphous phase exhibited higher reactivity of the polymerization reaction.

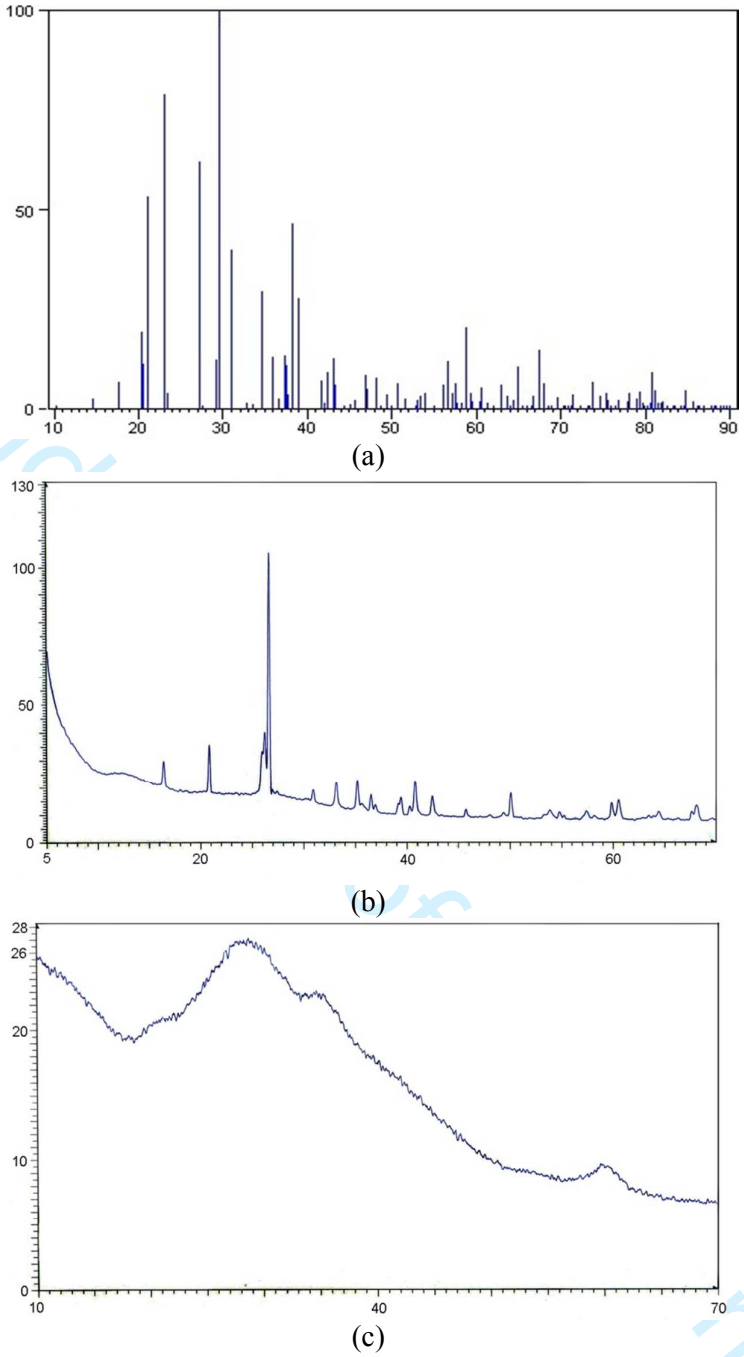

Figure 7. XRD patterns of samples (a) R2, (b) R12, and (c) R24

3.6 Thermogravimetric analysis

TGA traces of powdered specimens were collected for samples R2 and R24. Powdered specimens were used to ensure thermal stability throughout the transient heating (Kong and

Sanjayan, 2008). Figure 8a and Figure 8b respectively trace the TGA weight losses for samples R2 and R24. A sharp loss in mass around 100 °C for sample R2 arose from loss of evaporable water (Figure 8a). An endothermic peak was observed at approximately 70–90 °C in the DTA curve (Figure 8b), associated with the mass loss from evaporation of free pore water (Duxson *et al.*, 2006). This temperature range has already been identified and used as an optimized curing temperature (specifically 85 °C) for geopolymer composite preparation in an oven (Dutta and Ghosh, 2018). The rate of weight loss slowed at 100 °C in the analysis and steady weight was observed around 600 °C. The average weight remaining at this stage was 77.71%. The TG/DTA pattern of sample R24 was dissimilar to that of sample R2; weight loss of only about 2.5% was observed, and occurred between 350 and 600 °C (Figure 8a). This slight weight change might have arisen from degradation of the isolated organic part. The average total percentage of weight remaining at 600 °C was 97.5%. The thermogravimetric results clearly confirmed the more amorphous characteristics of sample R24, which was subjected to a longer rest period, thereby confirming the results of XRD and FESEM analysis.

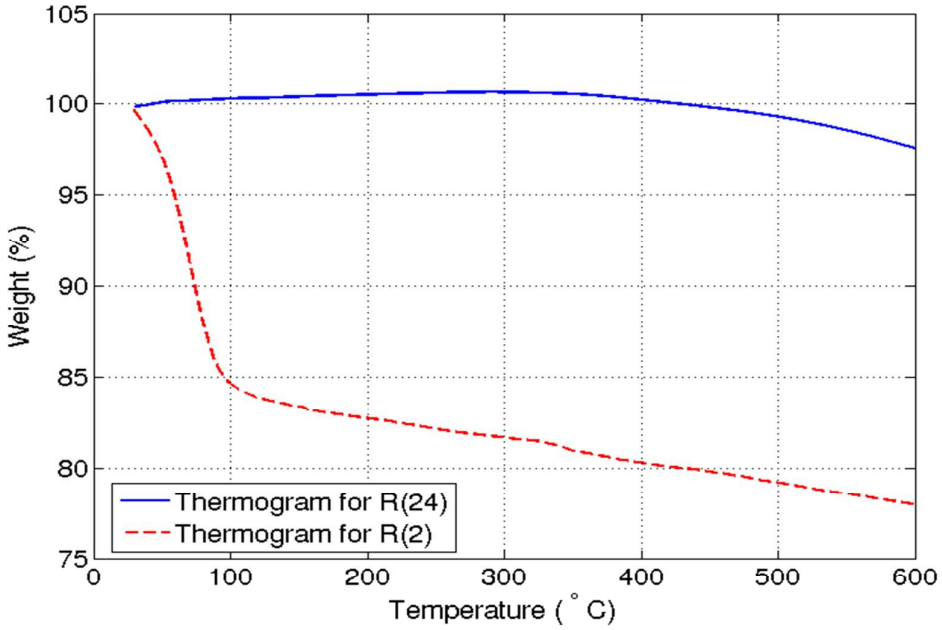

Figure 8a. Thermograms for samples R2 and R24: remaining weight versus temperature

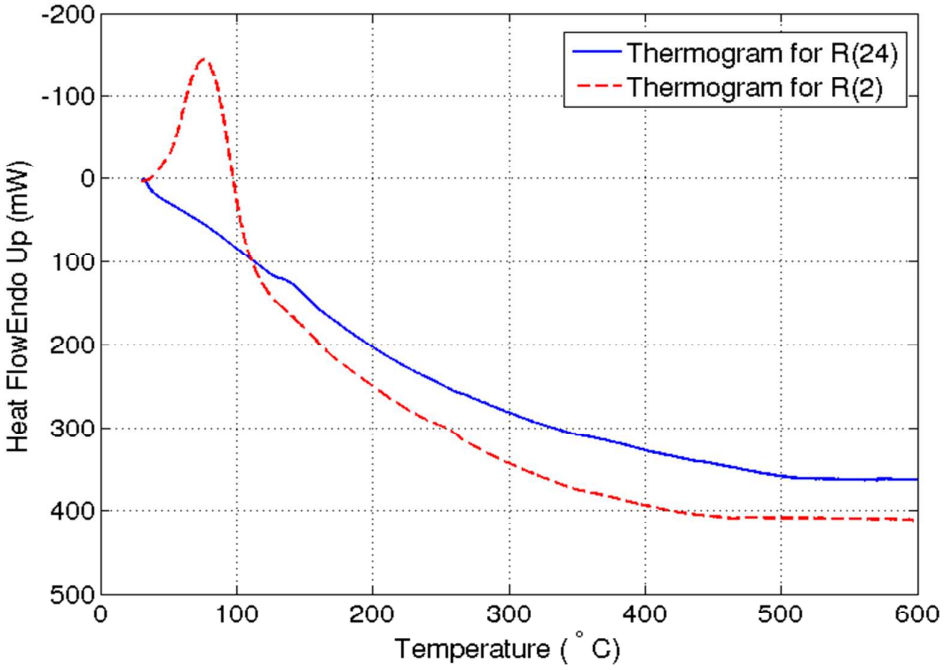

Figure 8b. Thermograms for samples R2 and R24: heat flow out of each sample during TGA analysis

3.7 Change in weight during environmental exposure

Including SCMs such as GGBS in geopolymers avoids the durability issues of cement, thus making geopolymers more durable against extreme environmental exposures and chemical attacks (Mohammadreza and Riding, 2015). The mineralogical and microstructural characterization results obtained in the present study were confirmed by results on the performance of alkali-activated samples subjected to severe environmental exposure. Two distinct series of samples R2 and R24 were subjected to cyclic freezing and thawing in sulfate exposure. The changes in weight of the two sample types were dissimilar (Figure 9a), confirming the importance of the rest period in the formation of dissimilar structures with different performance. The R2 samples showed the greatest reductions in weight and strength during environmental exposure, whereas the R24 samples showed comparatively good resistance to weight change. R24 samples showed a small increment in weight (1.78%) but R2 samples showed the maximum increment (27.94%), possibly due to the ionic transaction between nonreacted alkali hydroxide within the pores with the magnesium sulfate in solution.

3.8 Change in strength during environmental exposure

After exposure to cyclic freezing and thawing in sulfate solution (Figure 8), the strength change of R24 after exposure was quite less than that of R2 (Figure 9b). The residual strength dropped remarkably for R2 after the second cycle of freezing. The residual strength of R2 samples dropped by 52% relative to their initial values after 6 months of exposure, whereas R24 samples retained 79.21% of their initial strengths at this time. This was similar to the performance trends observed for cement paste samples under saline exposure. Figure 6h clearly indicates the presence of non-reacted alkali within the body of an R24 sample; thus, the minor weight and strength gains observed for these samples may have arisen from ionic transfer under saline exposure. After 1 year of saline exposure under cyclic freezing and thawing, sample R24 exhibited 70.93% residual strength but the R2 sample showed zero strength under loading. The role of the rest period thus affected the mineralogical characteristics, microstructural characteristics, and mechanical performance.

Figure 8c. Exposure of specimens to cyclic freezing and thawing

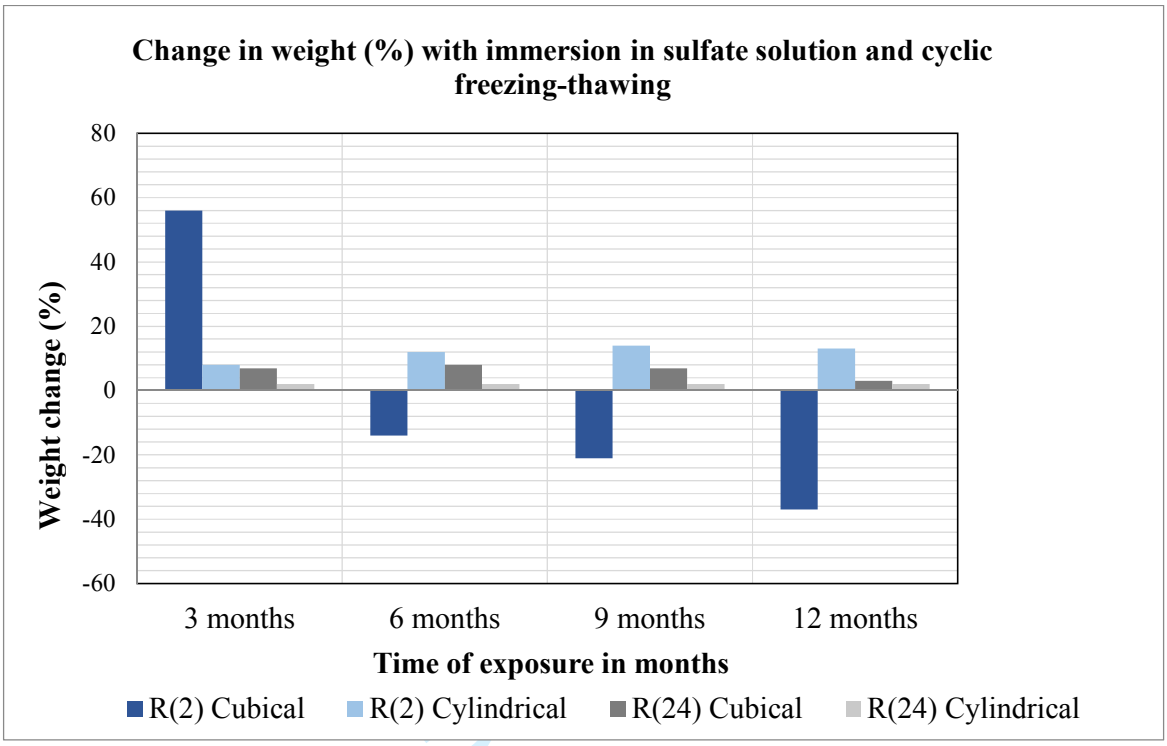

Figure 9a. Changes in weight during severe exposure for one year

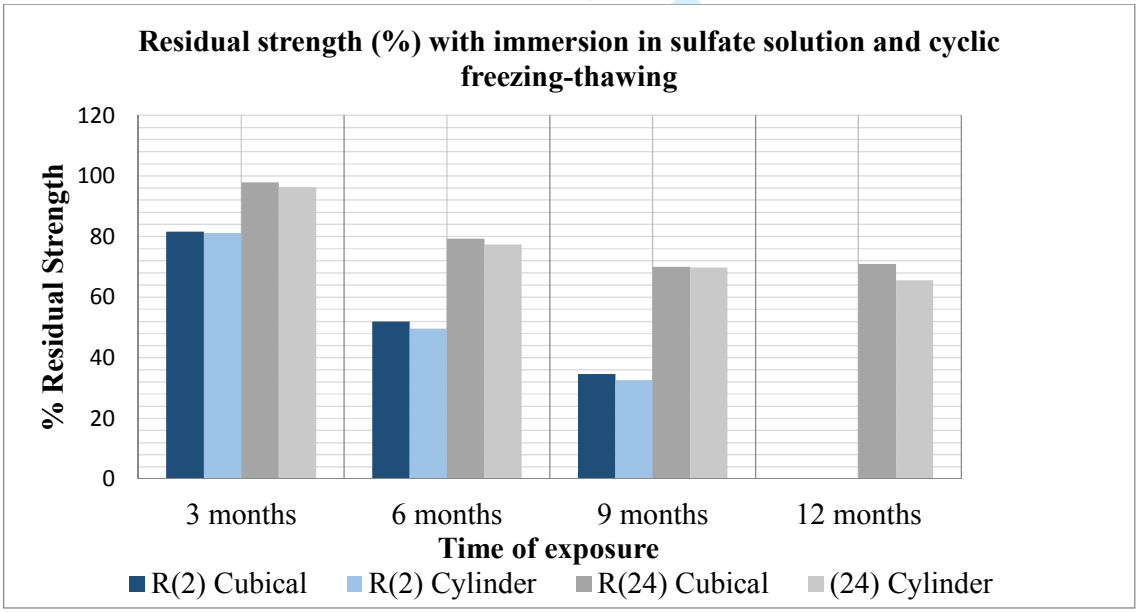

Figure 9b. Residual strengths during severe exposure for one year

4. Summary and conclusions

The effect of delayed water curing upon the mechanical and microstructural properties of geopolymer paste based upon AAFA blended with GGBS was investigated in this work by testing samples subjected to various aging periods (rest period) of 2 to 24 h prior to water curing. The rest period proved to be a crucial parameter determining the performance of blended AAFA-based geopolymer paste. The conclusions of this study are summarized as follows.

1) Geopolymers based upon AAFA blended with GGBS exhibited quick setting; the area factor fell rapidly with time after mixing. Samples reached the end of the plastic state between 35 and 40 min, indicated by the area factor reaching unity in workability tests.
2) AAFA-based geopolymer paste samples subjected to longer rest periods showed rapid early strength gaining under water curing compared to those subjected to shorter rest periods. R24 and R2 attained 95% and 16% of their final strengths after the first 1 d of water curing.
3) Leaching was observed for samples subjected to longer rest periods of 12 h and more. Longer rest periods brought about the formation of more amorphous polymeric structure, which promoted the ejection of alkali from the geopolymer matrix**.**
4) A specific crystalline texture consisting of needle-like structures was observed for samples subjected to the shortest rest period tested. This showed that the length of the rest period influenced the development of amorphous versus non-amorphous texture.
5) Multiple inherent crystalline phases, namely quartz and mullite, were recognized in XRD patterns of sample R2. Sample R12 showed an amorphous phase having short-range order within the 2θ range of 20° to 40°. Sample 24 showed almost completely amorphous phase, with a broad hump in the XRD pattern within the 2θ range of 5° to 60° and attenuated monoclinic peaks compared to R2.
6) Dissimilar sample performance arose from variations in the duration of the rest period applied. R2 showed a sharp drop (16%) in its thermogram at around 100 °C, attributed to loss of evaporable water in the geopolymer. The average total weight losses for samples R2 and R24 during heating up to 600 °C were respectively 22.29% and 2.5%.
7) The residual strengths of two samples subjected to severe environmental exposure were found to be dissimilar; the maximum strength loss at every sampling period was associated with a sample subjected to the shorter rest period. After 12 months of saline exposure with cyclic freezing and thawing, sample R2 showed zero strength under loading, whereas samples subjected to longer rest periods showed comparatively good resistance to the harsh environment. Sample R24 exhibited 70.93% of its initial strength after 12 months of exposure. The maximum increment in

weight (27.94%) was observed for sample R2, although sample R24 showed a slight increment in weight (1.78%).

References

1. Alonso, S. and Palomo, A. (2001a), "Alkaline activation of metakaolin and calcium hydroxide mixtures: influence of temperature, activator concentration and solids ratio", *Materials Letters*, 47(1–2), pp. 55–62.
2. Alonso, S. and Palomo, A. (2001b), "Calorimetric study of alkaline activation of calcium hydroxide–metakaolin solid mixtures", *Cement and Concrete Research*, 31(1), pp. 25–30.
3. Breck, D. W. (1974), "Zeolite Molecular Sieves, Structure, Chemistry and Use", John Wiley and Sons, New York.
4. Castel, A. and Foster, S.J. (2015), "Bond strength between blended slag and Class F fly ash geopolymer concrete with steel reinforcement", *Cement and Concrete Research*, 72, pp. 48–53.
5. De Silva, P. and Sagoe-Crenstil, K. (2008), "Medium-term phase stability of Na_2O–Al_2O_3–SiO_2–H_2O geopolymer systems", *Cement and Concrete Research*, 38(6), pp. 870–876.
6. Dutta, D., Chakrabarty, S., Bose, C., and Ghosh, S. (2012), "Comparative Study of Geopolymer Paste Prepared from Different Activators", *Recent Trends in Civil Engineering and Technology*, 2(3), pp. 1–10.
7. Dutta, D. and Ghosh, S. (2014), "Microstructure of Fly Ash Geopolymer Paste with Blast Furnace Slag", *CACE*, 2(3), pp. 95–101.
8. Dutta, D. and Ghosh, S. (2018), "Comparative Study on the Performance of Blended and Non-Blended Fly Ash Geopolymer Composites as Durable Construction Materials", *Advances in Civil Engineering*, 2940169, 12 pp.
9. Duxson P., Lukey G.C., and Van Deventer J.S.J. (2006), "Thermal evolution of metakaolin geopolymers: Part 1 — Physical evolution", *Journal of Non-Crystalline Solids*, 352, 5541– 5555.
10. Feely, R.A., Sabine, C.L., Lee, K., Berelson, W., Kleypas, J., Fabry, V.J., and Millero, F.J. (2004), "Impact of anthropogenic CO_2 on the $CaCO_3$ system in the oceans", *Science*, 305(5682), pp. 362–366.
11. Fernández-Jiménez, A., Garcia-Lodeiro, I., and Palomo, A. (2007), "Durability of alkali-activated fly ash cementitious materials", *Journal of Materials Science*, 42(9), pp. 3055–3065.

12. Fernández-Jiménez, A. and Palomo, A. (2005), "Composition and microstructure of alkali activated fly ash binder: Effect of the activator", *Cement and Concrete Research*, 35(10), pp. 1984–1992.
13. Fletcher, R.A., MacKenzie, K.J., Nicholson, C.L., and Shimada, S. (2005), "The composition range of aluminosilicate geopolymers", *Journal of the European Ceramic Society*, 25(9), pp. 1471–1477.
14. Ganesan, N., Abraham, R., Raj, S.D., and Sasi, D. (2014), "Stress–strain behaviour of confined Geopolymer concrete", *Construction and Building Materials*, 73, pp. 326–331.
15. Hendricks, W.M., Bell, A.T., and Radke, C.J. (1991), "Effects of organic and alkali metal cations on the distribution of silicate anions in aqueous solutions.", *Journal of Physical Chemistry*, 95(23), pp. 9513–9518.
16. Huntzinger, D.N. and Eatmon, T.D. (2009), "A life-cycle assessment of Portland cement manufacturing: comparing the traditional process with alternative technologies", *Journal of Cleaner Production*, 17(7), pp. 668–675.
17. Inada, M., Eguchi, Y., Enomoto, N., and Hojo, J. (2005), "Synthesis of zeolite from coal fly ashes with different silica–alumina composition", *Fuel*, 84(2–3), pp. 299–304.
18. Khale, D. and Chaudhary, R. (2007), "Mechanism of geopolymerization and factors influencing its development: a review", *Journal of Materials Science*, 42(3), pp. 729–746.
19. Kong, D.L.Y. and Sanjayan, J.G. (2008), "Damage behavior of geopolymer composites exposed to elevated temperatures", Cement and Concrete Composites, Volume 30, Issue 10, Nov, pp. 986–991.
20. Kriven, W.M., Gordon, M., and Bell, J.L. (2004), "Geopolymers: nanoparticulate, nanoporous ceramics made under ambient conditions". *Microscopy and Microanalysis*, 10(S02), p. 404.
21. LaRosa, J.L., Kwan, S., and Grutzeck, M.W. (1992), "Zeolite formation in class F fly ash blended cement pastes", *Journal of the American Ceramic Society*, 75(6), pp. 1574–1580.
22. Mehta, P.K. and Burrows, R.W. (2001), "Building durable structures in the 21st century", *Indian Concrete Journal*, 75(7), pp. 437–443.
23. Mohammadreza, M. and Riding, K. A. (2015), "Influence of different particle sizes on reactivity of newly ground glass as supplementary cementitious material (SCM)", *Cement and Concrete Composites* 56, pp. 95–105.
24. Murayama, N., Yamamoto, H., and Shibata, J. (2002), "Mechanism of zeolite synthesis from coal fly ash by alkali hydrothermal reaction", *International Journal of Mineral Processing*, 64(1), pp. 1–17.

25. Nath, P. and Sarker, P.K. (2014), "Effect of GGBFS on setting, workability and early strength properties of fly ash geopolymer concrete cured in ambient condition", *Construction and Building Materials*, 66, pp. 163–171.

26. Palomo, A., Alonso, S., Fernandez-Jiménez, A., Sobrados, I., and Sanz, J. (2004), "Alkaline activation of fly ashes: NMR study of the reaction products", *Journal of the American Ceramic Society*, 87(6), pp. 1141–1145.

27. Palomo, A., Blanco-Varela, M.T., Granizo, M.L., Puertas, F., Vazquez, T., and Grutzeck, M.W. (1999), "Chemical stability of cementitious materials based on metakaolin", *Cement and Concrete Research*, 29(7), pp. 997–1004.

28. Panagiotopoulou, C., Kontori, E., Perraki, T., and Kakali, G. (2007), "Dissolution of aluminosilicate minerals and by-products in alkaline media", *Journal of Materials Science*, 42(9), pp. 2967–2973.

29. Provis, J.L., Lukey, G.C., and Van Deventer, J.S. (2005), "Do geopolymers actually contain nanocrystalline zeolites? A reexamination of existing results". *Chemistry of Materials*, 17(12), pp. 3075–3085.

30. Rashad, A. M. (2013) "Properties of alkali-activated fly ash concrete blended with slag". *Iran. J. Mater. Sci. Eng.*, 10(1), pp. 57–64.

31. Terzano, R., Spagnuolo, M., Medici, L., Vekemans, B., Vincze, L., Janssens, K., and Ruggiero, P. (2005), "Copper stabilization by zeolite synthesis in polluted soils treated with coal fly ash", *Environmental Science and Technology*, 39(16), pp. 6280–6287.

32. Van Jaarsveld, J.G.S., Van Deventer, J.S.J., and Lorenzen, L. (1998), "Factors affecting the immobilization of metals in geopolymerized fly ash", *Metallurgical and Materials Transactions B*, 29(1), pp. 283–291.

33. Van Jaarsveld, J.G.S., Van Deventer, J.S.J., and Lukey, G.C. (2003), "The characterisation of source materials in fly ash-based geopolymers", *Materials Letters*, 57(7), pp. 1272–1280.

34. Wang, K., Shah, S.P., and Mishulovich, A. (2004), "Effects of curing temperature and NaOH addition on hydration and strength development of clinker-free CKD-fly ash binders", *Cement and Concrete Research*, 34(2), pp. 299–309.

35. Xu, H. and Van Deventer, J.S. (2002), "Geopolymerisation of multiple minerals". *Minerals Engineering*, 15(12), pp. 1131–1139.

36. Yip, C.K., Lukey, G.C., and Van Deventer, J.S.J. (2005), "The coexistence of geopolymeric gel and calcium silicate hydrate at the early stage of alkaline activation", *Cement and Concrete Research*, 35(9), pp. 1688–1697.
37. Yip, C.K. and Van Deventer, J.S.J. (2003), "Microanalysis of calcium silicate hydrate gel formed within a geopolymeric binder", *Journal of Materials Science*, 38(18), pp. 3851–3860.

RJC

RASĀYAN *J. Chem.*
Vol. 11 | No. 3 |1018 - 1033 | July - September | 2018
ISSN: 0974-1496 | e-ISSN: 0976-0083 | CODEN: RJCABP
http://www.rasayanjournal.com
http://www.rasayanjournal.co.in

ENHANCING THE MECHANICAL AND MICRO-STRUCTURAL PROPERTIES OF SILICA FUME BLENDED FLY ASH BASED GEOPOLYMER USING MURRAM AS A TERTIARY SUPPLEMENT

Debabrata Dutta[1,*] and Somnath Ghosh[2]

[1]Research Scholar, Department of Civil Engineering, Jadavpur University, 188, Raja S. C. Mallick Road, Kolkata-700032, India

[2]Professor, Department of Civil Engineering, Jadavpur University, 188, Raja S. C. Mallick Road, Kolkata-700032, India

*E-mail: ddebabrata83@gmail.com

ABSTRACT

The present study aims to investigate the compressive strength and the underlying micro-structural change of fly ash geopolymer paste with silica fume and murram as supplements up to 10% and 2.5% of the total weight respectively. The workability property of the geopolymer paste samples was evaluated at a green state using a unique methodology based on the polar graph. Besides, various geopolymer paste samples were subjected to heat curing at different temperatures and also for different durations to find the influence of heat curing to the obtained compressive strengths. The present study also probed into the underlying micro-structural changes of the corresponding geopolymer paste samples through SEM (Scanning Electron Microscopy), MIP (Mercury Intrusion Porosimetry) and EDX (Energy Dispersive X-Ray Analysis). Through the present analysis, it can be concluded that blending of silica fume and murram with fly ash based geopolymer paste results in a sustainable high performance binder even at lower alkalinity with lower heat consumption as well as lower water content which can be considered as a better alternative of cement concrete binder to march towards environmental sustainability.

Keywords: Geopolymer, Fly ash, Silica fume, Murram, Strength, Micro-structure, High Performance.

INTRODUCTION

Ordinary Portland cement (OPC) is continuing to be used as an indispensable building material for decades. However, the production of OPC is associated with a lot of energy consumption and is a significant contributor towards the huge amount of greenhouse gases emissions triggering the threat of global warming[1]. Cement industry produces a huge amount of carbon dioxide in the atmosphere[2]. With growing environmental consciousness, there is a renewed interest among the environmentalists to reduce the effluence of cement and others industry as much as possible which enforced the material scientists to look for greener alternatives[3]. Beside this, the sustainable performance of Portland cement is another major limitations[4]. Recently, geopolymers have been investigated extensively as an alternative binder with a view to producing green, durable and sustainable concretes[5,6]. Various alternative cementitious materials (like fly ash, slag, metakaoline and others) are found to have potential application to resolve the durability aspects of cement concrete[7]. Again, an enormous surplus of fly ash all over the world has also boosted its usage to produce alternative binders[8].

Principally, geopolymer, a novel inorganic polymer binding material, is prepared by the activation of base material consisting silica and alumina like fly ash in presence of strong alkali like sodium hydroxide and sodium silicate resulting in a three-dimensional amorphous aluminosilicate network with better binding properties[9-11].

CrossMark

Fly ash is amorphous spherical particles. But the content of fly ash usually varies with the types of coal and plants[9]. Geopolymer based on fly ash, may be utilized as a binder instead of cement to mix with aggregates in a manner to form geopolymer concrete. Performance of geopolymer is proved better than cement in different aspects like high early strength, resistance to chemical attack and higher compressive strength etc.[9-11]. Substantial studies are already available on fly ash based geopolymer concrete[9-12]. Recently a few important studies have been focused on blended geopolymer to meet advanced properties of it[42].

Silica fume, a secondary sequel in the production of silicon amalgams, is treated as highly reactive pozzolana and is widely used in conventional concrete to enhance its various strength and durability properties[17]. The basic fundamental cause of using siliceous mineral in conventional concrete is to emphasize secondary CSH formation[18]. Geopolymers was announced as an amorphous three-dimensional aluminosilicate binder material by Davidovits[19]. Combative materials like fly ash consisting of silica and alumina are quickly disbanded into the strong alkaline solution to make liberated silico-aluminate tetrahedral components. These tetrahedral units are linked through a rotator mode to reach into amorphous geopolymers during the poly-condensation reaction[19-20]. In alkalinity, the base material dissolves progressively to form oligomers; then precipitation of geopolymers are formed. Nevertheless, a very rare study on fume silica in geopolymer is available in the existing literature. Limited works have focussed on studying the performance of silica fume blended fly ash based geopolymer concrete[13-16]. Chindaprasirt et al. concluded that silica fume as supplements improves the performance of fly ash geopolymer in connection with strength and durability[13]. Lee et al. have shown that the reactivity of geopolymer concrete is enhanced when a combination of fly ash, slag, and silica fume is used as binder[14]. Okoye et al. have recently reported that fume silica in fly ash geopolymer improves the physical performance[15]. Very recently, Duan et al. investigated the performance of silica fume blended activated fly ash in micro and macro level after temperature fluctuating cycles with different heating temperatures of 200ºC; 400ºC and 800ºC, replacing fly ash by 0% to 30% silica fume with an interval of 10%, by weight[16].They commented that blended geopolymer emphasizes rapid strength development in geopolymer.

A few recent studies have reported the diverse effect of silica fume on the consistency of geopolymer which in fact marginalize the massive usage of this composite indeed. Also, the maximum strength of silica fume based geopolymer is dropped remarkably under thermal fluctuation but this drop after thermal cycles is independent of silica fume content[16]. Therefore, there is a need to explore the possibilities of other contentious materials like murram (having similar property as red mud) to be blended together with fumed silica in the geopolymer with FA as a base material, to cut off the limitations. The advantageous part is that murram and fly ash is environmentally safe. Moreover, these materials can be procured free of cost in India. Few studies have investigated the potential of red mud to be used in geopolymer concrete. Kumar et al. used Red Mud and Fly ash in Geopolymer for developing a paving block and showed that incorporation of supplements effects on the better reaction rate and hardened properties of the blended geopolymer; 5-20% red mud is found to be optimum in the improvement in setting time and compressive strength[21]. Ye et al. applied a thermal pre-treatment to correlate it with the dissolution of supplements and its rate of geopolymerisation[22]. This research found the effect of red mud to reduce the adverse effect of iron in alkaline solution. Again this study was focused on the transformation of phase in the midst of thermal treatment. Zhang et al. investigated the various properties in micro and macro level for the red mud blended geopolymer with varying composition of the material and curing pattern[23]. They found that an increase in geopolymer strength with increasing Si/Al and Na/Al ratios up to 25 weeks.

In natural clay material, the approach of aluminosilicate is governed by calcination. Calcination is a thermal healing process in presence of oxygen applied to ores, to bring about a thermal decomposition, phase transition or removal of a volatile fraction[24]. This formation is projected through three steps: firstly; construction of a gas, secondly; improvement in viscous nature thirdly; progressive association. These steps execute three basic occurrences like (a) production of di-hydrogen (b) silicon oxidation (c) development of silicon hydride class as demonstrated earlier[25].

The chemistry states that excessive presence of reactive silica may cause porous character by the generation of hydrogen[26]. Contributions of various ingredients in alkali-activated fly ash based geopolymer are needed to be discussed. In activation of fly ash, the pozzolana freely dilutes in alkali and consequently emphasizes geopolymerisation[19].

$Si^0 \rightarrow Si^{4+} + 4e^-$ (1)

$4H_2O + 4e^- \rightarrow 2H_2 + 4OH^-$ (2)

$4H_2O + Si^0 \rightarrow 2H_2 + Si(OH)_4$ (3)

Alkali metal hydroxide contributes to the cations (Na, K, Ca and other metallic cations) which are required to maintain the structure neutrality (as aluminium is of four-fold). The purpose of the alkali cations is to balance the extra ionic charges. Here the term structural neutrality implies neutralization of ionic charges. Reactive silica-alumina in the alkaline medium cannot produce geopolymer unless it is introduced with heat. Investigations of Kirschner et al. elaborate that geopolymer formation in room temperature is not feasible [27].

The research was designed to develop blended fly ash based geopolymer paste, keeping the following parameter as targets.

1. Geopolymer strengthening at low Alkalinity (< 8% K_2O of total base particles)
2. Geopolymer strengthening at low Silicate Modulus (< 1.0)
3. Geopolymer workability at low water content (< 0:33 = Water/Fly Ash)
4. Geopolymer strengthening at a low temperature of heat curing (< 85°C)
5. Geopolymer strengthening at less curing duration (< 48 Hrs)

The replacement of traditional construction materials by new materials like geopolymer has already risen. Most of the studies were carried out to compare the geopolymer with the conventional construction material. Recently research has been employed to the properties blended fly ash geopolymer. The combinational study is essential to develop advanced geopolymer products that consume less alkali and heat energy in preparation. The study deals with blended geopolymer with better workability, strength, and microstructure which require less alkali and heat for preparation. The study will be effective to the production of cost-effective geopolymer as non-conventional sustainable material in concrete industry. These materials are very much novel with substantial potential to be used as commercially.

EXPERIMENTAL

Present research elaborately represents comprehensive results of 14 different laboratory trial mixes. An extensive parametric study has been carried out considering the strength of the alkaline solution, the water content in the mixture, base material, supplementary material, heat curing profile. Moreover, the paste samples have been studied in plastic as well as the hardened state. Compressive Strength Test, Area Factor Test, MIP, SEM, and EDX have been carried out to evaluate the performance of various kinds of geopolymer binder with a view to choosing an optimal mix design.

Materials and Methods

The chemical composition of the Fly Ash conforms to class F in accordance with ASTMC618 and was supplied by Kolaghat Thermal Power Plant, Murram were supplied by Ujjwal Chemical Works, Ranaghat, Kolkata, India and Silica Fume were supplied by Oriental Trexim Pvt. Ltd. The detail composition is reported in Table-1. The loss of ignition LOI is seen possibly due to the presence of hydrated compounds and residual organic matter. Scanning electron microscopy results of fly ash, murram and silica fume are given in Fig.-1. Different ranges of particle sizes are seen to be present in these three raw materials which are clearly observed from magnified pictures. The magnification had to varied for different samples to have a clear picture. In the case of murram, the magnification was kept less in comparison to others as its particle size was larger. However, it was higher for fly ash to pinpoint the fraction of very finer particles comprised with the larger particles.

More than 75% of grain size was less than 45μ with 380m^2/Kg as specific surface area. Fume silica of specific gravity of 2.36 and surface area (BET) of 8900m^2/kg was used. Typical values of murram were also accounted. It indicates that 85% of the volume was below 75 μm. The specific surface area (BET) of murram was 171 m^2/Kg.85 percent pure potassium hydroxide in pellet form and sodium silicate solution (Na_2O, SiO_2, H_2O were 8%,26.5%, and 65.5% respectively). For the silicate solvent, silicate modulus and bulk density were kept 3.3 and 1410 kg/m^3 respectively. All the alkali solutions were brought from Loba

Chemie Ltd, India. To prepare the alkaline activator solution, the required quantity of potassium hydroxide pellets was first dissolved directly into the water and was left at room temperature for 24 hours (shown in Fig.-2b).

Table-1: Chemical Analysis Report of Fly Ash, Silica Fume and Murram (In percentage)

Materials	SiO_2	Al_2O_3	Fe_2O_3	TiO_2	CaO	MgO	K2O	Na_2O	SO_3	P_2O_5	LOI
Fly Ash	56.01	29.80	03.58	01.75	02.36	00.30	00.73	00.61	00.00	00.44	00.40
Silica Fume	92.00	00.46	01.60	00.00	00.29	00.28	00.61	00.51	00.19	00.00	01.00
Murram	21.06	26.01	13.02	04.21	17.12	02.22	02.04	05.30	00.00	00.00	09.02

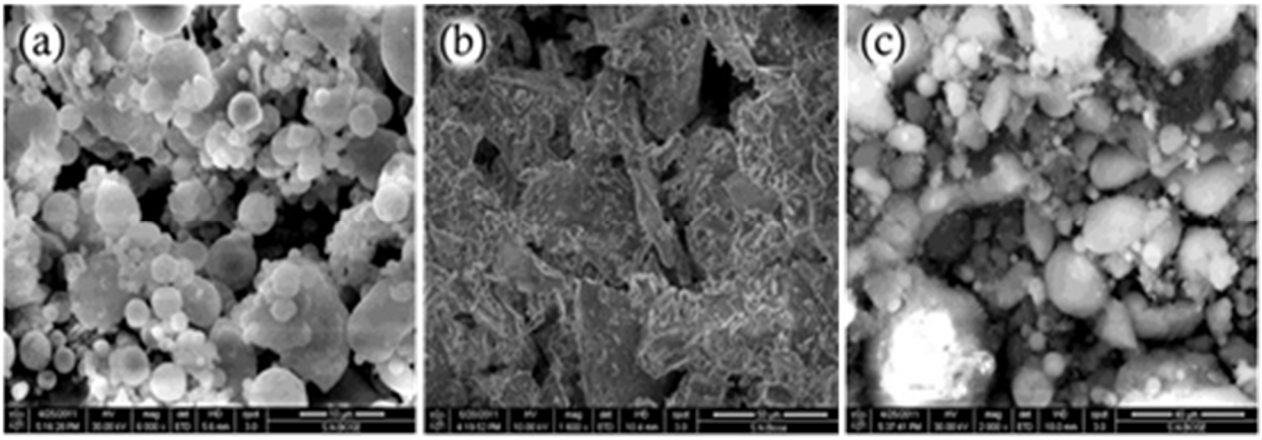

Fig.-1: SEM images of- (a) Fly ash, (b) Murram, (c) Silica Fume

Fig.-2: (a) Hobart Mixture, (b) Alkaline activator

The silicate solution was mixed around three hours earlier the preparation of geopolymer pastes. Dissolution of potassium hydroxide pellets in water is an exothermic reaction. Hence, the generation of heat from the solution indicates the progress of the reaction. Although in the earlier study it is mentioned that one-night stay of the solution is sufficient[28]. A duration of 24 hrs is kept constant for every case to be assured of the completion of the process. When the reaction of potassium hydroxide solution with sodium silicate is an exothermic reaction and takes few hours to get cool. However excessive time delay brings in white precipitation within the solution. So, 3 hrs. rest was optimized and made fixed in this research. These activator solutions had K_2O content equal to either 6.0% or 8.0% of fly ash. SiO_2/ (K_2O + Na_2O) ratio in

activator solution was maintained equal to either 0.0 or 0.77. Sodium silicate was used as the source of SiO_2 in activator solution. SiO_2/K_2O is the apparent silicate modulus. The Hobart mixture of model P660 of capacity 600cc and speed of 60 cps was used for the mixing of paste. Mixing proportion of the geopolymer paste is specified in Table-2a.

Table-2a: Mix Proportion of Geopolymer Pastes

Sample Id.	Silica Fume*	Murram*	K2O in activator*	SiO2 in activator*	SiO2/K2O in activator	Water*
GPK1	0.0%	0.0%	8%	8%	1.0	33%
GPK2	0.0%	0.0%	8%	0%	0.0	33%
GPK3	0.0%	0.0%	6%	6%	1.0	33%
GPK4	0.0%	0.0%	6%	0%	0.0	33%
GPK5	10%	0.0%	8%	8%	1.0	33%
GPK6	10%	0.0%	8%	0%	0.0	33%
GPK7	10%	0.0%	6%	6%	1.0	33%
GPK8	10%	0.0%	6%	0%	0.0	33%
GPK9	10%	2.5%	8%	8%	1.0	33%
GPK10	10%	2.5%	8%	0%	0.0	33%
GPK11	10%	2.5%	6%	6%	1.0	33%
GPK12	10%	2.5%	6%	0%	0.0	33%
GPK13	10%	2.5%	8%	8%	1.0	25%
GPK14	10%	2.5%	6%	6%	1.0	25%

**% of (fly ash + silica fume+ murram) in weight*

The typical mix composition for 1000 gm. of the base material (fly ash + silica fume + murram) is given in Table-2b. Here in this research, the K_2O% with respect to (fly ash + silica fume + murram) in weight and the apparent silicate modulus (SiO_2/K_2O) are taken as the input parameters of the mix. The actual silicate modulus or solution modulus is calculated from $SiO_2/ (K_2O + Na_2O)$. The water content (as given in Table-2c) is total of H_2O molecules coming from (i) KOH dissolution, (ii) water added for making KOH solution, (iii) Sodium silicate solution and (iv) additional water for mixing.

Table-2b: Sample Calculations of Different Mixes

Sample Id	Fly Ash (gm.)	Silica Fume (gm.)	Murram (gm.)	K_2O (gm.)	Apparent Silicate modulus	SiO_2 (gm.)	Sodium Silicate (SS) (gm.)	Na_2O From (SS) (gm.)	KOH (gm.)	Pure KOH (gm.)	Silicate Modulus
GPK1	1000	0	0	80	1	80	301.89	24.24	95.30	109.60	0.77
GPK2	1000	0	0	80	0	0	0.00	0.00	95.30	109.60	0.00
GPK3	1000	0	0	60	1	60	226.42	18.18	71.48	82.20	0.77
GPK4	1000	0	0	60	0	0	0.00	0.00	71.48	82.20	0.00
GPK5	900	100	0	80	1	80	301.89	24.24	95.30	109.60	0.77
GPK6	900	100	0	80	0	0	0.00	0.00	95.30	109.60	0.00
GPK7	900	100	0	60	1	60	226.42	18.18	71.48	82.20	0.77
GPK8	900	100	0	60	0	0	0.00	0.00	71.48	82.20	0.00
GPK9	875	100	25	80	1	80	301.89	24.24	95.30	109.60	0.77
GPK10	875	100	25	80	0	0	0.00	0.00	95.30	109.60	0.00

GPK11	875	100	25	60	1	60	226.42	18.18	71.48	82.20	0.77
GPK12	875	100	25	60	0	0	0.00	0.00	71.48	82.20	0.00
GPK13	875	100	25	80	1	80	301.89	24.24	95.30	109.60	0.77
GPK14	875	100	25	60	1	60	226.42	18.18	71.48	82.20	0.77

Table-2c: Sample Calculation for water and density of mixes

Sample Id	Fly Ash (gm.)	Silica Fume (gm.)	Murram (gm.)	Water From (SS) (gm.)	Water From KOH (gm.)	Extra Water (gm.)	Total Water	The density of mix gm./cc
GPK1	1000	0	0	197.74	15.32	116.94	330	2.46
GPK2	1000	0	0	0.00	15.32	314.68	330	2.12
GPK3	1000	0	0	148.30	11.49	170.21	330	2.37
GPK4	1000	0	0	0.00	11.49	318.51	330	2.12
GPK5	900	100	0	197.74	15.32	116.94	330	2.4
GPK6	900	100	0	0.00	15.32	314.68	330	2.07
GPK7	900	100	0	148.30	11.49	170.21	330	2.32
GPK8	900	100	0	0.00	11.49	318.51	330	2.07
GPK9	875	100	25	197.74	15.32	116.94	330	2.39
GPK10	875	100	25	0.00	15.32	314.68	330	2.07
GPK11	875	100	25	148.30	11.49	170.21	330	2.31
GPK12	875	100	25	0.00	11.49	318.51	330	2.06
GPK13	875	100	25	197.74	15.32	36.94	330	2.59
GPK14	875	100	25	148.30	11.49	90.21	330	2.49

Paste sample was chosen to predict the properties of the binder itself. The incorporation of aggregates brings multi-phase in a composite like a geopolymer mortar or concrete. In this study, the paste is considered to compare the performance of binder at gel and hardening phase. Cubical (50mm × 50mm × 50mm) geopolymer paste specimen were investigated for typical hardened properties.

Detection of Various Constraints

Effect of Supplements on Alkali Hydroxide

Strong alkali activated silicon & aluminium, present in the base material, is the main contributor to have a partially or totally compacted activated composite[29]. The requirement of sodium silicate to emphasize the initial polymerization may be reduced by the application of highly reactive silica source like silica fume[30]. In higher solution modulus Na+ is less effective for the stabilization of larger oligomer which can be effectively stabilized by cation like K^+ having larger size[31]. Here the concentration of sodium silicate in the activator solution is indicated by the silicate modulus or solution modulus. Practical investigation depicts that, a combination of potassium hydroxide and sodium silicate show better performance at higher silicate modulus of activator. SiO_2 / (K_2O + Na_2O) results better than SiO_2 / Na_2O when both the value is kept one[32]. Addition of higher silicate solution increases larger silicate composed molecules which is better coordinated by potassium ions[19].Thus, an extra source of silica accelerates the rate of geopolymerization. So, the effect of silica fume at different alkalinity can be monitored by changing the percentage of K_2O in the activator.

Effect of Supplements on Silicate Modulus

The function of sodium silicate is to start the polymerization essentially in an earlier stage. The condensation process in the dissolution of geopolymer follows two stages; one is fast while another is slow[33]. Again, the degree of aluminosilicate polymerization depends on the concentration of silicate solution[34,35]. E. Prud'homme et al. confirm the existence of "in situ inorganic foam" in the presence of silica fume as an

external agent in TGA-MS[25,26]. Here also, the effect of silica fume as supplementary of silicate solution can be investigated.

Effect of Supplements on Water Content

The addition of silica fume in geopolymer mixture enhances di-hydrogen due to oxidation of free silicon in the alkaline medium during synthesis[25]. The favourable effect in workability has already been established in literature[36]. Higher consistency was expected even at lower water content in presence of silica fume. The change in consistency may be quantified in this study by using the typical polar chart as workability setup.

Effect of Supplements on Curing Temperature

The polymeric reaction is emphasized in high-temperature curing[37]. Low temperature or ambient temperature curing for geopolymer exhibits poor structure formation due to delayed setting[27]. The viscosity of geopolymer mixture is in fact increased with the rise in curing temperature[26,27]. All of the aspects like the viscosity of gel, the polarity of gel, stabilization of geopolymer, production of binder product is emphasized by the higher rate of reaction which is a function of curing temperature. The presence of highly reactive silica from silica fume, which is not segregated like kaolinite causes highly soluble and reactive geopolymer system. Here the term segregation refers isolation of nonreactive particles under alkali activation which is largely present in kaolinite. The effect of silica fume on the curing temperature can be further studied to gain more insights behind the previous hypothesis.

Effect of Supplements on Curing Duration

A critical review of existing Literature depicts that increasing curing time improves the polymerization process by maintaining the dissolution of reactive species. Curing of geopolymer at high temperature for a longer period provides lower compressive strength. It is because of the breaking of the granular structure in geopolymer. Again, excessive dehydration and shrinkage affect in the same way[26]. Addition of more reactive silica fume in fly ash geopolymer may enhance amorphous to the semi-crystalline structure. While this semi-crystalline structure gets more affected by longer curing time[38]. The duration of curing time may be optimized with additional silica fume.

Detection Method

Workability at Green State

At the green level, the geopolymer gel was subjected to workability test. The workability was determined by a typical experimental setup. A polar chart was used. Fifty concentric circles and 40 radial lines were present in the chart. Smaller areal segments were best fitted to measure the slump. Every n^{th} circle confirms diameter of n cm. Typical brush cylinder (6 cm diameter, 8cm height) and a circular glass slab were used. The thickness and diameter of the glass slab were 7mm and 50cm respectively (as shown in the Fig.-3a).

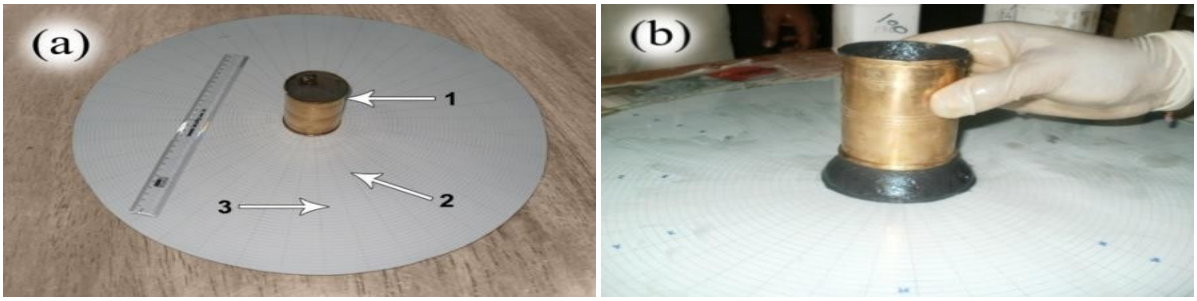

1. Brass cylinder 2. Polar chart 3. Circular shaped glass

Fig.-3: (a) Workability set up, (b) Raising of the cylinder

The polar graph was placed below the glass slab. Then brass cylinder was placed confirming that the centers of cylinder and slab coincide. The brass cylinder was used to hold the paste sample. The mold was filled by the paste sample immediately after 10 mints revolution in Hobart mixture. After one minute of

detention period, the cylinder was elevated to permit the flow of the paste. After a certain time of flow (>1 minute), reading corresponding to the outer most periphery of the flow was taken. The change in the rate of poly-condensation is reflected in the workability. Workability was expressed by the term Area factor. Where "Area Factor" represents the ratio of the area of unconfined paste to that of confined paste. This typical workability measurement procedure was implemented to find the spread of geopolymer paste in our earlier work[31].

Compressive strength at hardened state

Compressive strength test of the specimen was tested by digital compression testing machine of model no. EM500 supplied by ENKAY Enterprise. The least count was 0.001 KN. The direct strength of hardened samples was determined after 3 days along with 28 days in a 2000kN capacity compression testing machine(digital)[39]. The cube strength was determined as per ASTM C109. In each case, three or more than three identical specimens were measured as per ASTM C-109-02, average data were taken as strength.

Microstructure characteristics by SEM and EDX analysis

QUANTA 2000 of capacity 2.4 nm at 30 kv at high vacuum condition was used to find the surface texture and internal morphology. Energy Dispersive X-Ray Analysis (EDX analysis) by ED spectrometer was conducted to find typical elemental configuration. At the time of crushing the samples were collected in a form of chips. The factor like an age for each sample was kept fixed so as to remove the concern like the effect of time on surface texture. The size of the samples was kept at about 5-8 mm in size. The dimension of any sample did not exceed 8 mm.

Pore morphology by MIP analysis

Mercury Intrusion Porosimetry (MIP) was done to evaluate the PSD distribution curve for permeable pores in the form of pore volume versus apparent pore entry radius. The detail features are briefed in Table-2d. MIP was used to examine a numerical link between pore size, distribution and its total volume. Again it also determines the bulk density and apparent porosity at the same time. The intrusion pressure was moved up to 53500 psi for this case. In this method mercury is intruded under pressure in an evacuated sample and volume of intruded mercury is monitored against pressure. Mercury being a non-wetting liquid for most of the solids (especially for cement-based materials and ceramics), the intrusion process follows Washburn's equation that relates pressure to equivalent pore entry radius. Thus radius versus intruded volume curves can be obtained. In this test, the distribution function specifies the portion in a function of any range of pore sizes which in fact yield volume of the pores within those assortments.

RESULTS AND DISCUSSION

Workability

Mobility or consistency is desired only with good strength characteristics. A sample having higher fluidity is not treated as favorable until it provides good enough strength characteristics. In conventional cement concrete, the basic feature at green state is controlled by water/cement ratio and water implies the added free water. To maintain the different mode of operation workability is tuned according to an appropriate mix design to obtain the desired compressive strength. Contrastingly, for geopolymer paste, the scenario is quite different as in this case, the raw materials contain a good amount of water content. Besides the progress of oxidation of Silicon di-hydrogen, more water is accumulated later on. Therefore, consistency is a function of the degree of reaction in the right mode.

Table-2d: Typical Setup of Quantachrome Poremaster and Sample Style

Set up Name	Micromeritics Autopore II
Set up Position	CGCRI, Kolkata
Pressure Range	0-60,000 pis
Hg Surface Tension	480.00 erg/cm^2
Minimum Delta Vol.	0.000% FS

Hg Contact Angle	(I) 140.00^0, (E) 140.00^0
Moving Point Average	11 (Scan Mode). Mercury volume normalized by sample weight
Operating Software	Quantachrome poremaster for Windows Data Report version 7.01
Sample Size	¼ inch diameter and ½ inch height
Bulk Sample Volume:	1.0000 cc

Table-3: Consistency Test Reports of Geopolymer at Green State.

Specimen Id	Primary Diameter (D1) (cm)	Ultimate Equivalent Diameter (D2) (cm)	Primary Area (A1) (cm^2)	Ultimate Area After Flow (A2) (cm^2)	Area Factor =A2/A1
GPK1	6	24	28.26	452.16	16.0
GPK2	6	6	28.26	28.26	1.0
GPK3	6	20	28.26	314	11.1
GPK4	-	-	-	-	-
GPK5	6	36	28.26	1017.36	36.0
GPK6	6	15	28.26	176.63	6.25
GPK7	6	33	28.26	854.87	30.3
GPK8	6	11	28.26	95	3.4
GPK9	6	34	28.26	907.46	32.1
GPK10	6	31	28.26	754.39	26.7
GPK11	6	30	28.26	706.5	25.0
GPK12	6	27	28.26	572.265	20.3
GPK13	6	28	28.26	615.44	21.8
GPK14	6	31	28.26	754.385	26.7

14 individual samples had a typical level of expansion or flow as reported in Table-3. As stated already that alkali cations play a major role for charge compensation of alumina which emphasis the poly-condensation. The consistency of GPK3 was drastically changed from GPK1 as GPK3 had less KOH content. As explained earlier, sodium silicate initiates the polymerization. Sample GPK2 and GPK4 had slight to no plasticity after mixing (as shown in Fig.-3g) due to the absence of Sodium Silicate. Sample GPK5 and GPK7 had higher consistency. It is because of the faster formation of Si-O-Si in the presence of excessive reactive silica. Insufficient alumina is not desirable for the framework structure (tetrahedral) formation which causes weak bonding after curing. This problem can be compensated with the application of external alumina or its equivalent. Appreciable consistency with enhanced structure was obtained for sample GPK9 to sample GPK14. Sample GPK9, GPK10, GPK11 and GPK12 have better consistency in compare to GPK1, GPK2, GPK3 and GPK4 respectively. Most significant observation is that the sample GPK13 and GPK14 have better consistency even at low water content in comparison to that of GPK1 and GPK3.

Compressive Strength

Twenty cubical (50mm × 50mm × 50mm) samples from each series were considered for strength testing. Mean compressive strength value is stated in Table-4. The compressive strengths of paste samples, cured at 85^0 for 48 hours, are given in the first column of Table-4. The silica fume addition (by 10% of total weight) in the presence of murram (2.5% by total weight) gave a better result for every case. Typical volumetric increment (as shown in Fig.-5a) was noticed for Sample GPK5 and GPK7. It may be because of the formation of chain structure instead of frame work structure. Sample GPK5 and GPK7 were not appropriate for testing strength. The geometry of cured GPK5 and GPK7 samples (as shown in Fig.-4a) were not perfect for the compressive strength test. This volumetric increment was reduced by the application of 2.5% murram (by total weight). The replacement of fly ash by a certain amount of silica fume and murram gave a favorable increment of compressive strength. Sample GPK9 showed around 26.25%

increment from GPK1 and Sample GPK11 showed around 58.03% increment from GPK3. Interestingly sample GPK2 and GPK4 had the poor result in absence of sodium silicate solution which allows the primary geopolymerisation as discussed earlier. But GPK10 and GPK12 showed better result even at zero sodium silicate. This result supports that silica fume acted as a partial compensator of sodium silicate solution. As mentioned earlier, external reactive silica emphasizes the oxidation which causes the continuous production of the di-hydrogen at the time of mixing. Due to this fact appropriate consistency was available for sample GPK13 and GPK14 at lower water content. The reduction of excess water (8% drop in water content) gave 14.55% and 20.91% increment in compressive strength from sample GPK9 and GPK11 respectively.

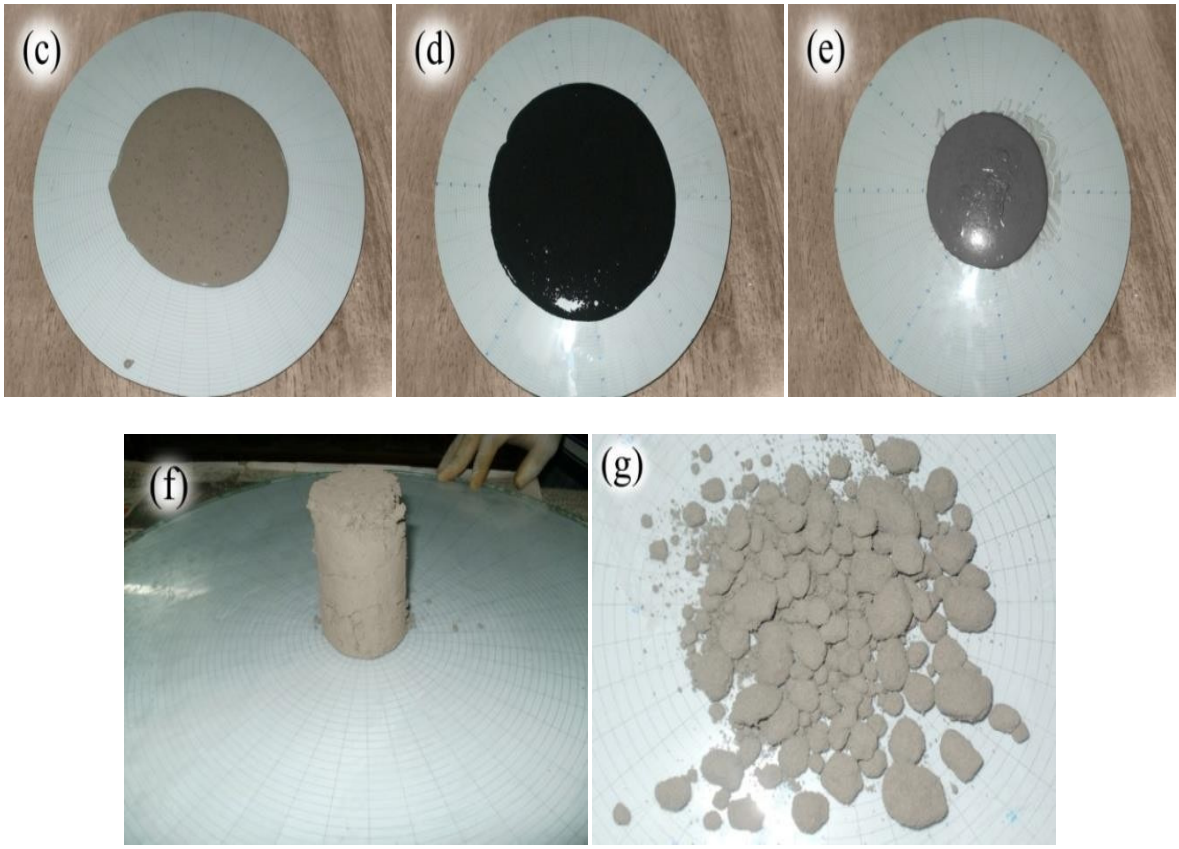

Fig.-3: (c) Sample GPK1, (d) Sample GPK10, (e) Sample GPK3, (f) Sample GPK2, (g) Sample GPK4

Reduction in curing temperature and duration had an adverse effect for every case. The drop in compressive strength for sample GPK9, GPK11, GPK13, and GPK14 were minimum. Due to the reduction in curing temperature from 85^0C to 55^0C, the compressive strength was seen to drop by 7.6% and 8.03% for sample GPK13 and GPK14 respectively. The drop in the strengths were about 37.52%, 68%, 11.42%and 11.86% for sample GPK1, GPK3, GPK9 and GPK11 respectively for the same. Less impact of curing temperature (within a range of 55^0C to 85^0C) on sample blended with silica fume in presence of murram was indicated by the result. Similarly, the reduction in curing period had little to no effect on sample blended with silica fume and murram. A reduction in curing period from 48 hours to 24 hours (at a controlled curing temperature of 85^oC) imposed 7.28% and 2.95% reduction in compressive strength for sample GPK1 and GPK9 respectively. Very little changes in compressive strength were observed in the case of GPK13 and GPK14.Best result was achieved for GPK13.

Scanning Electron Microscopy

Significant change in microstructure of geopolymer paste comprising different mixture combination was exhibited by SEM analysis. The excessive presence of silica enhances the porosity due to the di-hydrogen

produced by water. The typical volumetric increment after 10% replacement of fly ash by silica fume in the primary mix (GPK1) was found as shown in Fig.-5a (representing GPK5). The volumetric enlargement was reduced with the application of murram. For sample GPK10 comparatively compacted and less porous morphology was observed as shown in Fig.-5d The microstructure of sample GPK6 comprising of interconnected pores was observed through SEM (shown in Fig.-5c).

Table-4: Compressive Strengths of Geopolymer Paste Specimens

Sample Id.	Compressive strength (MPa) after heat curing at different temperature and time			
	85^0C for 48 hrs.	85^0C for 24 hrs.	85^0C for 48 hrs.	85^0C for 24 hrs.
GPK1	27.1	25.1	16.9	14.2
GPK2	3.9	3.1	0.0	0.0
GPK3	14.3	11.3	4.6	4.0
GPK4	-	-	-	-
GPK5	-	-	-	-
GPK6	15.8	13.0	10.1	10.1
GPK7	-	-	-	-
GPK8	8.11	7.6	6.6	5.9
GPK9	34.2	33.1	30.3	29.2
GPK10	18.1	16.2	10.6	6.1
GPK11	22.5	21.3	19.9	17.8
GPK12	10.0	9.8	3.5	3.2
GPK13	39.1	39.0	36.1	35.9
GPK14	27.2	27.1	25.1	25

Sometimes the presence of excessive interconnected pores is responsible for low mechanical strength in geopolymer. The micro structure of Geopolymer sample GPK10 had a better surface morphology which was suitably correlated with its attainment of maximum compressive strength. The SEM investigation depicts that better mechanical properties are the outcome of improved micro structural homogeneity. The SEM images for sample GPK11 and GPK12 are represented by Fig.-5a and Fig.-5b respectively. In these cases, the products were better in compare to GPK2 and GPK4, as cultured physically. But the presence of loose precipitates of non-reacted material in GPK12 was indicative of poor reaction. Better bonding was found for sample GPK11.In fact the level of the non-reacted material varies from specimen to specimen may be assumed to provide varying effects on their strength accordingly[40]. The incorporation of external silica emphasizes porous structure due to less formation of Si-O-Al-O than Si-O-Si link, which cannot be stabilized unless there is an additional source of aluminium ions. Further addition of external alumina source (murram) can better stabilize the system resulting in a far better geopolymer. Usually, for fly ash geopolymer (activated with different alkali concentration), better morphology is expected for higher alkalinity. The most interesting observation is that sample GPK4 (non-blended fly ash activated with 6% K_2O) was failed to form full or partial geopolymer structure due to the absence of Sodium Silicate in mixture whereas quite better structure was formed for sample GPK12 (fly ash blended with silica fume and murram, activated by 6% K2O) even at zero silicate modulus of activator. Sample GPK1 cured at different curing profile (85^oC for 48 Hrs. and 55^oC for 48 Hrs.) were cultured at very high magnification SEM images, as represented by Fig. 4b and Fig. 4c. Presence of non-contributed alkali was found entrapped within the pores of sample GPK1, cured at 55^oC for 48 hrs. Comparatively, intact structure was found for sample GPK9 cured at 55^oC for 48 hours, as shown in Fig. 5d. Few micro cracks were developed due to shrinkage and that was effectively reduced by minimizing the curing duration. It is confirmed by SEM investigation that better fly ash based geopolymer structure can be formed at low alkalinity and low level of heat curing, by incorporating silica fume and murram.

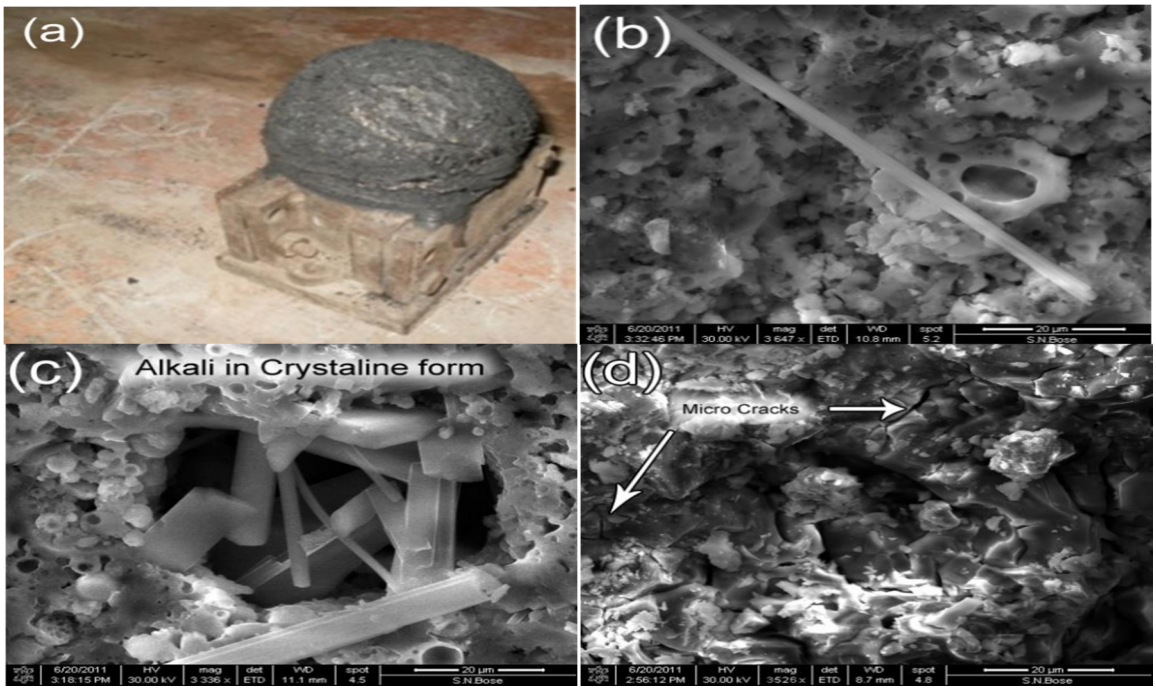

Fig.-4: (a) Sample GPK5,(b) SEM Image of GPK1 cured at 85^{0}C for 48 hrs (mag 3647x), (c) SEM Image of GPK1 cured at 55^{0}C for 48hrs (mag 3336x) and (d) SEM Image of GPK9 cured at 55^{0}C for 48 hours (mag 3526x)

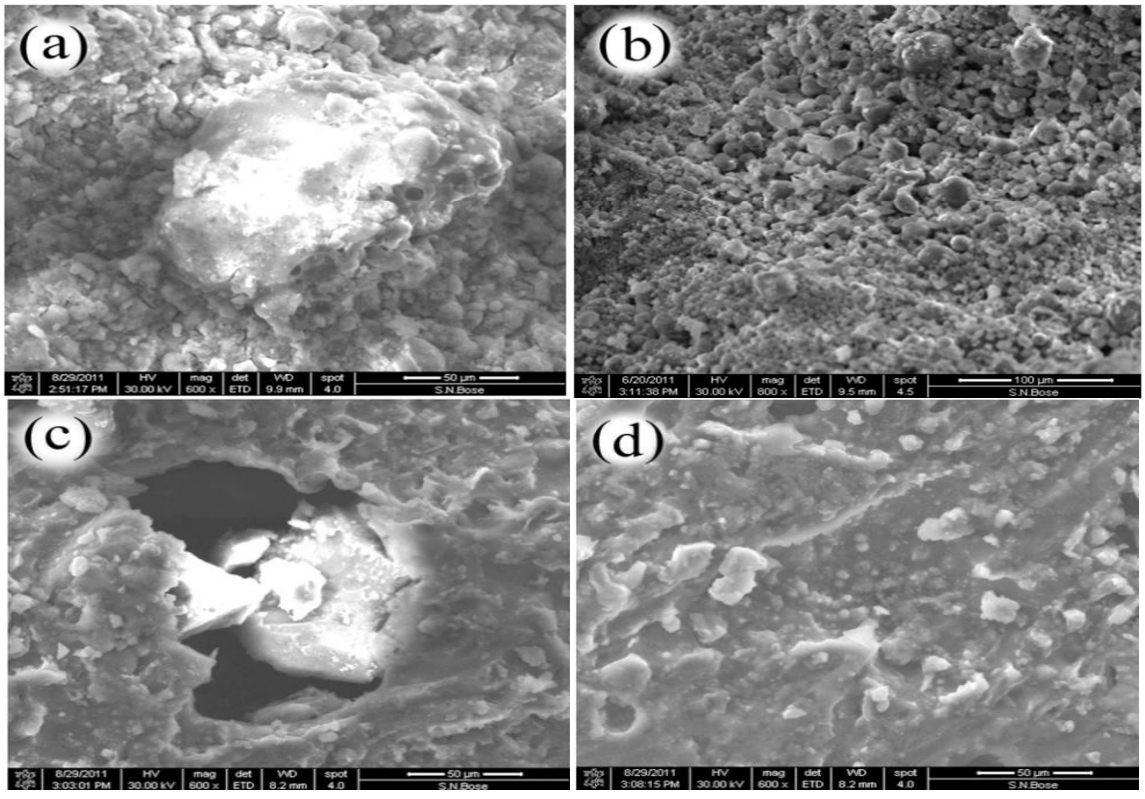

Fig.-5: SEM images of samples
(a) GPK11 (mag 600x), (b) GPK12 (mag 800x), (c) GPK6 (mag 600x), (d) GPK10 (mag 600x)

EDX (Energy Dispersive X-Ray Analysis)

The spectrums of 4 different samples (GPK1, GPK5, GPK9 and GPK11) are shown in Figure-6 for the samples. Each result was selected from thirty individual EDX analysis. The supplementation of silica fume and murram was indicated by the peak in Silicon and Aluminium content as indicated by EDX analysis. The presence of an element like Magnesium, Calcium and Iron was found in almost every case. The greater presence of oligomers, reflecting the higher Si/Al ratio in the reaction product was examined by EDX analysis. In sample GPK1 lower presence of reactive SiO_2 was specified by the increase in K/Si, K/Al ratio and a decrease in the Si/Al ratio. The condition was opposite in GPK5 for the presence of a higher value of SiO2. With the presence of excessive reactive silicon in the form of the composed molecule, the value of K/Si and K/Al ratio were decreased. A higher quantity of potassium and aluminum (Fig.-6c) was exhibited by the EDX analysis of GPK9. This was because of the better stabilization of Si-O-Al due to the presence of additional aluminium acted as the charge balancer alkali cation (Potassium). A little drop in aluminium, potassium content and a corresponding rise in oxygen, silicon was observed in EDX analysis as depicted in Fig.-6d. This time lower KOH was indicated by the successive drop in K/Si. Better elementary distribution was observed by the analysis report of sample GPK9 that was established by the compressive strength of the sample.

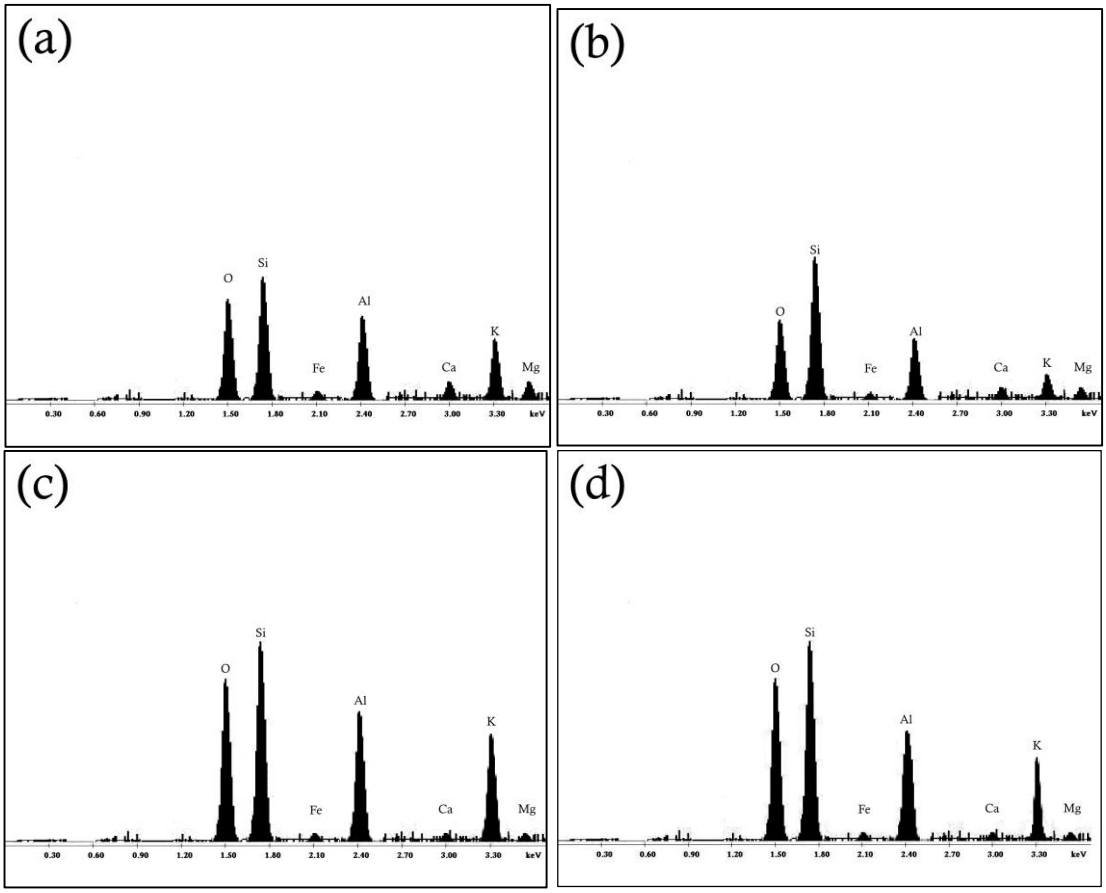

Fig.-6: Electron dispersive spectroscopy (EDS) of samples: (a) GPK1, (b)GPK5, (c) GPK9, (d)GPK1

MIP of Hardened Samples

Pore volume is affected remarkably by the replacement of fly ash with silica fume. Geopolymer sample blended with silica fume and murram provide comparatively intact structure. The replacement of fly ash by silica fume insists the rate of polymerization which in-fact enhances the evaporation of water rapidly. The geopolymer paste sample GPK1 (Cured at 85^0C for 48 hrs.) have a pore distribution contributing from 3.0μ to 0.009μ. Sample GPK9 (Cured at 85^0C for 48hrs) allows the intrusion within a range of 5.0μ to 0.15μ. Mercury intrusion porosimetry has some limitations regarding the information on the pore

characteristics [41]. In this study MIP is used to obtain perfect conclusion even within the limit in connection with porosity and pore size simultaneously. The maximum applied intrusion pressure for sample GPK1 and sample GPK9 are about 53194.551 psi and 53228.703 psi respectively. In this test, pore volume distribution represents a function F equal to -dV/ dlogD. Here, V equal to the combined pore capacity. In Fig.-7 pore volume distribution function is plotted with pore diameter for sample GPK1 and GPK9. The geopolymer sample GPK1 shows significant intrusion within a diameter, range of 5 micrometres to 0.2 micrometer and maximum peak intrusion appears at 2 micrometres. The sample GPK9 gives prominent intrusion within a range of 2 micrometer to 0.009 micrometer and the maximum peak has been attended at 0.075 micrometer. This phenomenon clearly indicates the drop in average pore size for the sample GPK9. Fig.-8 and Fig.-9 show noticeable difference in the pressure responsible for the sudden change in delta volume. At a pressure of 398.638 psi a sudden increment in delta volume (0.0228 cc/g) occurs for sample GPK9 whereas a sudden increment of delta volume (0.0326cc/g) has been observed for sample GPK1 at a pressure of 93.746 psi. The pore diameters responsible for the sudden change in delta volume are 2.276 micrometer and 0.535 micrometer for sample GPK1 and GPK9 respectively. In both the cases, the hysteresis loop between the intrusion and extrusion are visible which indicates the amount of fluid unable to extrude. It is found that the mode of extrusion curve has been discontinued for sample GPK1 which is basically due to the breaking of the specimen for excessive internal pressure. Physically it can be explained that the bottle neck shape of pores allows the smoother intrusion but restricts the extrusion in the same way. Though the range of pores responsible for intrusion is quite larger in case of sample GPK9, but it happens comparatively at a higher intensity of pressure. It is noticeable that around 41.85% and 87.67% volume are intruded at a pressure of 1022.157 psi for sample GPK9 and 943.212 psi for sample GPK1 respectively. This depicts that percent volume intrusion is almost twice for sample GPK1 in compare to sample GPK9 even at same pressure intensity. Parallel to that smoother extrusion curve indicates no breakage of sample GPK9 which supports the strong integrity of the structure.

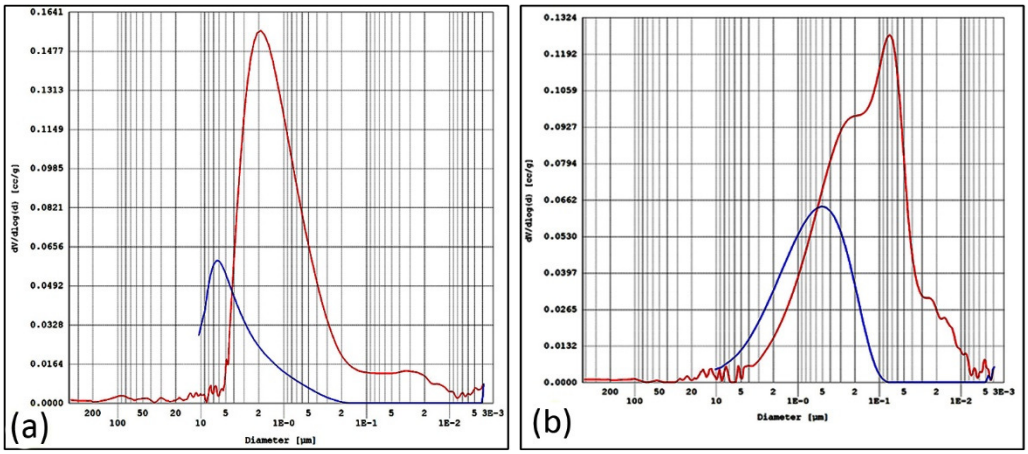

Fig.-7: MIP distribution curve of samples (a) GPK1 and (b) GPK9

CONCLUSION

A detailed micro-structural study and a comparative performance analysis have been performed for the developed blended geopolymer paste by replacing fly ash with fume silica and murram in the present experimental study.

The major findings of this papers are as follows:

- Murram as a tertiary input in silica fume blended fly ash improves the mechanical properties of the geopolymers. Although the addition of only silica fume reduces the mechanical properties of geopolymer due to the lesser formation of three-dimensional geopolymeric aluminosilicate network, the effect of silica fume is found to be favorable in the presence of murram. In its presence, silica fume is likely to result in initial polymerization even in absence of sodium silicate.

- Moreover, higher consistency is quantified for samples blended with silica fume even at lower water content and lower alkalinity. Geopolymer samples blended with silica fume and murram exhibit better performance.
- The presence of the extra alkaline solution in fly ash based geopolymer caused by partial dissolution of the fly ash spheres is found to be absent for samples blended with silica fume and murram. This reflects the increment in dissolution rate of fly ash, which is favorable in the reduction of efflorescence.
- A high strength geopolymer with high workability was successfully made even at lower water content and lower curing heat consumption.
- Rising of curing temperature and duration have little to no effect on the strength of blended geopolymer in the presence of silica fume & murram. It may be because of the silica fume and murram which introduce acceleration to the rate of polymerization with a reduced external parameter.
- The inception data of the intruded volume pore sizes and corresponding pressure indicate better micro-structure of y ash based geopolymer blended with silica fume and murram.
- It is found that the coexistence of silica fume and murram in a moderate amount is responsible for the better strength, consistency, micro-structure for every case, even at lower alkalinity, lesser water content and lesser heat energy consumption.

The present research was inclined towards the development of sustainable construction materials by utilizing environmental outcomes (called disposals) to take a step further towards a greener environment. The authors are currently focussing on the development of fly ash based geopolymer activated with naturally available alkali like sludge etc. The effect of different acids and salts of different concentration on blended geopolymer are currently being evaluated.

Prolonged microstructural study on blended and non-blended fly ash Geopolymer with time and its impact on strength and stability are the future scopes of this study. Evaluation of the economic stand of the blended fly ash based geopolymer should also be justified in future.

REFERENCES

1. D. N. Huntzinger and T. D. Eatmon, *J. Clean Prod.,* **17(7)**, 668(2009), **DOI:** 10.1016/j.jclepro.2008.04.007
2. V. M. Malhotra and P. K. Mehta, *High-Performance, High-Volume Fly Ash Concrete: Materials, Mixture Proportioning, Properties, Construction Practice, and Case Histories,* Supplementary Cementing Materials for Sustainable Development Inc., Ottawa, p. 1-124 (2005).
3. R.A. Feely, C. L. Sabine et al., *Science,* **305**, 362(2004), **DOI:** 10.1126/science.1097329
4. P. K. Mehta and R.W. Burrows, *ICJ*, **75(7)**, 437(2001), **DOI:**10.1.1.475.5570
5. A. Castel and S. J. Foster, *Cem. Concr. Res.,* **72,** 48(2015), **DOI:**10.1016/j.cemconres.2015.02.016
6. N Ganesan and et al., *Constr. Build. Mater.*, **73**, 326(2014), **DOI:** 10.1016/j.conbuildmat.2014.09.092
7. M. Mohammadreza and K. A. Riding, *Cem. Concr. Comp.,* **56**,95(2015), **DOI:** 10.1016/j.cemconcomp.2014.10.004
8. A. Nadeem, S. Ali Memon, and T. Yiu Lo, *Constr. Build. Mater.*, **38**, 338(2013), **DOI:** 10.1016/j.conbuildmat.2012.08.042
9. Mehta, P. Kumar, High-performance, *Proceedings of the international workshop on sustainable development and concrete technology. Ames, IA, Iowa State University*, May 20-21, 03, (2004).
10. J. Temuujin, R. P.Williams, and A.V. Riessen, *J. Mater. Process. Technol.,* **209(12-13)**, 5276(2009), **DOI:** 10.1016/j.jmatprotec.2009.03.016
11. P. Sarker, R. Haque, and K.V. Ramgolam, *Mater. Des.,* **44**, 580(2013), **DOI:** 10.1016/j.matdes.2012.08.005
12. K. Somna, C. Jaturapitakkul, P. Kajitvichyanukul, P. Chindaprasirt and et al., *Fuel,* **90(6)**, 2118(2011), **DOI:** 10.1016/j.fuel.2011.01.018
13. P. Chindaprasirt, P. Paisitsrisawat and U. Rattanasak, *Adv. Powder Technol.,* **25(3),** 1087(2014), **DOI :**10.1016/j.apt.2014.02.007
14. N. K. Lee, G. H. An, K.T. Koh and G. S. Ryu, *Adv. Mater. Sci. Eng.,* **2016,** Article ID 2192053(2016), **DOI:**10.1155/2016/2192053

15. Okoye, N. Francis, S. Prakash, and N. B. Singh, *J. Clean. Prod.*, **149**, 1062(2017), **DOI:**10.1016/j.jclepro.2017.02.176
16. P. Duan, C. Yan, and W. Zhou, *Cem. Concr. Comp.*, **78**, 108(2017), **DOI:** 10.1016/j.cemconcomp.2017.01.009
17. K. Kohno, *In Proceedings of the third international conference on the use of fly ash, silica fume, slag and natural pozzolans in concrete, Trondheim, Norway,* 1989, *American Concrete Institute Publication* SP-114, 815826, (1989),
18. H. Cheng-Yi, R. F. Feldman, *Cem. Concr. Comp.*, **15**, 585592 (1985), **DOI:**10.1016/0008-8846(85)90056-0
19. J. Davidovits, *Geopolymer Chemistry and Applications,* Geopolymer Institute (2008).
20. H. Xu, J. S. J. Van Deventer, *Int. J. Miner. Process.,* **59(3)**, 247(2000), **DOI:**10.1016/S0301-7516(99)00074-5
21. A. Kumar and S. Kumar, *Constr. Build. Mater.,* **38**, 865(2013), **DOI:** 10.1016/j.conbuildmat.2012.09.013
22. Ye Nan and et al., *J. Am. Ceram. Soc.*, **97(5)**, 1652(2014), **DOI:**10.1111/jace.12840
23. Mo. Zhang and et al., *Fuel* **134**, 315(2014), **DOI:** 10.1016/j.fuel.2014.05.058
24. M. W. Grutzeck, D.D. Siemer, *J. Am. Ceram. Soc.*, **80(9)**, 24492458 (1997), **DOI:**10.1111/j.1151-2916.1997.
25. D. Khale and R. Chaudhary, *J. Mater. Sci.*, **42(3)**, 729-746 (2007), **DOI:**10.1007/s10853-006-0401-4
26. E. Prudhomme and et al., *J. Eur. Ceram. Soc.*, **30**, 1641(2010), **DOI:** 10.1016/j.jeurceramsoc.2010.01.014
27. Kirschner, Andrea, Harald Harmuth, *Ceram. Silik.*, **48 (3)**, 117(2004)
28. S. Thokchom, P. Ghosh and S. Ghosh, *J. Civ. Eng. Manag.*, **17 (3)**, 393(2011), **DOI :**10.3846/13923730.2011.594225
29. A. Palomo, M. W. Grutzeck and M. T. Blanco, *Cem. Concr. Res.*, **29(8)**, 1323(1999), **DOI:**10.1016/S0008-8846(98)00243-9
30. J.T. Gourley, *conference on adaptive materials for a modern society, Sydney, Institute of materials engineering Australia,* **49 (15-26)**, 1455(2003).
31. D. Dutta, S. Chakrabarty, C. Bose, S. Ghosh, *STM Journals*, **2**, 1(2012).
32. D. Dutta, S. Ghosh, *Adv. Civ. Eng.*, **12**, 2940169 (2018), **DOI:**10.1155/2018/2940169
33. P. Duxson, A. Fernandez-Jimenez, J.L. Provis, G.C. Lukey, A. Palomo, J.S.J. van Deventer, *J. Mater. Sci.*, **42**, 2917(2007), **DOI:**10.1007/s10853-006-0637
34. E. Obonyo, E. Kamseu, U. C. Melo, C. Leonelli, *Sustainability,* **3(2)**, 410(2011), **DOI:**10.3390/su3020410
35. Mohd. N. Qureshi and S. Ghosh, *Adv. Civ. Eng. Mater.*, **2 (1)**, 62(2013), **DOI:** 10.1520/ACEM20120029.
36. F. A. Memon, M.F. Nuruddin, N. Shafiq, *Int. J. Min. Met. Mater.,* **20 (2)**, 205(2013), **DOI:** 10.1007/s12613-013-0714-7.
37. J. J. Brooks, *ACI Mater. J.*, **99 (6)**, 591(2002).
38. J.G.S. Van Jaarsveld, J.S.J. Van Deventer and G.C. Lukey, *Chem. Eng. J.,* **89(1-3)**, 63(2002), **DOI:** 10.1016/s1385-8947(02)00025-6.
39. D. Dutta, S. Ghosh, *Cur. Adv. Civ. Eng. (CACE), American V-King Scientific Publishing,* **2(3)**, 96 (2014).
40. P. Duxson, J. L. Provis, G. C. Lukey, S. W. Mallicoat, W. M. Kriven and J. S.J. van Deventer, *Colloids Surf. A. Physicochem. Eng. Asp.,* **269(1-3)**, 4758 (2005), **DOI:** 10.1016/j.colsurfa.2005.06.060.
41. J. Van Brakel, *Powder Tech.*, **29**, 201(1981).
42. K. Ghosh and P. Ghosh, *Rasayan J.Chem.*, **11(1)**, 426(2018), **DOI:** 10.7324/RJC.2018.1112036

[RJC-3046/2018]

Microstructure of Fly Ash Geopolymer Paste with Blast Furnace Slag

Debabrata Dutta*[1], Somnath Ghosh[2]

Department of Civil Engineering, Jadavpur University, Kolkata, India

ddebabrata83@gmail.com

Abstract- **An experimental investigation has been carried out to study the physical, mechanical and microstructural properties due to incorporation of blast furnace slag in the fly ash based geopolymer. Geopolymer specimens has been prepared by activating class F fly ash with sodium hydroxide and sodium silicate, blast furnace slag has been incorporated as substitute in the mix @ 0%, 10% and 15% by weight of fly ash. Substitution of blast furnace slag stabilise the mechanical feature which was a function of time earlier. The basic objective of this work is to recognize the constancy of compressive strength which in fact represents the permanence of geopolymer structure. The successive development of crystallise compound within the pores for time being increase the internal pore pressure. This developed pressure increase the compressive load carrying capacity for the fly ash geopolymer paste to some extent with time being but insist development of crack later on due to excessive tensile pressure. The change in physical property due to slag integration has been evaluated with mercury instruction porosimeter. MIP results indicate sharp drop in pore sizes for the specimen prepared with blast furnace slag. The microstructural characterization of the geopolymer specimens were also done by a scanning electron microscopy and EDAX analysis. SEM micrographs showed more homogeneous and amorphous microstructure for specimens incorporated with blast furnace slag.**

Keywords- Fly Ash; Blast Furnace Slag; Geopolymer; MIP; Compressive Strength; SEM; EDAX

I. INTRODUCTION

Modern Industrial process generates vast quantities of materials which are used to a limited extent and are primarily treated as wastes. This wastes leads to pollution in the environment directly. Waste utilization is of great importance for the scientists and engineers. With increasing demand for production, the rate of waste production has also increased day to day. Gainful utilization of these wastes is needed attention.

Ground granulated blast furnace slag and fly ash are being used in cement production up to a certain extent. In the year 1970; Joseph Davidovits has introduced a synthetic material which was termed as 'Geopolymer'. A plenty of research and development on this subject has proved geopolymer can be prepared from these waste materials, by activating these with suitable alkaline solution. Waste materials such as metakaolin, fly ash, blast furnace slag, silica fume etc are used as source materials. Geopolymer can be defined as "the material that results from the geosynthesis of polymeric alumino-silicates and alkali-silicates, yielding a three-dimensional polymeric framework of linked SiO_4 and AlO_4 tetrahedra" [2].

Geopolymer materials are reported to possess high early strength, higher durability and have almost no alkali-aggregate reaction [1]. These materials are therefore projected as alternate to conventional cement in future [3]. The $Na_2O/SiO_2$and Na_2O/Al_2O_3 ratios have great impact on its mechanical properties of geopolymer.Thakur [4] observed that when the Na_2O/SiO_2 or Na_2O/Al_2O_3 ratio increases the compressive strength increases , [5] reported that the increase of water/ Na_2O ratio reduces the compressive strength of geopolymer. Higher Na_2O:SiO_2 and NaOH molarity shows better performance in compressive strength [6]. The tetrahedral structure enhances the porous nature of geopolymer.

As porosity directly affect the compressive strength, a concept of blended geopolymer by the use of additives or dopants emerged out to improve the porosity as well as the strength and other properties. Moderate amount of minerals addition to a geopolymer can significantly improve the geopolymer structure and properties.Temuujin [7] suggested that the addition of calcium compounds CaO and $Ca(OH)_2$ improves mechanical properties of the fly ash-based geopolymers cured at ambient temperature.

In this study blast furnace slag was used as a substitute. An extensive study on the effect of blast furnace slag substitution in fly ash based geopolymer received special attention on its microstructural and mechanical properties. This paper represent the analysis report of geopolymers synthesised at 85^OC temperature for 48 hours by using class F fly ash as the source material, blast furnace slag was used as substitute and NaOH and Na_2SiO_3as activator.

II. EXPERIMENTAL

A. Materials

Class F fly ash used in the research was collected from Kolaghat Thermal Power Plant near Kolkata, India. About 75% of particles were finer than 45 micron and Blaine's specific surface was $380m^2/kg$. The chemical composition of fly ash is given in Table-1. The blast furnace slag used was in powdered form having specific gravity 2.8, bulk density 1236 kg/m^3, consisting of 39.07% CaO. The average particle size of blast furnace slag was varied between 35µ to 65µ. The chemical composition of blast furnace slag is given in Table 2.

Laboratory grade sodium hydroxide in pellet form (98 percent purity) and sodium silicate solution (Na_2O= 8%, SiO_2 =26.5% and 65.5% water) with silicate modulus ~ 3.3 and a bulk density of 1410 kg/m^3 was supplied by Loba Chemie Ltd, India.

Fig. 1 SEM Image of Fly Ash

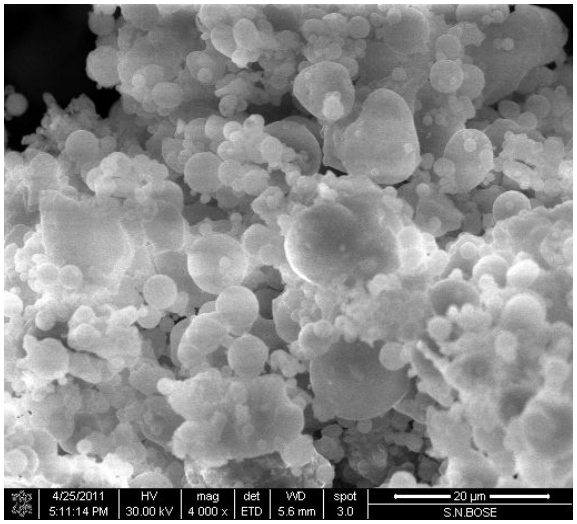

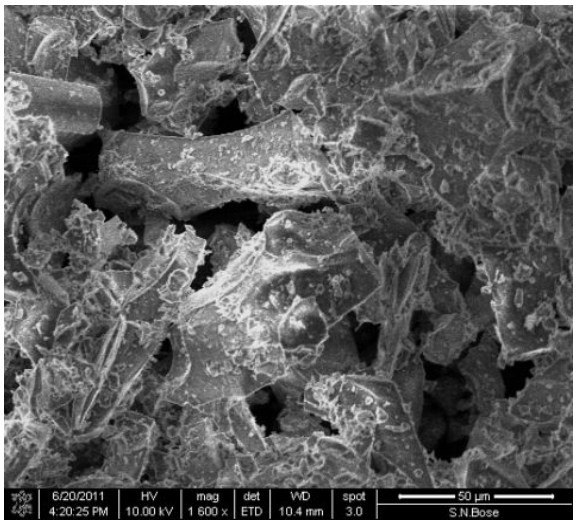

Fig. 2 SEM Image of blast furnace slag

TABLE I CHEMICAL PROPERTIES OF FLY ASH

Chemical composition	SiO_2	Al_2O_3	Fe_2O_3	TiO_2	CaO	MgO	K_2O	Na_2O	SO_3	P_2O_5	Loss on Ignition
Fly Ash	56.01%	29.8%	3.58%	1.75%	2.36%	0.30%	0.73%	0.61%	Nil	0.44%	0.40%

TABLE II CHEMICAL ANALYSIS REPORT OF BLAST FURNACE SLAG

Chemical composition	CaO	MgO	Fe_2O_3	MnO	Al_2O_3	SiO_2	Loss on ignition
Blast furnace slag	39.07%	8.95%	1.87%	0.44%	15.18%	30.26%	0.04%

B. Preparation of Solution, Specimens and Testing

The alkaline activating solution was prepared by dissolving required quantity of sodium hydroxide pellets directly into water .The activator solution (sodium hydroxide and water) was left at room temperature for 24 hours after that predetermined quantity of sodium silicate solution was added 3 hours before casting of geopolymer specimens. It had Na_2O content and SiO_2 content as 8.0% of fly ash, thereby making SiO_2/Na_2O ratio of 1. Water to Fly ash ratio was of 0.33.

In a Hobart mixer, fly ash, with or without blast furnace slag (according to Table 3) was mixed with predetermined quantity of activator solution for 5 minutes. The geopolymer mix exhibited a thick sticky nature with good workability. The mix was transferred into 50 x 50 x 50 mm cubes followed by table vibration for 2 minutes to expel any entrapped air. After 60 minutes of air dry, the cubes were cured in a hot air oven for a period of 48 hours at 85^OC and then allowed to cool inside the oven [8]. Specimens were removed and stored at ambient temperature in a dry place before testing. Geopolymer paste mixture composition and curing environment is given in Table 3.

The geopolymer specimens were tested for its water absorption. The compressive strength was tested with digital compressive testing machine. The microstructural properties were studied with scanning electron microscope and electron diffraction spectrum. Pore characteristics were studied by mercury intrusion porosimeter, using Quantachrome Pore master 60, at a contact angle 140^O which measured total intruded volume of mercury into the specimens.

TABLE III MIXTURE COMPOSITION OF GEOPOLYMER PASTES

Sample ID	Na_2O content in activator (%) of (fly ash + slag) in wt.	SiO_2 content in activator (%) of (fly ash + slag) in wt.	Blast furnace slag (%) of (fly ash + slag) in wt.	Type of specimen	Water / fly ash ratio	Curing temp. and duration
GP1	8	8	0	Paste	0.33	85^0C and 48 hrs
GB1	8	8	10	Paste	0.33	85^0C and 48 hrs
GB2	8	8	15	Paste	0.33	85^0C and 48 hrs

III. RESULTS AND DISCUSSIONS

A. Mercury Intrusion Porosimetry (MIP)

Mercury intrusion porosimetry was used to investigate the total porosity and the pore size distribution of the geopolymer specimens. The bulk volume of each test specimen was 1cc and maximum applied intrusion pressure during the test was about 53500 psi. In the feature of this very test pore volume distribution is presented as a distribution function, F Where

$$F = - dV / d \log D$$

V = collective pore volume

It indicates the part under a function of any pore diameter range capitulate pore volume of pores in that range.

Pore volume distribution function and pore diameter of the paste specimens are plotted in Figure 3. It can be noticed that substitution of fly ash by blast furnace slag in the mix has a significant influence on the average pore sizes. In case of geopolymer mix GB2 (specimen blended with 15% blast furnace slag) the significant intrusion is prominent from diameter range 0.02 to 1.5 micro meter, whereas for geopolymer mix GP1 (geopolymer without blast furnace slag) the same ranges between 0.1 to 10 micrometer. Peak intrusion appears at 0.3 micrometer and 0.4 micrometer for GB2 and GP1 respectively. The volume of larger pores may seem smaller due to bottle-neck shapes of pores [9].It is clear that the pore size in calcium blended geopolymer is distributed at the order of lesser pore diameter. Figure indicates the ultimate breaking of sample for GP1 through the absence of extrusion curve. This may occur due to larger pore pressure offered by the mercury without getting the provision of expulsion. Structural crumple may be due to empty spaces that are unapproachable on the way to the mercury. A lag in the volume extruded vs. the volume intruded at the similar pressure is clearly observed even in Figure 3 for GB2, forming a hysteresis loop in the intrusion and extrusion curves. Significant variation in mean median pore sizes is noticed due to blast furnace slag substituted into the geopolymer mix.

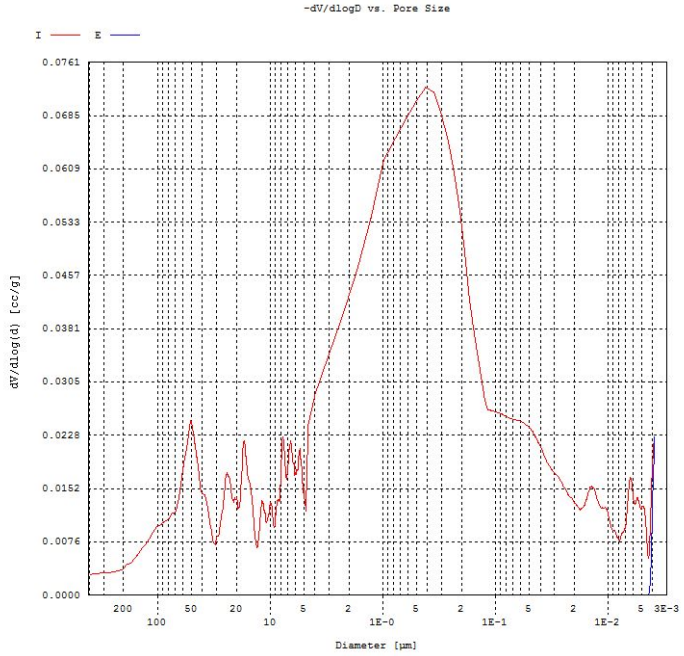

(GP1)

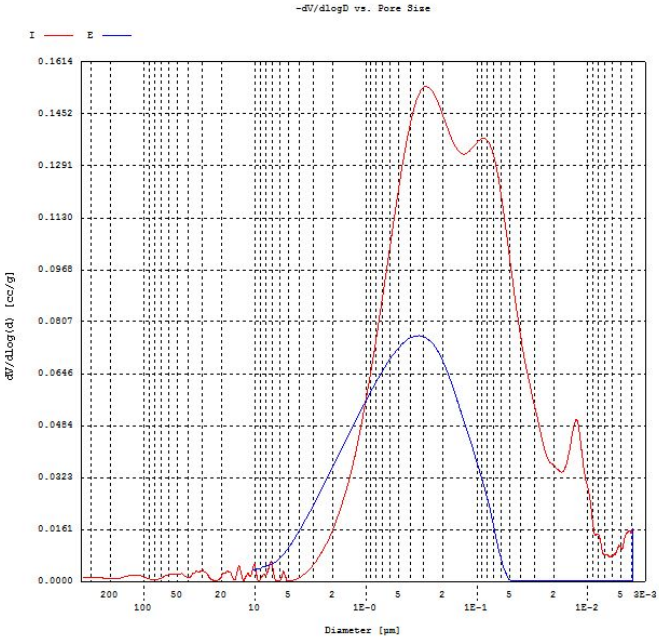

(GB2)

Fig.3 Relationship of Pore volume distribution function with pore diameter

B. Microstructural Investigation by Scanning Electron Microscopy

SEM analysis was conducted to understand pore morphology and view the reacted and unreacted regions of the samples. Fig. 4, 5, and 6 presents the ESEM micrographs for geopolymer paste specimens GP1, GB1 and GB2 along with their EDAX traces. In all the micrographs of specimens, it depicts a microstructure having some unreacted and partly reacted particles embedded in the geopolymer gel. The micrographs reveal mostly an amorphous phase with pores of various sizes. GP1 specimen that is prepared without blast furnace slag appears to be more porous than other specimens GB1 and GB2 which contain 10% and 15% blast furnace slag respectively. Another significant observation is that surface texture is smoother and compact in specimens with blast furnace slag addition which was observed in higher magnification. The magnification corresponding GP1, GB1 and GB2 are 600 x, 1200x and 1600x respectively.

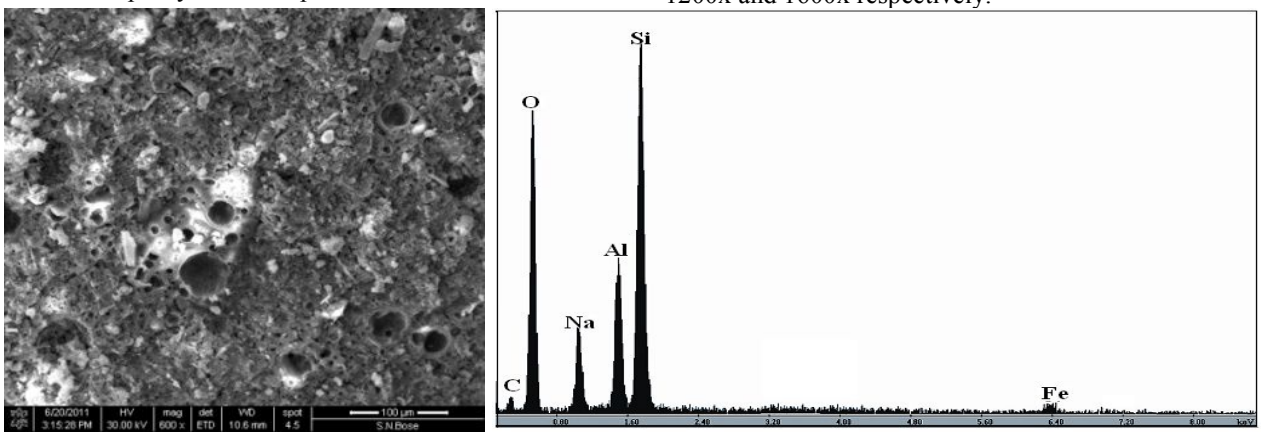

Fig. 4 SEM @ 600x zoom and EDAX of Sample GP1

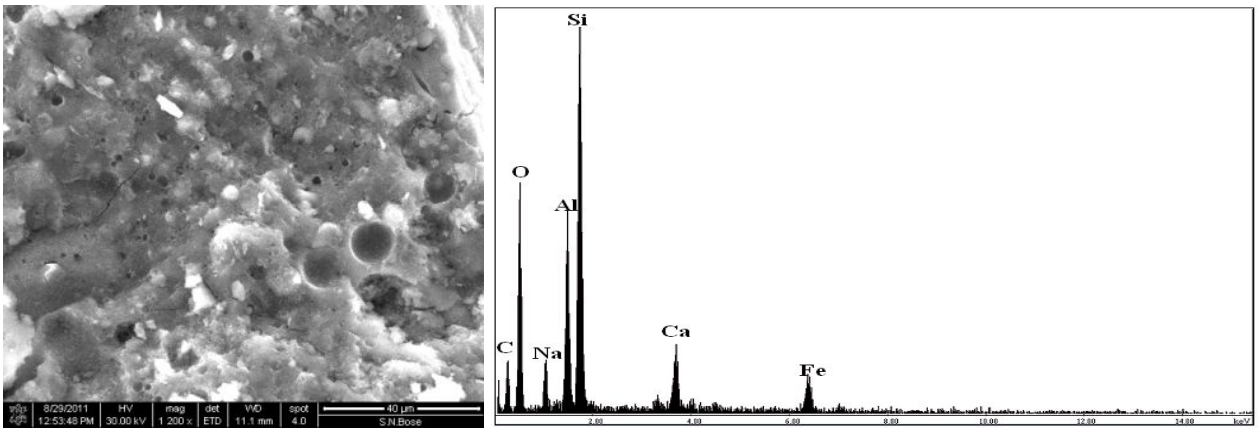

Fig. 5 SEM @ 1200 x zoom and EDAX of Sample GB1

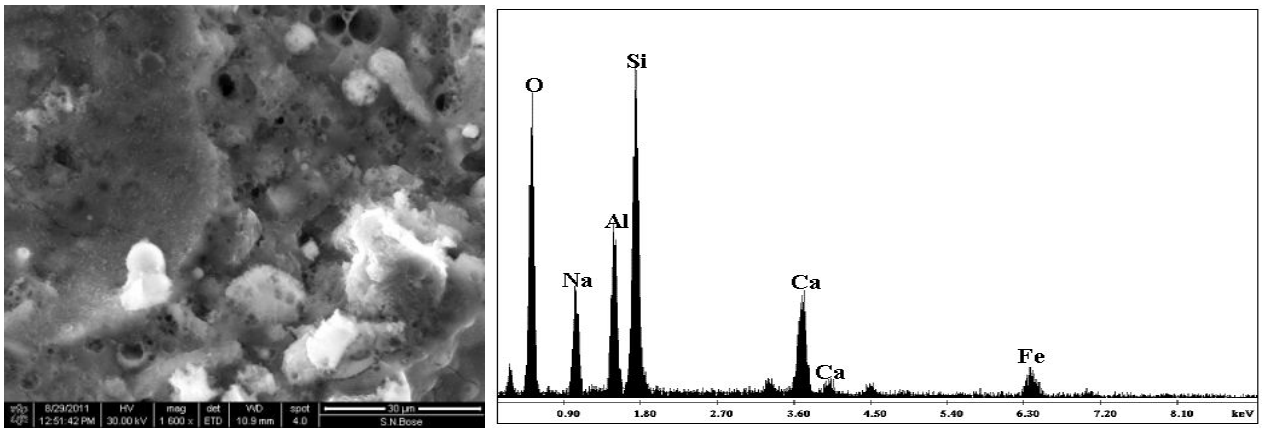

Fig. 6 SEM@ 1600x zoom and EDAX of Sample GB2

Larger magnification of GP1 specimen shows (Fig. 4a, Fig. 4b, Fig. 4c, Fig. 4d, Fig. 4e and Fig. 4f) some regular structure within the pores. Despite being amorphous by definition, the existence of regular structure does not

support the pure amorphous character of geopolymer. Beside this it proves the presence of crystalline feature. The transformation from liquid precursor to "solid" gel and the mechanisms of densification gives the means to control the nanostructure, porosity and properties of geopolymers again the gelation results from hydrolysis–polycondensation of aluminum and silicon included species, resulting in a complex network inflamed by water trapped in the pores [10]. As per EDAX spectra(Fig. 4g) taken on that very crystalline portion having a diameter of 152 nm indicate the presence of crystallise Sodium compound.EDAX spectra of specimens shows major elements such as carbon (C), oxygen (O), aluminium (Al), silicone (Si), calcium (Ca) and sodium (Na). The weight percentages of some important elements were Si (15.95%), Al (8.38%), Na (3.71%) and Ca (0.85). GB1 having a blast furnace slag content of 10% also has similar elements. However, the weight percentages of important elements are different for GB1 which shows Si (19.93%), Al (9.13%), Na (4.94%) and Ca (3.32). For GB2 specimen prepared with addition of 15% blast furnace slag, the weight percentages from EDAX analysis yielded as Si (26.54%), Al (8.46%), Na (5.33%) and Ca (10.52). EDAX analysis supports the formation of Na-aluminosilicate hydrates. This smooth texture of GB1, GB2 may be due to the formation of C-S-H and the formation of geopolymer, leading to a fine and homogeneous structure [11].

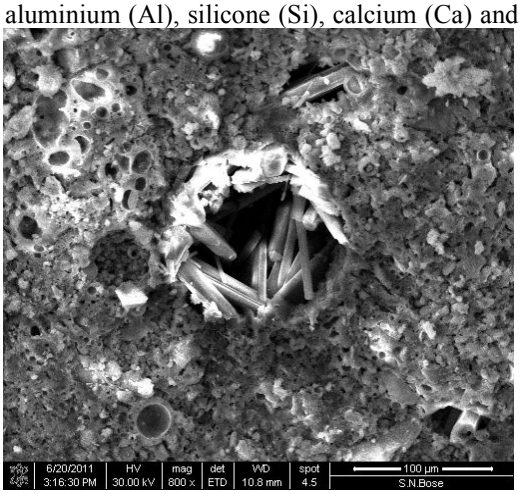

Fig. 4a. SEM of Sample GP1@800x zoom

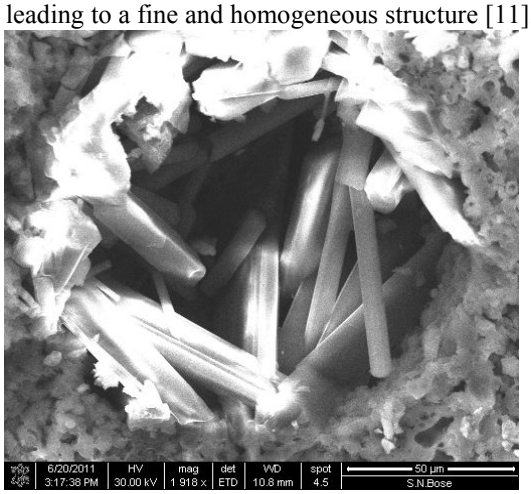

Fig. 4b SEM of Sample GP1@1916x zoom

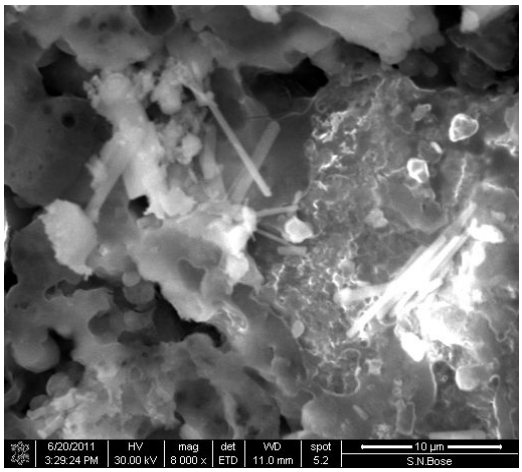

Fig. 4c SEM of Sample GP1@8000x zoom

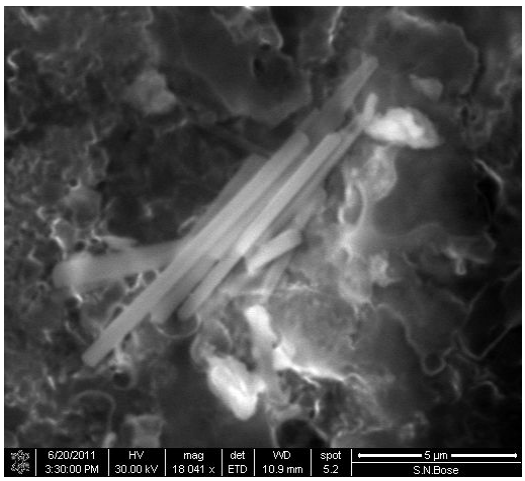

Fig. 4d SEM of Sample GP1@18041x zoom

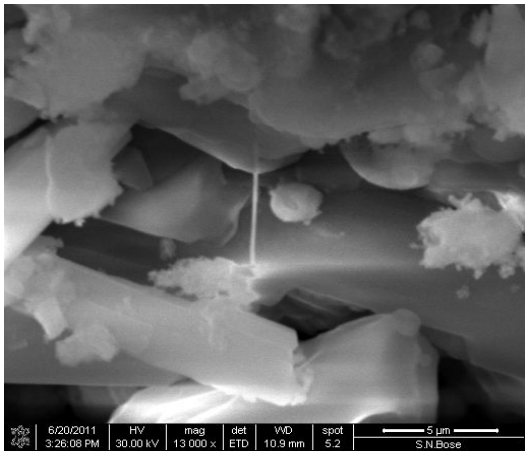

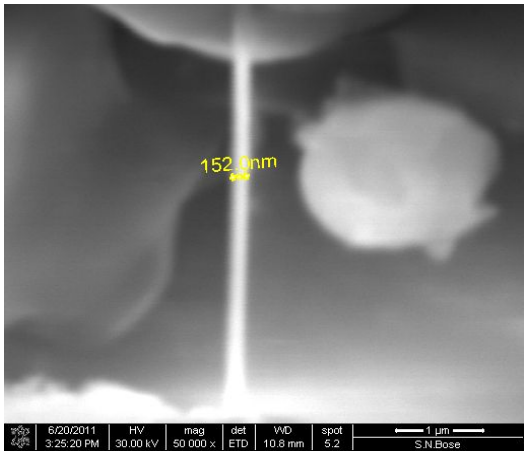

Fig. 4f SEM of Sample GP1@50000 x zoom

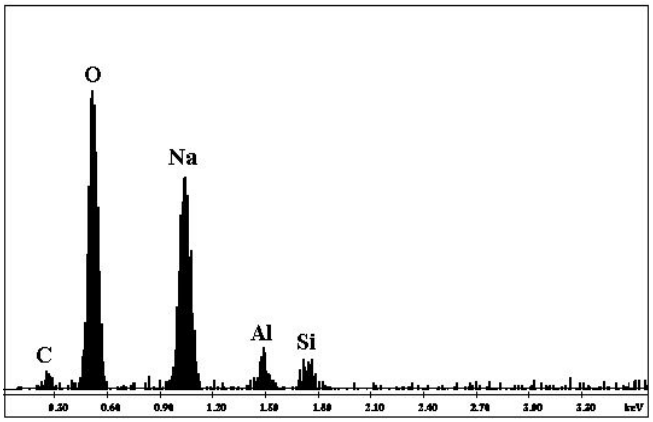

Fig. 4g EDAX of crystalline compound within the pore

C. Compressive Strength and its Consistency

High calcium content mixes give quick hardening behavior which minimize the time of hardening of fly ash based geopolymer. Higher $CaCO_3$ content may results in faster geopolymerisation due to the formation of semi-crystalline Ca-Al-Si gel [12]. The compressive strength of the geopolymer paste was determined after 3 days of synthesis. Ten specimens for each mix composition were subjected to compression in a digital compressive strength testing machine and the average is reported in Figure 7a. GP1 specimen prepared without blast furnace slag has a compressive strength of 37 MPa. Significant increases of strength occurred for GB1 specimen (39 MPa) which contained 10% blast furnace slag. Similarly, the compressive strength further increased (41 MPa) with additional blast furnace slag of 15%. It accounts a strength increase of 10.81% for GB2 compared to GP1. The results clearly indicate successive increment in compressive strength of the specimens with higher blast furnace slag addition.

But the motto of this work is to understand the stability of compressive strength which in fact represents the stability of geopolymer structure. The successive formation of crystallise compound within the pores for time being increase the internal pore pressure. This developed pressure increase the compressive load carrying capacity for the GP1 specimen with time being to some extent. As the developed tensile stress acts against the compressive load which is imposed externally. This phenomena emphasis compressive strength for a little period but the nature of crystalline feature is very much unstable. Due to the successive formation of crystallise compounds the internal pore pressure is increased which causes generation of micro cracks. This may cause a drop in compressive strength.A result of 90 days study has been represented in Figure 7b.No further remarkable increase in compressive strength was observed for specimens GB1 and GB2 with time. Whereas compressive strength for sample GP1 ceases 74 MPa after 90 days even. Again development of partial crystallise structure was proofed with the evaluation of metallic sound at the time of crushing. But most of the samples within GB1 and GB2 do not exhibit the same. Again GB1 and GB2 samples were accounted as single break crush. Larger Ca

Fig. 4e SEM of Sample GP1@13000x zoom

content decreases the microstructural porosity of geopolymer by forming amorphous structure Ca–Al–Si gel during geopolymerization [14],[15],[16]. This phenomena is also sustained by the investigation [17] of ground granulated blast furnace slag ,states that calcium included compounds such as calcium silicates, calcium aluminate hydrates, and calcium-silico-aluminates are produced during geopolymerization of fly ash, which influence the setting and workability of the mix [13].

Most remarkable drawback for GP1 specimens is that it major percentage shows hair crack after 15-16 weeks from preparation which allows the sudden drop in compressive strength. This phenomenon is due to the consistent progress in pore pressure.

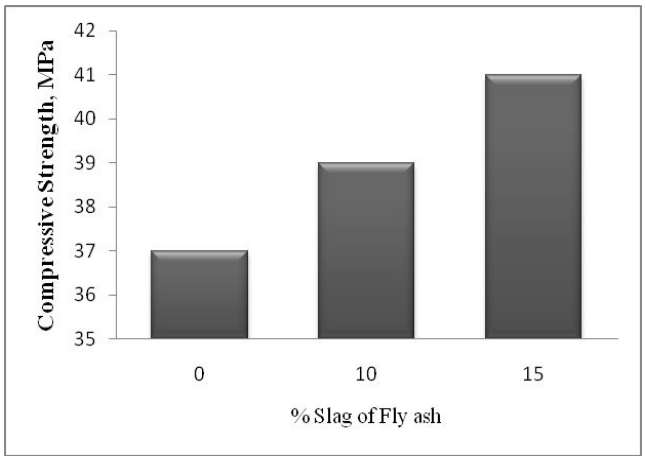

Fig. 7a 3 day compressive strength of geopolymer specimens.

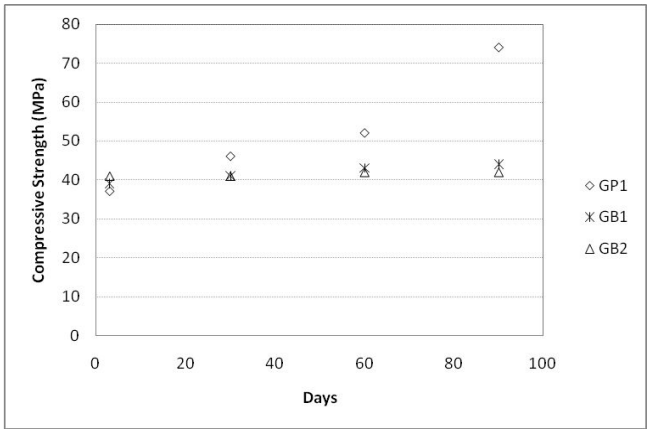

Fig. 7b Compressive strength of geopolymer specimens with time

D. Water Absorption

Water absorption test was conducted for all the geopolymer specimens to relate with total porosity results obtained from MIP.

Fig. 8 presents the variation of water absorption of specimens. Blast furnace slag addition causes a reduction in water absorption for the geopolymer specimens. GP1 specimen having no additive showed 12.23% water absorption. Addition of blast furnace slag results in reduction of water absorption to 11.72% and 10.89% for GB1 and GB2 respectively.

It is significant to note that GB1 and GB2 specimens had improved porosities when compared to GP1. The rate of water absorption was found higher for blast furnace slag blended geopolymer as the drop in mean size increase the rate of suction.

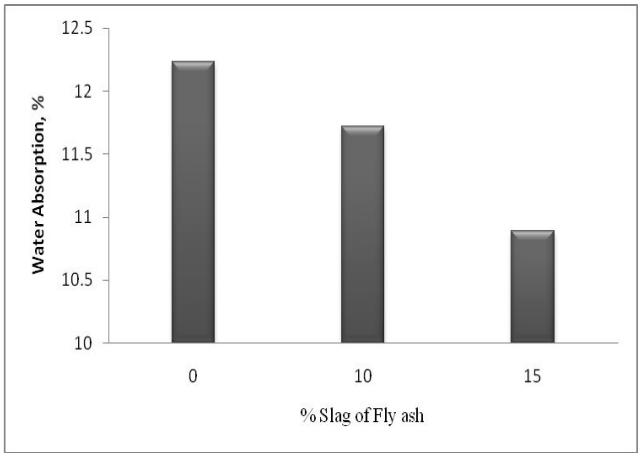

Fig. 8 Water absorption of geopolymer specimens

IV. CONCLUSIONS

A stabilised characteristics regarding strength was obtained by addition of GGBS as a source of Calcium. The Ultimate strength was achieved by 3 days strength of geopolymer blended with GGBS.No further increment of compressive strength which is caused basically due to the formation of crystallise sodium compound, was omitted by the addition of supplementary slag. It is due to the formation of amorphous Ca–Al–Si structure additionally during geopolymerization.MIP result indicates reduction of larger pores after addition of blast furnace slag into geopolymer paste sample. This has a favourable effect on microstructure resulting in lesser water absorption and higher compressive strength.Incorporation of blast furnace slag enhances the compressive strength of paste specimens .This could be due to the notable variations of porosity between the specimens prepared with or without blast furnace slag.Water absorption showed a decreasing trend with increase in blast furnace slag content in fly ash based geopolymer.Scanning electron microscopy shows better surface texture due to the addition of blast furnace slag in fly ash based geopolymer. In larger zoom regular crystallise compounds were found only in GP1 specimen where as in higher magnification this type of crystallize formations were not found in blended geopolymer (GB1, GB2).9Rate of water absorption is higher for blast furnace slag blended geopolymer as suction rate through surface is accelerated due to reduction in average pore sizes.

REFERENCES

J.Davidovits, Geopolymer, "Man-made Rock Geosynthesis and the Resulting Devolopment of Very Early High Strength Cement," Journal of Materials Education, 16 (2-3), pp: 91-137, (1994).

J. Davidovits, "Properties of geopolymer cements. Proceedings," First International Conference on Alkaline Cements and Concretes. Scientific Research Institute on Binders and Materials, Kiev State Technical University. 9 ,pp:131-149, (1994).

A.Palomo, M.W. Gruztek, M.T. Blanco "Alkali activated fly ashes. A cement for the future," Cement and Concrete Research. 29 ,pp:1323-1329, (1999).

R. N Thakur, S.Ghosh, "Effect of mix composition on compressive strength and microstructure of fly ash based geopolymer composites," ARPN Journal of Engineering and Applied Sciences. 6, pp:70-71, (2009).

Hardjito and B. V. Rangan, "Development and properties of low-calcium fly ash –based geopolymer concrete," Research Report GC. Faculty of Engineering, Curtin University of Technology, Perth, Australia, 1 pp: 130, (2005) .

S.Songpiriyakij , "Engineering Properties of Mae Moh Fly Ash Geopolymer Concrete," International Conference on Pozzolan Concrete and Geopolymer, Khon Kaen, Thailand, 24-25, pp:219-225, (2006).

J Temuujin, A van Riessen, R Williams, "Influence of calcium compounds on the mechanical properties of fly ash geopolymer pastes," Journal of Hazardous Materials, 167(1–3) ,pp:82–88, (2009).

R.Thakur, S. Ghosh, "Fly ash based geopolymer composites," Proceedings of 10th NCB International seminar on cement and building materials, New Delhi, India, 3 ,pp:442-451, (2007).

F.Skvara,Tomas Jilek, Lubomir Kopecky, " Geopolymer Materials Based on Fly Ash," Ceramics, 49 (3) ,pp:195-154, (2005).

Peter Duxsona, John L. Provis , Grant C. Lukey , Seth W. Mallicoat ,Waltraud M. Kriven , Jannie S.J. van Deventer, "Understanding the relationship between geopolymer composition, microstructure and mechanical properties," Colloids and Surfaces A: Physicochem. Engg. Aspects ,269, pp:47–58, (2005).

H. M. Khater, "Effect of Calcium on Geopolymerization of Aluminosilicate Waste," J. Mater. Civil. Eng. 24(92), pp: 92-101, (2012).

C.K.Yip,, JSJ Van Deventer, " Effect of granulated blast furnace slag on geopolymerisation." CD ROM Proceedings of 6th World Congress of Chemical Engineering, Melbourne, Australia, pp: 23–27, September, (2001).

JGS Jaarsveld, JSJ Deventer, L Lorenzen, " Factors affecting the immobilisation of metals in geopolymerised fly ash." Metallurgical Material Transaction B, 29, pp: 283–291, (1998).

JGS Jaarsveld, JSJ Deventer, GC. Lukey, " The characterisation of source materials in fly ash-based geopolymers." Materials Letters. 12, pp:72–80, (2003).

H Xu, JSJ Deventer, SJ. Jannie, " Geopolymerisation of multiple minerals."Mineral Engineering, 15 , pp: 1131–1139, (2002).

K Wang, SP Shah, A Mishulovich ,"Effects of curing temperature and NaOH addition on hydration and strength development of clinker-free CKD-fly ash binders," Cement Concrete Research ,34, pp:299–309, (2004).

CK Yip, JSJ van Deventer, "Microanalysis of calcium silicate hydrate gel formed within a geopolymeric binder," J Material Science, 38(18), pp: 3851–3860, (2003).

International Journal of Emerging Technology and Advanced Engineering
Website: www.ijetae.com (ISSN 2250-2459, Volume 2, Issue 11, November 2012)

Effect of Lime Stone Dust on Geopolymerisation and Geopolymeric Structure

Debabrata Dutta[1] and Somnath Ghosh[2]
[1]Research Scholar, Department of Civil Engineering, Jadavpur University, Kolkata- 700032, W.B, India,
[2]Professor, Department of Civil Engineering, Jadavpur University, Kolkata- 700032, W.B, India.
Email: ddebabrata83@gmail.com , Ph: +919547876984

***Abstract*— In this paper, synthesis of geopolymer from fly ash with sodium hydroxide as activator was studied. Fly ash was replaced by Lime stone dust in various proportions (10% and 15%) where Fly ash was used as source material for synthesis of geopolymer. Sodium silicate (Na_2SiO_3) and sodium hydroxide (NaOH) solutions were mixed maintaining a silicate modulus (Na_2O / SiO_2) at 1. Scanning electron microscopy (SEM), mercury intrusion porosimetry was carried out to characterize the geopolymer specimens. Compressive strength and water absorption were also tested on geopolymer pastes. The results illustrate that high strength geopolymer pastes can be produced using mixture of fly ash with Lime stone dust in lower curing temperature. The compressive strength of geopolymer paste specimens with 15% Lime stone dust were increased about 44% when cured for 48 hours at 65^{O}C. Specimens incorporated with Lime stone dust showed better microstructure and exhibited lesser porosity. The average pore diameters get reduced due to the addition of Lime stone dust which has a favourable effect on geopolymer structure as building material.**

***Keywords*— Geopolymer, Sodium Silicate, Fly ash, Lime stone dust, ESEM, MIP.**

I. Introduction

Basically, alkali metal (Na or K) silicate or hydroxide is often used as an activator for synthesis of the metakaolin-based or fly ash-based geopolymers [1, 2].At present, fly ash based geopolymers have received tremendous attention as fly ash has huge potential and are abundantly available as wastes from thermal power plants. It is necessary to explore new pathways for fly ash-based geopolymerization and improve the properties of the materials. High CaO content decreases the microstructural porosity as well as strengthens the geopolymer by establishing amorphous structure Ca–Al–Si gel during geopolymerization [3, 4, 5, 6]. This is also supported by the investigation [7] that ground granulated blast furnace slag which explains that calcium containing compounds such as calcium silicates, calcium aluminate hydrates, and calcium-silico-aluminates are formed during geopolymerization of fly ash, that affects the setting and workability of the mix [4]. The geopolymers manufactured from calcined material were found to have higher early strength, while those formed from non-calcined materials possessed higher increase in strength during the later stages of curing [5]. Jaarsveld et al. [3] reported anomalous result; greater strength was obtained for the geopolymers containing kaolin. Temuujin et al. [8] suggested that the accumulation of calcium compounds CaO and $Ca(OH)_2$ improves mechanical properties of the fly ash-based geopolymers cured at ambient temperature again. A thought of blended geopolymer came out by the sense to improve the porosity as well as the strength and other properties. The addition of moderate amount of minerals to a geopolymer can have significant improvements on the geopolymer structure and properties.

In this study Lime stone dust was utilized as an additive for fly ash-based geopolymer. The products obtained were characterized by means of their microstructure and hardened property.

II. Materials and Method

A. Materials

Low calcium Class F fly ash used in the present research work was collected from Kolaghat Thermal Power Plant near Kolkata, India. It had chemical composition as given in Table-1. About 75% of particles were finer than 45 micron and Blaine's specific surface was 380m^2/kg. The Limestone dust was brought from BCC Limited, Dhanbad, Jharkhand, India. The Lime stone dust is a solid composite having specific gravity 2.7, bulk density 1425 kg/m^3.It has an average particle size of 25 micron while particle size varies between ranges of 10µ to 70µ. The chemical analysis report of Lime stone dust is provided in Table 2. Scanning electron micrographs of fly ash and Lime stone dust is given in figure 1 and 2.

Laboratory grade sodium hydroxide in pellet form (98 percent purity) and sodium silicate solution (Na_2O= 8%, SiO_2 =26.5% and 65.5% water) with silicate modulus ~ 3.3

International Journal of Emerging Technology and Advanced Engineering
Website: www.ijetae.com (ISSN 2250-2459, Volume 2, Issue 11, November 2012)

and a bulk density of 1410 kg/m^3 was supplied by LobaChemie Ltd,India. The alkaline activating solution was prepared by dissolving required quantity of sodium hydroxide pellets directly into predetermined quantity of sodium silicate solution. It hadNa_2O content and SiO_2 content as 8.0% of fly ash, thereby making SiO_2/Na_2O ratio of 1. Water to Fly ash ratio was of 0.33. The activator solution was left at room temperature overnight before being used to manufacture geopolymer specimens.

TABLE 1.

CHEMICAL COMPOSITION OF FLY ASH

Chemical composition	Fly ash (%)
SiO_2	56.01
Al_2O_3	29.8
Fe_2O_3	3.58
TiO_2	1.75
CaO	2.36
MgO	0.30
K_2O	0.73
Na_2O	0.61
SO_3	Nil
P_2O_5	0.44
Loss on ignition	0.40

TABLE 2.

CHEMICAL COMPOSITION OF LIME STONE DUST

Chemical Composition	Percentage
CaO	51.01
MgO	0.28
Fe_2O_3	0.36
Al_2O_3	2.74
SiO_2	3.92
K_2O	0.04
Na_2O	Nil
TiO_2	0.09
Loss on ignition	41.56

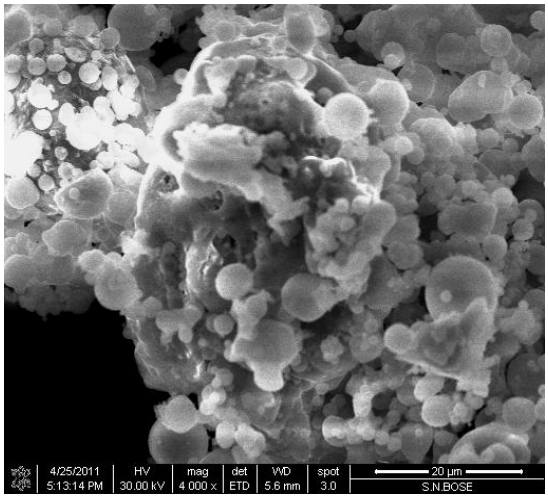

FIGURE 1

.SEM IMAGE OF FLY ASH

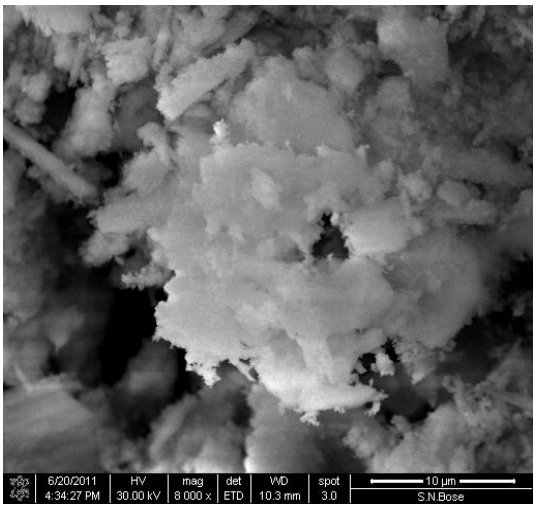

FIGURE 2

.SEM IMAGE OF LIME STONE DUST

B. Sample preparation

a. General

Sodium hydroxide pellets was mixed into water as required to maintain water to fly ash ratio in the activator solution as 0.33. The Sodium hydroxide solution thus prepared was kept for one day before mixing with sodium silicate solution. The mixture of Sodium hydroxide solution and sodium silicate solution again was kept for few hours until its temperature came down. The curing regime

International Journal of Emerging Technology and Advanced Engineering
Website: www.ijetae.com (ISSN 2250-2459, Volume 2, Issue 11, November 2012)

adopted was after Thakur and Ghosh [9]. At the very outset Lime stone dust was mixed with fly ash as 10%, 15% by weight of fly ash. This Lime stone dust added fly ash was mixed with the activator solution for 5 minutes in a Hobart mixture for preparing paste. Paste were then transferred into 50mm x 50mm x 50mm cubical moulds and vibrated on a vibrating table for 2 minutes. Specimens were cured along with the moulds in an oven for a period of 48 hours at 65^0C and allowed to cool inside the oven before being removed to room temperature. Specimens were removed and stored at room temperature at a dry place before testing. Some data of the present study are given in the Table 3.After 28 days from casting, the geopolymer specimens were tested for its pore characteristics, water absorption, compressive strength and microstructural properties including scanning electron microscopy, pore characteristics were studied by mercury intrusion porosimetry test.

TABLE 3.

DETAILS OF GEOPOLYMER PASTE AND PASTE SPECIMENS

Sample ID	Na_2O Content in activator (%)	SiO_2 content in activator (%)	Lime stone dust (% by Wt of fly ash)	Type of specimen	Water / fly ash ratio	Curing temp. and duration
AGP1	8	8	0	Paste	0.33	65^0C and 48 hrs
GL1	8	8	10	Paste	0.33	65^0C and 48 hrs
GL2	8	8	15	Paste	0.33	65^0C and 48 hrs

III. RESULTS AND DISCUSSION

A. Mercury intrusion porosimetry (MIP)

MIP samples were made by cutting a cylinder of ¼ in. dia. to ½ in. height, having a bulk sample volume of 1.00cc which were tested on a Micromeritics Auto pore II set up in CGCRI , Kolkata, MIP from 0-60,000 pis ,with a Hg surface tension 480.00 erg/cm2, contact angle (I) 140.000, (E) 140.000.MIP was used to examine a statistical comparison of the tested samples in terms of mean and median pore size and pore distribution.MIP data are related more to pore connectivity and the values of larger pores may seem smaller due to bottle-neck shapes of pores[10]. The bulk volume of each test specimen was 1cc and maximum applied intrusion pressure during the test was about 53500 psi. Plots of the rate of mercury intruded into specimens and pore diameter of the paste specimens are shown in Figure 3 and Figure 4. It can be noticed that addition of Lime stone dust in the mix has a significant influence on the average pore sizes. In case of sample GL2 (specimen blended with 15% Lime stone dust) the significant intrusion is prominent from diameter range 0.005 micro meter to 2 micro meter where as for the case of AGP1 (geopolymer not blended) the significant intrusion ranges between 0.01 micrometer to 20 micrometer. Pick intrusion appears at 0.04 micrometer and 0.1 micrometer for GL2 and AGP1 respectively. It is evident that due to presence of calcium the samples responded in relatively lower pore size ranges rather than higher. But higher pore sizes require lesser pressure effort. This signifies that there had been absence of larger pores in calcium blended sample. That is the pore size in calcium blended geopolymer is distributed at the order of lesser pore diameter. This indicates more compactness resulting higher strengths. Bulk density was seemed to be improved about 22%.Considerable variation in average pore sizes is noticed due to the different quantities of Lime stone dust added into the geopolymer mix. Skvara et al. [11] found that the Na2O content and SiO_2/Na_2O of geopolymer mix significantly affects pore characteristics and compressive strength. In the present experimental investigation, the least porosity is obtained in GL2 specimen having highest Lime stone dust content. As Lime stone dust contains a large amount of $CaCO_3$ which produces Ca+ ions. The Ca+ may reimburse the charge of aluminum atoms in spite of Na+. It is supposed that reinforcing effect was caused by the unreacted Lime stone dust particles. Semi crystalline Ca-Al-Si may also be formed at the presence of higher calcium. [12].

International Journal of Emerging Technology and Advanced Engineering
Website: www.ijetae.com (ISSN 2250-2459, Volume 2, Issue 11, November 2012)

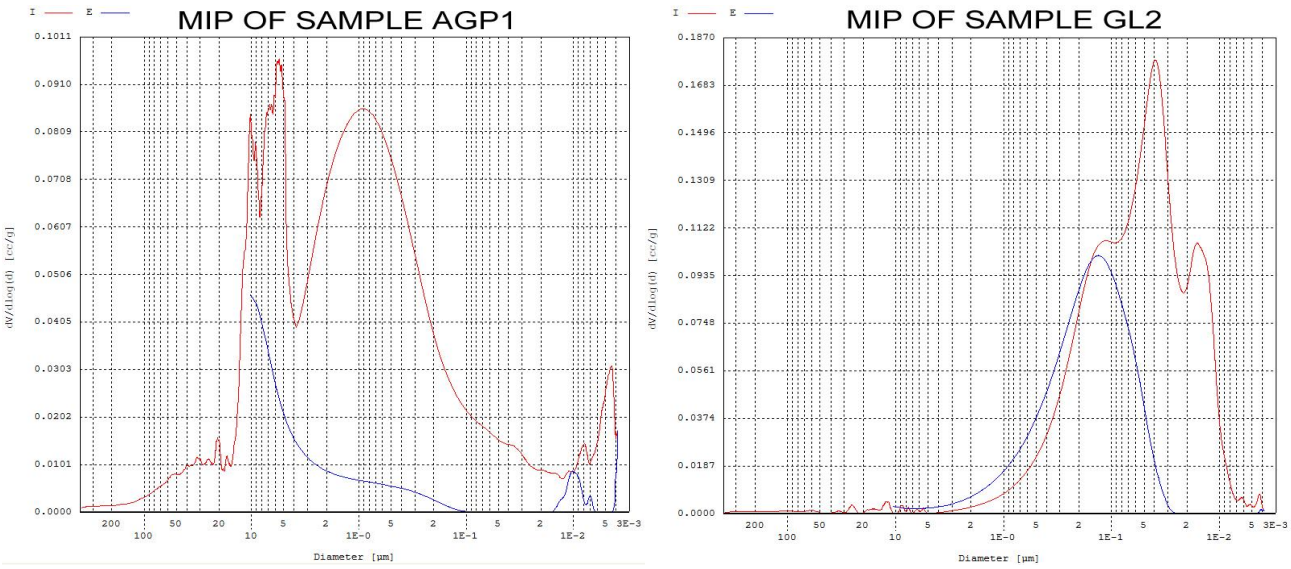

FIG. 3 & FIG. 4

RELATIONSHIP OF RATE OF MERCURY INTRUSION WITH PORE DIAMETER

B. Compressive strength

The compressive strength of the geopolymer paste was determined after 28 days from manufacture. There was slow increment in compressive strength with time beyond 28 days for the samples without Lime stone dust the strength trends were likely to change over time as high NaOH geopolymer leaned to cure more slowly [13]. Three specimens for each series were crushed in a digital compression testing machine and the average is reported. As fracture behavior of the samples was often unpredictable as few areas were chip of prior to ultimate facture, successful samples were indicated only when there was a single break of the materials [14]. Compressive strength obtained for the specimens are presented in Figure 5. The key role played by the Ca ions in the geopolymer skeleton. Infact the high $CaCO_3$ content effects in quicker geopolymerisation and the development of semi-crystalline Ca-Al-Si gel [15] .AGP1 specimen prepared without Lime stone dust has a compressive strength of 25 MPa. Addition of Lime stone dust caused increase in compressive strength of specimens. Significant increases of strength occurred for GL1 specimen (30 MPa) which contained 10% Lime stone dust. Similarly, the compressive strength further increased (36 MPa) with additional Lime stone dust of 15%. It amounted to a strength increase of 20% and 44% for GL1 and GL2 respectively. The results clearly indicate successive increment in compressive strength of the specimens. Porosity has been accounted to be principal microstructural variable limiting the mechanical properties of geopolymers[16].The variation of compressive strength should be due to significant differences in their porosity as noticed from the MIP results. It was noticed from the MIP results that porosity improves with addition of Lime stone dust in case of geopolymer specimens. Hence, the compressive strength shows a corresponding increase.

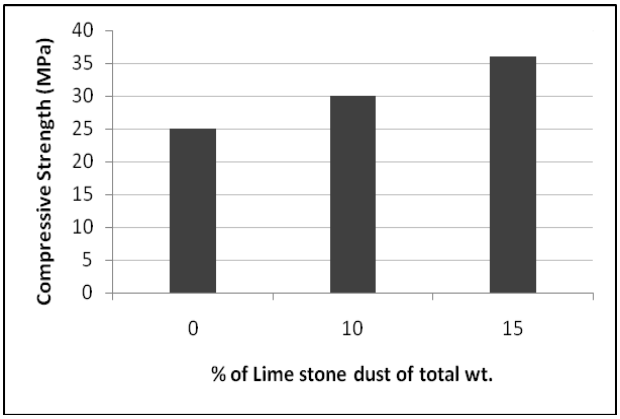

FIGURE 5.

COMPRESSIVE STRENGTH OF SPECIMENS

International Journal of Emerging Technology and Advanced Engineering
Website: www.ijetae.com (ISSN 2250-2459, Volume 2, Issue 11, November 2012)

C. Microstructural investigation with ESEM/EDAX

Model quanta 200 mk 2 made in Netherland Scanning Electron Microscope was used. In study of porosity.SEM analysis covers a much smaller area in compare to MIP. Because at least 25 mm^2 of sampling area is needed to obtain a reliable result [17]. However, SEM analysis was not interred to be used as a method to obtain statistical information regarding pore size. It was performed in order to study pore morphology and to view the reacted and unreacted regions of the samples. Figure 6 presents the ESEM micrographs for geopolymer paste specimens AGP1, GL1 and GL2 along with their EDAX traces. In all the micrographs of specimens, it depicts a microstructure having some unreacted and partly unreacted particles embedded in the geopolymer gel. The micrographs reveal mostly an amorphous phase with pores of various sizes. AGP1 specimen which is prepared without Lime stone dust appear to be more porous than other specimens GL1 and GL2 which contain 10% and 15% Lime stone dust. Another significant observation is that surface texture is more smooth and compact in specimens where Lime stone dust has been added in the mix. EDAX spectra of AGP1 specimen shows major elements such as carbon (C), oxygen (O), aluminium (Al), silicone (Si), calcium (Ca) and sodium (Na). The weight percentages of some important elements were Si (15.80%), Al (8.04%), Na (12.95%) and Ca (0.25). GL1 having a Lime stone dust content of 10% also has similar elements. However, the weight percentages of important elements are different which shows Si (18.18%), Al (10.92%),Na (11.76%) and Ca(5.22). For GC2 specimen prepared with addition of 15% Lime stone dust, the weight percentages from EDAX analysis yielded the following: Si(19.54%), Al(9.12%) , Na(7.33%)and Ca (7.28).

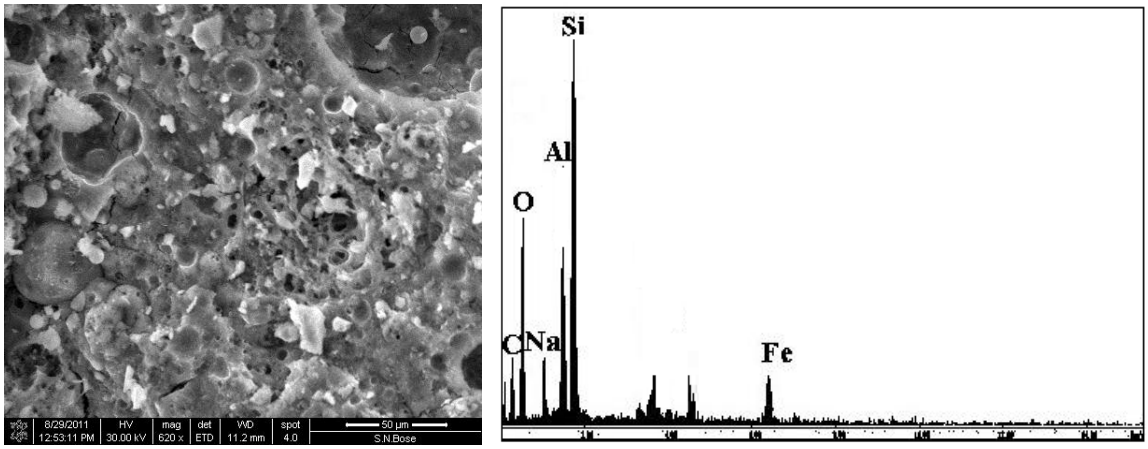

[A] AGP1 specimen

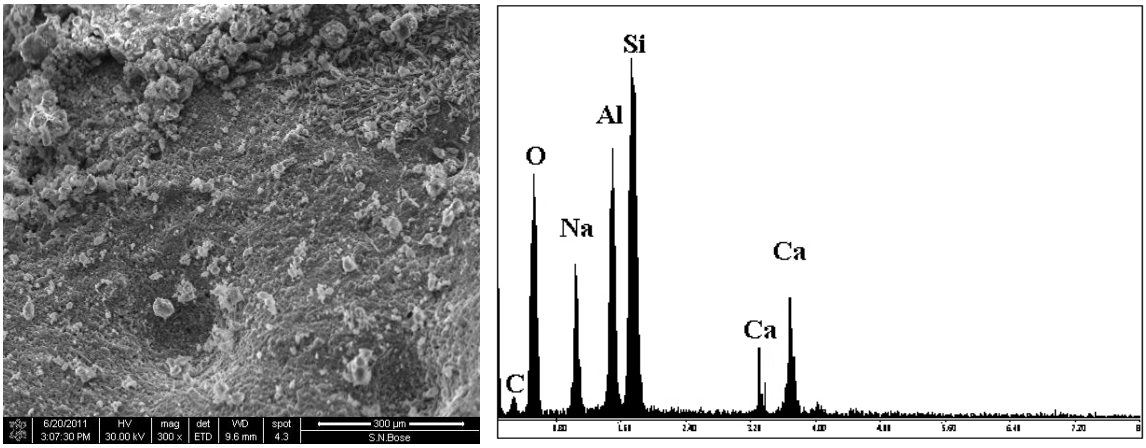

International Journal of Emerging Technology and Advanced Engineering
Website: www.ijetae.com (ISSN 2250-2459, Volume 2, Issue 11, November 2012)

[B] GL1 specimen

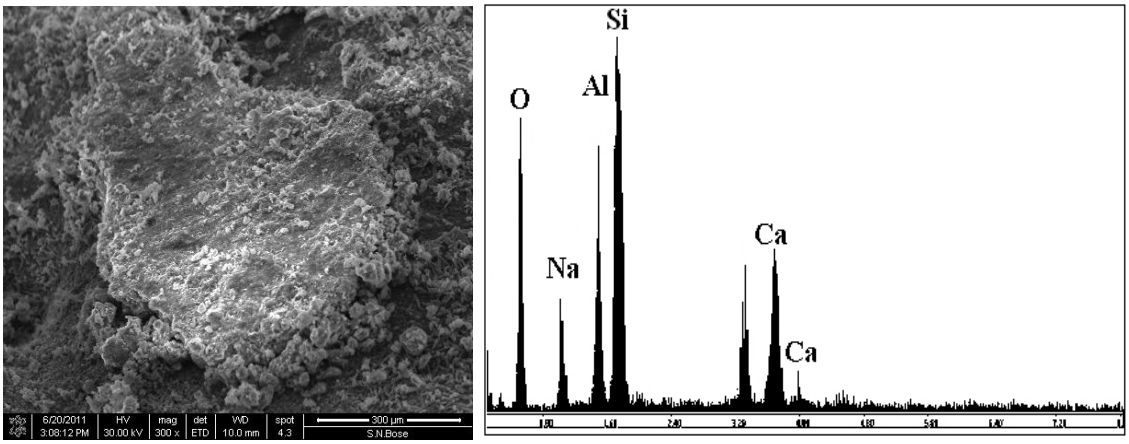

[C] GL2 specimen

FIGURE 6.

ESEM MICROGRAPHS AND EDAX SPECTRA FOR GEOPOLYMER PASTE SPECIMENS

D. Water absorption

To determine the water absorption of specimens, six cubes from each series were taken after curing at a temperature of 65^0C for 48 hours and its weight determined as initial weight. The samples were then immersed in water for 24 hours and its saturated surface dry weight was recorded as the final weight. Water absorption of specimens is reported as the percentage increase in weight. The temperature was kept under 65^0C to avoid any change in structural configuration which may cause due to the exposure temperature over curing one. The procedure followed was after Thokchom and Ghosh [18].

Water absorption was measured by using the following equation.

$$\text{Water absorption} = [(WS-WD)/WD] \times 100\%$$

Where,

WS = weight of specimen after immersion in water for 24 hours

WD = weight of specimen after oven curing at 65^0C for 48 hours

Figure 7 presents the variation of water absorption of specimens. As expected, using Lime stone dust as additives caused a reduction in water absorption for geopolymer specimens. AGP1 specimen having no additive showed 9.5% water absorption. Addition of Lime stone dust resulted in reduction of water absorption to 7.98% and 5.69% for GL1 and GL2 respectively. It is significant to note that GL1 and GL2 specimens had improved porosities when compared to AGP1. It should be mentioned that rate of water absorption is higher for Lime stone dust blended geopolymer as suction rate through surface is accelerated due to reduction in average pore sizes. It can be concluded from the results that water absorption is proportionally related to porosity of the specimens.

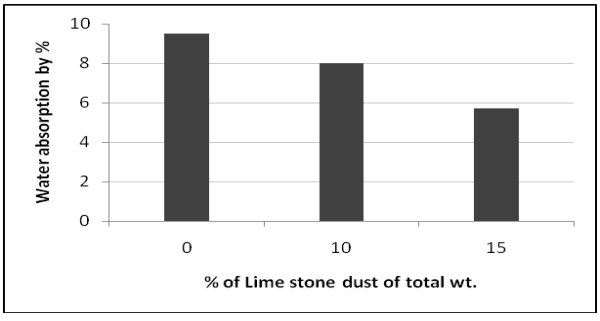

FIGURE 7

International Journal of Emerging Technology and Advanced Engineering
Website: www.ijetae.com (ISSN 2250-2459, Volume 2, Issue 11, November 2012)

IV. CONCLUSION

The following conclusions were made on the basis of the results from the experimental investigation.

1. Pore sizes get reduced after addition of Lime stone dust into geopolymer paste sample. This phenomena influences water absorption and compressive strength.

2. Incorporation of Lime stone dust up to 15% increases the compressive strength of paste specimens about 44%.This could be due to the notable variations of porosity between the specimens prepared with or without Lime stone dust.

3. Water absorption values were found directly related to total porosity of specimens. For paste specimens, water absorption showed a decreasing trend in water absorption with increasing Lime stone dust content.

4. SEM images shows surface texture is less porous and compact in specimens where Lime stone dust has been added in the mix. EDAX reports that a little amount of weakly crystalline CSH phases could be formed.

5.The reduction in compressive strength due to lower curing temperature may be compensated by incorporation of calcium compound which can accelerate the rate of geopolymerisation even at low temperature.

REFERENCES

[1] H. Xu, S. J. Van Deventer, "The Effect of Alkali Metals on the Formation of Geopolymeric Gels from Alkali-feldspars," in Colloids and SufacesA :Physicochem . Eng. Aspects 00 1-18 (2003) .

[2] Frantisek Skvara , Tomas Jilek , LubomirKopecky Geopolymer Materials Based on Fly Ash April 20 , 2005 .

[3] Van Jaarsveld JSG, Van Deventer JSJ, Lorenzen L (1998), Factors affecting the immobilisation of metals in geopolymerised fly ash, Metal Mater Trans B 29:283,

[4] Van Jaarsveld JGS, Van Deventer JSJ, Lukey GC (2003), The Characterisation of source material in fly ash based geopolymer ,Mater Lett 57:1272

[5] Xu H, Van Deventer JSJ (2002), Geopolymerisation of multiple minerals, Miner Eng 15:1131

[6] Wang K, Shah SP, Mishulovich A (2004), Effects of curing temperature and NaOH addition on hydration and strength development of clinker-free CKD-fly ash binders Cement Concrete Res 34:299

[7] Yip, C.K. & Van Deventer, J.S.J., Microanalysis of calcium silicate hydrate gel formed within a geopolymeric binder,Journal of Materials Science, 2003, 38(18): 3851-3860. Yip CK, Van Deventer JSJ (2003) J Mater Sci 38:3651

[8] Temuujin J, van Riessen A, Williams R. Influence of calcium compounds on the mechanical properties of fly ash geopolymer pastes. J Hazard Mater 2009

[9] [9] R.Thakur, S. Ghosh,(2007) Fly ash based geopolymer composites, Proceedings of 10th NCB International seminar on cement and building materials, New Delhi, India 3, 442-451

[10] Frantisek Skvara , Tomas Jilek , LubomirKopecky Geopolymer Materials Based on Fly Ash April 20 , 2005 .

[11] F.Skvara, L.Kopecky, J.Nemecek ,Z.Bittnar, (2006) Microstructure of Geopolymer Materials based on fly ash, Ceramics-Silikaty 50 (4) 208-215.

[12] Lee, W.K.W., Van Deventer, J.S.J., 2002. The effect of ionic contaminants on the early-age properties of alkali-activated fly ash-based cements. Cement and Concrete Research 32, 577–584.

[13] H. Xu , S. J. Van Deventer , "The Effect of Alkali Metals on the Formation of Geopolymeric Gels from Alkali-eldspars ," Colloids and Sufaces A : Physicochem . Eng. Aspects 00 1-18 (2003) .

[14] Waltrud M. Kriven and Jonathan L. Bell University of Illinois at Urbana Champaign 105 Materials Science and Engineering Blgd. 1304 W. Green St. Urbana, IL 61801 Effect Of Alkali Choice On Geopolymer Properties .

[15] Yip, C.K., Van Deventer, J.S.J. Effect of granulated blast furnace slag on geopolymerisation. In: CD-ROM Proceedings of 6th World Congress of Chemical Engineering, Melbourne, Australia, 23–27 September 2001

[16] B.A. Latella, D.S. Perera, D. Durce,E. G. Mehrtens, J. Davis, Mechanical properties of metakaolin-based geopolymers with molar ratios of Si/Al ≈ 2 and Na/Al ≈1, J Mater Sci 43 (2008) 2693–2699.

[17] J. Van Brakel (ed) , "A special Issue Devoted to Mercury Porosimetry, "Powder Tech. 29 [1] 1-209 (1981) .

[18] Thokchom Suresh , Ghosh Partha , Ghosh Somnath 2009 Effect of Water Absorption , Porosity and Sorptivity on Durability of Geopolymer Pastes ARPN Journal of Engineering and Applied Sciences , vol 4 , no. 7 , Sep 2009 .